

Redescription of a rarely encountered species *Travisia chinensis* Grube, 1869 (Annelida, Traviidae), including a description of a new species of *Travisia* from Amoy, China

Deyuan Yang^{1,2}, Xuwen Wu³, Zhi Wang⁴, Xiaoyu Zhao²,
Jiangshiou Hwang^{1,5,6}, Lizhe Cai²

1 Institute of Marine Biology, National Taiwan Ocean University, Keelung 20224, Taiwan **2** College of the Environment and Ecology, Xiamen University, Xiamen 361102, Fujian, China **3** Institute of Oceanology, Chinese Academy of Sciences, Qingdao 266071, China **4** State Key Laboratory of Marine Environmental Science, College of Ocean and Earth Sciences, Xiamen University, Xiamen 361102, China **5** Center of Excellence for Ocean Engineering, National Taiwan Ocean University, Keelung 20224, Taiwan **6** Center of Excellence for the Oceans, National Taiwan Ocean University, Keelung 20224, Taiwan

Corresponding authors: Jiangshiou Hwang (jshwang@mail.ntou.edu.tw), Lizhe Cai (cailizhe@xmu.edu.cn),
Xuwen Wu (wuxuwen@qdio.ac.cn)

Academic editor: Christopher Glasby | Received 6 July 2022 | Accepted 29 August 2022 | Published 4 November 2022

<https://zoobank.org/6FDCCA3C-97AC-4E83-B072-8BEDB9E0B2A5>

Citation: Yang D, Wu X, Wang Z, Zhao X, Hwang J, Cai L (2022) Redescription of a rarely encountered species *Travisia chinensis* Grube, 1869 (Annelida, Traviidae), including a description of a new species of *Travisia* from Amoy, China. ZooKeys 1128: 1–17. <https://doi.org/10.3897/zookeys.1128.90020>

Abstract

The original description of *Travisia chinensis* Grube, 1869 was incomplete, leading to confusion with other species. To clarify the status of this species, we provide a redescription of, and remarks on, *T. chinensis* based on an examination of the type specimen. We also describe *Travisia amoyanus* **sp. nov.**, collected from Xiamen (Amoy), China, and originally identified as *T. chinensis* by Monro (1934). The new species can be distinguished from its congeners by a combination of the following characters: the total number of segments (34 or 35) and chaetigers (33 or 34), parapodial lappets first from chaetiger 15, and a pygidium with a large ventral triangular cirrus and about six encircling lateral cirri. Genetic distances and phylogenetic analyses based on the mitochondrial (*16S rRNA*) and nuclear (*18S rRNA*) genes support the identity of the new species.

Keywords

Morphology, phylogeny, Polychaeta, stinkworms, taxonomy

Introduction

Currently, the polychaete family Traviidae Hartmann-Schröder, 1971 contains a single genus, *Travisia* Johnston, 1840, which includes 37 recognized species (Read and Fauchald 2022). *Travisia* is easily recognized by its noticeably fetid odor which makes them known as stinkworms. Because their external features are very simple, the taxonomic characters are mainly based on quantitative morphological characters, such as the total number of segments, chaetigers, branchiae, and pygidial lobes (Dauvin and Bellan 1994; Rizzo and Salazar-Vallejo 2020). Although some reviews (Dauvin and Bellan 1994; Augener 1922) and regional studies (e.g., Hartman 1969; Yang and Sun 1988; Maciolek and Blake 2006) had been conducted on *Travisia*, there are still many species with incomplete descriptions, and species boundaries need to be re-evaluated.

Travisia chinensis Grube, 1869 was originally described based on a single specimen collected from Chinese waters, but the exact type locality was not given. Later, Augener (1922) redescribed *T. chinensis* based on the type material and considered *Travisia olens* Ehlers, 1879, *T. kerguelensis* McIntosh, 1885, and *T. chinensis* as the same species, based on their similar number of segments. Unfortunately, none of these authors provided illustrations, and some main characters (e.g., the number of branchiae, and the position and shape of parapodia lappets) were not clearly described. Since these early descriptions, Monro (1934) identified a specimen collected from Amoy (Xiamen) as *T. chinensis* based on Augener's (1922) statement. However, the main characters of *T. chinensis* sensu Monro, 1934 are not consistent with Grube and Augener's descriptions, mainly differing in the number of chaetigers (33 or 34 vs 29) and the number of segments (34 or 35 vs 30). *Travisia chinensis* has not been recorded anywhere since its original description (Dauvin and Bellan 1994) and has rarely been compared with other *Travisia* species by subsequent authors. To clarify the taxonomic confusion, we examined the holotype of *T. chinensis* (ZMB 0629) deposited in Zoological Museum, Berlin (ZMB) with the help of Dr Birger Neuhaus. Detailed descriptions of *T. chinensis* are provided and compared with the related species.

The first author examined all materials of *Travisia* deposited in the Marine Biological Museum (MBM) of the Chinese Academy of Sciences (IOCAS). Newly collected *Travisia* specimens revealed that the specimens from the coastal region of Xiamen agree well with *T. chinensis* sensu Monro (1934) in most morphological characters, such as body with 33 or 34 chaetigers and parapodial lappets present from chaetiger 15. In addition, both our materials and Monro's specimen were collected from Amoy (Xiamen), southern East China Sea. In this study, we consider them as a new species to science, *Travisia amoyanus* sp. nov.

Our study aims to provide redescrptions and comments on the rarely known *T. chinensis* Grube, 1869, as well as to erect a new species, *T. amoyanus* sp. nov., collected from Xiamen Fujian, China. To confirm the taxonomic status of the new species, we studied the morphology of the specimens and performed phylogenetic analyses based on partial sequences of *16S rRNA* and *18S rRNA* genes. We also provide the *28S rRNA* gene sequence of this new species.

Materials and methods

Specimen collection and morphological study

The type material of *T. chinensis* (holotype, ZMB 0629) was examined at the Zoological Museum, Berlin (ZMB) by Dr Birger Neuhaus in June 2020. Twenty-five specimens of the undescribed species were collected from the coastal regions of Xiamen and deposited in the Marine Biological Museum of the Chinese Academy of Sciences in the Institute of Oceanology in Qingdao, China. Sampling information of the examined specimens is summarized in the Suppl. material 1: table S1. Methyl green (MG) stain saturated in 80% ethanol was used to highlight the external morphological characters and characterize MG staining patterns following the methods of Maekawa and Hayashi (1999). Specimens were observed using a Zeiss Discovery V20 or Motic SMZ-168 stereomicroscope. Macrophotographs of whole animals were photographed using a Canon EOS 6D Mark II with a 100 mm macro lens or and Olympus E-M1 Mark II with a 60 mm lens with LED lighting. Micrographs were taken using an AxioCam 512 digital camera mounted on the microscope. All image stacks were obtained using Helicon Focus v. 7. To assess intraspecific variation of morphological characters, for each complete specimen, we measured the total length (TL), maximum width (at widest segments of the body), counted the total number of segments and chaetigers, the number of branchiae (including the starting and end segments of branchiae), and the starting segment of parapodia lateral lappets. A statistical analysis was carried out using Microsoft Excel. The morphological terminology follows Blake and Maciolek (2020). The definition of the total number of segments follows the recent proposal of Rizzo and Salazar-Vallejo (2020). The following abbreviations are used: Toc, total number of chaetigers; Tos, total number of segments; Mob, Maximum of branchiae; Sopl, start of parapodial lappets on chaetiger; Sob, start of branchiae; pr, prostomium; per, peristomium; nuO, nuchal organ; mo, mouth; br, branchiae; chaet, chaetiger; IntP, interramal pore; Pl, parapodia lateral lappet; np, nephridial pore; ntc, notochaetae; npc, neurochaetae; Py, pygidium; Vc, Pygidial ventralmost cirrus; MG, Methyl Green.

DNA extraction, amplification, and sequencing

Genomic DNA was extracted from branchiae or tissue of ethanol-preserved specimens using the Qiagen DNeasy Blood and Tissue Kit, following the DNeasy Protocol provided in the manufacturer's instructions. Two nuclear gene markers: 28S and 18S and one partial mtDNA gene marker 16S were amplified and sequenced. Polymerase chain reactions (PCR) for the 28S and 18S genes followed the protocols of Glover et al. (2016), and 16S gene followed the protocols described by Law et al. (2014) and Kobayashi and Kojima (2021). The primers and PCR annealing temperatures are summarised in Suppl. material 1: table S2. Polymerase chain reactions (PCR) were conducted in a total volume of 50 µl containing 25 µl PCR Mix (Dongsheng Biotech Co., Ltd, Guangdong,

China), 2 μ l forward- and reverse-primer each (10 μ M), 2 μ l template DNA, and 20 μ l ddH₂O. All PCR reactions were performed in a Veriti 96-Well Thermal Cycler (Applied Biosystems, Thermo Fisher Scientific). The PCR products were electrophoresed on a 1.5% agarose gel, then Sanger sequencing was performed by Sangon Biotech (Shanghai) Co., Ltd. SeqMan v. 11.1.0 (DNASTar, WI, USA) was used to assess the forward and reverse DNA strands of each gene, then blasted in GenBank to check for potential contamination. The newly obtained sequences were submitted to GenBank (<http://www.ncbi.nlm.nih.gov>) in the National Centre for Biotechnology Information (NCBI).

Phylogenetic analyses

For phylogenetic comparisons, we used all available *Travisia* sequences downloaded from GenBank and our newly obtained sequences. As outgroups, the sequences of *Ophelia limacine* (Rathke, 1843), *Scalibregma inflatum* Rathke, 1843, and *Polyphysia crassa* (Örsted, 1843) were used. All sequences used in this study were listed in Suppl. material 1: table S3. The online version of MAFFT v. 7 (Katoh et al. 2019) was used to align multiple sequences of each marker, with default values except for the parameter “Adjust direction according to the initial sequence,” which was turned on. The subsequent phylogenetic analysis steps were performed in PhyloSuite v. 1.2.2 (Zhang et al. 2020) with the help of its plug-in programs (Gblocks, ModelFinder, Partion-Finder2, IQ-TREE v. 1.6.8, and MrBayes v. 3.2.6). Gblocks v. 0.91b (Talavera and Castresana 2007) was used to remove ambiguously aligned sites. Three data sets (16S, 18S, and 16S+18S) were conducted for the phylogenetic analysis with maximum likelihood (ML) and Bayesian inference (BI) analysis. ModelFinder (Kalyaanamoorthy et al. 2017) and PartionFinder2 were used to select the best-fit model for single gene (16S or 18S) and the concatenated sequences (16S and 18S) using the Bayesian Information Criterion (BIC). ML was performed using IQ-TREE (Nguyen et al. 2015) based on 10000 ultrafast bootstrap replicates. BI was performed using MrBayes (Ronquist et al. 2012). Analyses were run for 10 million generations, in which the initial 25000 sampled data were discarded as burn-in. The resulting ML and Bayesian trees were visualized in iTOL (<https://itol.embl.de/>).

Nucleotide divergence (p -distance and Kimura2-parameter) over sequence pairs within and between species of *Travisia* were calculated in MEGA X (Kumar et al. 2018).

Results

Phylogenetic analyses

The results of phylogenetic analyses (ML and BI) based on partial 16S rDNA (417 bp), 18S rDNA (1671 bp), and their concatenated sequences (2088 bp), showed different topologies and support values, but analyses of ML and BI based on each dataset have the same topologies.

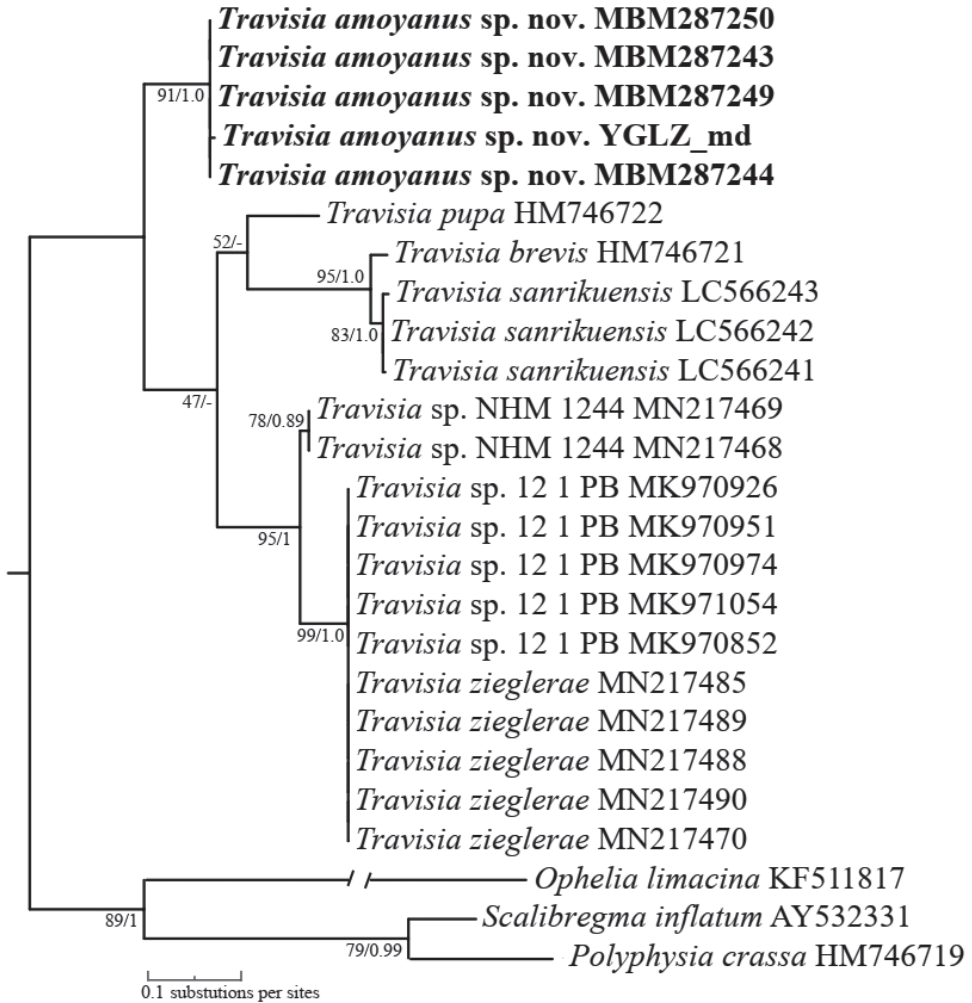


Figure 1. Maximum likelihood (ML) tree of Traviidae based on 16S sequences under IM2+F+G4 model, GTR+G+F model was used for Bayesian inference (BI) analysis. Node support values based on 10000 ultrafast bootstraps from ML followed by posterior probability values from BI analyses.

Phylogenetic analysis based on 16S or 18S sequences indicated that *Travisia amoyanus* sp. nov. was sister to all the other species of *Travisia* (BS = 89%, PP = 1.0 and BS = 100%, PP = 1.0, respectively; Figs 1, 2). However, phylogenetic analysis based on the concatenated sequences showed that *T. amoyanus* sp. nov. was sister to the clade consisting of *T. pupa* Moore, 1906, *T. kerguelensis* McIntosh, 1885, *T. zieglerae* Wiklund et al. 2019 and *Travisia* sp. (BS = 49%, PP = 0.53), and all the above species were sister to the clade consisting of *T. sanrikuensis* Kobayashi & Kojima, 2021 and *T. brevis* Moore, 1923 (Suppl. material 2). The pairwise genetic distances between *T. amoyanus* sp. nov. and the other species of *Travisia* ranged from 17.5% to 20.7%

(Kimura2-parameter) and 15.4–17.9% (uncorrected p -distance) for 16S (Table 1), 3.4–3.9% (Kimura2-parameter) and 3.4–3.8% (uncorrected p -distance) for 18S (Suppl. material 1: table S4), while the intraspecific distance within *T. amoyanus* sp. nov. was 0.08% for 16S and 0.1% for 18S. Such large genetic distance ranges for 16S and 18S, much larger than for compared species, were sufficient to distinguish the *T. amoyanus* sp. nov. from those species.

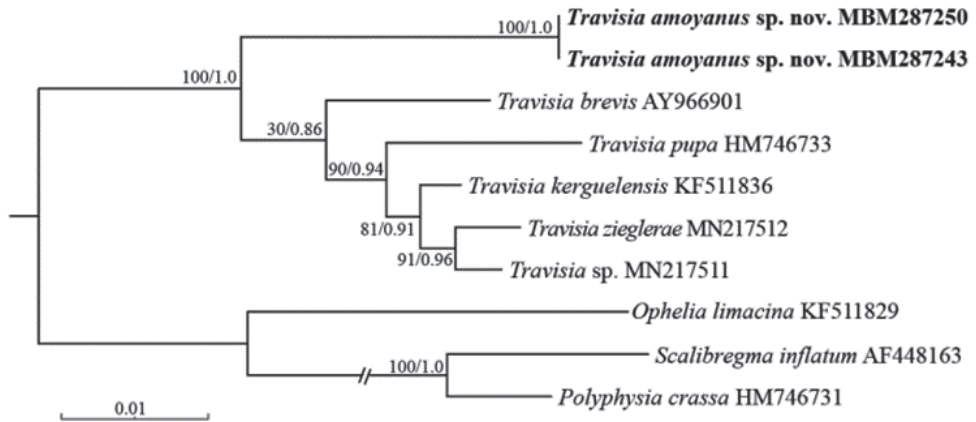


Figure 2. Maximum likelihood (ML) tree based on 18S rRNA gene sequences under TIM3+I+F model, K2P+I model for Bayesian inference (BI) analysis. Node support values based on 10000 ultrafast bootstraps from ML followed by posterior probability values from BI analyses.

Table 1. Pairwise distances using 16S within and among species of *Travisia*: values in the lower left corner were based on the Kimura2-parameter, and in the upper right corner were based on the p -distance model. Note: red numbers indicate the intraspecific genetic distance (p -distance and Kimura2-parameter show similar value).

Species of <i>Travisia</i>	<i>N</i>	1	2	3	4	5	6	7
1 <i>T. amoyanus</i> sp. nov.	5	0.001	0.170	0.171	0.179	0.167	0.162	0.154
2 <i>T. zieglerae</i>	21	0.195	0.001	0.001	0.058	0.132	0.172	0.151
3 <i>Travisia</i> sp.	10	0.197	0.001	0.001	0.060	0.136	0.172	0.155
4 <i>Travisia</i> sp. NHM 1244	2	0.207	0.061	0.063	0.001	0.109	0.153	0.144
5 <i>T. pupa</i>	1	0.191	0.146	0.151	0.118	n/c	0.153	0.127
6 <i>T. sanrikuensis</i>	3	0.186	0.198	0.199	0.172	0.174	0.006	0.032
7 <i>T. brevis</i>	1	0.175	0.170	0.175	0.160	0.140	0.033	n/c

Taxonomy

Family Traviidae Hartmann-Schröder 1971

Genus *Travisia* Johnston, 1840

Type species. *Travisia forbesii* Johnston, 1840.

Diagnosis (based on Rizzo and Salazar-Vallejo 2020). Body subfusiform or grub-like. No obvious ventral or lateral groove. Segments annulated, with integument

papillated. Prostomium small, conical or truncate, with no eyes and prostomial processes. Nuchal organs present. Parapodia reduced to two fascicles of capillary chaetae, with no dorsal or ventral cirri. Parapodial lappets or lobes present above and below the fascicles of chaetae in some species. Branchiae present or absent. A series of interramal sensory organs or pores present between dorsal and ventral fascicles of chaetae. Nephridial pores present. Pygidium ovoid or cylindrical.

Remarks. Three genera (*Dindymenides*, *Kesunis*, and *Travisia*) were included in the subfamily Traviinae Hartmann-Schröder, 1971, and later *Dindymenides* and *Kesunis* were synonymized with *Travisia* by Dauvin and Bellan (1994). Blake and Maciolek (2020) elevated Traviinae Hartmann-Schröder, 1971 to family Traviidae, with *Travisia* as the only valid genus. However, the synonymization of these three genera by Dauvin and Bellan (1994) was only based on the morphological study and a molecular phylogenetic analysis has yet to have been done.

***Travisia chinensis* Grube, 1869**

Fig. 3A–C

Travisia chinensis Grube, 1869: 66; China Sea, North-western Pacific.

Travisia chinensis Augener, 1922: 38–40.

Diagnosis. Body with 30 segments and 29 chaetigers. Branchiae cirriform from chaetiger 2, more than 25 pairs. Neuropodial lappet from chaetiger 16, notopodial lappet from chaetiger 19. Annulation pattern of segments: 1–15 triannulate, 16–26 biannulate, 26–30 uniannulate.

Material examined. *Holotype.* ZMB 0629, Chinese waters (“Chinesische Gewässer”), Coll. GRUBE.

Description. Body fusiform. Whitish in alcohol. About 30 mm in length (Fig. 3A). Prostomium twisted, anteriorly pointed (Fig. 3B). The mouth between chaetiger 1 and chaetiger 2 (Fig. 3B). Branchiae cirriform, except one trifid present chaetiger 10 on the right side, more than 25 pairs, start on chaetigers 2 and to at least chaetigers 26 (Fig. 3A). Most branchiae shorter than body width.

Chaetigers 1–15 without parapodial lappets. Chaetiger 16 with a small neuropodial lappet, below the bundle of neurochaetae on the right side of the body (Fig. 3C). Notopodial lappet above the bundle of notochoetae starting on chaetiger 19. Notopodial and neuropodial lappets well developed from chaetiger 19, but missing on segments 29 and 30 (Fig. 3C). Nephridial pores from chaetigers 3–14, the first four and last four small, the remainder larger (Fig. 3A).

Neuropodial and notopodial chaetal rami well separated. Chaetae arising directly from body wall, with 29 chaetigers. All chaetae hair-like, smooth and without a fringe. Interramal pores from the first chaetigers segment to almost all segments except the last one segment. Segments 2–15 with three annulations, segments 16–26 with two annulations, last five segments with one annulation (Fig. 3A). Pygidium as long as last three segments, with about 10 indentations.

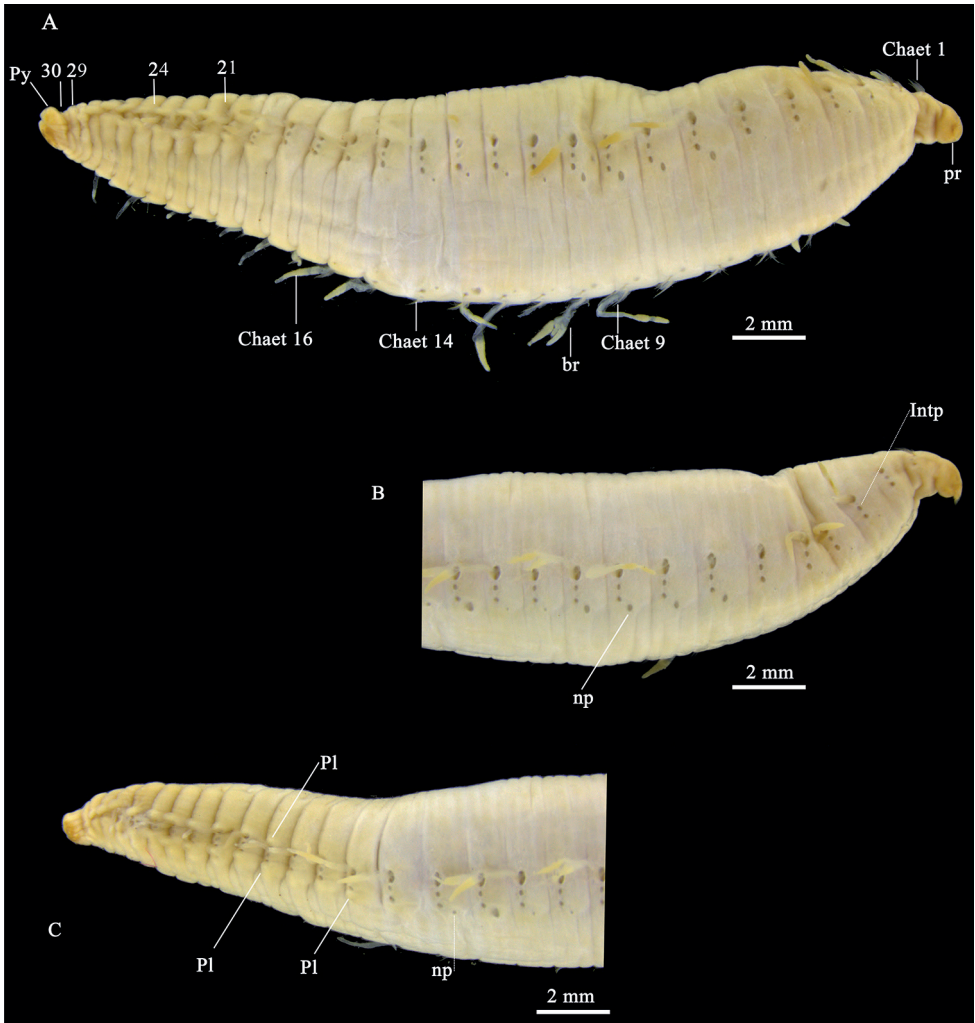


Figure 3. *Trivisia chinensis* Grube, 1866 (holotype, ZMB 0629) **A** complete specimen in lateral view **B** anterior part in lateral view **C** posterior part in lateral view. Abbreviations: pr, prostomium; nuO, nuchal organ; mo, mouth; br, branchiae; chaet, chaetiger; IntP, interramal papilla; Pl, parapodia lateral lappet; np, nephridial pores; Py, pygidium.

Remark. The original description of *Trivisia chinensis* was not detailed. Thus, it was seldom compared with the other *Trivisia* species. According to the original description, *T. chinensis* has one trifid branchia, while most other *Trivisia* species have cirriform branchiae, except for *T. arborifera* Fauvel, 1932 from Indian Ocean and *T. filamentosa* León-González, 1998 from California which were reported with strongly branched branchiae. Some researchers accepted that the trifid branchia might make *T. chinensis* a distinctive species (Kükenthal 1887; Fauvel 1932), while according to our observation, the trifid branchia is also present in a specimen of *Trivisia* cf. *pupa* from the Yellow Sea

(unpublished data), which is supposed to have only cirriform branchiae. Therefore, the presence of one bifid or trifid branchia might actually be an intraspecific variation and should not be regarded as a valid characteristic in distinguishing *Travisia* species.

Travisia chinensis (30 segments, 29 chaetigers) resembles the following six species in have a similar number of segments and chaetigers (29–31): *Travisia amadoi* Elías et al., 2003, *Travisia olens* Ehlers, 1897, *Travisia araciae* Rizzo & Salazar-Vallejo, 2020, *Travisia hobsonae* Santos, 1977, *Travisia brevis* Moore, 1923, and *Travisia forbesii intermedia* Annenkova, 1937.

Travisia chinensis differs in the start of parapodial lappets (chaetiger 19) from *T. amadoi* (chaetiger 12), *T. araciae* (chaetiger 13), and *T. hobsonae* (chaetiger 1). *Travisia chinensis* differs from *T. brevis* in the following morphological characters: the number of branchiae (>25 pairs in *T. chinensis* vs 22 pairs in *T. brevis*); the shape of the prostomium (conical vs short blunt cone), and segments without parapodial lappets (last four segments vs last two segments).

Travisia forbesii intermedia and *T. olens* are not easily distinguished from *T. chinensis* more by lack of information. According to the original description, the former two lack exact data on the position of parapodial lappets, and a re-examination of the types of the two species is needed.

Type locality. According to Salazar-Vallejo et al. (2014), the type locality was probably the coastal waters of Qingdao. Dauvin and Bellan (1994) also stated that the holotype was from the North-western Pacific. Until now, we have not found any other specimens of *T. chinensis* in the seas of China, based on the materials of MBM.

***Travisia amoyanus* sp. nov.**

<https://zoobank.org/0211D399-6360-4932-9AB6-993260F8A26C>
Figs 4A–O, 5A–H

Travisia chinensis Monro, 1934: 374, fig. 8.

Material examined. Holotype. Complete MBM287243: Xiamen, China, 24°27.14'N, 118°11.19'E, 24 July 2021, ethanol. **Paratypes.** One complete (MBM193597), two complete (MBM286089), Xiamen, China, 24°35.04'N, 118°10.09'E, 19 April 1963, formalin. Five complete (MBM286088), Xiamen, China, 24°26.30'N, 118°10.11'E, 2014–2016, formalin. Four complete (MBM286075), Xiamen, China, 24°30.49'N, 118°16.30'E, 2014–2016, formalin. One complete (MBM287244), one complete (MBM287245), one complete (MBM287248), one complete (MBM287249), one complete (MBM287250), same data as the holotype, ethanol one complete (MBM287246), one complete (MBM287247), same data as the holotype, formalin.

Diagnosis. Prostomium pointed, conical. Body with 34 or 35 segments and 33 or 34 chaetigers. Branchiae cirriform from chaetiger 2 to chaetiger 28–32. Larger triangular lateral parapodia lobes or lappets well developed from chaetiger 15. Pygidium with a larger ventral triangular cirrus and about six lateral cirri around.

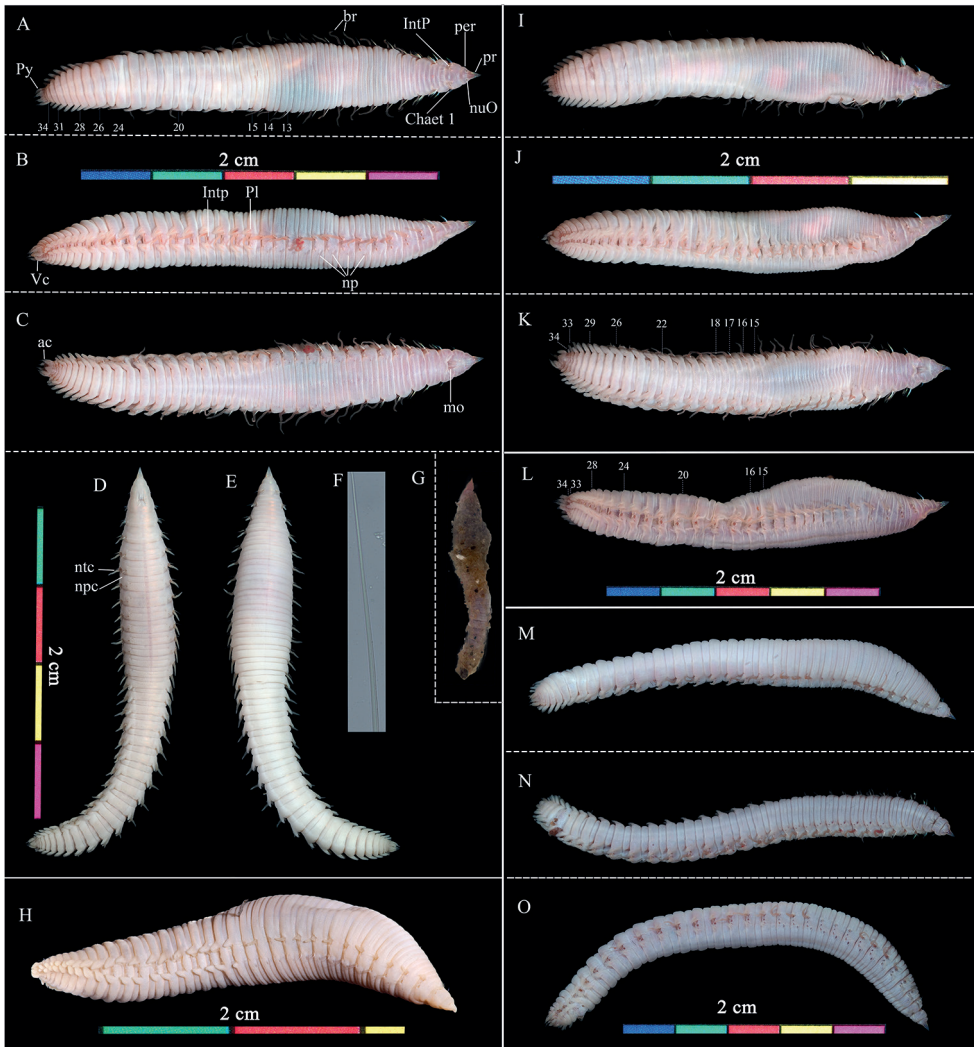


Figure 4. *Trivisia amoyanus* sp. nov. **A–F** holotype (MBM287243) **H–O** paratypes (**H** MBM193597; **I–K** MBM287249; **L** MBM287248; **M–O** MBM287244) **A–C** living specimen in dorsal, lateral, and ventral view, respectively **D** fixed specimen in ventral view **E** same, in dorsal view **F** detail of capillary chaeta **G** tube **H** fixed specimen in lateral view **I–K** alive, in dorsal, lateral, and ventral views, respectively **L** alive, in lateral view **M–O** alive, dorsal, lateral, and ventral views, respectively. Abbreviations: pr, prostomium; per, peristomium; nuO, nuchal organ; mo, mouth; br, branchiae; chaet, chaetiger; IntP, interramal papilla; Pl, parapodia lateral lappet; np, nephridial pores; ntc, notochaetae; npc, neurochaetae; Py, pygidium; ac, anal cirri; Vc, Pygidial ventralmost cirrus.

Description. Preserved specimens white to grey, and living specimens reddish (Fig. 4D, F, G). Body length 18.0–45.0 mm (holotype, 30.0 mm) and 2.0–5.6 (holotype, 3.0 mm) width at widest segment. Prostomium conical, distally pointed. Eyes and prostomial processes absent (Fig. 4A–C, H–N). Peristomium with a pair of nuchal

organs (Fig. 4A, H, L). Mouth opening between chaetiger 1 and 2 (Fig. 4C, D, M). Body surface with fine papillae except the distal part of prostomium and branchiae (Fig. 4A–E, G–M).

Branchiae simple, cirriform with 27–31 pairs (holotype: 31 pairs on the left side, 30 pairs on the right side), from chaetigers 2 to chaetigers 28–32. In preserved specimens, branchiae length nearly uniform except for chaetiger 2 and about the last 10 chaetigers.

Body with 34 or 35 segments and corresponding 33 or 34 chaetigers. All chaetae capillary, with a narrow wing (limbate) at one side (Fig. 5 F).

Parapodia biramous, without pre- and postchaetal lobes, notopodial and neuropodial chaetal rami well separated except the posterior end. Interramal pores or lateral sense organs between notopodial and neuropodial chaetal rami from chaetiger 1 to every succeeding segment, except that occasionally hidden or absent on segment 34 or 35.

Prominent parapodia lateral lappets from chaetiger 15, well developed. Notopodial lobes (lappets) above the bundle of notochaetae. Neuropodial lobes below neurochaetae but missing on last one or two chaetigers. Notopodial and neuropodial lobes triangular except toward the anus, where they become longer and more cylindrical.

Nephridial pores present on chaetigers 3–14, anterior and posterior pores smaller than middle ones. First chaetiger biannulate, chaetigers 2–19 triannulate ventrally and dorsally, chaetigers 20–27 biannulate, 28–34 (35) segments uniannulate. Posterior margin of the last seven or eight segments with more or less obvious crenulations dorsally. Midventral groove absent, if have, present from last four segments (Fig. 4D).

Pygidium as long as about last three segments with a larger triangular mid-ventral process and six lobes. Inner anus with many cirriform papillae.

MG staining pattern. The body surface of specimens has a distinctive staining pattern: the posterior part of the first and the third ring of chaetigers 2–14 show significant staining; from chaetigers 15 to the posterior end the body is deeply stained (Fig. 5).

Variations. Morphological comparison of 23 specimens is provided (Suppl. material 1: table S5). Maximum length ranged from 1.8 to 4.5 mm. Branchiae distribution is frequently asymmetrical on both sides of the body, most specimens have a narrow range ($N = \pm 1$), except MBM286089-spec.3 (28 pairs on left, 31 pairs on right).

The maximum number of branchiae ranged from 27–31 pairs among individuals (Fig. 6). Eighteen specimens had 34 segments, and five specimens had 35 segments. Fourteen specimens had 34 chaetigers, and nine specimens had 33 chaetigers.

Body subfusiform in preserved specimens, swollen medially (Fig. 5D, E), while in living specimens, the segments are nearly equal between the prostomium and the anus, usually swollen at the anterior part of the body because of the worm's peristalsis (Fig. 5A–C, H–N).

Type locality. Coastal waters of Xiamen, China.

Etymology. The specific epithet, *amoyanus*, refers to the type locality of Amoy, the pronunciation of local dialect of Xiamen, a coastal city in Fujian Province, China.

Biology. *Travisia amoyanus* inhabits sandy sediments from the intertidal to the subtidal (1–2 m depth). It can be strongly malodorous, and the body surface is covered by a viscous mucus tube with sand grains adhering (Fig. 5F).

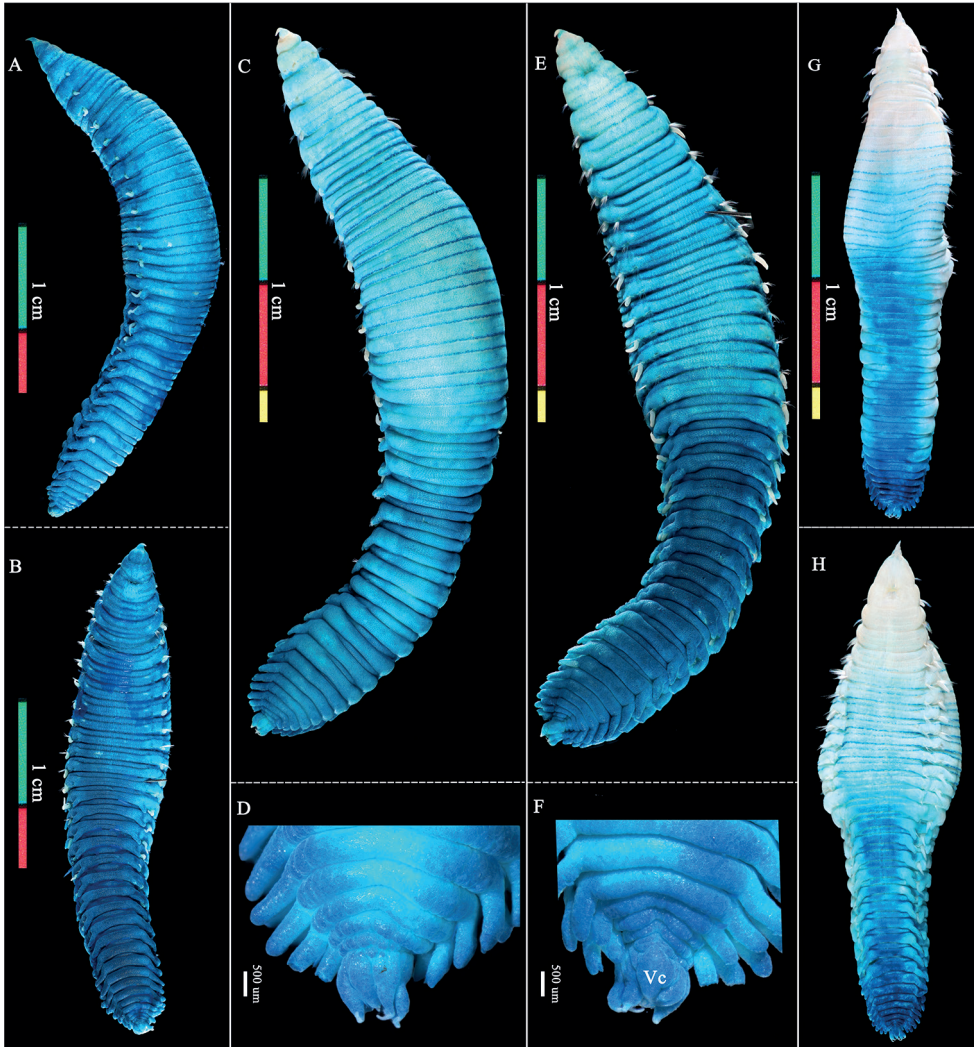


Figure 5. *Travisia amoyanus* sp. nov., stained with methyl green. Paratypes (**A, B** MBM286089-spec.1; **C–F** MBM286089-spec.2) and non-type specimen (**G, H** MBM286088-Spec.1) **A, C, G** whole body in dorsal view **B, E, H** whole body in ventral view **D** posterior end in dorsal view **F** posterior region in ventral view Abbreviations: Vc, Pygidial ventralmost cirrus.

Remarks. *Travisia amoyanus* sp. nov. clearly differs from *T. chinensis* in the total number of segments and chaetigers, the beginning of parapodial lappets, and the shape of pygidium. In *T. amoyanus* (34 or 35 segments, 33 or 34 chaetigers), parapodial lappets start from chaetiger 15 and the pygidium with a large triangular mid-ventral process, whereas in *T. chinensis* (30 segments, 29 chaetigers), neuropodial lappets start from chaetiger 16 and notopodial lappets from chaetiger 19 and the pygidium bears no large triangular mid-ventral lobe.

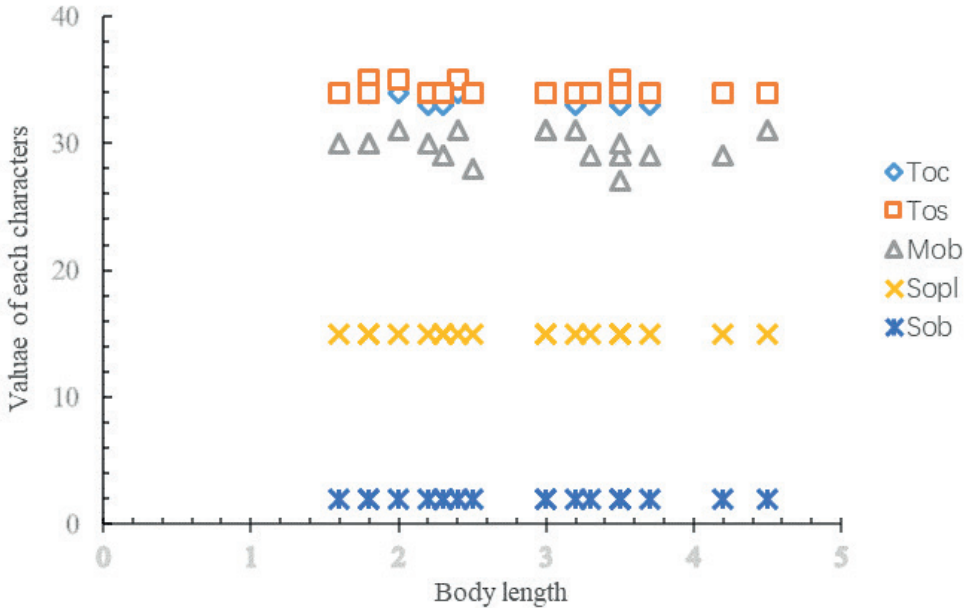


Figure 6. Scatter diagram illustrating variability of five key characters with the body length. Abbreviations: Toc, total number of chaetigers; Tos, total number of segments; Mob, Maximum of branchiae; Sopl, start of parapodial lappets on chaetiger; Sob, start of branchiae.

Travisia amoyanus sp. nov. resembles several species in having a similar number of segments and chaetigers (35–36), such as *T. concinna* (Kinberg, 1866) (35 segments and chaetigers) from South Africa, *T. arborifera* (36 chaetigers) from Indian Ocean, and *T. filamentosa* (35–36 segments, 35 chaetigers) from California. However, *T. amoyanus* sp. nov. can be distinguished from *T. arborifera* and *T. filamentosa* by having cirriform branchiae, the latter two species have branched branchiae. *Travisia amoyanus* sp. nov. differs still from *T. concinna* in having 31 (vs 33) pairs of branchiae, and parapodial lappets starting from chaetiger 15 (vs 17 or 18). In addition, *T. amoyanus* sp. nov. has 31 pairs of branchiae and parapodial lappets from chaetigers 15, while *T. fusiformis* Kudenov, 1975 has 34 pairs of branchiae, notopodial lappets from chaetigers 2 and neuropodial lappets from chaetiger 17.

Travisia amoyanus sp. nov. is much closer to *T. japonica* Fujiwara, 1933 from Japan and *T. gigas* Hartman, 1938 from California in the starting segments of parapodial lappets. But, the new species and *T. gigas* can be distinguished in the following aspects: (1) 34 or 35 segments and 33 or 34 chaetigers in *T. amoyanus*, 46 segments and 46 chaetigers in *T. gigas*; (2) 31 pairs of branchiae in *T. amoyanus*, 44 pairs in *T. gigas*; (3) pygidium with a large triangular mid-ventral process and six cylindrical lobes in *T. amoyanus*, without triangular mid-ventral process in *T. gigas*.

Travisia japonica is considered to have a wide-ranging body segment count (32–43 segments), and the species has been recorded from a wide range of geographic regions

(Dauvin and Bellan 1994). However, Fujiwara (1933) stated explicitly that *T. japonica* has a relatively fixed number of segments (39, seldom 40) based on examination of a considerable number of specimens. Therefore, in this comparison, we used the original description data and suggest that records of *T. japonica* from non-Japanese areas need to be re-evaluated and might represent potentially undescribed species.

Travisia amoyanus sp. nov. is distinguishable from *T. japonica* by the following characters: the number of segments (34 or 35 in *T. amoyanus* vs 39 or 40 in *T. japonica*), the number of chaetigers (33 or 34 in *T. amoyanus* vs 39 or 40 in *T. japonica*), the number of branchiae (27–31 pairs in *T. amoyanus* vs 25 pairs in *T. japonica*), the distribution of interramal pores (1–33 or 34 chaetigers in *T. amoyanus* vs 1–29 chaetigers in *T. japonica*), the number of nephridial pores (12 pairs in *T. amoyanus* vs 11 pairs in *T. japonica*). In fact, the difference between these two species also had been noticed by Monro (1934: p374): “*T. japonica* Fujiwara is close to *T. chinensis* (regarded herein as *T. amoyanus*), but has 39 to 40 chaetigers”.

Distribution. Currently only found from Xiamen coastal waters.

Acknowledgements

We deeply thank Dr Birger Neuhaus and Lukas Kirschey for providing us with the photograph and translating the original description of *Travisia chinensis*. We thank Julio Parapar, Naoto Jimi, James A. Blake, Nancy J. Maciolek, and Sergio I. Salazar-Vallejo for providing valuable references during this study. Many thanks to Dandan Zhong, Zeyang Lin, Yinlin Shi, Shen Zhong, and Quan Ma for their help with the collection of samples. We are particularly grateful to Alexandra Rizzo, one anonymous reviewer, and Chris Glasby and Robert Forsyth, ZooKeys editors for their constructive comments on the manuscript.

This research was supported by the China Postdoctoral Science Foundation (no. 2021M691866), the Biological Resources Program, Chinese Academy of Sciences (no. KFJBRP-017-46), the MEL Outstanding Postdoctoral Scholarship, and the Undergraduate Innovation and Entrepreneurship Training Programs at Xiamen University (no. 202110384077).

References

- Annenkova NP (1937) Polychaete fauna of the northern part of the Japan Sea. Issledovaniya fauny morei. Zoologicheskii Institut Akademii Nauk USSR Explorations des Mers de l'URSS 23: 139–216. [In Russian]
- Augener H (1922) Revision der australischen Polychaeten-Typen von Kinberg. Arkiv för Zoologi 14(8): 1–42. <https://doi.org/10.5962/bhl.part.7728>
- Blake JA, Maciolek NJ (2020) Traviidae Hartmann-Schröder, 1971, new family status. In: Blake JA, Maciolek NJ (Eds) Handbook of Zoology. Annelida. Volume 2: Pleistoannelida, Sedentaria II. Walter de Gruyter, Berlin, 302–311. <https://doi.org/10.1515/9783110291681-009>

- Dauvin JC, Bellan G (1994) Systematics, ecology and biogeographical relationships in the family Traviinae (Polychaeta, Opheliidae). *Mémoires du Muséum National d'Histoire Naturelle* 162: 169–184.
- Fauvel P (1932) Annelida Polychaeta of the Indian Museum. *Calcutta Memoirs of the Indian Museum* 12(1): 1–262.
- Fujiwara T (1933) On a new species of Japanese Polychaeta, *Travisia japonica* sp. nov. *Journal of Science of the Hiroshima University, Series B, Division 1 (Zoology)* 2: 91–103.
- Glover A, Dahlgren T, Wiklund H, Mohrbeck I, Smith C (2016) An end-to-end DNA taxonomy methodology for benthic biodiversity survey in the Clarion-Clipperton Zone, Central Pacific Abyss. *Journal of Marine Science and Engineering* 4(1): e2. <https://doi.org/10.3390/jmse4010002>
- Grube AE (1869) Familie der Opheliaceen. *Schlesische gesellschaft für vaterlandische kultur Breslau Jahresbericht* 46: 59–68.
- Hartman O (1938) Descriptions of new species and new generic records of polychaetous annelids from California of the families Glyceridae, Eunicidae, Staurotereidae and Opheliidae. *University of California Publications in Zoology* 43: 93–111.
- Hartman O (1969) Atlas of the sedentary polychaetous annelids from California. Allan Hancock Foundation, University of Southern California, Los Angeles, 812 pp.
- Johnston G (1840) *Miscellanea Zoologica*. British annelids. *Annals and Magazine for Natural History London* 1(4): 368–375. <https://doi.org/10.1080/00222934009512507>
- Kalyaanamoorthy S, Minh BQ, Wong TKF, von Haeseler A, Jermini LS (2017) Model Finder: Fast model selection for accurate phylogenetic estimates. *Nature Methods* 14(6): 587–589. <https://doi.org/10.1038/nmeth.4285>
- Katoh K, Rozewicki J, Yamada KD (2019) MAFFT online service: Multiple sequence alignment, interactive sequence choice and visualization. *Briefings in Bioinformatics* 20(4): 1160–1166. <https://doi.org/10.1093/bib/bbx108>
- Kobayashi G, Kojima S (2021) *Travisia sanrikuensis*, a new species of Traviidae (Annelida) from the Lower Bathyal Zone of the Northwestern Pacific. *Species Diversity : An International Journal for Taxonomy, Systematics, Speciation, Biogeography, and Life History Research of Animals* 26(2): 131–136. <https://doi.org/10.12782/specdiv.26.131>
- Kudenov JD (1975) Sedentary polychaetes from the Gulf of California. *Journal of Natural History* 9(2): 205–231. <https://doi.org/10.1080/00222937500770131>
- Kükenthal W (1887) Die Opheliaceen der Expedition der “Vettore Pisani”. *Jenaische Zeitschrift für Naturwissenschaft* 21: 361–373. <https://www.biodiversitylibrary.org/page/8612269>
- Kumar S, Stecher G, Li M, Knyaz C, Tamura K (2018) MEGA X: Molecular Evolutionary Genetics Analysis across computing platforms. *Molecular Biology and Evolution* 35(6): 1547–1549. <https://doi.org/10.1093/molbev/msy096>
- Salazar-Vallejo SI, Carrera-Parra LF, Muir AI, de León-González JA, Piotrowski C, Sato M (2014) Polychaete species (Annelida) described from the Philippine and China Seas. *Zootaxa* 3842(1): 1–68. <https://doi.org/10.11646/zootaxa.3842.1.1>
- Law CJ, Dorgan KM, Rouse GW (2014) Relating divergence in polychaete musculature to different burrowing behaviors: A study using Opheliidae (Annelida). *Journal of Morphology* 42: 548–571. <https://doi.org/10.1002/jmor.20237>

- Maciolek NJ, Blake JA (2006) Opheliidae (Polychaeta) collected by the R/V Hero and the USNS Eltanin cruises from the Southern Ocean and South America. *Scientia Marina* 70(S3): 101–113. <https://doi.org/10.3989/scimar.2006.70s3101>
- Maekawa N, Hayashi I (1999) Taxonomic study on the genus *Onuphis* (Polychaeta, Onuphidae) from Japan and adjacent seas, with descriptions of six new species. *Bulletin of the National Science Museum, Tokyo, Series A* 25: 163–214.
- Monro CCA (1934) On a collection of Polychaeta from the coast of China. *Annals and Magazine of Natural History (Series 10)* 13: 353–380. <https://doi.org/10.1080/00222933408654824>
- Moore JP (1923) The polychaetous annelids dredged by the U.S.S. “Albatross” off the coast of southern California in 1904. IV. Spionidaeto Sabellariidae. *Proceedings. Academy of Natural Sciences of Philadelphia* 75: 179–259.
- Nguyen LT, Schmidt HA, von Haeseler A, Minh BQ (2015) IQ-TREE: A fast and effective stochastic algorithm for estimating maximum-likelihood phylogenies. *Molecular Biology and Evolution* 32(1): 268–274. <https://doi.org/10.1093/molbev/msu300>
- Read G, Fauchald K [Eds.] (2022) World Polychaeta Database. *Travisia* Johnston, 1840. World Register of Marine Species. <https://www.marinespecies.org/aphia.php?p=taxdetails&id=129417> [Accessed on 2022-06-26]
- Rizzo A, Salazar-Vallejo SI (2020) A new species of *Travisia* (Annelida, Traviidae) from Campos Basin, Brazil. *Studies on Neotropical Fauna and Environment* 56(1): 1–9. <https://doi.org/10.1080/01650521.2020.1752512>
- Ronquist F, Teslenko M, van der Mark P, Ayres D, Darling A, Höhna S, Larget B, Liu L, Suchard M, Huelsenbeck J (2012) MrBayes 3.2: Efficient Bayesian phylogenetic inference and model choice across a large model space. *Systematic Biology* 61(3): 539–542. <https://doi.org/10.1093/sysbio/sys029>
- Talavera G, Castresana J (2007) Improvement of phylogenies after removing divergent and ambiguously aligned blocks from protein sequence alignments. *Systematic Biology* 56(4): 564–577. <https://doi.org/10.1080/10635150701472164>
- Wiklund H, Neal L, Glover AG, Drennan R, Muriel R, Dahlgren TG (2019) Abyssal fauna of polymetallic nodule exploration areas, eastern Clarion-Clipperton Zone, central Pacific Ocean: Annelida: Capitellidae, Opheliidae, Scalibregmatidae, and Traviidae. *ZooKeys* 883: 1–82. <https://doi.org/10.3897/zookeys.883.36193>
- Yang D, Sun R (1988) Polychaetous annelids commonly seen from Chinese waters. China Agriculture Press, Beijing, 352 pp. [in Chinese]
- Zhang D, Gao F, Jakovlić I, Zou H, Zhang J, Li WX, Wang GT (2020) PhyloSuite: An integrated and scalable desktop platform for streamlined molecular sequence data management and evolutionary phylogenetics studies. *Molecular Ecology Resources* 20(1): 348–355. <https://doi.org/10.1111/1755-0998.13096>

Supplementary material 1

Tables

Authors: Deyuan Yang, Xuwen Wu, Zhi Wang, Xiaoyu Zhao, Jiangshiou Hwang, Lizhe Cai

Data type: Morphological, phylogenetic.

Explanation note: **Tables: table S1:** Sampling information and museum registration numbers of *Travisia amoyanus* sp. nov.; **table S2:** Primers and annealing temperatures used in this study; **table S3:** Information on taxa and sequences used in phylogenetic analyses; **table S4:** Pairwise distances in 18S fragment within and among species of *Travisia* based on Kimura 2-parameter (the lower-left corner) and p-distance model (the upper right corner); **table S5:** Main morphological characters of studied specimens of *Travisia amoyanus* sp. nov.

Copyright notice: This dataset is made available under the Open Database License (<http://opendatacommons.org/licenses/odbl/1.0/>). The Open Database License (ODbL) is a license agreement intended to allow users to freely share, modify, and use this Dataset while maintaining this same freedom for others, provided that the original source and author(s) are credited.

Link: <https://doi.org/10.3897/zookeys.1128.90020.suppl1>

Supplementary material 2

ML tree based on 16S and 18S

Authors: Deyuan Yang, Xuwen Wu, Zhi Wang, Xiaoyu Zhao, Jiangshiou Hwang, Lizhe Cai

Data type: Phylogenetic.

Copyright notice: This dataset is made available under the Open Database License (<http://opendatacommons.org/licenses/odbl/1.0/>). The Open Database License (ODbL) is a license agreement intended to allow users to freely share, modify, and use this Dataset while maintaining this same freedom for others, provided that the original source and author(s) are credited.

Link: <https://doi.org/10.3897/zookeys.1128.90020.suppl2>

Palearctic seed beetle *Bruchus affinis* (Coleoptera, Chrysomelidae, Bruchinae) new to North America, arrival, distribution, and autecology

Hume B. Douglas¹, Stéphane Dumont², Karine Savard¹,
Graham S. Thurston³, Marilyn H. S. Light⁴

1 Canadian National Collection of Insects, Arachnids and Nematodes, Agriculture and Agri-Food Canada, Ottawa, ON, K1A 0C6, Canada **2** Département de biologie et de biotechnologies, Collège Ahuntsic, 9155 rue Saint-Hubert, Montréal, H2M 1Y8, QC, Canada **3** Canadian Food Inspection Agency, Ottawa Plant Laboratory, Building 18, 960 Carling Avenue, Ottawa, ON, K1A 0Y9, Canada **4** 174, rue Jolicoeur, Gatineau, QC J8Z 1C9, Canada

Corresponding author: Hume B. Douglas (Hume.Douglas@agr.gc.ca)

Academic editor: Ron Beenen | Received 6 July 2022 | Accepted 13 October 2022 | Published 4 November 2022

<https://zoobank.org/6BCF63CD-0179-4BA9-AB9B-0248ADE3F790>

Citation: Douglas HB, Dumont S, Savard K, Thurston GS, Light MHS (2022) Palearctic seed beetle *Bruchus affinis* (Coleoptera, Chrysomelidae, Bruchinae) new to North America, arrival, distribution, and autecology. ZooKeys 1128: 19–31. <https://doi.org/10.3897/zookeys.1128.90016>

Abstract

First North American records are presented for *Bruchus affinis* Frölich, 1799 (Coleoptera, Chrysomelidae, Bruchinae), as confirmed by morphology from multiple sites in Canada: British Columbia, Ontario, and Québec. Diagnostic information is presented for *B. affinis* in North America. This insect is expected to reduce plant reproductive output in infested *Lathyrus latifolius* L., *Lathyrus sylvestris* L., and other potential *Lathyrus* (Fabaceae) hosts. Impacts on broad bean (*Vicia faba* L.) production are expected to be small. Potential reproductive impact on native North American *Lathyrus* species remains unknown. The United States of America and Canada are now known to be home to 69–79 species of adventive Chrysomelidae including 16–18 Bruchinae. We have found two dead, teneral *B. affinis* individuals inside *Lathyrus* seeds imported from Europe, and we hypothesise that this species was introduced to Canada from Europe via seeds for planting sometime before 2007. At our study sites, *Lathyrus* flowering began in mid June followed by oviposition in late June with first adults emerging in late August, requiring about 60 days from egg to adult stage. *Dinarmus basalis* (Rodani, 1877) (Hymenoptera, Pteromalidae) was newly recorded as parasitoid of *Bruchus affinis* in Canada, and caused about 10% mortality in *B. affinis* at our sites.

Keywords

Invasive alien species, biological control

Introduction

The univoltine seed beetle *Bruchus affinis* Frölich, 1799 is native to most countries of the western Palearctic Region (Anton 2010). It has been found there as a seed predator of several species of *Lathyrus* and to some extent *Vicia faba* L. (broadbeans) (Bashar et al. 1987, 1990; Delobel and Delobel 2006). *Bruchus affinis* adults use pollen and nectar of various *Lathyrus* species for food but require feeding on pollen of *L. latifolius* L. or *L. sylvestris* L. to terminate sexual diapause and commence oviposition on newly formed pods (Bashar et al. 1987, 1990). This species has not been observed to infest dried seeds (requirement for immature seeds is better documented for congener *Bruchus pisorum* Linnaeus, 1758; e.g. Howe and Currie 1964). So, although it damages seeds, *B. affinis* is not a pest of stored products.

Lathyrus latifolius (Fabaceae) is a perennial flowering vine introduced to North American gardens perhaps as early as the 1700s. It is now established as an ornamental and weedy species in Canada and USA. *Lathyrus sylvestris* was introduced sometime before 1827 when seeds of both plants were listed in a Canadian nursery catalogue (Woodhead 1998). This study began in July 2020, when ML found the beetles (Figs 1, 2) emerging from seeds from the first pods of a solitary cultivated *L. latifolius* in Gatineau, Québec, Canada. This plant was started from seed in 2019 in a garden that otherwise did not contain *Lathyrus* plants. In 2021, ML found dead teneral *Bruchus affinis* beetles within seeds inside a commercial packet of *L. latifolius* seeds imported from Europe. We aimed to investigate the range and invasion history of *Bruchus affinis* first in that garden, and then more broadly in Canada.

We also examined the phenology and behaviour of *B. affinis* with *L. latifolius* and *L. sylvestris* in two Gatineau localities. This was to learn how *B. affinis* interacts with plant hosts in Canada. In particular, we examined the timing of flowering and the *B. affinis* egg to adult interval. We asked: at what date does *B. affinis* first appear on the hosts, mate, and begin oviposition? We also investigated the period required for eggs to hatch and for adult beetles to emerge from infested seeds.

Methods

The first pods of *L. latifolius* to ripen in 2020 in the Gatineau garden represent the first infestation cohort for the site and plant (hereafter the index plant). Fifty-four seeds were harvested from that plant and dried at room temperature. Over the next few weeks, 18 beetles emerged, with a total seed infestation rate of 33%. Beetles were submitted to HD via the Agriculture and Agri-Food Canada Entomology National Identification Service. All specimens are deposited at the Canadian National Collection of Insects, Arachnids, and Nematodes (CNCI), 960 Carling Ave., Ottawa, Canada.

In 2021, all authors searched for additional populations of Bruchinae associated with *Lathyrus* spp. in Canada, examining growing plants, insect collections, and on-

line photograph-sharing websites for specimens and observations. HD also contacted biologists with the Canadian Food Inspection Agency's Plant Health Survey Unit to search *Lathyrus* plants for *Bruchus* beetles in other parts of Canada. Stephen Paiero checked the University of Guelph insect collection (Guelph, Ontario) for additional specimens of *B. affinis*, but found none. No comprehensive field survey has been conducted to determine the full range of this species in North America.

Beetle behaviour study locations were in Gatineau QC, a private garden, with only the *L. latifolius* index plant (45.464, -75.761). Additional beetles were observed in nearby roadsides, with eight patches of *L. sylvestris*, 45.4562, -75.7638 (2 m diameter); 45.4571, -75.7672 (3 m diameter); 45.4551, -75.7612 (3 m diameter); 45.455, -75.761 (2 m diameter); 45.4546, -75.7604 (5 m diameter); 45.4544, -75.7601 (1 m diameter); 45.4542, -75.7598 (6 m diameter); and 45.454, -75.7594 (2 m diameter). Historical weather data for Ottawa International Airport (Ontario, Canada) was obtained from Environment (Canada 2022).

Plant material

Behavioural observations began with daily monitoring of the garden *L. latifolius* plant by ML for flowering and beetle activity from June through September 2021. First inflorescences having flowers open were tagged and then tracked. The first available pods were monitored for oviposition. Tagged pods remained on the plant until mature when they were harvested and permitted to dehisce. All remaining closed pods were opened manually two months after harvest. Seed infestation and parasitoid presence were assessed for all seeds from all tagged pods. Herbarium vouchers from both *Lathyrus* species were collected, for deposition in herbaria (CAN/DAO) (Fig. 3A, B).

Adult beetles were hand collected (i.e. not using a net) from *L. sylvestris* at behavioural study sites by ML in early morning. Specimens were preserved in 95% ethanol with several voucher specimens mounted. Stem tagging was not possible at the *L. sylvestris* roadside localities. So, randomly selected stems were used for study. Pods at varying developmental stages were examined and/or collected on several mornings from June to October. All seeds retained for rearing were stored at room temperature and examined daily for presence of emergent beetles. Maturing green to yellow seeds were opened within 24 hours of collection using a scalpel to view their contents (Fig. 5B). Mature brown seed samples, that floated when placed in water, were cracked open using a vacuum vise with exposed steel jaws. Seeds that sank in water and could not be cracked open were scored as uninfested. Additional pods were kept at 20 °C until January 2022 for further emergence of beetles or parasitoids.

Field photography was conducted by ML using an Olympus 12.5× Super Wide Optical Zoom camera. Macro photography was done using an Olympus EM5 MkII with macro lens according to subject and an Olympus T10 Ring Flash or an Olympus RFII Ring Flash for larger subjects. An Epson Perfection Scanner V550 Photo was used to document *Lathyrus* stems and herbarium specimens.

Results and discussion

Distributional records

The external morphology and male genitalia of Canadian specimens closely matched taxon concepts of *B. affinis* from Brandl (1981) and Borowiec (1988). A. Delobel, and L. Borowiec also confirmed our initial identifications based on submitted photographs. Specimens identified also matched Canadian National Collection specimens identified by Anton, Natterer, and Bottimer in morphology of the pronotum, male mesotibia, and aedeagus.

We found *B. affinis* at the following localities in **Canada: British Columbia:** Vancouver, 49.2162, -123.1713, 22.VI.2021, ex. *L. latifolius*, B. Spencer, 4 ex; **Québec:** Gatineau, 45.463, -75.765, reared from *L. latifolius* seeds from garden, M.H.S Light, 8 ex., CNC1053109 to CNC1053117; Gatineau, 5.IX.2021, M.H.S. Light; Wakefield, 45.6466, -75.9298, reared from *L. sylvestris* seeds of field edge patch, 15.VIII.2021, M.H.S. Light, 12 ex.; Gatineau, boul. Cité des Jeunes, 45.4544, -75.7601, mating on flowering *L. sylvestris* of roadside patch, 27.VI.2021, M.H.S. Light, 5 ex.; Gatineau, 45.4546, -75.7604, 27.VI.2021, M.H.S. Light, 18 ex.; Gatineau, 45.464, -75.761, reared from *L. latifolius* seeds from garden, 18.VIII.2021, M.H.S. Light, 1 ex.; Gatineau, 45.71, -75.7672, reared from *L. sylvestris* seeds of a roadside patch, 15.VIII.2021, M.H.S. Light, 5 ex.; Gatineau, 45.4551, -75.7612, reared from *L. sylvestris* seeds, 15.VIII.2021, M.H.S. Light, 8 ex.; Gatineau, 45.464, -75.761, infesting *L. latifolius* seeds; Gatineau QC, eggs on pod 25.VI.2021, eggs hatch 6.VII, beetles hatch 18.VIII.2021, M.H.S. Light, 8 ex.; Gatineau, 45.464, -75.761, Dead *Bruchus affinis* from two seeds in a sealed commercial package of 25 *L. latifolius* seeds, 18.21.III.2021, M.H.S. Light, 2 ex.; Farm Point, 45.6092, -75.8975, 23.VI.2021, ex. roadside *Lathyrus* flowers, H. Douglas, 6 ex.; Laval, Boisé Papineau (Près St. Martin) sur marguerite, 45.60229, -73.68096, 19.VI.2013, S. Dumont, 1 ex.; Laval, Boisé Papineau, 45.60704, -73.68082, battage spirée en fleurs, 21.V.2014, S. Dumont, 1 ex.; Laval, Boisé Papineau, 45.603, -73.681, sur *Lathyrus*, 29.VII.2014, S. Dumont, 3 ex.; Laval, Contrecoeur, Camp des Grèves 45.979, -73.182, sur *Lathyrus*, 7.VIII.2009, S. Dumont, 3 ex.; Laval, Berge Olivier-Charbonneau 45.698, -73.529, sur *L. latifolius*, 21.VII.2021, S. Dumont, 22 ex.; Montréal, Anjou, près Parc Roger Rousseau 45.617, -73.545, sur *L. latifolius*, 22.VII.2021, S. Dumont, 20 ex.; Notre-Dame-de-l'île-Perrot (Vaudreuil), 4.VII.2007, Battage *Lathyrus* sp., Pierre de Tonnancour, 2 ex.; Notre-Dame-de-l'île-Perrot (Vaudreuil), 20.V.2011, Battage *Caragana* sp., Pierre de Tonnancour, 1 ex.; Notre-Dame-de-l'île-Perrot (Vaudreuil), 14.VI.2011, Battage *Cirsium arvense*, Pierre de Tonnancour, 1 ex.; Notre-Dame-de-l'île-Perrot (Vaudreuil), 20.V.2011, Battage *Rubus odoratus*, Pierre de Tonnancour, 1 ex.; Notre-Dame-de-l'île-Perrot (Vaudreuil), 31.VIII.2011, Battage *Lathyrus latifolius*, Pierre de Tonnancour, 1 ex.; Notre-Dame-de-l'île-Perrot (45.3775, -73.9431), 7.VI.2019, fauchage, champ humide, Pierre de Tonnancour, 1 ex. **Ontario:** Ottawa, Hurdman Bridge, 45.418, -75.664, 3.VII.2021, ex. *Lathyrus* flowers, 8 ex., H. Douglas (field photographs: <https://www.inaturalist.org/observations/85903171>). An additional female *Bruchus*

specimen from near Québec City, seen only in internet photographs also has pronotal morphology matching *B. affinis* (<https://www.inaturalist.org/observations/38795458>), suggesting that *B. affinis* may also be established in that region.

We present evidence of 79 specimens from multiple sites in three provinces, separated by over 3500 km over 14 years, and rearing evidence of successful reproduction in nature. Together, these lead us to conclude that multiple populations of *B. affinis* are established in Canada.

Bruchus affinis can be distinguished from other North American *Bruchus* by the following combination of characters (adapted from key by Kingsolver 2004 using Borowiec 1988): antennae with three or four basal antennomeres red-brown; pronotum with lateral spines situated before pronotal midlength in anterodorsal view (Fig. 1D); male mid tibiae with two spines on ventral surface near apex (Fig. 2A); hind legs with femoral spine (Fig. 2B) extending apicad (not protruding ventrad beyond basal part of ventral surface, like Kingsolver 2004 fig. 257), mucro twice longer than lateral denticle (Fig. 2B); protibiae with some red-brown colouration on basal half, mesotibiae black (Fig. 1B). The broadly obtuse apex of the aedeagus is also unique among North American species (Fig. 2D). For rapid assessments, no other species has lateral spines situated on the anterior half of the pronotum and all black mesotibiae.

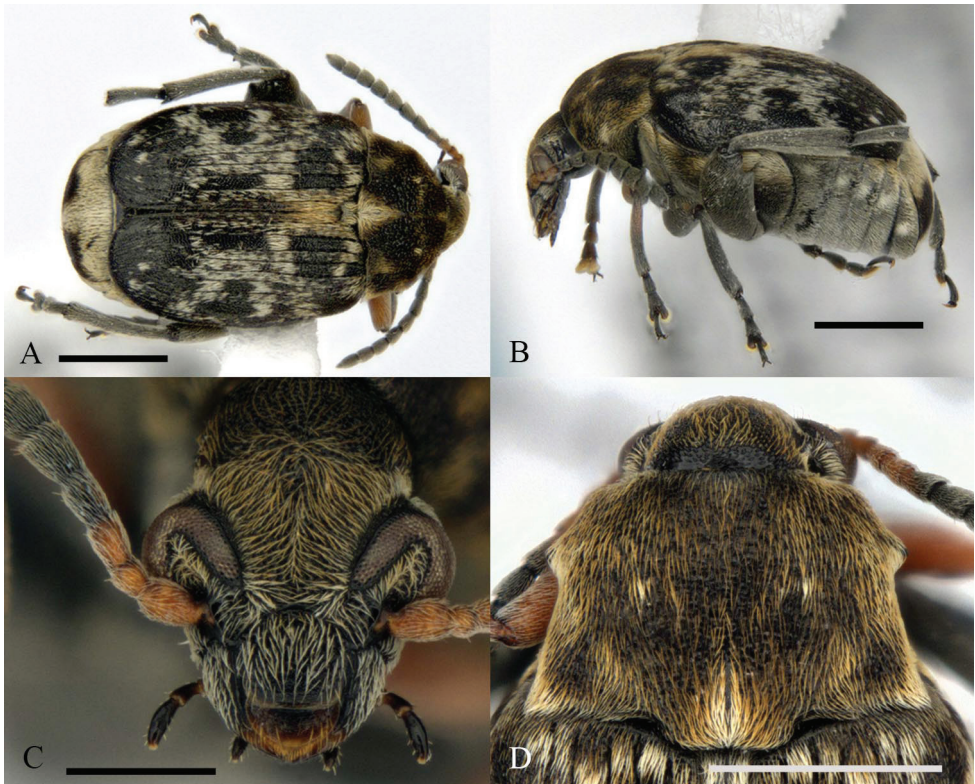


Figure 1. Morphology of a male of *Bruchus affinis* from Québec, Canada **A** dorsal habitus **B** lateral habitus **C** anterior view of head **D** dorsal view of pronotum. Scale bars: 1 mm (**A, B, D**); 0.5 mm (**C**).



Figure 2. Morphology of a male of *Bruchus affinis* from Québec, Canada **A** posterior view of mesotibia **B** lateral view of hind femur and tibia **C** pygidium **D** aedeagus. Scale bars: 0.5 mm.

Adventive species biology

It was initially unknown whether the infestation of the index plant could represent the first establishment of a new population of *B. affinis* in Canada. Alternatively, we thought this infestation could have spread from a pre-existing adventive population. Later we found nearby patches of *B. affinis*-infested *L. sylvestris*. Finding these specimens as well as others from elsewhere in Canada (many collected before 2020) is consistent with spread of a pre-established adventive population rather than establishment of a new adventive population in the garden of the index plant resulting from planting infested seeds there.

Our finding of *B. affinis* specimens within seeds of *L. latifolius* that were commercially imported from Europe suggests that import of infested seed is a likely pathway for the introduction of this species to Canada. The discovery of *B. affinis* in Québec, Ontario, and British Columbia over only 15 years is consistent with multiple introductions over several years since our earliest specimen collection date in 2007. This is also consistent with movement of infested seed rather than haphazard introduction

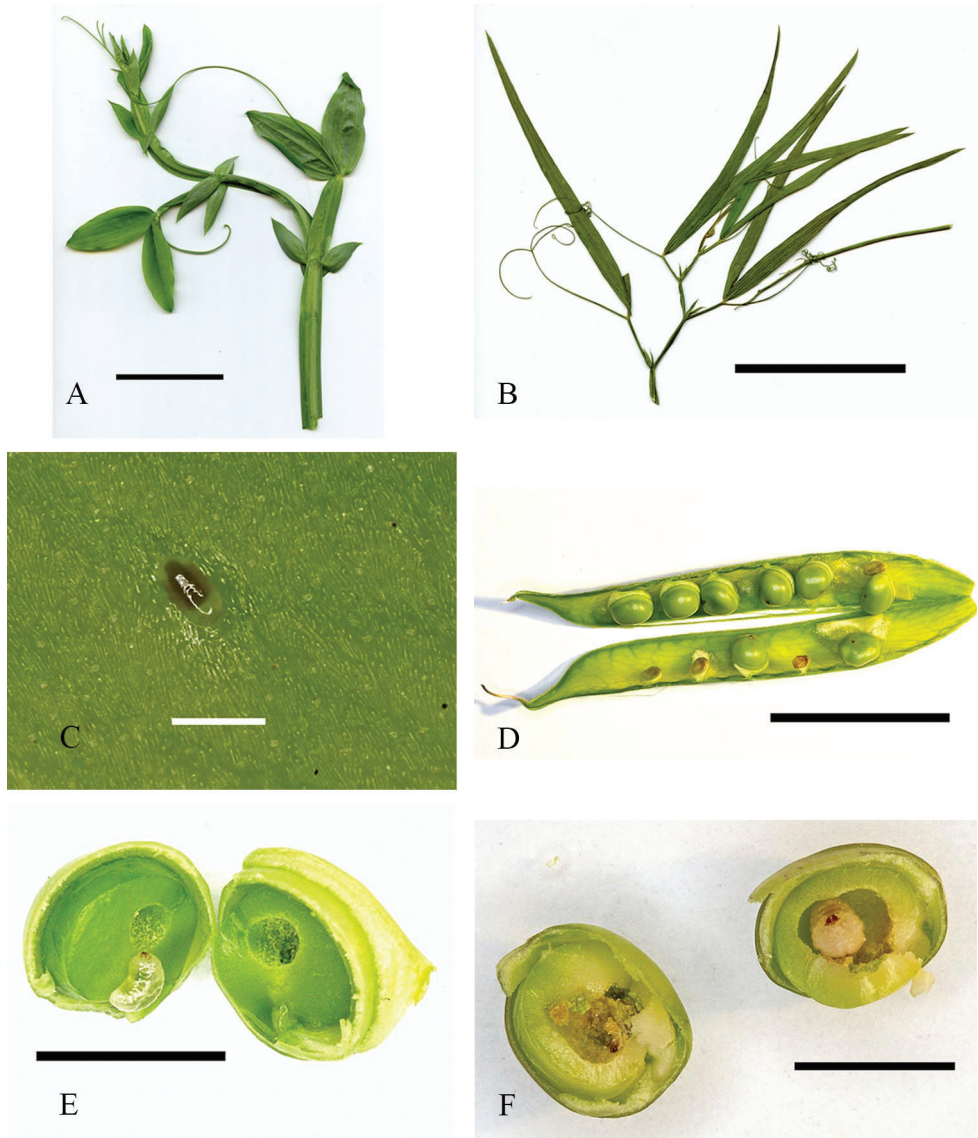


Figure 3. Morphology of *Lathyrus* spp. and *B. affinis* from Québec, Canada **A** apex of *L. latifolius* stem, garden plant (45.464, -75.561) **B** *L. sylvestris* stem, pressed (45.457, -75.767) **C** egg of *B. affinis* on outer pod wall of *L. sylvestris* **D** opened pod of *L. sylvestris* with seed entry holes of *B. affinis* larvae and white inner pod wall tissue developing beneath oviposition sites **E** infested seed of *L. sylvestris* with first instar larva of *B. affinis* **F** same with second instar larvae. Scale bars: 50 mm (**A**, **B**); 0.5 mm (**C**); 25 mm (**D**); 5 mm (**E**, **F**).

of adults (e.g. live beetles accidentally trapped in shipping containers). This evidence indicates that *B. affinis* was present in Canada for 15 or more years.

Bruchus affinis is known to infest seed pods of *L. grandiflorus*, Sibth. & Smith, *L. latifolius*, *L. sylvestris*, and *L. tuberosus* L. (Kergoat et al. 2007), all introduced species

to North America, and *Vicia* sp. (Fabres et al. 1986). Knowledge that *B. affinis* harms only seeds indicates that it will not harm the ability of these plants to grow or perform ornamental and erosion control functions. The moderate observed impact of *Bruchus* predation on their seeds may somewhat reduce these plants' ability to propagate. USA and Canada are also home to 29 named native *Lathyrus* species (USDA, 2022) plus other native Fabaceae. It remains unknown whether *B. affinis* can harm the reproductive outputs of these native species.

Bruchus affinis is also known to use *Vicia faba* as host in Europe (Segers et al. 2021), where it appears to act as a minor pest. In Europe, several species of *Bruchus* infest fava beans in the field. Of these, *B. rufimanus* is the most destructive (Segers et al. 2021). *Bruchus rufimanus* is listed as present in Canadian provinces producing fava beans (Bousquet et al. 2013); however, we were unable to find evidence that it causes economic damage to Canadian fava bean crops (e.g. Agrinova 2017). Together, these two findings may suggest that *B. affinis* is unlikely to cause substantial harm to fava beans in Canada.

This new North American record, added to the species counts by Douglas et al. (2021), indicate that Canada and the USA are together known to host 69–79 species of adventive Chrysomelidae, including 16–18 Bruchinae. Of these, 52–60 adventive Chrysomelidae are known from Canada, and 56–66 are known from the USA.

Behavioural observations

Flowering of both *Lathyrus* species began the week of June 15, 2021. The first *L. latifolius* pods developed by June 23 with the first eggs appearing on pods June 25: hatching began July 6. Mature, undehisced pods were collected from August 2 to August 12. Twenty-one *B. affinis* emerged from the 76 seeds (22 pods) on August 18–26 only: there were no further emergences. Seed infestation rate was 27.6%, averaging about one *B. affinis* larva per pod. Of the 21 tagged pods, 20 contained eggs (range 1–8 eggs per pod; median 3 eggs per pod). Overall, beetle reproduction on *L. latifolius* commenced as soon as flowers developed. Development of the new beetle generation was complete by the end of August, with about one quarter of seeds killed by beetles.

On *L. sylvestris*, 30 *B. affinis* adults were observed on June 27 on plants at five of eight roadside patches. Few *B. affinis* were seen after decrease in flower production in mid-July. The first 43 *B. affinis* individuals reared indoors emerged on August 14. Emergence of *B. affinis* collected from all eight patches on July 28 (104 pods/606 seeds) occurred mainly during two peak periods with warm weather: August 14–21 (preceded by five days of hot weather, 30–31 °C; indoor 27 °C), 68 beetles; and August 25–26 (daily max. 32.8–32.7 °C; indoor 27 °C; 92 beetles). Of all 215 beetles eclosed in August 2021, 160 were from these two periods. The infestation rate of the 606 seeds was 35% (13.5–73.5% across patches). If a pod had not yet dehisced, emerging beetles chewed exit holes to exit through the pod wall. The sound of chewing was audible outdoors from up to 2 m away. All observed beetles initiated flight immediately after exiting pods outdoors or within rearing containers. Flying behaviour in containers continued for several hours, after which emerging beetles no longer attempted flight. Dehisced or manually opened pods of both species revealed white tissue developing

from the inner pod wall beneath egg positions (Fig. 3D). Beetle activity periods and seed infestation rates on *L. sylvestris* were similar to those on garden grown *L. latifolius*.

The earliest evidence of parasitism was September 1 when two different hymenopter larvae were found within *B. affinis*-infested seeds. Hymenoptera parasitoids of *B. affinis* first emerged from mature seeds of *L. sylvestris* (collected September 5, 10, and 11). These were identified as *Dinarmus basalis* (Rodani, 1877), a cosmopolitan parasitoid of Bruchinae in legume seeds (Schmale et al. 2003) by John Huber and Gary Gibson (CNCI). *Bruchus affinis* and parasitoid emergence holes from seeds were distinguishable, allowing ML to score beetle and parasitoid infestation rates. Holes made by reared *B. affinis* were circular, $1.5\text{--}2.1 \pm 0.02$ mm in diameter ($n = 63$, median: 1.9 mm), while those from parasitoids were smaller and circular: $0.6\text{--}1.2 \pm 0.02$ mm ($n = 27$, 0.8 mm). The 438 seeds collected for rearing from patch 5 on September 5 resulted in 19 parasitoid emergence holes plus one pre-emergent parasitoid or 8% parasitism of developing *B. affinis*. *Bruchus affinis* was confirmed as host of the parasitoid by examination of the host remains by ML. In most cases, the remains of the beetle, including elytra and mandibles, could be used to confirm that a pupa (Fig. 4) was

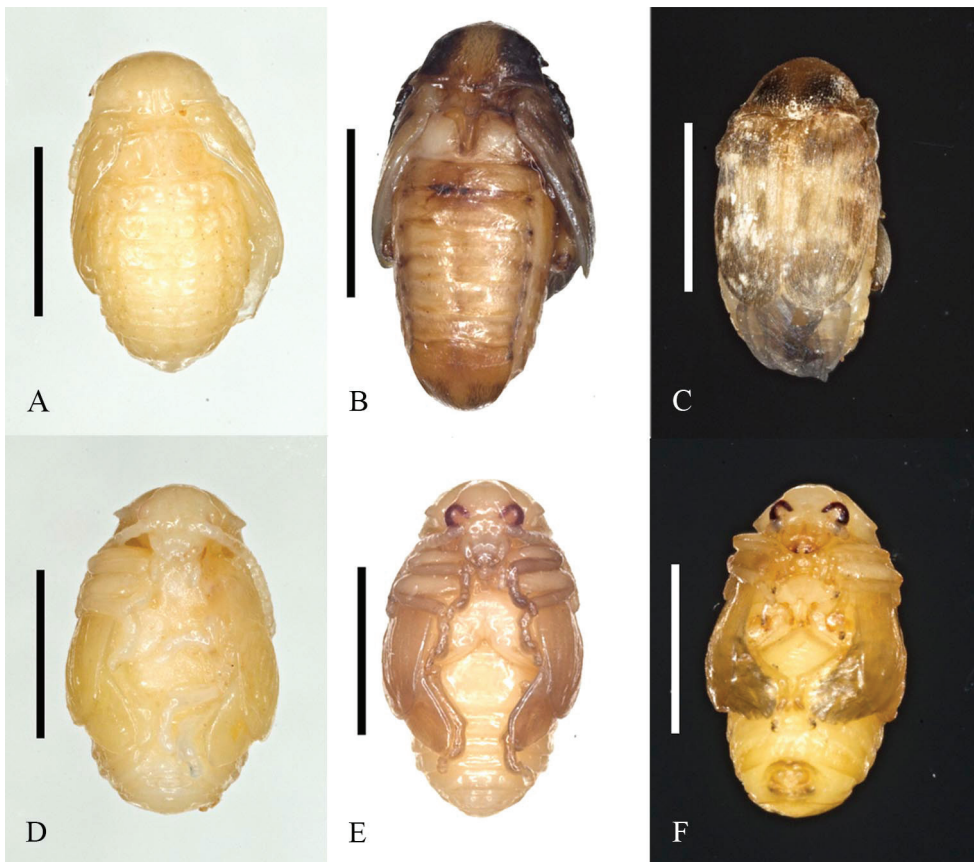


Figure 4. *Bruchus affinis* pupal stages in seeds of *L. sylvestris* from Québec, Canada. Scale bars: 2 mm.

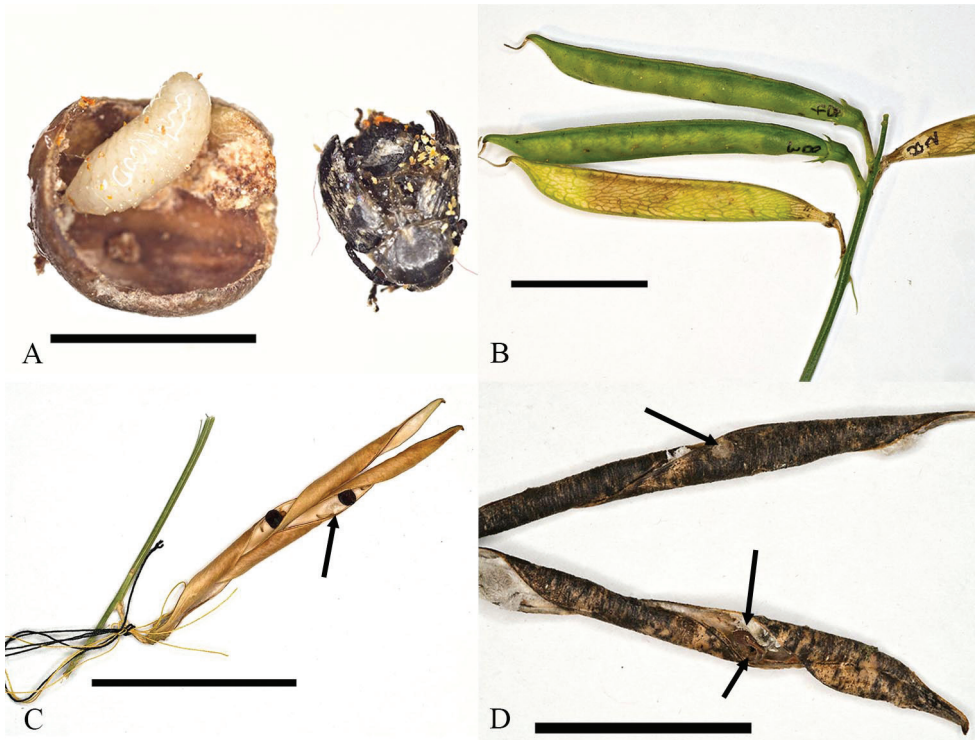


Figure 5. **A** *Bruchus affinis*, parasitized by Hymenoptera larvae in seed of *L. sylvestris* **B** maturing pods of *L. sylvestris* with hatched and unhatched eggs **C** dehiscent pod of *L. latifolius* **D** dehiscent pod of *L. sylvestris* showing *B. affinis* exit holes in pod wall and seed. Scale bars: 2 mm (**A**); 25 mm (**B**); 50 mm (**C**); 20 mm (**D**).

host to the parasitoid. Fig. 5A shows a parasitoid larva was feeding on a teneral beetle when a field-collected seed was opened on October 26. Here, the parasitoid may have continued feeding later into the autumn because of warmer indoor rearing conditions.

Reproductive phenology

Onset of host flowering was about two weeks earlier in Québec (mid-June) than reported from France (early July) (Bashar et al. 1987). Fabres et al. (1986) reported that adult *B. affinis* in France lived about 11 months after emergence including a nine-month reproductive diapause reporting that first pods appropriate to oviposition were present in mid-July with a maximum number of available pods for oviposition present in mid-August. We found that eggs were laid at our study site slightly earlier (about June 25). The period of sexual reproduction of *B. affinis* was short. We observed few *B. affinis* on *Lathyrus* plants after mid-July.

In summary, we report the following from North America (Québec): infestation of *L. latifolius* and *L. sylvestris* (Fabaceae) by *Bruchus affinis*; rearing of *B. affinis* from

both hosts; oviposition in 2021 beginning late June, to adult emergence beginning mid August; observation of *B. affinis* adults chewing holes to exit undehisced pods of *L. sylvestris*; parasitization of *B. affinis* by *Dinarmus basalis* in Québec. We also found that the seed emergence hole diameter of *B. affinis* was consistently larger than that of parasitoid emergence holes, such that we could reliably distinguish between exit hole types. We quantified *B. affinis* seed infestation rates of *L. latifolius* (17–28%), and of *L. sylvestris* (13.5–73.5%) for 2021.

Conclusions

Bruchus affinis is established in North America in Canada in Québec, Ontario, and British Columbia since 2007 or earlier using introduced *Lathyrus latifolius* and *L. sylvestris* as hosts. These populations may have originated from imports of infested seed for planting. Numbers of recorded adventive Chrysomelidae for Canada and America north of Mexico are updated to reflect this finding. Beetle development involved an approximately two-month period from oviposition to emergence. Phenological milestones of adult flight activity, oviposition, and adult emergence were estimated for study populations. Parasitoids were documented to use *B. affinis* as a host in Canada, but had a minor impact on infestations, accounting for about 10% mortality of pre-emergent pupae.

Acknowledgements

We thank A. Delobel (Muséum National d'Histoire Naturelle, France); G. Kergoat (French National Research Institute for Agriculture); G. Morse, University of San Diego, and L. Borowiec (University of Wrocław) for assistance in determining the identity of our specimens. We thank I. Nei (Canadian Food Inspection Agency, CFIA), B. Spencer (Vancouver, British Columbia), and P. de Tonnancour (Vaudreuil, Québec) for specimens, and T. Kimoto (CFIA) and S. Paiero (University of Guelph) for searching. Thanks to iNaturalist website participants who posted photographs of *Lathyrus* and *Bruchus* specimens that we investigated. We also acknowledge that V. Belov (Texas A & M) University correctly identified B. Spencer's photographed beetles as *B. affinis* in 2020 (<https://bugguide.net/node/view/1852275>); we appreciate that international identifiers like V. Belov sometimes notice new adventive insects in Canada. Thanks to M. Vankosky (AAFC), J. Tansey (Government of Saskatchewan), and J. Gavloski (Government of Manitoba) for information on pests of fava bean in Canada. Thanks to G. Kenicer (Royal Botanic Garden, Edinburgh) for assistance with identification of *L. latifolius* and *L. sylvestris*, to O. Lonsdale, G. Gibson, and J. Huber (CNCI) for parasitoid identifications, and to M. MacConaill for equipment and photography help. Thanks to an anonymous reviewer for helpful comments.

References

- Agrinova (2017) Guide pour la production de la gourgane dans la région du Saguenay-Lac-Saint-Jean. <https://www.agrinova.qc.ca/wp-content/uploads/2017/03/Guide-gourgane-version-finale-mars-2017.pdf> [accessed December 7, 2021]
- Anton KW (2010) Subfamily Bruchinae Latreille, 1802. In: Löbl I, Smetana A (Eds) Catalogue of Palaearctic Coleoptera. Volume 6. Chrysomeloidea. Apollo Books, Stenstrup, 339–353.
- Bashar A, Fabres G, Hosseart M, Valero M, Labeyrie V (1987) *Bruchus affinis* and the flowers of *Lathyrus latifolius*: an example of the complexity of relations between plants and phytophagous insects. In: Labeyrie V, Fabres G, Lachaise D (Eds) Insects–Plants. Dr W Junk, Dordrecht, 189–194.
- Bashar A, Fabres G, Labeyrie V (1990) Nocturnal rest and displacement patterns of *Bruchus affinis* (Col. Bruchidae) on specific *Lathyrus* spp. (Leguminosae) populations. In: Szentesi Á, Jermy T (Eds) Insects–plants '89, Akadémiai Kiadó, Budapest, 249–254.
- Borowiec L (1988) Fauna Polski, 11, Bruchidae (Insecta: Coleoptera), Polska Akademia Nauk, Instytut Zoologii, Warszawa, 219 pp.
- Bousquet Y, Bouchard P, Davies A, Sikes D (2013) Checklist of Beetles (Coleoptera) of Canada and Alaska. Second edition. Pensoft, Sofia, 402 pp. <https://doi.org/10.3897/zookeys.360.4742>
- Brandl P (1981) Bruchidae. In: Freude H, Harde KW, Lohse GA (Eds) Die Käfer Mitteleuropas. Band 10. Bruchidae, Anthribidae, Scolytidae, Platypodidae & Curculionidae. Goecke & Evers Verlag, Krefeld, 7–21.
- Delobel B, Delobel A (2006) Dietary specialization in European species groups of seed beetles (Coleoptera: Bruchidae: Bruchinae). *Oecologia* 149(3): 428–443. <https://doi.org/10.1007/s00442-006-0461-9>
- Douglas HB, Dumont S, Savard K, Chantal C (2021) Two adventive species of European Chrysomelidae (Coleoptera) new to North America: *Cryptocephalus moraei* (Cryptocephalinae) and *Psylliodes dulcamarae* (Galerucinae: Alticini), and the origins of adventive Chrysomelidae in Canada and United States of America. *Canadian Entomologist* 153(6): 774–786. <https://doi.org/10.4039/tce.2021.20>
- Environment Canada (2022) Historical weather data for Ottawa International Airport (Ontario, Canada). https://weather.gc.ca/city/pages/on-118_metric_e.html [accessed April 2, 2022]
- Fabres G, Bashar A, Hossaert-McKey M, Labeyrie V (1986) Adaptation à sa plante hôte d'un phytophage spécialiste de la consommation de graines et influence sur la biologie de ses populations: cas de *Bruchus affinis* (Col. Bruchidae) et de *Lathyrus* spp. Collection Nationale CNRS "Biologie des Populations", Lyon: 4–6 Septembre 1986.
- Howe RW, Currie JE (1964) Some laboratory observations on the rates of development, mortality and oviposition of several species of Bruchidae breeding in stored pulses. *Bulletin of Entomological Research* 55(3): 437–477. <https://doi.org/10.1017/S0007485300049580>
- Kergoat GJ, Silvain JF, Delobel A, Tuda M, Anton K-W (2007) Defining the limits of taxonomic conservatism in host-plant use for phytophagous insects: molecular systematics and evolution of host-plant associations in the seed-beetle genus *Bruchus* Linnaeus (Coleoptera: Chrysomelidae: Bruchinae). *Molecular Phylogenetics and Evolution* 43(1): 251–269. <https://doi.org/10.1016/j.ympev.2006.11.026>

- Kingsolver JM (2004) Handbook of the Bruchidae of the United States and Canada. Volume 1. Agricultural Research Service, United States Department of Agriculture, 324 pp.
- Schmale I, Wäckers FL, Cardona C, Dorn S (2003) Combining parasitoids and plant resistance for the control of the bruchid *Acanthoscelides obtectus* in stored beans. *Journal of Stored Products Research* 39(4): 401–411. [https://doi.org/10.1016/S0022-474X\(02\)00034-6](https://doi.org/10.1016/S0022-474X(02)00034-6)
- Segers A, Dumoulin L, Caparros Medigo R, Jacquet N, Cartryesse C, Malumba Kamba P, Pierreux J, Richel A, Blecker C, Francis F (2021) Varietal and environmental effects on the production of faba bean (*Vicia faba* L.) seeds for the food industry by confrontation of agricultural and nutritional traits with resistance against *Bruchus* spp. (Coleoptera: Chrysomelidae, Bruchinae). *Agriculture, Ecosystems & Environment* 327: 107831. <https://doi.org/10.1016/j.agee.2021.107831>
- USDA NRCS (2022) The PLANTS Database National Plant Data Team, Greensboro. <http://plants.usda.gov> [accessed May 1 2021]
- Woodhead E (1998) Early Canadian Gardening: an 1827 Nursery Catalogue. Illustrated edition. McGill-Queen's University Press, Montréal, 304 pp.

A new species of *Monstrilla* (Copepoda, Monstrilloida) from the western Caribbean with comments on *M. wandelii* Stephensen, 1913 and *M. conjunctiva* Giesbrecht, 1893

Eduardo Suárez-Morales¹

¹ *El Colegio de la Frontera Sur (ECOSUR), Unidad Chetumal, 77014 Chetumal, Mexico*

Corresponding author: Eduardo Suárez-Morales (esuarez@ecosur.mx)

Academic editor: Kai Horst George | Received 3 May 2022 | Accepted 20 October 2022 | Published 4 November 2022

<https://zoobank.org/D446044C-473C-449F-BEB9-B4CC0FCD2CFB>

Citation: Suárez-Morales E (2022) A new species of *Monstrilla* (Copepoda, Monstrilloida) from the western Caribbean with comments on *M. wandelii* Stephensen, 1913 and *M. conjunctiva* Giesbrecht, 1893. ZooKeys 1128: 33–45. <https://doi.org/10.3897/zookeys.1128.84944>

Abstract

The taxonomic study of monstrilloid copepods is hampered by incomplete early descriptions, uncertain synonymies, and the difficulty of reliably matching males and females of species. A re-evaluation of male monstrilloid specimens collected from two reef areas of the Mexican Caribbean allowed me to clarify the status of *Monstrilla mariaeugeniae* Suárez-Morales & Islas-Landeros, 1993 and *M. wandelii* Stephensen, 1913 based on a comparison of males attributed to each of these species. Males from the Puerto Morelos reef system, northern Mexican Caribbean coast, were first proposed as a tropical subspecies of the subarctic *M. wandelii*; later on, morphologically close males collected from the Mahahual reef area, southern Mexican Caribbean coast, were designated as the males of *M. mariaeugeniae*. Their status is here corrected with the description of *M. mahahualensis* **sp. nov.** based on the Mahahual males; the new species shares the same type of genitalia with the antarctic *M. conjunctiva* Giesbrecht, 1892 and the subarctic *M. wandelii*; Park (1967) linked a single male from Vancouver to *M. wandelii*. It was realised that Park's (1967) males from the Vancouver area and the two Mexican Caribbean groups of males represent different, undescribed species. I here reassign the males earlier attributed to *M. mariaeugeniae* as a new species of *Monstrilla* which is herein described. The new species differs from the males of *M. conjunctiva* and *M. wandelii* by details of the genitalia, length of the setae of the fifth legs, armature and integumental structures of the antennules, and size of the outer exopodal spines of legs 1–4. This is the third known species of *Monstrilla* with a *M. conjunctiva*-like male genitalia and the first one known from tropical areas. The male of both *M. mariaeugeniae* and *M. wandelii* remain unknown.

Keywords

Mexican Caribbean, Monstrillidae, morphology, protelean endoparasites, taxonomy

Introduction

Monstrilloid copepods are protelean endoparasites infecting different groups of marine invertebrates including polychaetes, molluscs, and sponges (Huys et al. 2007; Suárez-Morales 2011, 2018; Jeon et al. 2018) and are frequently recorded as adults in plankton samples. Their taxonomic and nomenclatural history is complex and uncertain (Grygier and Ohtsuka 2008; Suárez-Morales 2011, 2018; Suárez-Morales and Grygier 2021), particularly in reference to old records, early species descriptions, and the recognition and matching of males and females of the species (Grygier 1994, 1995; Suárez-Morales 2010, 2011, 2018; Suárez-Morales and Grygier 2021). The re-examination of collection specimens and the analysis of material from new sites with updated taxonomic criteria are valuable tools to solve some of these taxonomic problems (Grygier 1994; Suárez-Morales 2000a, b; Suárez-Morales and Gasca 2004).

Materials and methods

During the examination of zooplankton samples from Mahahual reef, southern coast of the Mexican Caribbean, several male monstrilloids were re-examined. They were tentatively identified by Suárez-Morales (1998) as the males of *M. mariaeugeniae* Suárez-Morales & Islas-Landeros, 1993, originally described from females collected at Puerto Morelos (PM) reef, on the northern coast of the Mexican Caribbean. Suárez-Morales (1996) designated PM males as a tropical subspecies of the Arctic *M. wandelii* Stephensen, 1913.

In order to determine the status of the northern and southern Mexican Caribbean males, which was still uncertain, I re-examined the Mahahual male specimens. I sorted five adult males closely resembling those that were previously named by me (Suárez-Morales 1996) as a subspecies (i.e., *Monstrilla wandelii tropica*) from the northern Mexican Caribbean reef (PM) and subsequently designated as the males of *M. mariaeugeniae* (Suárez-Morales 1998) to determine their status in the light of their resemblance to males from PM and to other species. As an outcome of this new evaluation using the descriptive criteria by Grygier and Ohtsuka (1995), the male individuals from Mahahual are here recognized as a new species, *M. mahahualensis* sp. nov., and not a *M. wandelii* subspecies nor the males of *M. mariaeugeniae*. The new species from Mahahual is fully described including examination with SEM and compared with similar species and male specimens from PM. The female of the new species remains unknown, like the true males of *M. mariaeugeniae*. Also, the male of *M. wandelii* from Vancouver, as described by Park (1967), is likely to represent an undescribed species; the male of *M. wandelii* from Greenland remains unknown.

Results

Taxonomy

Subclass Copepoda Milne Edwards, 1840

Order Monstrilloida Sars, 1901

Family Monstrillidae Dana, 1849

Genus *Monstrilla* Dana, 1849

Monstrilla mahahualensis sp. nov.

<https://zoobank.org/4761E010-CB8C-4F53-AC2B-F94E18AA6E16>

Figs 1–4

Type material. Adult male *holotype*, partially dissected (ECO-CH-Z 10595); specimen mounted in glycerine, sealed with acrylic varnish; two slides, collected by L. Vásquez-Yeomans and A. González-Vera, December 31 1990, plankton sample; **Paratypes:** 3 adult males (ECO-CH-Z 10596), one mounted on slide, undissected, and 2 males in vial, ethanol-preserved, undissected; collection data as holotype. Additional non-type material: one adult male prepared for SEM examination following the procedures described by Silva-Briano et al. (2013).

Type locality. Reef lagoon of Mahahual (18°43'11.42"N, 87°42'11.01"W), southern coast of the Mexican Caribbean.

Etymology. The species epithet, a toponym in singular, refers to the reef system of Mahahual, the type locality of this species. The gender is feminine.

Diagnosis. Male *Monstrilla* with light cuticular reticulation of cephalothorax covering cephalic area and 2/3 of post-oral cephalothorax surface. Antennule 5-segmented, geniculate, segments 3 and 4 indistinctly segmented, intersegmental division marked by constriction. First antennular segment unarmed, segments 3 and 4 each with discoid integumental structures of unknown function; armature of segments 4 and 5 reduced. Element 4d1 (Grygier and Ohtsuka 1995) robust, spinulate. Legs 1–4 with relatively long outer exopodal spines. Genital complex type II (Suárez-Morales 2000c) with short, thick shaft carrying pair of lappets subdistally. Lappets simple, conical, weakly asymmetrical, with outer surface furnished with rows of spinules. Fifth legs represented by pair of bulbous processes armed with long distal seta reaching beyond posterior margin of caudal rami.

Description of adult male. Body size of holotype 2.56 mm, of one paratype 2.72 mm measured from forehead margin to posterior end of anal somite. Body tagmiosis as usual in males of *Monstrilla* (Suárez-Morales and Castellanos-Osorio 2019; Suárez-Morales 2000c; Suárez-Morales 2022). First pedigerous thoracic somite incorporated into cephalothorax. Cephalothorax long, cylindrical, relatively robust, representing about 60% of total body length. Oral cone located at 40% of way back along ventral surface of cephalothorax (Fig. 1B). Cephalic region anteriorly subquadrate, forehead flat (Fig. 1A). Ocelli poorly developed, almost unpigmented. Small oval hyaline bodies (see Suárez-Morales 2018; Fig. 1A) adjacent to rounded ocelli. Cuticular or-

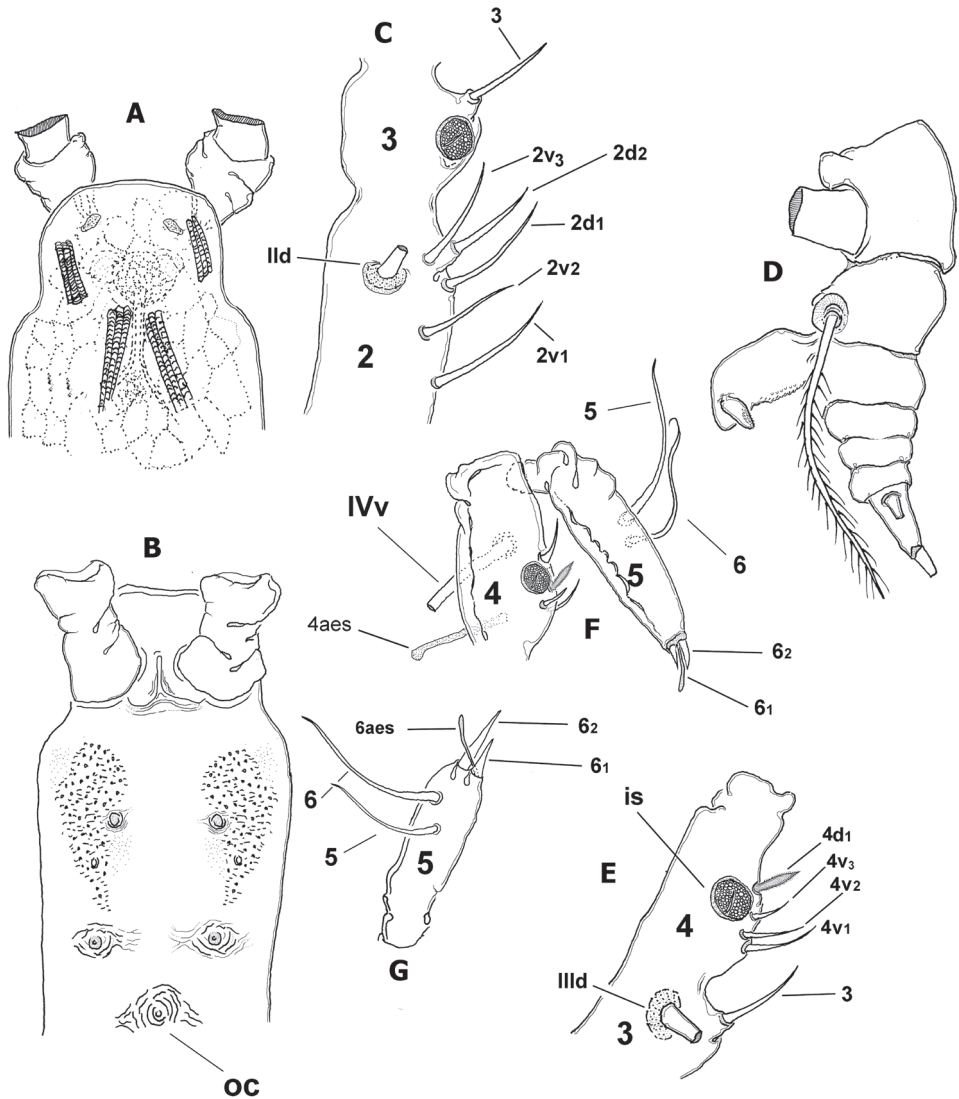


Figure 1. *Monstrilla mahahualensis* sp. nov., holotype adult male from Mahahual, Mexico **A** cephalic region showing weak reticulation pattern, dorsal view **B** perioral area showing oral cone (oc), cuticular processes and ornamentation, ventral view **C** antennule segments 2 and 3 showing setation pattern and position of integumental structure **D** urosome showing fifth legs and genital complex, lateral view **E** third and fourth antennule segments showing setation pattern and position of integumental structure (is) **F** fourth and fifth antennule segments showing setation pattern and position of integumental structure **G** fifth antennule segment showing setation pattern Scale bars: 50 μ m (**A–G**).

namentation of cephalothorax including light cuticular reticulation showing irregular pattern covering cephalic area and almost 2/3 of post-oral cephalothoracic surface (Fig. 1A). On ventral surface, three pairs of nipple-like processes present between oral cone and antennule bases (Fig. 1B); two foremost ventral processes with adjacent pattern

of minute transverse wrinkles and small papillae (Figs 1B, 2C). Oral cone moderately produced, with adjacent field of faint, transverse striae (oc in Fig. 1B).

Urosome consisting of five somites: fifth pedigerous somite (largest of urosome, with fifth legs), genital somite (with genital complex on ventral surface), two free somites, and short anal somite. Length ratio of urosomites (from proximal to distal) being: 44.1: 24.4: 12.6: 10.1: 8.8 = 100 (Figs 1D, 2F, 3F).

Antennules representing about 40% of total body length, and almost 65% of cephalothorax length. As usual in males of *Monstrilla*, antennules indistinctly five-segmented, geniculation between segments 4 and 5 (Figs 1F, 2A, B). Following setal nomenclature proposed by Grygier and Ohtsuka (1995) for female monstrilloid copepod antennules. First segment lacking setal element 1. Second segment carrying six elements, including short elements $2v_{1-3}$, and $2d_{1,2}$ plus long seta II_d , with broad socket (Fig. 1C). Second and third segments separate. Third segment short, globose, with setiform flexible medial element 3 reaching about proximal 1/3 of fourth segment; inner surface of segment with discoid integumental structure of unknown function (Fig. 1C, *is* in Figs 1E, 3E, 4C, D) at insertion of element 3; structure present in the right antennule only. Setae III_d , III_v absent. Fourth segment fused with third, division marked by moderate constriction; segment armed with five setal elements: $4d_1$, $4v_{1-3}$, IV_v , and long aesthetasc ($4aes$) (Fig. 1F, 4D); discoid integumental structure like that on third segment present at insertion of elements $4d_1$ and $4v_{1-3}$ (Figs 1E, 2D, 3E). Setal element $4v_1$ longer than $4v_2$, 3; element $4d_1$ robust, spiniform, pinnate (Fig. 1E). Distal fifth segment geniculate, slightly longer than preceding fourth segment (Fig. 1F), with reduced armature, armed with six setal elements (*sensu* Huys et al. 2007) (see Table 2). Spiniform apical elements 61 and 62 (*sensu* Grygier and Ohtsuka 1995), or 1,2 (*sensu* Huys et al. 2007) present, unequally long (Figs 2A, 4A). Length ratio of antennular segments (proximal to distal): 11.4: 19.8: 11.4: 27.8: 29.6 = 100 (Fig. 2A, B).

First incorporated pedigerous thoracic somite and succeeding three thoracic somites each bearing well-developed biramous swimming legs (Figs 2E, 3D). Swimming legs 1–4 as in *M. mariaeugeniae* (Suárez-Morales and Islas-Landeros 1993, fig. 1c, d, i, j), all with triarticulate endopodites and exopodites and same armament pattern except for leg 1 exopodite, bearing one seta fewer on distal segment (Fig. 1E). Exopodites longer than endopodites. Distal spiniform seta of third exopodite with denticles along outer margin, inner margin weakly setulose in all legs (* in Fig. 3D). Outer spines of exopodal segments 1 and 3 of all legs noticeably long (arrowheads in Fig. 3D). Basis of swimming legs 2–4 with short basipodal seta; basipodal seta on legs 1 and 2 not observed; seta on leg 3 long. All natatory setae lightly and biserially plumose. Huys and Boxshall (1991) was followed for general and setation nomenclature. Armament formula of legs 1–4 as in Table 1.

Table 1. Armature of swimming legs 1–4 including basipodites, exopodites and endopodites. Roman numerals indicate spiniform elements, Arabic numbers indicate setiform elements.

	Basipodite	Endopodite	Exopodite
Leg 1	1-0	I-1;0-1;2.2.1	I-0;0-1; I,2,2
Legs 2–4	1-0	0-1;0-1;2,2,1	I-1;0-1; I,2,2,1

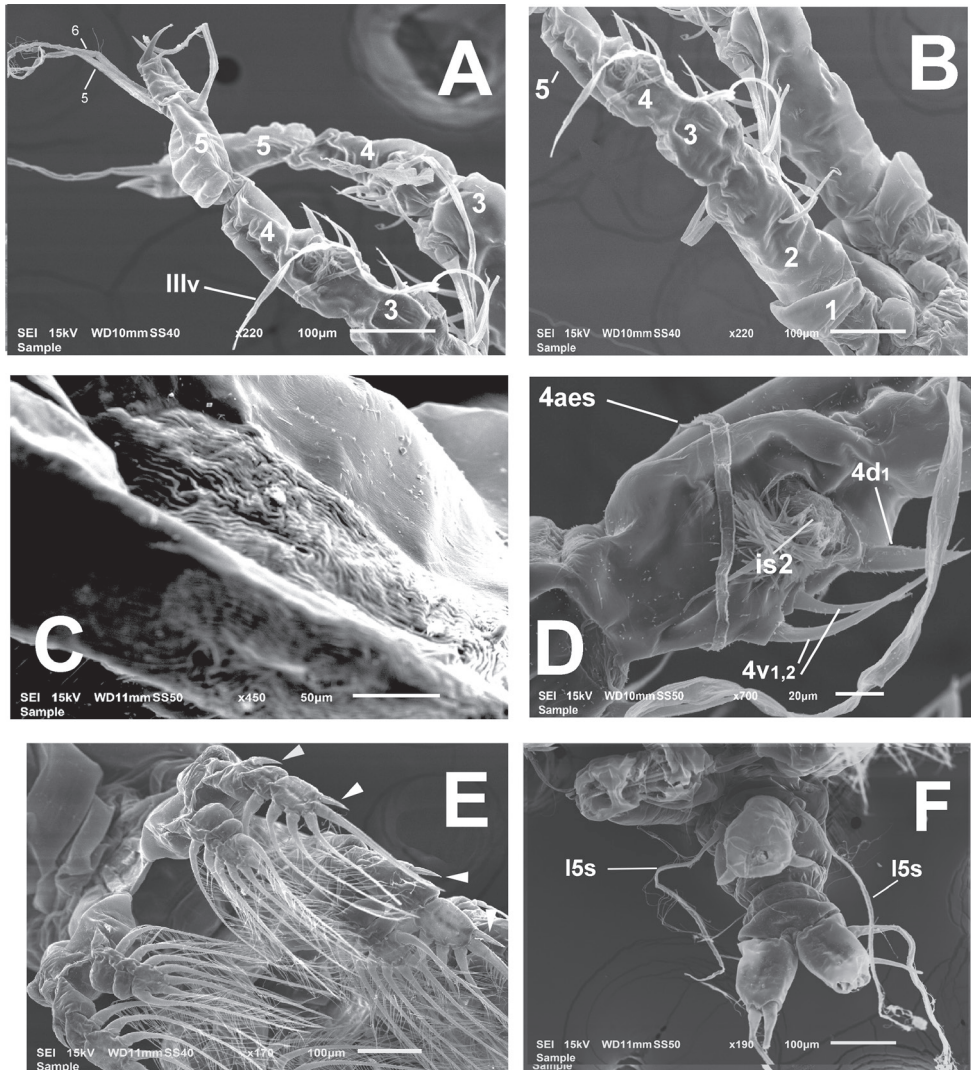


Figure 2. *Monstrilla mahabualensis* sp. nov., SEM-prepared adult male from Mahahual, Mexico **A** antennules, ventral view indicating purported segments 3–5 **B** same, semi-lateral view indicating purported segments 1–5 **C** detail of wrinkled cuticular field on perioral surface, ventral view **D** purported fourth antennular segment showing setation pattern and second integumental structure (is2) **E** legs 1–3 showing endopodal and exopodal rami general setation pattern, arrows indicate relatively long outer exopodal spines, ventral view **F** urosome with fifth legs armed with long setae, and genital complex, ventral view. Setal elements on antennule segments 1–4 labeled following Grygier and Ohtsuka's (1995) nomenclature.

Fifth legs reduced, represented by pair of small globose protuberances on ventral surface of fifth pedigerous somite armed with long single seta reaching beyond posterior margin of caudal rami (Figs 1D, *l5s* in Figs 2F, 3F, 4B). Genital somite carrying genital complex consisting of short, thick medially curved shaft bearing paired subdistal

genital lappets (Figs 2F, 3A–C, 4B, E). Lappets divergent, conical, tapering distally, ornamented with rows of spinules on inner surface (Fig. 3A, B); genital complex carrying genital opening with pair of rounded opercular flaps in apical position (*offl* in Fig. 3C).

Caudal rami subrectangular, each ramus approximately 1.3 times as long as wide, bearing four caudal setae (setae II–V; Huys and Boxshall 1991), armature incomplete in some specimens, but sockets indicate setal insertions (Figs 2F, 3F, 4B).

Female. Unknown.

Discussion

The male specimens studied here can be included in the genus *Monstrilla* by 1) the presence of two urosomites between the genital somite and the anal somite, 2) the structure of its genital complex that is typical for the genus, in this case, type II (Suárez-Morales 2000d); 3) the presence of well-developed or reduced paired fifth legs, 4) the possession of 4–6 caudal setae in both sexes, and 5) branched antennular setae sometimes present. This combination of characters is unique among the known genera of monstrilloids (Grygier and Ohtsuka 2008; Suárez-Morales and McKinnon 2014; Jeon et al. 2018).

The males of *Monstrilla conjunctiva* Giesbrecht, 1902, *M. wandelii sensu* Park (1967), and *M. mahahualensis* sp. nov., share a similar structure of the genitalia. This type of male genital complex was first described and depicted for *M. conjunctiva* by W. Giesbrecht from a male collected in Antarctic waters (Giesbrecht 1902). There are no other known species of *Monstrilla* with the *M. conjunctiva*-like male genitalia; therefore, the comparisons in this work include the three nominal species of monstrilloids sharing this character (Table 2). The shape, structure, and ornamentation of the genital lappets, the length of the fifth leg setae, body size, and antennule setation pattern show some differences among these three taxa, as follows: the genital lappets are simple, leaf-like, distally acute in *M. conjunctiva* (Giesbrecht 1902, fig. 12.3) whereas they are chelate and smooth in *M. wandelii* (see Park 1967, fig. 2C, D); in *M. mahahualensis* sp. nov., the lappets are simple, conical, and ornamented with rows of spinules (Fig. 3A, B). Also, in both *M. conjunctiva* (Giesbrecht 1902, figs XII.3, 4) and *M. wandelii sensu* Park (1967, fig. 2C, D), the leg 5 setae are relatively short, not reaching the distal margin of the caudal rami. In the new species, *M. mahahualensis*, the fifth leg setae reach well beyond the posterior margin of the caudal rami (Figs 2F, 3F, 4B). The new species shares with *M. wandelii sensu* Park (1967) the relatively long outer exopodal spines of legs 1–4, and the antennule segmentation and armature pattern (see Table 2). It shares with *M. conjunctiva* the caudal rami setation pattern and the antennule setation (Table 2).

The rounded integumental structures resembling those here observed in *M. mahahualensis* sp. nov. were first depicted, but not described, by Suárez-Morales (1996, fig. 2A, B) in males of PM. These structures were not reported by Giesbrecht (1902) or Park (1967) and are present in the female holotype of *M. mariaeugeniae*

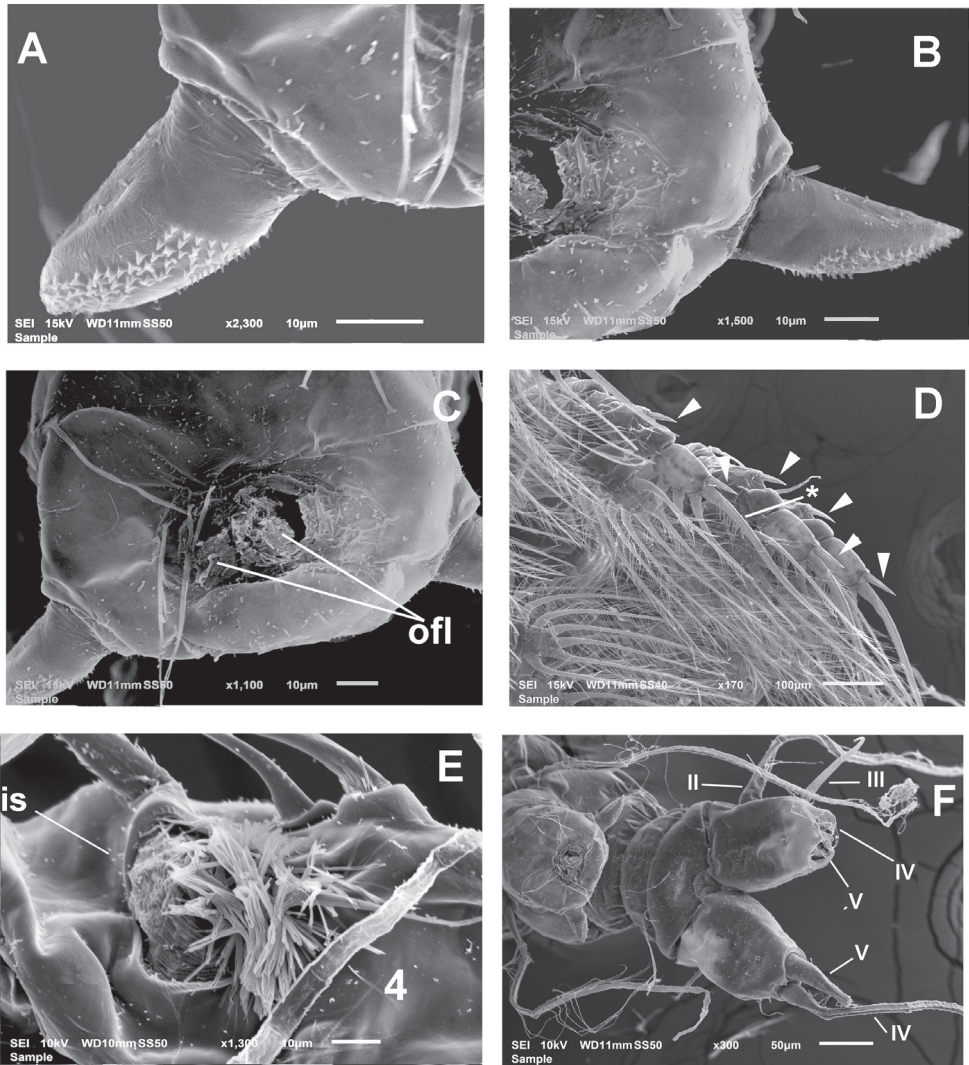


Figure 3. *Monstrilla mahahualensis* sp. nov., SEM-prepared adult male from Mahahual, Mexico, female holotype **A** detail of right genital lappet showing cuticle ornamentation, ventral view **B** same, left genital lappet, semi-lateral view **C** apical surface of genital complex showing genital opening and paired opercular flaps (ofl), ventral view **D** swimming les 2–4 showing setation pattern and long exopodal spines (arrowheads) **E** integumental structure on antennule segment 4, ventral view **F** urosome, genital complex, and caudal rami showing setation pattern (setae II–V).

(pers. obs.), thus agreeing with Suárez-Morales' (1996) notion that the PM males, and the Mahahual males (Suárez-Morales 1998) were linked to *M. mariaeugeniae*.

There are two distinct types of male genitalia among species of *Monstrilla* and of the related genus *Caromiobenella* Jeon, Lee & Soh, 2018 (McAlice 1985; Jeon et al.

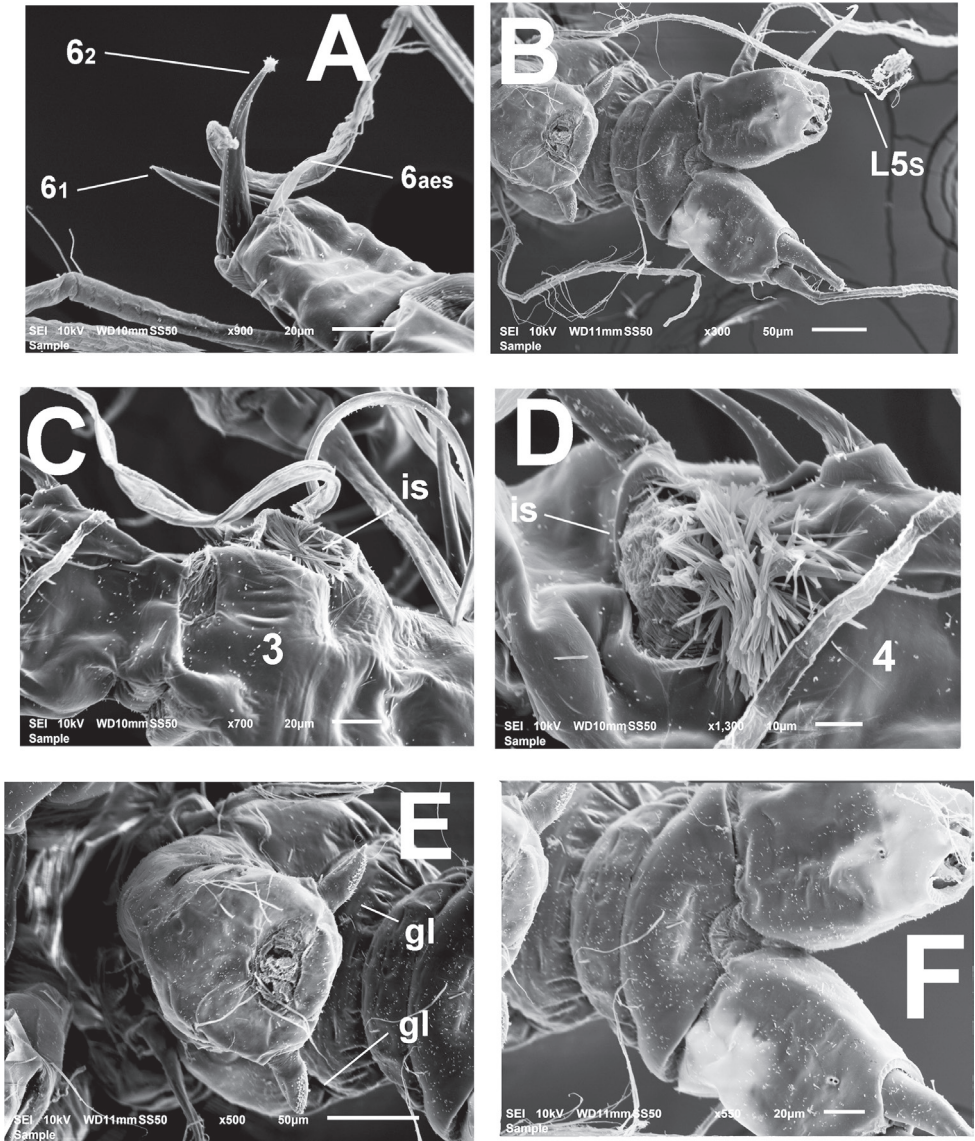


Figure 4. *Monstrilla mahabualensis* sp. nov., SEM-prepared adult male from Mahahual, Mexico **A** right antennule fifth segment showing terminal setal elements, ventral view **B** distal part of urosome showing genital complex, fifth legs with long setae (L5s) **C** integumental structure 1 (*is*), on third antennulary segment, semi-lateral view **D** integumental structure 2 (*is*) on fourth antennulary segment, ventral view **E** genital complex showing genital opening and paired genital lappets (*gl*) **F** detail of anal somite, ventral view. Setal elements on segments 1–4 labeled following Grygier and Ohtsuka's (1995) nomenclature; armature of fifth segment labeled following Huys et al. (2007); ae2 on distal segment follows Huys et al. (2007) sequence notation of antennulary aesthetascs. Arrows indicate proximal rounded protuberance on fifth antennulary segment. Scale bars: 75 μ m (**A**, **B**).

2018; Suárez-Morales 2000d; Cruz Lopes da Rosa et al. 2021): the first one (type I) shows a genital shaft of variable length and thickness bearing a deep distal notch between the distally set lappets; this medial notch is frequently ornamented with spinules or teeth on its inner surface. A second type (type II) is distinguished by the presence of a smooth, rounded medial protrusion instead of a notch in the same position. The male genitalia displayed by the three species: *M. wandelii sensu* Park (1967), *M. conjunctiva*, and *M. mahahualensis* sp. nov. are assignable as a modified type II male genitalia, in which lappets are widely divergent, probably resulting from a strong development of the broad medial protrusion between them.

The antennule segmentation, with fused segments 3 and 4 is another character shared by the three species, *M. wandelii*, *M. conjunctiva*, and *M. mahahualensis* sp. nov., including their reduced setation of segments 1, 4, and 5. The setation patterns of segments 1–4 were compared following Grygier and Ohtsuka's (1995) nomenclature for the first time. The differences among these species and Caribbean males are presented in Table 2.

Table 2. Comparison of male antennule armature patterns of different species and populations with *M. conjunctiva*-like genitalia. Identification of elements on A1 segments 1–4 followed Grygier and Ohtsuka's (1995) nomenclature; for elements on A1 segment 5, Huys et al.'s (2007) nomenclature was followed.

A1 elements (<i>sensu</i> Grygier and Ohtsuka 1995)	<i>M. mahahualensis</i> sp. nov.	<i>M. conjunctiva</i> Giesbrecht, 1902	<i>M. wandelii</i> Park (1967)
61/62 ratio	0.66	0.4	0.9
Element 1	absent	absent	absent
Elements on S2	2v ₁₋₃ , 2d _{1,2} , II d	2v ₁₋₃ , 2d _{1,2}	2v ₁₋₃ , 2d _{1,2} , II d
Elements on S3	III v, III d, 3	III v, III d, 3	III v, III d, 3
Elements on S4	4v ₁₋₃ , 4d ₁ , 4aes, IV v	4v ₁₋₃ , 4d ₁ , 4aes, IV d	4v ₁₋₃ , 4d _{1,2} , 4aes, IV v
Elements on S5*	1,2,6, C,B AE2	1, 2, 4, 6, C, AE2	1, 2, 4, 6,C, AE2

The PM males share several characters with *M. mahahualensis* sp. nov., namely: 1) antennule segmentation pattern, 2) body proportions, cephalothorax ornamentation, 3) caudal armature, 4) antennule armature (see Table 1), 4) position of the oral papilla (~ 40% of way back along ventral surface of cephalothorax), and 5) the presence of integumental structures on the antennule (Suárez-Morales 1996, fig. 2A, B). There are, however, some important differences between the PM males and *M. mahahualensis* sp. nov. from Mahahual (southern Mexican Caribbean), as follows: In the PM males the fifth legs setae are relatively short, not reaching beyond the posterior margin of the caudal rami (Suárez-Morales 1996, figs 1B, 2C), thus diverging from the clearly longer fifth leg setae of *M. mahahualensis* sp. nov. reaching well beyond the distal margin of the caudal rami; 2) in addition, the genital lappets of the PM males are bilobed, chela-like (Suárez-Morales 1996, figs 2C, 3A) vs. simple, conical in *M. mahahualensis* sp. nov. (Fig. 3A, B). Also, the PM males have two integumental structures on antennular segment 2 (Suárez-Morales, 1996, fig. 2A, B), but not on segments 3 and 4, as observed in *M. mahahualensis* sp. nov. (Figs 1E, F, 2D, 3E). Antennular segments 6₁ and 6₂ are

equally long in the PM males (Suárez-Morales 1996, fig. 2A, B) and unequally long in *M. mahahualensis* sp. nov. (Figs 1G, 2A, 4A, Table 1). Thus, it is likely that the PM males represent a different species closely related with *M. mahahualensis* sp. nov. The holotype of the PM species is deposited in the USNM collection as *Monstrilla wandelii tropica* (USNM-259668) and is probably a different species (see Suárez-Morales 1996), whose link with *M. mariaeuigeniae* is yet to be determined.

Acknowledgements

I thank El Colegio de la Frontera Sur (ECOSUR-Chetumal) for full support during the taxonomic analysis of these samples. Rosa Ma. Hernández and José Angel Cohuo (ECOSUR) deposited and catalogued specimens of this species in the collection of Zooplankton at ECOSUR-Chetumal. Manuel Elías-Gutiérrez kindly guided my SEM sessions with ECOSUR's SEM equipment (JEOL JSM-6010LA) at El Colegio de la Frontera Sur (ECOSUR) Chetumal, Mexico. Part of this material was studied during my sabbatical year at the USNM in Washington, D.C. and I appreciate the continuous support from Chad Walter and for cataloguing the PM male specimens in the USNM collection. The comments and suggestions from two anonymous reviewers allowed me to improve an earlier version of this work.

References

- Cruz Lopes da Rosa J, Dias CO, Suárez-Morales E, Weber LI, Gomes Fischer L (2021) Record of *Caromiobenella* (Copepoda, Monstrilloida) in Brazil and discovery of the male of *C. brasiliensis*: Morphological and molecular evidence. *Diversity* 13(6): 241. <https://doi.org/10.3390/d13060241>
- Giesbrecht W (1902) Zoologie Copepoden. Expédition Antarctique Belge- Resultats du Voyage de S.Y. Belgica en 1897–1898–1899 sous le commandement de A. Gerlache de Gomery. Rapports Scientifiques publiés aux frais du Gouvernement Belge, sous la direction de la Commission de la Belgica, m Taf. I–XIII, 1–49.
- Grygier MJ (1994) [dated 1993] Identity of *Thaumatoessa* (= *Thaumaleus*) *typica* Krøyer, the first described monstrilloid copepod. *Sarsia* 78(3–4): 235–242. <https://doi.org/10.1080/00364827.1993.10413537>
- Grygier MJ (1995) Annotated chronological bibliography of Monstrilloida (Crustacea: Copepoda). *Galaxea* 12: 1–82.
- Grygier MJ, Ohtsuka S (1995) SEM observation of the nauplius of *Monstrilla hamatapex*, new species, from Japan and an example of upgraded descriptive standards for monstrilloid copepods. *Journal of Crustacean Biology* 15(4): 703–719. <https://doi.org/10.2307/1548820>
- Grygier MJ, Ohtsuka S (2008) A new genus of monstrilloid copepods (Crustacea) with anteriorly pointing ovigerous spines and related adaptations for subthoracic brooding. *Zoological Journal of the Linnean Society* 152(3): 459–506. <https://doi.org/10.1111/j.1096-3642.2007.00381.x>

- Grygier MJ, Suárez-Morales E (2021) Recognition and partial solution of nomenclatural issues involving copepods of the family Monstrillidae (Crustacea: Copepoda: Monstrilloida). *Zootaxa* 4486(4): 497–509. <https://doi.org/10.11646/zootaxa.4486.4.5>
- Huys R, Boxshall GA (1991) *Copepod Evolution*. The Ray Society, London, 468 pp.
- Huys R, Llewellyn-Hughes J, Conroy-Dalton S, Olson PD, Spinks JN, Johnston DA (2007) Extraordinary host switching in siphonostomatoid copepods and the demise of the Monstrilloida: Integrating molecular data, ontogeny and antennular morphology. *Molecular Phylogenetics and Evolution* 43(2): 368–378. <https://doi.org/10.1016/j.ympev.2007.02.004>
- Jeon D, Lee W, Soh HY (2018) A new genus and two new species of monstrilloid copepods (Copepoda: Monstrillidae): integrating morphological, molecular phylogenetic and ecological evidence. *Journal of Crustacean Biology* 38: 45–65.
- McAlice BJ (1985) On the male of *Monstrilla helgolandica* Claus (Copepoda, Monstrilloida). *Journal of Crustacean Biology* 5(4): 627–634. <https://doi.org/10.2307/1548240>
- Park TS (1967) Two unreported species and one new species of *Monstrilla* (Copepoda: Monstrilloida) from the Strait of Georgia. *Transactions of the American Microscopical Society* 86(2): 144–152. <https://doi.org/10.2307/3224681>
- Silva-Briano M, Adabache A, Guerrero-Jiménez G (2013) Additions to the taxonomy of *Brachionus josefinae* (Rotifera: Monogononta: Brachionidae). *Hidrobiológica* 23(3): 450–455.
- Suárez-Morales E (1996) On a tropical subspecies of *Monstrilla wandelii* (Copepoda: Monstrilloida) from the Mexican coasts of the Caribbean Sea. *Crustaceana* 69(1): 34–40. <https://doi.org/10.1163/156854096X00042>
- Suárez-Morales E (1998) On the male of *Monstrilla mariaeugeniae* Suárez-Morales & Islas-Landeros (Copepoda: Monstrilloida) from the Mexican Caribbean Sea. *Crustaceana* 71(3): 360–362. <https://doi.org/10.1163/156854098X00347>
- Suárez-Morales E (2000a) A new species and new geographic records of *Monstrilla* (Copepoda: Monstrilloida) from the Philippines. *Journal of Crustacean Biology* 20(4): 680–686. <https://doi.org/10.1163/20021975-99990092>
- Suárez-Morales E (2000b) Redescription of two species of *Cymbasoma* from Southwest Britain and from Indonesia (Copepoda: Monstrilloida) with notes on taxonomy. *Beaufortia/Bulletin of the Zoological Museum of Amsterdam* 50: 139–149.
- Suárez-Morales E (2000c) The male of *Cymbasoma quintanarooense* (Suárez-Morales) (Copepoda, Monstrilloida) from the Caribbean with an identification key for the known males of *Cymbasoma*. *Marine Biology Research* 85(3): 203–210. <https://doi.org/10.1080/00364827.2000.10414573>
- Suárez-Morales E (2000d) Taxonomic report on some monstrilloids (Copepoda, Monstrilloida) from Toulon Bay, France. *Bulletin de l'Institut Royal de Sciences Naturelles de Belgique. Biologie* 70: 107–118.
- Suárez-Morales E (2010) On the taxonomic status of *Monstrilla leucopsis* Sars (Crustacea: Copepoda: Monstrilloida) from Norway, with comments on the male of *M. longiremis* Giesbrecht. *Zootaxa* 2510: 55–67. <https://doi.org/10.11646/zootaxa.2510.1.3>
- Suárez-Morales E (2011) Diversity of the Monstrilloida (Crustacea: Copepoda). *PLoS ONE* 6(8): e22915. <https://doi.org/10.1371/journal.pone.0022915>

- Suárez-Morales E (2018) Monstrilloid copepods: the best of three worlds. *Bulletin of the Southern California Academy of Sciences* 107(2): 92–103. <https://doi.org/10.3160/3646.1>
- Suárez-Morales E (2022) A new species of *Monstrilla* (Crustacea: Copepoda: Monstrilloida: Monstrillidae) collected by the R / V *Albatross* (1908) from the Sulu Sea, Philippines. *Journal of Natural History* 55(47–48): 3041–3052. <https://doi.org/10.1080/00222933.2022.2032444>
- Suárez-Morales E, Castellanos-Osorio I (2019) A new species of *Monstrilla* (Copepoda, Monstrilloida, Monstrillidae) from the plankton of a bay system of the northwestern Caribbean, with a key to species. *ZooKeys* 876: 111–123. <https://doi.org/10.3897/zookeys.876.38400>
- Suárez-Morales E, Gasca R (2004) On the invalidity of *Strilloma* Isaac (Copepoda: Monstrilloida): observations from the type species. *Zoological Studies* 43(2): 292–299.
- Suárez-Morales E, Grygier MJ (2021) Mediterranean and Black Sea monstrilloid copepods (Copepoda: Monstrilloida): rediscovering the diversity of transient zooplankters. *Water (Basel)* 13(8): 1036. <https://doi.org/10.3390/w13081036>
- Suárez-Morales E, Islas-Landeros M (1993) A new species of *Monstrilla* (Copepoda: Monstrilloida) from a reef lagoon off the Mexican coast of the Caribbean Sea. *Hydrobiologia* 271: 45–48. <https://doi.org/10.1007/BF00005694>
- Suárez-Morales E, McKinnon AD (2014) The Australian Monstrilloida (Crustacea: Copepoda) I. *Monstrillopsis* Sars, *Maemonstrilla* Grygier & Ohtsuka, and *Australomonstrillopsis* gen. nov. *Zootaxa* 3779(3): 301–340. <https://doi.org/10.11646/zootaxa.3779.3.1>

New faunistic records of the families Bolitophilidae and Keroplatidae (Diptera, Sciaroidea) from Morocco

Ouafaa Driauch^{1,2}, Peter J. Chandler³,
Mohamed Amin El Mouden¹, Boutaina Belqat¹

1 LESCURL/CNRST N°18, FS, Abdelmalek Essaadi University, Tetouan, Morocco **2** Biotechnology, Environmental Technology and Valorization of Bio-Resources Team, FSTH, Abdelmalek Essaadi University, Tetouan, Morocco **3** 606B Berryfield Lane, Melksham, Wiltshire SN12 6EL, UK

Corresponding author: Boutaina Belqat (belqat@gmail.com)

Academic editor: Marc De Meyer | Received 19 April 2022 | Accepted 28 September 2022 | Published 7 November 2022

<https://zoobank.org/ADA965F5-57D6-439F-BCB3-025DB7FB399A>

Citation: Driauch O, Chandler PJ, Amin El Mouden M, Belqat B (2022) New faunistic records of the families Bolitophilidae and Keroplatidae (Diptera, Sciaroidea) from Morocco. ZooKeys 1128: 47–52. <https://doi.org/10.3897/zookeys.1128.85536>

Abstract

The family Bolitophilidae is recorded for the first time from Morocco with one species *Bolitophila* (*Bolitophila*) *saundersii* (Curtis, 1836). Ten new species are added to the Moroccan fauna of Keroplatidae, known until now by only two species, raising the number of species currently known in Morocco to 12.

Keywords

Biodiversity, fungus gnats, new records

Introduction

The Keroplatidae are among the larger and most conspicuous fungus gnats. The family has a worldwide distribution, with about 1000 species belonging to 90 genera (Pape et al. 2011).

Keroplatids are commonly found in moist forests, but also in other ecosystems, where they are often associated with fungi, rotten wood, and similar substrates. Their larvae live in webs and either feed on fungal spores or are predaceous on small invertebrates caught in their webs. The webs may include droplets of fluid containing oxalic acid which immobilises prey. Adults are often found in dark, humid places, including caves. Keroplatids

can be collected by sweeping in low vegetation, under hanging rocks, tree trunks, and along stream banks. They are also frequently caught in Malaise traps (Evenhuis 2006).

The Bolitophilidae is a small family of fungus gnats, currently comprising 61 extant species in a single genus, *Bolitophila* Meigen, 1818, which has two subgenera, *Bolitophila* s. str. and *Cliopisa* Enderlein, 1936 (Bechev and Chandler 2011). This is a principally Holarctic family, with only one species previously recorded from North Africa, in Algeria (Burgehele-Balacesco 1966). Their larvae develop internally in soft fungi.

The fungus gnats of the families Bolitophilidae and Keroplatidae of Morocco are practically unstudied. This paper is the first contribution to specifically treat both families from Morocco. The family Bolitophilidae is recorded for the first time from Morocco by one species *Bolitophila* (*Bolitophila*) *saundersii* (Curtis, 1836). The Moroccan fauna of keroplatids was represented by only two species, *Macrocera fasciata* Meigen, 1804 (Becker and Stein 1913; Chandler and Ribeiro 1995; Evenhuis 2006; Kettani et al. 2022) and *Keroplatus reaumurii* (Dufour, 1839) (Matile 1986; Chandler et al. 2006; Evenhuis 2006). The new findings increase the number of Moroccan keroplatids to 12. Of the 10 species recorded from Morocco for the first time, six are new to North Africa.

Material and methods

A total of 25 specimens of Keroplatidae were collected by sweeping. Between 2013 and 2022, 15 sites were sampled in mountainous areas, such as the Rif and the High Atlas.

Most of the material was collected by B. Belqat and O. Driauach, and Dr M. Ebejer provided additional material that he had collected. All the material is preserved in 70% ethanol and was identified by P. Chandler. A list of sampling sites, with coordinates and altitudes, is given in Table 1. General and North African distributions of the species are separately given.

Table 1. Sampling sites (in alphabetical order) harbouring the species collected in Morocco, in the present study, with localities, geographical coordinates and elevations.

Station	Locality	Elevation (m)	Geographical coordinates
RIF			
Aïn Ras El Ma	Majjou	856	35°06.873'N, 5°11.388'W
Bab Rouida	Parc National Talassemrane	1512	35°06.881'N, 5°08.270'W
Daya Amsemlil	Jbel Bouhachem	1059	35°15.596'N, 5°25.917'W
Douar Belwazen	Belwazen	176	35°40.368'N, 5°25.116'W
Lower Loukkos saltmarsh	5 km E of Larache	2	35°12.274'N, 6°08.222'W
Halouma Kitane	Kitane, Tétouan	140	35°31.912'N, 5°19.861'W
Jbel Zemzem	Jbel Zemzem	216	35°45.457'N, 5°22.189'W
Marabout El Khaloua	Dar Khenouss	788	35°29.039'N, 5°20.678'W
Maison forestière	Parc National Talassemrane	1674	35°08.076'N, 5°08.262'W
Oued Aârate	Dardara	269	35°07.381'N, 5°17.456'W
Oued Majjou	Majjou Village	799	35°06.186'N, 5°10.935'W
Oued Tizga	Amsa	516	35°26.237'N, 5°13.694'W
Oued Sahel	Ben Karrich, Tétouan	40	35°29.238'N, 5°26.352'W
Oued Sidi Yahya Aârab	Sidi Yahya Aârab	62	35°17.545'N, 4°53.503'W
High Atlas			
Douar Akhlij Tnine Ourika	Ourika, Marrakech	870	31°22.385'N, 7°46.608'W

List of species

Family Bolitophilidae

Genus *Bolitophila* Meigen, 1818

Bolitophila saundersii (Curtis, 1836)

Material examined: Daya Amsemlil, 1 ♂ 1 ♀, 26 Mar. 2016.

General distribution: Palaearctic.

North African distribution: Algeria. **New record for Morocco.**

Family Keroplatidae

Subfamily Macrocerinae

Genus *Macrocera* Meigen, 1804

Macrocera fasciata Meigen, 1804

Material examined: Ain Ras El Ma, 1 ♂, 1 ♀, 27 Mar. 2013.

General distribution: Palaearctic.

North African distribution: Morocco.

Macrocera nigricoxa Schiner, 1863

Material examined: Oued Aârate, 2 ♂♂, 26 Mar. 2014; Oued Sahel, 1 ♂, 5 Apr. 2014.

General distribution: Palaearctic.

North African distribution: first record for Morocco and North Africa.

Macrocera phalerata Meigen, 1818

Material examined: Daya Amsemlil, 1 ♂, 23 Apr. 2016.

General distribution: Palaearctic.

North African distribution: Tunisia. **First record for Morocco.**

Macrocera pusilla Meigen, 1830

Material examined: Lower Loukkos saltmarsh, 4 ♀♀, 10 May 2012, Ebejer Leg.

General distribution: Palaearctic.

North African distribution: Algeria and Tunisia. **First record for Morocco.**

Subfamily Keroplatinae Rondani, 1856**Tribe Keroplatini Rondani, 1856****Genus *Keroplatus* Bosc, 1792*****Keroplatus reaumurii* (Dufour, 1839)**

Material examined: Douar Belwazen, 1 ♂, 2 Feb. 2022.

General distribution: Palearctic.

North African distribution: Morocco.

Tribe Orfeliini Malloch, 1917**Genus *Antlemon* Loew, 1871*****Antlemon halidayi* Loew, 1871**

Material examined: Daya Amsemblil, 1 ♂, 23 Apr. 2016; Halouma Kitane, 1 ♂, 1 Jan. 2015; Oued Majjou, 3 ♂♂, 9 Apr. 2013.

General distribution: Palearctic.

North African distribution: Algeria and Tunisia. **First record for Morocco.**

***Antlemon servulum* (Walker, 1836)**

Material examined: Bab Rouida, 1 ♂, 17 Jun. 2014.

General distribution: Palearctic.

North African distribution: first record for Morocco and North Africa.

Genus *Macrorrhyncha* Winnertz, 1846***Macrorrhyncha gallica* Chandler & Blasco-Zumeta, 2001**

Material examined: Maison forestière, 1 ♂, 7–17 Jun. 2014, Malaise trap.

General distribution: Europe.

North African distribution: first record for Morocco and North Africa.

Genus *Neoplatyura* Malloch, 1928***Neoplatyura biumbrata* (Edwards, 1913)**

Material examined: Douar Arikji Ltnin Ourika, 1 ♂, 28 Apr. 2015; Jbel Zemzem, 1 ♂, 17 Apr. 2014.

General distribution: Europe.

North African distribution: first record for Morocco and North Africa.

***Neoplatyura nigricauda* (Strobl, 1893)**

Material examined: Marabout El Khaloua, 1 ♂, 3 Jun. 2018.

General distribution: Palearctic.

North African distribution: Tunisia. **First record for Morocco.**

Genus *Orfelia* Costa, 1857***Orfelia persimilis* Caspers, 1991**

Material examined: Bouhachem, 1 ♂, 14 Jul. 2013; Oued Tizga, 1 ♂, 25 Jun. 2014;
Oued Sidi Yahya Aârab, 1 ♂, 25 Apr. 2015.

General distribution: Europe.

North African distribution: first record for Morocco and North Africa.

Genus *Pyratula* Edwards, 1929***Pyratula ebroensis* Chandler & Blasco-Zumeta, 2001**

Material examined: Maison forestière, 1 ♂, 7 Jun. 2014.

General distribution: Europe.

North African distribution: first record for Morocco and North Africa.

Acknowledgements

We are grateful to Dr Martin Ebejer who kindly provided material that he collected in Morocco and for permitting us to publish his new records. We also warmly and sincerely thank Dr Paul Beuk for his support to our PhD students and his continues help in identifying species of some Diptera families. We thank the reviewers and editor, Dr. Marc De Meyer, for their constructive comments on the manuscript.

References

- Bechev D, Chandler PJ (2011) Catalogue of the Bolitophilidae and Diadocidiidae of the World (Insecta: Diptera). *Zootaxa* 2741(1): 38–58. <https://doi.org/10.11646/zootaxa.2741.1.2>
- Becker T, Stein P (1913) Dipteren aus Marokko. *Annuaire du Musée zoologique de l'Académie impériale de Sciences de St.-Petersbourg* 18: 62–95.
- Burghele-Balacesco A (1966) Les Mycetophilidae (Diptères) cavernicoles de la collection Biospeologica (IV^e–VIII^e séries des “Grottes visitées”). *International Journal of Speleology* 2(4): 319–334. <https://doi.org/10.5038/1827-806X.2.4.3>

- Chandler PJ, Ribeiro E (1995) The Sciaroidea (Diptera) (excluding Sciaridae) of the Atlantic Islands (Canary Islands, Madeira and the Azores). *Boletim do Museu Municipal do Funchal (Suplemento 3)*: 1–170. [História Natural]
- Chandler PJ, Bechev DN, Caspers N (2006) The fungus gnats (Diptera: Bolitophilidae, Diadocidiidae, Ditomyiidae, Keroplatidae and Mycetophilidae) of Greece, its islands and Cyprus. *Studia Dipterologica* 12: 255–314.
- Evenhuis NL (2006) Catalog of Keroplatidae of the World (Insecta: Diptera). *Bishop Museum Bulletin in Entomology* 13: 1–178.
- Kettani K, Ebejer MJ, Ackland DM, Bächli G, Barraclough D, Barták M, Carles-Tolrà M, Černý M, Cerretti P, Chandler P, Dakki M, Dauterion C, De Jong H, Dils J, Disney H, Droz B, Evenhuis N, Gatt P, Gracioli G, Grichanov IY, Haenni J-P, Hauser M, Himmi O, Macgowan I, Mathieu B, Mouna M, Munari L, Nartshuk EP, Negrobov OP, Oosterbroek P, Pape T, Pont AC, Popov GV, Rognes K, Skuhrová M, Skuhrový V, Speight M, Tomasovic G, Trari B, Tschorsnig H-P, Vala J-C, von Tschirnhaus M, Wagner R, Whitmore D, Woźnica AJ, Zatwarnicki T, Zwick P (2022) Catalogue of the Diptera (Insecta) of Morocco—An annotated checklist, with distributions and a bibliography. *ZooKeys* 1094: 1–466. <https://doi.org/10.3897/zookeys.1094.62644>
- Matile L (1986) L'identité du “ver de la tipule de l'Agaric” de Réaumur, et notes taxonomiques sur les *Keroplatus* paléarctiques (Diptera, Mycetophiloidea, Keroplatidae). *Annales de la Société Entomologique de France* 22: 353–367.
- Pape T, Blagoderov V, Mostovski MB (2011) Order Diptera Linnaeus, 1758. In: Zhang ZQ (Ed.) *Animal biodiversity: an outline of higher-level classification and survey of taxonomic richness*. *Zootaxa* 3148: 222–229. <https://doi.org/10.11646/zootaxa.3148.1.42>

A fossil species found living off southern California, with notes on the genus *Cymatinoa* (Mollusca, Bivalvia, Galeommatoidea)

Paul Valentich-Scott¹, Jeffrey H. R. Goddard²

¹ Santa Barbara Museum of Natural History, 2559 Puesta del Sol, Santa Barbara, California 93105, USA

² Marine Science Institute, University of California, Santa Barbara, Santa Barbara, California 93106, USA

Corresponding author: Paul Valentich-Scott (pvsconfig@sbnature2.org)

Academic editor: Graham Oliver | Received 21 September 2022 | Accepted 17 October 2022 | Published 7 November 2022

<https://zoobank.org/5A7D93B2-1D5A-4187-9CCE-66B64B7A0C64>

Citation: Valentich-Scott P, Goddard JHR (2022) A fossil species found living off southern California, with notes on the genus *Cymatinoa* (Mollusca, Bivalvia, Galeommatoidea). ZooKeys 1128: 53–62. <https://doi.org/10.3897/zookeys.1128.95139>

Abstract

A small bivalve mollusk previously only known from the Pleistocene of Los Angeles County has recently been found living intertidally near Santa Barbara, California. The bivalve has been determined to be *Cymatinoa cooki* (Willett, 1937), a member of the Galeommatoidea J.E. Gray, 1840. We document the habitat for the newly discovered *C. cooki*, and compare it to *C. electilis* (Berry, 1963), the other extant member of this genus recorded from the region. *Cymatinoa cooki* is rare, and while many galeommatoid species have been shown to be commensal with other invertebrates, we have been unable to determine any specific commensal relationships for it.

Keywords

Commensal, intertidal zone, Pleistocene, taxonomy

Introduction

The invertebrates inhabiting the rocky intertidal zone of southern and central California are among the most studied and documented in the world (Morris et al. 1980; Ricketts et al. 1985; Carlton 2007). The bivalve mollusks of this region and in this

habitat have also been extensively researched (Coan et al. 2000; Coan and Valentich-Scott 2007). It is thus a surprise that a bivalve previously known only from the Pleistocene has been recently discovered living on the underside of intertidal rocks at Naples Point in Santa Barbara County, California. This small, translucent bivalve is clearly identifiable as a member of the frequently cryptic yet exceedingly diverse superfamily Galeommatoida J.E. Gray, 1840.

Our recently collected specimens belong to the poorly understood genus *Cymatioa* Berry, 1964. The only other living representative of this genus in southern California is *C. electilis* (Berry, 1964). We examined the type specimens of *C. electilis* and concluded they were not the same as our Naples Point species. With subsequent research, we determined our species matched the holotype of *C. cooki* (Willett, 1937) from the Baldwin Hills Pleistocene of Los Angeles County.

Galeommatoidan bivalve mollusks have been extensively documented for nearly 200 years (Turton 1825; Deshayes 1856; Morton and Scott 1989; Goto et al. 2012; Li et al. 2012). Members of the superfamily are exceptionally diverse, with both free-living and commensal species (Li et al. 2016). Those with commensal relationships have been documented living in association with many different invertebrate hosts, including echinoderms, crustaceans, and annelids (Morton and Scott 1989; Goto et al. 2012).

Willett (1937) documented the molluscan fauna at Baldwin Hills, central Los Angeles, during the time a sewer line was being installed. The sewer trench uncovered a 20–30 cm thick Pleistocene deposit of invertebrate and vertebrate fossils, approximately four feet below ground level. In his publication, Willett recognized 296 species of mollusks and described two new species of galeommatoidan bivalves, *Rochefortia reyana* and *Bornia cooki* [now *Cymatioa cooki*].

Bandy and Marinovich (1973) estimated the Baldwin Hills deposits to be between 36,000 and 28,000 years before the present. The deposits range from 78 to 146 m above current sea level and are approximately 10 km from the modern coastline.

The environment at Naples Point was described in detail by Sousa (1979), who conducted ecological research there (termed the Ellwood Boulder Field) and by Goddard et al. (2020), who conducted a long-term study of heterobranch sea slugs at the point. Common macro-invertebrates observed under boulders and cobbles by the latter included Striped Shore Crabs *Pachygrapsus crassipes* Randall, 1840, juvenile Bat Stars *Patiria miniata* (Brandt, 1835), juvenile Purple Sea Urchins *Strongylocentrotus purpuratus* (Stimpson, 1857), the Banded Turban Snail *Tegula eiseni* Jordan, 1936, the chitons *Stenoplax conspicua* (Dall, 1879), *Lepidozonia pectinulata* (Carpenter in Pilsbry 1893), and *Leptochiton rugatus* (Carpenter in Pilsbry 1892), the Tidepool Ghost Shrimp *Neotrypaea bifari* (Holthuis, 1991) and its commensal goby *Typhlogobius californiensis* (Steindachner, 1879), the Peanut Worm *Phascolosoma agassizii* Keferstein, 1866, the brittle star *Ophioplocus esmarki* Lyman, 1874, and juvenile two-spot octopuses (*Octopus* sp.). It was near the end of the study by Goddard et al. (2020) that he found the living galeommatid bivalve described herein.

Materials, methods, site details, and abbreviations

The galeommatid bivalve we describe here was collected by hand by the second author at Naples Point, located on the south coast of Santa Barbara County, 24 km west of Santa Barbara (approximately 34.43, -119.95). This area is within the Naples State Marine Conservation Area. The second author also found two living specimens, shell length about 10 mm, on 23 November 2018, under a low intertidal boulder and photographed but did not collect them (Fig. 1C, D). On 4 March 2019, the second author found a third specimen, shell length 7.4 mm, on the underside of a low intertidal boulder, about 10 m east from where the first two specimens were found. After the third specimen was photographed *in situ* and collected, additional images were taken following relaxation in MgCl_2 (Fig. 1A, B). On 10 December 2019, a fourth specimen, a left shell valve 8.8 mm long, was found underneath a low intertidal boulder (Fig. 2A–C). Subsequent visits to the same locality did not yield any additional shells or living animals.

Abbreviations: CASIZG, Invertebrate Zoology and Geology, California Academy of Sciences, San Francisco, California, USA; SBMNH, Invertebrate Zoology, Santa Barbara Museum of Natural History, Santa Barbara, California, USA; LACMIP, Invertebrate Paleontology, Natural History Museum of Los Angeles County, Los Angeles, California, USA.

Systematic account

Superfamily Galeommatoidea J.E. Gray, 1840

Family Galeommatidae J.E. Gray, 1840

***Cymatioa* Berry, 1964**

Crenimargo Berry, 1963, not Cossmann, 1902. Type species (monotypy): *Crenimargo electilis* Berry, 1963. Recent, eastern Pacific.

Cymatioa Berry, 1964, new name for *Crenimargo* Berry, not Cossmann.

Description. Shell ovate; subequilateral; exterior surface finely punctate; sculpture of sparse, broad, low, radial ribs; ventral margin undulate; right valve with one anterior cardinal tooth; left valve with two anterior cardinal teeth.

Commensal relationships. Baldwin (1990) reported *Cymatioa electilis* from Nayarit, Mexico, 20 cm deep and byssally attached to the walls of the burrows of the ghost shrimp, *Axiopsis serratifrons* (Milne-Edwards, 1873).

Discussion. Huber (2015) suggested a number of species that might fall within *Cymatioa* based on their punctate sculpture and undulate ventral margin. While the type species of *Cymatioa* was described from Colima, Mexico, the species he included in this genus are distributed in tropical locations around the globe.

***Cymatinoa cooki* (Willett, 1937)**

Figs 1A–H, 2A–C

Bornia cooki Willett, 1937: 389, pl. 5, figs 3–6.

Description. *Shell:* thin, fragile, subovate; inequilateral, posterior end much longer; anterior and posterior ends broadly rounded; dorsal margin gently sloping on each side of umbos; ventral margin broadly gaping in living animal; beaks small, sharply pointed; prodissoconch 200 μm in diameter; sculpture of irregular, slightly wavy com-marginal striae, and fine, dense punctae; ventral margin with sparse, broad, low radial undulations; periostracum thin, light beige, silky; hinge plate narrow; right valve with one short anterior cardinal tooth, one elongate posterior lateral tooth; left valve with two minute anterior cardinal teeth, one elongate posterior lateral tooth; ligament internal, opisthodontic, elongate; resilifer narrow, elongate; ventral margin slightly wavy internally; adductor muscle scars subovate, subequal; pallial line entire; strong accessory muscle scars dorsal to pallial line. Length to 11.4 mm (Willett 1937).

Mantle: large, reflected, covering most of outer shell surface when fully extended, including umbones (Fig. 1A); mantle can be mostly retracted into the shell; reflected portion of mantle sparsely papillate (Fig. 1A); slightly fused posteroventrally; two anterior and two posterior tentacles, short, slightly extending past shell margins (Fig. 1A, B).

Foot: large, translucent, exceeding the length of the shell when fully extended, spathate, with distinct pointed heel; bright white stripe extending from the tip of foot to the shell margin, presumably related to byssal formation (Fig. 1A). This species is an active crawler (Fig. 1C).

Type locality. Baldwin Hills Pleistocene deposit, Los Angeles County, California; 33.9658, -118.4264; LACMIP locality 59.

Locality of living specimens. USA, California, Santa Barbara County, off Naples Point; 34.4339, -119.9500; intertidal zone, in boulders and cobbles. SBMNH 629938, conjoined shell and anatomy, length 7.4 mm, height 4.5 mm (Fig. 1A, B); SBMNH 641848, (Fig. 2A–C), one left valve length 8.8 mm, height 5.5 mm.

Habitat and potential commensal relationships. All three living specimens were found near the seaward edge of a boulder field centered at 34.4339, -119.9500 and located on a broad, gently sloping, wave-cut bench of Monterey Shale. This boulder field extends vertically from a tidal height of approximately +0.3 m above mean lower low water to -0.4 m. The surfgrass *Phyllospadix torreyi* S. Watson, 1879, dominates much of the surrounding bench. At low tide, a shallow lagoon lies just landward of the boulder field, and behind that are more shale bench, a narrow sand beach, and then cliffs up to 20 m high consisting of Monterey shale overlain by terrestrial deposits. Sand levels on the beach and in the lagoon fluctuate seasonally, with nearly all of the beach scoured away in winter, but the boulder field as a whole is never significantly inundated, especially at its seaward edge where the *Cymatinoa* was found. Vertical relief in the boulder field is fairly low, with most boulders under 0.5 m diameter. A few rock outcrops just to the west are only about 1 m high.

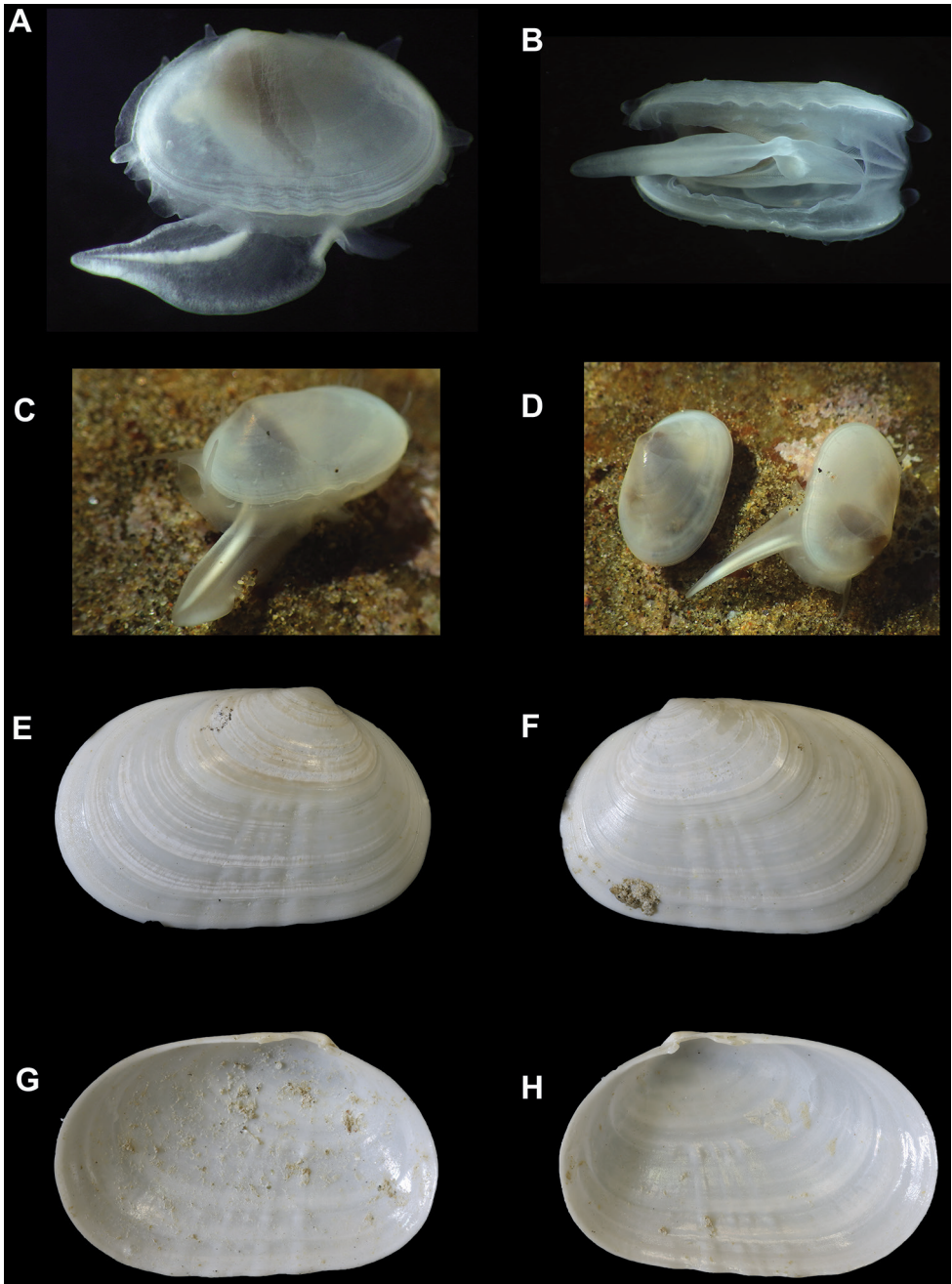


Figure 1. *Cymatinoa cooki*. **A, B** living animal from Naples Point, SBMNH 629938, length = 7.4 mm **A** lateral view with extended foot, note mantle papillae anteriorly and dorsally **B** ventral view with wide, long mantle gape **C, D** animals on native substratum **E-H** holotype, LACMIP 59.2., length = 9.7 mm **E** exterior of right valve **F** exterior of left valve **G** interior of left valve **H** interior of right valve.

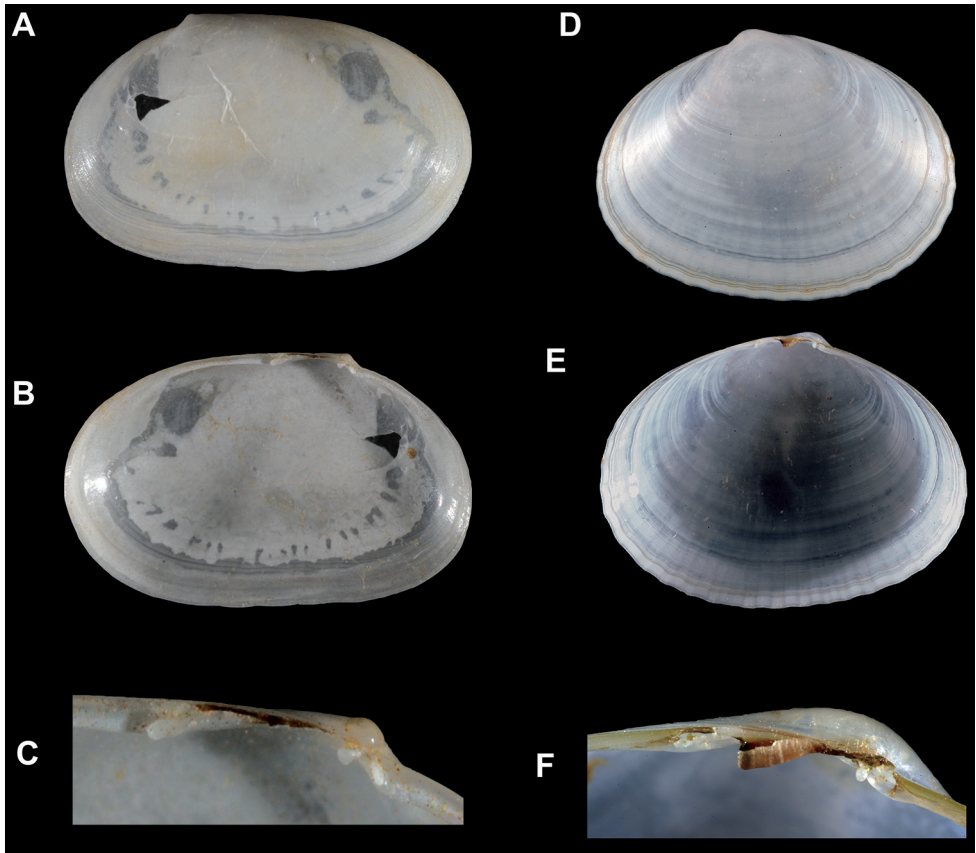


Figure 2. **A–C** *Cymatinoa cooki*, shell of left valve collected at Naples Point, SBMNH 641848, length 8.8 mm **A** exterior of valve **B** interior of valve **C** close up of hinge **D–F** *Cymatinoa electilis*, left valve **D, E** holotype, CASIZG 043976, length = 16 mm **D** exterior of valve **E** interior of valve **F** paratype, SBMNH 34017, close up of hinge.

The specimens found on 23 November 2018 were on sand underneath a boulder (Fig. 1C, D). One of these was found at the entrance to a burrow of unknown origin, with its foot extended and tentaculate inhalant siphon extending into the burrow opening. The burrow may have been constructed by the Tidepool Ghost Shrimp, *Neotrypaea biffari* (Holthuis, 1991), which occur frequently under boulders at this site, usually with commensal Blind Gobies *Typhlogobius californiensis* Steindachner, 1879. This sighting is vouchered in eight images at <https://www.inaturalist.org/observations/18597683>, with the last image showing one of the specimens as first observed, next to the burrow entrance described above.

The specimen found on 4 March 2019 was on the underside of a boulder, among scattered tubes of the annelid *Spirorbis* sp. and small, scattered patches of an unidentified tan-colored encrusting sponge. Two small dorid nudibranchs, *Conualevia alba* Collier & Farmer, 1964; a single mussel, *Mytilisepta bifurcata* (Conrad, 1837); and an

adult chiton, *Stenoplax conspicua* (Dall, 1879), were also present, all within a few centimeters of the *C. cooki*. Burrow openings of unknown origin and 3–5 mm in diameter were also present on the undersurface of the boulder. This sighting is vouchered in six images at <https://www.inaturalist.org/observations/20962245>.

Comparisons. The shell morphology of *C. cooki* is closest to *C. electilis*, with both species sharing a commarginal and punctate sculpture and an undulate ventral margin (Fig. 2A–F). *Cymatinoa cooki* is subquadrate and inequilateral, with a much longer posterior end (Fig. 2A), whereas *C. electilis* is subovate with a slightly longer posterior end (Fig. 2D). The cardinal teeth in both species are quite small and similar; however, the posterior lateral tooth in *C. cooki* is longer and more robust (Fig. 2C) than that of *C. electilis* (Fig. 2F). Because the living animal is undocumented for *C. electilis*, we are unable to provide anatomical comparisons. However, based on other galeommatid taxa, many differences in mantle tentacles and papillae are likely.

Discussion

Previously only known from the Pleistocene of Los Angeles, *Cymatinoa cooki* is herein recorded living for the first time. Only three living specimens have been discovered to date. Despite *C. cooki*'s potential commensal relationship with burrowing invertebrates, we have not sampled the intertidal infauna deeply enough to discover the potential true habitat for this species.

Depending on the lifespan of *C. cooki*, the adults we observed at Naples Point may have been transported as larvae from much farther south during the marine heatwaves of 2014–2016, which drove northward numerous marine species distributions in the northeastern Pacific (Cavole et al. 2016; Sanford et al. 2019), including populations documented specifically at Naples Point (Goddard et al. 2016, 2018). This might explain why the second author did not find *C. cooki* at this site prior to 2018, despite intensively searching the same under-rock habitat for heterobranch sea slugs at Naples Point since 2002 (Goddard et al. 2020).

Other Baldwin Hills Pleistocene bivalves reported by Willett (1937) have been documented as living in southern California. *Mytilus adamsianus* [= *Brachidontes adamsianus* (Dunker, 1857)] is a common modern rocky intertidal species from Santa Cruz Island, California, to northern Peru (Coan and Valentich-Scott 2012). *Ensis californicus* [= *Ensis myrae* (Berry, 1953)] and *Petricola "tellimyalis"* [= *Petricola hertzana* (Coan, 1997)] are also found intertidally in southern California with the former in sandy protected environments and the latter associated with giant kelp holdfasts (Coan and Valentich-Scott 2012). The *Cymatinoa* specimen described by Willett (1937) was named for a Miss Edna T. Cook, who collected the specimens.

Given the small size, translucent shell, and cryptic habits of *C. cooki*, it is not surprising that living instances of the species have been overlooked for over 80 years. We are confident that its description here will lead to discovery of further examples in southern California and likely even further south into Mexico.

Acknowledgements

Austin Hendy and Lindsay Walker from LACMIP provided loans, images, and data for type specimens of *Cymatinoa cooki*. Eugene V. Coan and Robert Dees provided many useful comments and corrections on this manuscript.

Publication costs have been graciously provided by the Southern California Association of Marine Invertebrate Taxonomists Publication Grant (www.scamit.org). We appreciate the assistance of Megan Lilly and Erin Oderlin in facilitating our grant application.

References

- Baldwin AP (1990) *Cymatinoa electilis* (Berry, 1963) in association with the shrimp *Axius*. The Festivus 22: 92. [See correction of shrimp's name, The Festivus 22: 118]
- Bandy OL, Marinovich Jr L (1973) Rates of Late Cenozoic uplift, Baldwin Hills, Los Angeles, California. Science 181(4100): 653–655. <https://doi.org/10.1126/science.181.4100.653>
- Berry SS (1953) West American razor-clams of the genus *Ensis*. San Diego Society of Natural History, Transactions 11: 393–404. [pl. 29]
- Berry SS (1963) Notices of new eastern Pacific Mollusca — V. Leaflets in Malacology 1: 139–146.
- Berry SS (1964) Notices of new eastern Pacific Mollusca— VI. Leaflets in Malacology 1: 147–154.
- Brandt JF (1835) Prodomus descriptionis Animalium ab H. Mertensio in orbis terrarum circumnavigatione observatorum. Petropoli Museo Zoologica 1: 203–275.
- Carlton JT (2007) The Light and Smith Manual. Intertidal Invertebrates from Central California to Oregon, 4th edn. University of California, Berkeley, [xvii +] 1001 pp. <https://doi.org/10.1525/9780520930438>
- Cavole LM, Demko AM, Diner RE, Giddings A, Koester I, Pagniello CMLS, Paulsen M-L, Ramirez-Valdez A, Schwenck SM, Yen NK, Zill ME, Franks PJS (2016) Biological impacts of the 2013–2015 warm-water anomaly in the Northeast Pacific: Winners, losers, and the future. Oceanography 29(2): 273–285. <https://doi.org/10.5670/oceanog.2016.32>
- Coan EV (1997) Recent species of the genus *Petricola* in the eastern Pacific (Bivalvia: Veneroidea). The Veliger 40: 298–340.
- Coan EV, Valentich-Scott PH (2007) Bivalvia. In: Carlton JP (Ed.) Light's Manual: Intertidal Invertebrates from the Central California Coast. University of California, Berkeley, 807–859.
- Coan EV, Valentich-Scott PH (2012) Bivalve Seashells of Tropical West America. Marine Bivalve Mollusks from Baja California to Northern Perú. Santa Barbara Museum of Natural History, Monographs 6. Santa Barbara Museum of Natural History, Santa Barbara, [xv +] 1258 pp.
- Coan EV, Valentich-Scott PH, Bernard FR (2000) Bivalve Seashells of Western North America. Marine Bivalve Mollusks from Arctic Alaska to Baja California. Santa Barbara Museum of Natural History, Monographs 2. Santa Barbara Museum of Natural History, Santa Barbara, [viii +] 764 pp.
- Collier CL, Farmer WM (1964) Additions to the nudibranch fauna of the east Pacific and the Gulf of California. Transactions of the San Diego Society for Natural History 13: 377–396. <https://doi.org/10.5962/bhl.part.9602>

- Conrad TA (1837) Descriptions of new marine shells, from Upper California collected by Thomas Nuttall, Esq. *Journal of the Academy of Natural Sciences of Philadelphia* 7: 227–268.
- Cossmann M (1902) Appendice No. 3 au Catalogue illustré des coquilles fossiles de l'Éocène des environs de Paris. *Annales de la Société royale zoologique et malacologique de Belgique* 36: 9–110. [pls 2–7]
- Dall WH (1879) Report on the limpets and chitons of the Alaskan and Arctic regions, with descriptions of genera and species believed to be new. *Proceedings of the United States National Museum* 1(48): 281–344. <https://doi.org/10.5479/si.00963801.1-48.281>
- Deshayes GP (1856) Sur le genre *Scintilla*. *Zoological Society of London. Proceedings for 1855(23)*: 171–181.
- Dunker WBRH (1857) Mytilacea nova collectionis Cumingianae, descripta.... *Zoological Society of London. Proceedings for 1856(24)*: 358–366.
- Goddard JHR, Treneman N, Pence WE, Mason DE, Dobry PM, Green B, Hoover C (2016) Nudibranch range shifts associated with the 2014 warm anomaly in the NE Pacific. *Bulletin of the Southern California Academy of Sciences* 115(1): 15–40. <https://doi.org/10.3160/soca-115-01-15-40.1>
- Goddard JHR, Treneman N, Prestholdt T, Hoover C, Green B, Pence WE, Mason DE, Dobry PM, Sones JL, Sanford E, Agarwal R, McDonald GR, Johnson RF, Gosliner TM (2018) Heterobranch sea slug range shifts in the Northeast Pacific Ocean associated with the 2015–16 El Niño. *Proceedings of the California Academy of Sciences* 65(3): 107–131.
- Goddard JHR, Goddard WM, Goddard ZE (2020) Benthic heterobranch sea slugs (Gastropoda: Heterobranchia) from Santa Barbara County, California I. Review of the literature, and Naples Point, 2002–2019. *Proceedings of the California Academy of Sciences* 66(10): 275–298.
- Goto R, Kawakita A, Ishikawa H, Hamamura Y, Kato M (2012) Molecular phylogeny of the bivalve superfamily Galeommatoidea (Heterodonta, Veneroidea) reveals dynamic evolution of symbiotic lifestyle and interphylum host switching. *BMC Evolutionary Biology* 12(1): 172. <https://doi.org/10.1186/1471-2148-12-172>
- Gray JE (1840) Mollusks. In: *Synopsis of the Contents of the British Museum*, 42nd edn. G. Woodfall and Son, London, 105–152.
- Holthuis LB (1991) *FAO Species Catalogue. Vol. 13. Marine Lobsters of the World. An Annotated and Illustrated Catalogue of Species of Interest to Fisheries Known to Date.* *FAO Fisheries Synopsis* 125: 1–292.
- Huber M (2015) *Compendium of Bivalves 2.* ConchBooks, Hackenheim, 907 pp.
- Jordan EK (1936) The Pleistocene fauna of Magdalena Bay, Lower California. *Contributions of the Department of Geology, Stanford University* 1: 107–173.
- Keferstein W (1866) Untersuchungen über einige amerikanische Sipunculiden. *Nachrichten von der Königlichen Gesellschaft der Wissenschaften und der Georg-August-Universität zu Göttingen* 14: 215–228.
- Li J, Ó Foighil D, Middelfart PU (2012) The evolutionary ecology of biotic association in a megadiverse bivalve superfamily: Sponsorship required for permanent residence in sediment. *PLoS ONE* 7(8): e42121. <https://doi.org/10.1371/journal.pone.0042121>

- Li J, Ó Foighil D, Strong EE (2016) Commensal associations and benthic habitats shape macroevolution of the bivalve clade Galeommatoidea. *Royal Society of London: Proceedings B* 283: 20161006. <https://doi.org/10.1098/rspb.2016.1006>
- Lyman T (1874) Ophiuridae and Astrophytidae: New and old. *Bulletin of the Museum of Comparative Zoölogy at Harvard College* 3: 221–272.
- Milne-Edwards A (1873) Description de quelques crustacés nouveaux ou peu connus provenant du musée de M. C. Godeffroy. *Journal des Muséum Godeffroy* 1: 253–264. [pls 12, 13] <https://doi.org/10.5962/bhl.title.10644>
- Morris RH, Abbott DP, Haderlie EC (1980) *Intertidal Invertebrates of California*. Stanford University Press, Stanford, 690 pp.
- Morton B, Scott PH (1989) The Hong Kong Galeommatacea (Mollusca: Bivalvia) and their hosts, with descriptions of new species. *Asian Marine Biology* 6: 129–160.
- Pilsbry HA (1892) Monograph of the Polyplacophora. In: *Manual of Conchology*. Academy of Natural Sciences, Philadelphia 14: 1–128.
- Pilsbry HA (1893) Monograph of the Polyplacophora. In: *Manual of Conchology*. Academy of Natural Sciences, Philadelphia: 15: 129–350.
- Randall JW (1840) Catalogue of the Crustacea brought by Thomas Nutall and J.K. Townsend from the West Coast of North America and the Sandwich Islands, with descriptions of such species as are apparently new, among which are included several species of different localities, previously existing in the collection of the Academy. *Journal of the Academy of Natural Sciences of Philadelphia* 8: 106–147 [pls 3–7].
- Ricketts EF, Calvin J, Hedgpeth JW, Phillips DW (1985) *Between Pacific Tides*. 5th edn. Stanford University Press, Stanford, 682 pp. <https://doi.org/10.1515/9781503621329>
- Sanford E, Sones JL, García-Reyes M, Goddard JHR, Largier JL (2019) Widespread shifts in the coastal biota of Northern California during the 2014–2016 marine heatwaves. *Scientific Reports* 9(1): 4216. <https://doi.org/10.1038/s41598-019-40784-3>
- Sousa WP (1979) Experimental investigations of disturbance and ecological succession in a rocky intertidal algal community. *Ecological Monographs* 49(4): 228–254. <https://doi.org/10.2307/1942472>
- Steindachner F (1879) *Ichthyologische Beiträge (VIII.)*. *Sitzungsberichte der Akademie der Wissenschaften mathematisch-naturwissenschaftliche Klasse* 80: 119–191.
- Stimpson W (1857) On the Crustacea and Echinodermata of the Pacific shores of North America. *Boston Journal of Natural History* 6: 444–532. [pls 18–23] <https://doi.org/10.5962/bhl.title.59693>
- Turton W (1825) Description of some new British shells; accompanied by figures from the original specimens. *Zoological Journal* 2: 361–367. [pl. 13]
- Watson S (1879) Contributions to American botany: Revision of the North American Liliaceæ; descriptions of some new species of North American plants. *Proceedings of the American Academy of Arts and Sciences* 14: 213–303. <https://doi.org/10.2307/25138538>
- Willett G (1937) An upper Pleistocene fauna from the Baldwin Hills, Los Angeles County, California. *San Diego Society of Natural History, Transactions* 8: 379–406 [pls 25, 26]. <https://doi.org/10.5962/bhl.part.14904>

Genetic and morphometric analyses of historical type specimens clarify the taxonomy of the Ethiopian *Leptopelis gramineus* species complex (Anura, Arthroleptidae)

Sandra Goutte¹, Jacobo Reyes-Velasco^{1,2}, Abeje Kassie^{3,4}, Stéphane Boissinot¹

1 New York University Abu Dhabi, Saadiyat Island, Abu Dhabi, United Arab Emirates **2** Entorno Biotico A.C., Colima, Colima, Mexico **3** Ethiopian Biodiversity Institute, Addis Ababa, Ethiopia **4** Addis Ababa University, Addis Ababa, Ethiopia

Corresponding authors: Sandra Goutte (sg5533@nyu.edu), Stéphane Boissinot (stephane.boissinot@nyu.edu)

Academic editor: Angelica Crottini | Received 12 February 2022 | Accepted 5 September 2022 | Published 7 November 2022

<https://zoobank.org/74F7E96B-1198-487C-9EAF-56C63E958610>

Citation: Goutte S, Reyes-Velasco J, Kassie A, Boissinot S (2022) Genetic and morphometric analyses of historical type specimens clarify the taxonomy of the Ethiopian *Leptopelis gramineus* species complex (Anura, Arthroleptidae). ZooKeys 1128: 63–97. <https://doi.org/10.3897/zookeys.1128.82176>

Abstract

Frogs of the genus *Leptopelis* have diversified in the Ethiopian Highlands to occupy forests and montane grasslands both east and west of the Great Rift Valley. Genetic studies revealed that the endemic species *Leptopelis gramineus* (Boulenger, 1898) comprises multiple unnamed taxa. A careful examination of historical type specimens is, however, needed to fully resolve the taxonomy of the group. Here we use mitochondrial DNA and morphological analyses on a large sample of recently-collected Ethiopian *Leptopelis*, as well as century-old type specimens to demonstrate that the recently resurrected *L. montanus* Tiutenko & Zinenko, 2021 (previously *Pseudocassina ocellata* Ahl, 1924) is a junior synonym of *L. rugosus* (Ahl, 1924) and corresponds to the taxon found west of the Great Rift Valley, not east as previously thought. Our results show that populations inhabiting the mountains and plateaus east of the Rift constitute a distinct and undescribed species. We provide a re-description of *L. rugosus* and describe two new species inhabiting the Highlands east of the Great Rift Valley. We provide an identification key, as well as a description of the calls of the members of the *Leptopelis gramineus* species complex.

Keywords

African treefrogs, Afromontane, historical DNA, integrative taxonomy, *Leptopelis shebellensis* sp. nov., *Leptopelis xeniae* sp. nov., museomics, new species

Introduction

Leptopelis is a genus of sub-Saharan treefrogs, currently counting 54 species (Frost 2021). Members of this genus occupy a great diversity of habitats, from dry savannah to swamp forest and from lowland rainforest to montane grassland. Some species have abandoned the arboreal lifestyle of their ancestors and adopted a terrestrial or semi-fossorial life. In the Ethiopian Highlands, the genus *Leptopelis* has diversified into at least seven endemic species: four fully arboreal forms (*L. vanmutellii* (Boulenger, 1898), *L. ragazzi* (Boulenger, 1898), *L. susanae* Largen, 1977 and *L. yaldeni* Largen, 1977), two burrowing forms (*L. gramineus* (Boulenger, 1898) and *L. montanus* Tiutenko & Zinenko, 2021) and one species found either on low vegetation, ground or in shallow burrows (*L. diffidens* Tiutenko & Zinenko, 2021).

The Ethiopian burrowing treefrog *Leptopelis gramineus* was described as *Megalixalus gramineus* by Boulenger (1898), based on several individuals collected in southeast Ethiopia (“Between Badditù and Dimé”, see Fig. 1) during Captain Bottego’s expedition in 1895–1897. Two species, *Pseudocassina ocellata* and *Pseudocassina rugosa*, were subsequently described by Ahl (1924), based on individuals collected further north, during Oscar Neumann’s and Carlo von Erlanger’s expedition in 1900, but later synonymised with *Leptopelis gramineus* by Largen (1977). Largen also provided a distribution map of *L. gramineus*, which spanned habitats from 1,900 m to 3,900 m a.s.l. across the Ethiopian Highlands, both east and west of the Great Rift Valley (GRV). Using mitochondrial sequences and a small number of nuclear genes, Freilich et al. (2016) showed that *L. gramineus* was likely a species complex consisting of four taxa: one occupying the highlands west of the GRV (“West” clade in Freilich et al. 2016), one occupying the plateaus and mountains east of the GRV (“Arsi” clade) and two limited to the mountain forests of the southeast (the “Kibre Mengist” and the “Katcha” clades). Using a combination of mitochondrial sequences, nuclear sequences and ddRAD-sequencing data, Reyes-Velasco et al. (2018) confirmed the presence of the four clades of Freilich et al. (2016), but also detected additional population structures east and west of the GRV. Recently, Tiutenko and Zinenko (2021) restricted the use of the name *L. gramineus* to populations of the Gamo Goffa area (i.e. west of the GRV), based on the careful examination of the collection diary and described *L. diffidens*, which corresponds to the “Katcha” lineage of Freilich et al. (2016) and to the “Hareenna” lineage of Reyes-Velasco et al. (2018). In the same article, they removed the name *Leptopelis ocellatus* (= *Pseudocassina ocellata*) from the synonymy with *L. gramineus*, based on the genetic results of Reyes-Velasco et al. (2018) and a few specimens collected near the type locality and applied it to the mountain and plateau populations found east of the GRV (“Arsi” clade of Freilich et al. 2016 and “Bale Mountains” clade of Reyes-Velasco et al. 2018). As a species named *Leptopelis ocellatus* had been previously described from west Africa, Tiutenko and Zinenko assigned a new name to the species, *Leptopelis montanus* Tiutenko & Zinenko, 2021. These nomenclatural acts were, however, not supported

by the examination of any of the historical type specimens of *Leptopelis gramineus*, *Pseudocassina ocellata* or *P. rugosa*, but based only on their respective type localities. Finally, Tiutenko and Zinenko (2021) suggested the existence of two additional species, one found on the plateaus west of the GRV (*L. sp.* “Shewa”, corresponding to the “Northern” clade of Reyes-Velasco et al. 2018), which would correspond to *L. rugosus* (= *P. rugosa*) and one from the forests of the southeast (*L. sp.* “Borana/Sidamo”, corresponding to the “Kibre Mengist” clade of Freilich et al. 2016 and Reyes-Velasco et al. 2018), but did not name or describe either of them due to a lack of data.

Here, we use mitochondrial DNA and morphological data of individuals of the *Leptopelis gramineus* complex, including the holotypes of *L. gramineus* and *P. rugosa* and the lectotype of *Pseudocassina ocellata* to clarify the taxonomic status of multiple species and populations from the Ethiopian Highlands. Our results show that *Pseudocassina rugosa* and *P. ocellata* are conspecific and distinct from *L. gramineus*. Furthermore, the lectotype of *P. ocellata* is not conspecific with the population occurring in the Bale Mountains and considered as *L. montanus* (= *P. ocellata*) by Tiutenko and Zinenko (2021). The Bale Mountains lineage thus constitutes a new species, which we describe hereafter. We also describe a forest species and resurrect *Leptopelis rugosus* (= *P. rugosa*) from the synonymy with *L. gramineus* and provide a re-description of the species.

Materials and methods

Sampling

Methods of sampling are discussed in detail in Reyes-Velasco et al. (2018). In brief, we collected individuals of the *Leptopelis gramineus* species complex from the Highlands of Ethiopia between 2011 and 2018 (Fig. 1; Suppl. material 5: table S1). Our study was approved by the relevant Institutional Animal Care and Use Committee at Queens College and New York University School of Medicine (IACUC; Animal Welfare Assurance Number A32721–01 and laboratory animal protocol 19–0003). Frogs were sampled according to permits DA31/305/05, DA5/442/13, DA31/454/07, DA31/192/2010, DA31/230/2010, DA31/7/2011 and DA31/02/11 provided by the Ethiopian Wildlife Conservation Authority. We photographed individuals in life and euthanised them by ventral application of 20% benzocaine gel. We extracted tissue samples and stored them in RNAlater or 95% ethanol. Adult individuals were fixed in 10% formalin for 24 to 48 hours, rinsed in water and transferred to 70% ethanol. We took additional photographs of all individuals after preservation. All specimens were deposited at the Zoological Natural History Museum of Addis Ababa University (ZNHM), Ethiopia. Tissue samples are deposited at the Vertebrate Tissue Collection, New York University Abu Dhabi (NYUAD).

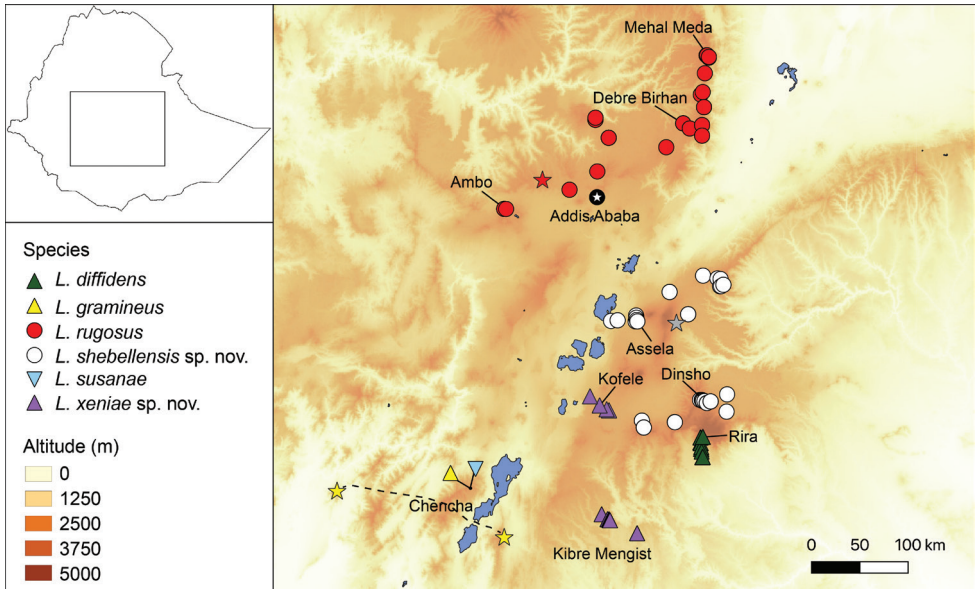


Figure 1. Distribution ranges of six species of the *Leptopelis gramineus* species complex. Small, more arboreal forms are represented by green (*L. diffidens*), yellow (*L. gramineus*) and purple (*L. xeniae* sp. nov.) triangles. Larger, semi-fossorial forms are represented by red (*L. rugosus*) and white (*L. shebellensis* sp. nov.) circles. The large arboreal *Leptopelis susanae* is represented by a light blue triangle. Stars indicate type localities given in the original descriptions of *L. gramineus* (yellow; dashed line between Badditù and Dimé), *Pseudocassina rugosa* (red) and *Pseudocassina ocellata* (grey), both synonymised here with *L. rugosus* (see the discussion in the main text).

DNA extraction and sequencing of type specimens

We obtained the authorisation from the Museum für Naturkunde Berlin (ZMB) to sample a small amount of muscle or liver tissue from the holotype of *P. rugosa* (ZMB-26915) and one of the two syntypes of *Pseudocassina ocellata*, which we here formally designate as lectotype (ZMB-26913; see species account below). Tissue sampling did not result in any major visible damage to the vouchers. We did not obtain tissue samples for the lectotype of *Leptopelis gramineus* (Genoa-28564). The types specimens had most likely been fixed in formalin or in spirit, which renders the extraction of DNA challenging and requires a different protocol than when using fresh tissue. We followed the DNA extraction protocol for formalin-preserved specimens, described by Shedlock et al. (1997) and modified in Reyes-Velasco et al. (2021). A standard potassium acetate DNA precipitation protocol was then followed. We used only new reagents and conducted all DNA extractions in a marine biology lab that does not work with amphibian samples. We used multiple negative controls during every step of the DNA extraction process.

We used a high sensitivity kit in a Qubit fluorometer (Life Technologies) to measure DNA concentration, while DNA fragment size distribution and concentration was estimated on a Bioanalyzer 7500 high sensitivity DNA chip (Agilent, Santa Clara, CA, USA). We used a NEBNext FFPE DNA Repair Mix (New England Biolabs) to repair damaged bases prior to library preparation. Library preparation was performed with the use of a NEB library preparation kit. During library preparation we skipped the shredding step due to the fragmented nature of historical DNA. All libraries were pooled and sequenced on an Illumina NextSeq 550 (75 bp paired-end) at the Genome Core Facility of New York University Abu Dhabi, UAE. We used the FASTx Toolkit (Gordon and Hannon 2010) to remove Illumina adaptors and low quality reads with a mean Phred score below 20. The final average read length post-trimming was 63 bp (Suppl. material 5: table S2). We then checked for biased base composition towards the end of the reads with the programme FastQC, as biased base composition is a common phenomenon in historical or ancient samples which results from de-amination (Dabney et al. 2013). We did not find a biased base composition in our reads. Summary statistics describing the sequencing data are available in Suppl. material 5: table S2. All sequences are deposited in GenBank (Suppl. material 5: table S3).

Assembly of mitochondrial genomes

Whole mitochondrial genomes of the type specimens of *Pseudocassina ocellata* and *Pseudocassina rugosa* were assembled from the Illumina reads using the programme MITObim (Hahn et al. 2013), which uses an iterative baiting method to generate mitochondrial contigs from short Illumina reads. We first used a published sequence of the mitochondrial genome of *Leptopelis vermiculatus* (Boulenger 1909; GenBank JX564875) as the reference mitogenome, with the default programme settings, except for a k-mer length of 21. We then re-ran the analysis using the resulting contigs from the first MITObim run. An additional eight mitochondrial genomes from other members of the *Leptopelis gramineus* species complex were also assembled following the same protocol (Suppl. material 5: table S3).

Phylogenetic analysis of mtDNA

To assess the relationships of the holotypes of *Pseudocassina ocellata* and *P. rugosa* and the validity of the names, we reconstructed phylogenetic relationships within the *Leptopelis gramineus* species complex using all the mitochondrial protein-coding genes, as well as the ribosomal RNA 12s and 16s of the individuals for which we had full mitochondrial genomes. We performed alignments using MAFFT version 7 (Katoh and Standley 2013) and used Geneious v.9.1.6 (Biomatters Ltd., Auckland, NZ) to manually trim any poorly-aligned regions and to ensure that the protein-coding sequences were in the correct reading frame. We performed Maximum Likelihood (ML) analysis in the programme RAxML-HPC BlackBox with 1,000 bootstraps, implemented on the CIPRES Science Gateway server (Miller et al. 2010; Suppl. material 1: fig. S1A).

We also performed a phylogenetic analysis using only sequences of the mitochondrial protein coding gene Cytochrome c oxidase I (COX1). The reason for choosing this gene is that many more sequences of COX1 are available for Ethiopian *Leptopelis* and this gene has been shown to be informative for estimating relationships in this group of frogs (Freilich et al. 2016; Reyes-Velasco et al. 2018), thus allowing for the accurate assignment of the type specimens to species or populations. In order to test whether the phylogenetic inferences, based on COX1, only are comparable with those based on full mitochondrial genomes, we first ran a ML analysis of COX1 using only the individuals for which we have the full mitochondrial genome and compared the topologies of the two phylogenetic trees (Suppl. material 1). We then analysed the full COX1 dataset, which includes all currently-known species and population of the *Leptopelis gramineus* group and consists of 534 bp for 42 individuals, plus an outgroup (vs. 10 individuals and 13,445 bp in the full mitogenome dataset). We selected a best-fit model of nucleotide evolution with the use of the Bayesian Information Criterion (BIC) in PartitionFinder v.1.1.1 (Lanfear et al. 2012; Suppl. material 5: table S4). We performed Bayesian phylogenetic inference (BI) in MrBayes v.3.2.2 (Ronquist et al. 2012) on the CIPRES Science Gateway server (Miller et al. 2010) and additionally performed Maximum Likelihood analysis (ML) in RAXML-HPC BlackBox with 1,000 bootstraps, also implemented on the CIPRES Science Gateway server (Fig. 2, Suppl. material 2).

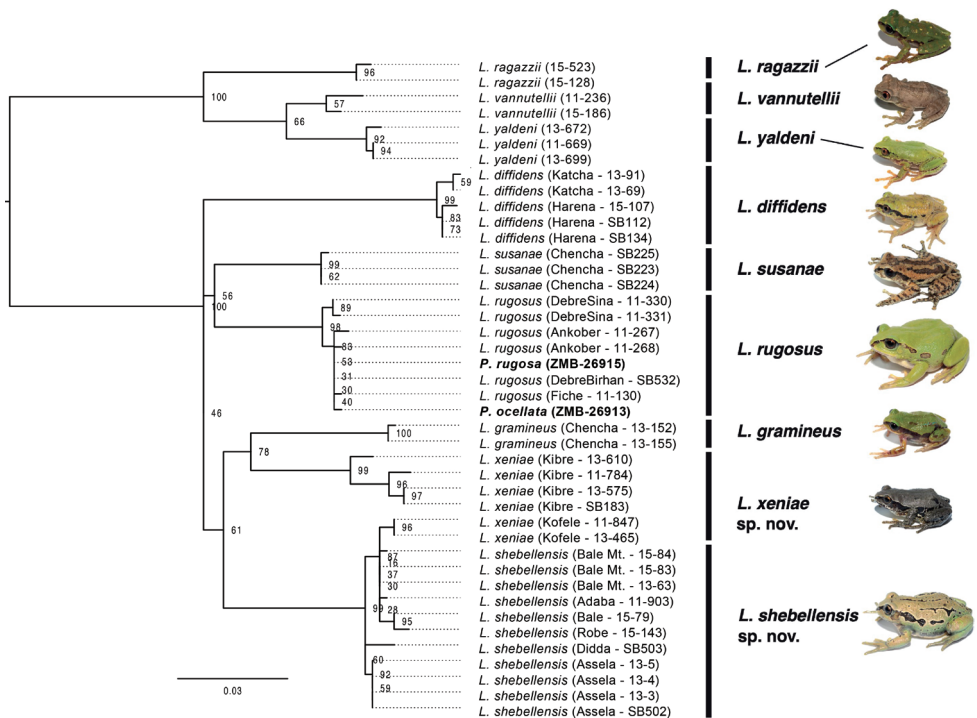


Figure 2. Phylogeny of the *Leptopelis gramineus* species complex. Maximum Likelihood phylogenetic inference, based on COX1. Names in bold represent historical type specimens of *Pseudocassina rugosa* (ZMB-26915) and *Pseudocassina ocellata* (ZMB-26913).

In certain studies of Ethiopian *Leptopelis*, species relationships were inferred using the ribosomal RNA 12s and 16s and no COX1 sequences were available for these specimens (Mengistu 2012; Tiutenko and Zinenko 2021). We thus performed an additional ML analysis on previously-published 16s sequences to establish the relationships between our samples and those collected in these studies (Suppl. material 3).

Genetic distances

We estimated pairwise genetic distances (uncorrected P distances) of the mitochondrial data (whole mitogenome and COX1), including all codon positions, both transitions and transversions and Gamma distributed rates amongst sites in the programme MEGA X (Kumar et al. 2018). Genetic distances are presented in Suppl. material 5: tables S5, S6.

Morphometric measurements

We measured 116 individuals that were collected in recent years, as well as type specimens of *Leptopelis gramineus* (lectotype Genoa-28564; paralectotypes Genoa-49850-1 & Genoa-49850-2), *Pseudocassina ocellata* (ZMB-26913) and *P. rugosa* (ZMB-26915) using a digital caliper (resolution ± 0.01 mm). We took 19 linear morphometric measurements for each specimen (Table 1, Suppl. material 5: table S7), which are defined in Watters et al. (2016) and were shown to be useful for morphological differentiation of anurans.

List of abbreviations: **ED** eye diameter; **EN** eye-nostril distance; **ETD** eye-tympanum distance; **FinDW** longest finger disc width; **FL** foot length; **FLL** forearm length; **HAL** hand length; **HL** head length; **HW** head width; **IND** inter-nares distance; **IOD** inter-orbital distance; **MTL** metatarsal tubercle length; **NS** snout-nostril distance; **SL** snout length; **SVL** snout-vent length; **THL** thigh length; **TD** tympanum diameter; **TL** tibia length; **Toe4DW** fourth toe disc width; **UEW** upper eyelid width.

Statistical analyses of linear morphometric measurements

We analysed males and females separately due to sexual dimorphism (Fig. 3; Table 1). We included the 18 adult individuals measured by Tiutenko and Zinenko in their recent paper (Tiutenko and Zinenko 2021) for a total sample size of 136 adults (108 males, 28 females). As sixteen measurements were shared in both datasets, we thus analysed the two datasets jointly using those measurements and excluding HAL, FL and FinDW from our dataset. We used the R package *FactoMineR* (Lê et al. 2008). As a result of shrinkage due to variable conditions of fixation and long-term preservation of type specimens, we ran discriminant analyses on recently-collected individuals only, in order to select the measurements best discriminating between species (removing the types of *Leptopelis gramineus*, *Pseudocassina rugosa* and *P. ocellata*). We then compared type specimens to the results. To determine the best discriminating morphometric measurements, we first ran a discriminant analysis and an ANOVA, followed by a Tukey HSD on each measurement selected by the discriminant analysis. Suppl. material 5: tables S8, S9 show the results of statistical analyses on linear morphometric measurements.

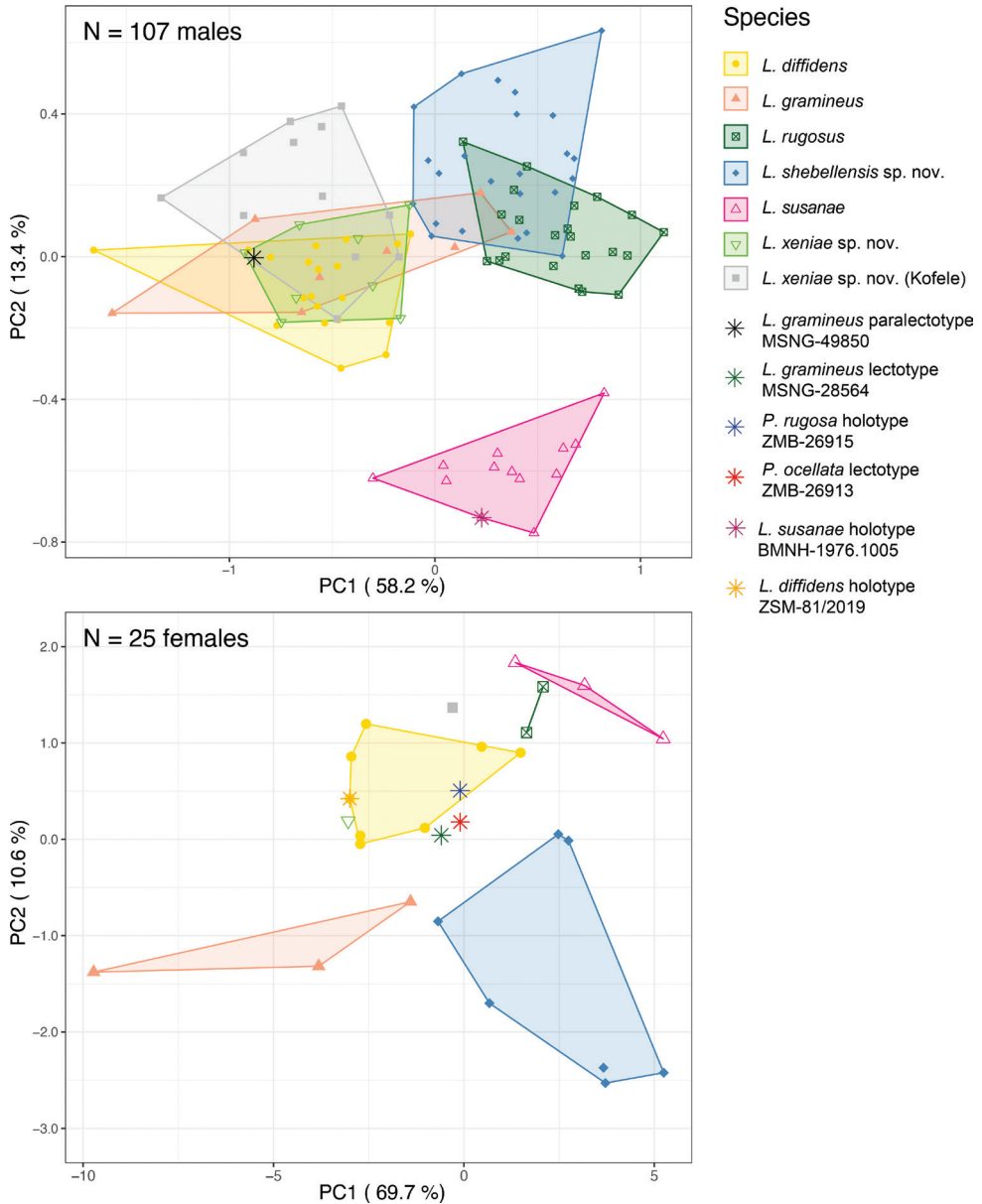
Table 1. Summary of the linear morphometric measurement for the *Leptopelis gramineus* species complex.

Species	sex	N	SVL	HW	HL	SL	NS	IND	EN	IOD	ETD	TD
<i>L. diffidens</i>	F	8	42 ± 5.5	15.6 ± 1.6	12.7 ± 1	5.5 ± 0.7	2.7 ± 0.5	3.3 ± 0.6	2.5 ± 0.3	3.9 ± 0.7	1.2 ± 0.3	1.8 ± 0.2
	M	20	27.5 ± 2.5	10.3 ± 1.1	9 ± 0.9	3.8 ± 0.3	2 ± 0.3	2.4 ± 0.3	1.7 ± 0.3	3.3 ± 0.4	0.7 ± 0.2	1.6 ± 0.4
<i>L. gramineus</i>	F	3	34.5 ± 8.8	13.9 ± 3.6	11.2 ± 2.5	5 ± 1.6	1.9 ± 0.9	2.5 ± 0.5	2 ± 0.6	4.2 ± 1.1	0.8 ± 0.6	1.8 ± 0.5
	M	8	30.3 ± 5.8	11.4 ± 2.7	9.5 ± 1.5	4.2 ± 0.6	2 ± 0.2	2.6 ± 0.2	1.7 ± 0.3	3.4 ± 0.8	0.7 ± 0.2	1.7 ± 0.4
<i>L. rugosus</i>	F	4	47.8 ± 5.3	16.4 ± 0.7	14.3 ± 0.7	6.7 ± 0.7	3.6 ± 0.4	4.4 ± 0.5	2.8 ± 0.4	4.3 ± 0.6	1.4 ± 0.6	2 ± 0.4
	M	22	38.7 ± 2.7	14.3 ± 1.4	11.8 ± 1.1	5.2 ± 0.4	2.9 ± 0.2	3.4 ± 0.3	2.1 ± 0.3	4.2 ± 0.5	0.9 ± 0.3	2.3 ± 0.4
<i>L. shebellensis</i> sp. nov.	F	8	53.4 ± 5.3	18.9 ± 2.3	15.8 ± 2.5	7 ± 1	3.8 ± 0.3	4.6 ± 0.5	3.3 ± 0.8	5.5 ± 0.8	1.2 ± 0.6	3.1 ± 0.5
	M	24	36.2 ± 3.3	13.2 ± 1.5	11.8 ± 1.3	5 ± 0.5	2.7 ± 0.3	3.1 ± 0.4	2.3 ± 0.3	3.8 ± 0.5	0.8 ± 0.3	2.1 ± 0.2
<i>L. susanae</i>	F	3	49.6 ± 6.6	18.1 ± 2.4	16.4 ± 2.2	7.4 ± 0.7	4.2 ± 0.2	4.6 ± 0.2	3.7 ± 0.4	5.9 ± 0.3	1.3 ± 0.4	2.6 ± 0.8
	M	12	33.2 ± 3.7	11.8 ± 1.3	11 ± 0.7	5 ± 0.4	2.6 ± 0.3	3.3 ± 0.3	2.4 ± 0.2	3.7 ± 0.3	0.9 ± 0.2	1.9 ± 0.3
<i>L. xeniae</i> sp. nov.	F	2	43.5 ± 5.7	15.9 ± 1.4	12.7 ± 0.4	5.1 ± 0.7	2.9 ± 0.4	3.2 ± 0	1.7 ± 0.3	3.3 ± 0.3	0.7 ± 0.1	2.1 ± 0.2
	M	20	27.6 ± 2.0	10.2 ± 0.6	9.1 ± 0.5	3.9 ± 0.3	2.2 ± 0.3	2.5 ± 0.3	1.7 ± 0.4	2.9 ± 0.4	0.7 ± 0.2	1.9 ± 0.3
			ED	UEW	FLL	HAL	FinDW	THL	TL	FL	Toe4DW	MTL
<i>L. diffidens</i>	F	8	4.5 ± 0.4	3 ± 0.4	9.6 ± 1.3	12.6 ± 1.9	1.5 ± 0.2	15.9 ± 3	15.6 ± 1.5	20.5 ± 2.6	1.4 ± 0.3	2.8 ± 0.5
	M	20	3.2 ± 0.4	2.5 ± 0.3	6.2 ± 0.9	8.1 ± 0.9	0.9 ± 0.1	10.9 ± 1.5	10.2 ± 0.9	12.5 ± 0.9	0.9 ± 0.1	1.8 ± 0.2
<i>L. gramineus</i>	F	3	4.2 ± 0.4	2.6 ± 0.5	8.5 ± 1.5	NaN ± NA	NaN ± NA	11.2 ± 2.1	11 ± 2.6	NaN ± NA	1.1 ± 0.2	1.8 ± 0.7
	M	8	3.6 ± 0.9	2.6 ± 0.5	6.3 ± 1.2	7.4 ± 0.5	0.8 ± 0.1	10.9 ± 1.2	10.3 ± 1.2	11.5 ± 1.2	0.9 ± 0.2	2 ± 0.7
<i>L. rugosus</i>	F	4	4.4 ± 0.3	3.5 ± 0.3	10.4 ± 1.3	13.5 ± 1	1.3 ± 0.3	20.5 ± 1.2	17.8 ± 1.4	21.3 ± 0.7	1.2 ± 0.4	3.7 ± 0.4
	M	22	4.1 ± 0.5	3.1 ± 0.2	7.8 ± 1.1	10.9 ± 0.8	1.2 ± 0.2	14 ± 1.5	13.2 ± 0.9	16.6 ± 1.3	1.1 ± 0.2	2.8 ± 0.4
<i>L. shebellensis</i> sp. nov.	F	8	5.8 ± 1.6	4.1 ± 1.1	10.8 ± 1.8	14.8 ± 1.8	1.3 ± 0.4	16.7 ± 2	16.1 ± 1.5	22.8 ± 2.5	1 ± 0.2	3.7 ± 0.6
	M	24	4.2 ± 0.7	2.8 ± 0.5	8 ± 1.2	10.2 ± 1	0.9 ± 0.2	12.7 ± 1.4	11.8 ± 1	14.8 ± 1.2	0.8 ± 0.2	2.4 ± 0.3
<i>L. susanae</i>	F	3	5.7 ± 1.3	3.9 ± 0.8	12.1 ± 1.3	16 ± 0.8	2.7 ± 0.2	22.5 ± 1	21.2 ± 2.1	24.6 ± 2.2	2.5 ± 0.3	2.9 ± 0.6
	M	12	4.2 ± 0.5	3.1 ± 0.6	7.4 ± 1.1	10.6 ± 0.8	1.8 ± 0.2	14.9 ± 0.9	14.8 ± 1	16.5 ± 1.4	1.6 ± 0.2	1.7 ± 0.2
<i>L. xeniae</i> sp. nov.	F	2	4.8 ± 0.4	3.3 ± 1.1	9.9 ± 1.8	12.8 ± 1.1	1.4 ± 0.1	16.8 ± 2.8	16 ± 3.4	20.2 ± 3.4	1.4 ± 0.1	2.4 ± 0.3
	M	20	3.3 ± 0.4	2.4 ± 0.3	6.1 ± 0.7	8.2 ± 0.7	0.8 ± 0.2	10.2 ± 1.4	9.9 ± 0.9	12 ± 1	0.8 ± 0.2	1.8 ± 0.3

Morphometric measurements were all log-transformed prior to analysis in order to approach normality. To correct for body size in our measurements, we used ratios of measurements over snout-vent length. We did not use other adjustment method such as the one proposed by Leonart et al. (2000) and used by others (e.g. Onn et al. 2018) to correct for allometric growth, because this method relies on coefficients calculated on populations and, therefore, artificially segregates individuals in a priori-determined groups. In addition, this method requires to measure multiple individuals of a given population before calculating the adjusted variables. Given that our goal here is to define characters that may be used for species identification without any a priori, we chose to resort to a size correction only based on the individual's own mensuration.

Recording and analysis of advertisements calls

Spontaneously calling males were located acoustically or visually between 20:00 and 02:00 h. We recorded advertisement calls in situ at a distance between 0.5–2 m to avoid near-field effects (Rossing 2007) or excessive attenuation or distortion of the sound. We used a Sennheiser ME66 directional microphone with a Sennheiser K6 powering module and an Olympus LS-100 or a Marantz PMD661 MKII recorder at a sampling rate of 44.1 kHz at 16 bits. Comments were recorded at the end of each recording using a Sennheiser ME62 microphone. The exact distance between the microphone and the calling male was measured with a Leica E7100i laser meter (precision: 3 mm)



after the capture of the frog. When possible, video recordings were taken simultaneously with an infrared camcorder (SONY DCR-SR85) and custom-made Colorado Para Tech infrared lights to ensure the identity of the focal individual. Videos were

subsequently used to select the focal male's calls in recordings containing vocalisations of multiple individuals. The audio recordings are available at the Fonoteca Zoologica sound collection (<https://www.fonozoo.com>).

Advertisement calls were analysed using Avisoft SAS (Sprecht 2017). We used a note-centred terminology scheme as described in Köhler et al. (2017), where the call constitutes a coherent unit and may contain one or several sub-units (notes), which, in turn, may contain distinct or indistinct pulses. We extracted six temporal and four spectral acoustic traits from our audio recordings (Table 2, Suppl. material 5: table S10): note duration, inter-call interval duration, number of pulses per note, inter-pulse interval duration, pulse rate, relative time of peak amplitude, call peak frequency, call frequency bandwidth, minimal and maximal call frequencies. Notes and pulses were labelled semi-automatically using the pulse train analysis function and subsequently by adjusting labels by eye. Sampling frequency was adjusted to 22,050 Hz. Spectral traits were extracted from the spectrogram using the automatic parameter measurement function on spectrograms using a Fast Fourier Transformation (FFT) length of 512, Hamming windowing, 50% frame size and 99.43% overlap between contiguous windows. All values were exported and averaged per individual and then per species in the R environment (R Core Team 2020; Table 2, Suppl. material 5: table S10). Spectrograms and oscillograms of the calls were plotted using the R package *seewave* (Sueur et al. 2008; Fig. 4).

Results

Phylogenetic analysis of mitochondrial DNA sequences

Results of both the Bayesian Inference (BI) and Maximum Likelihood (ML) analyses of the full COX1 dataset were largely congruent with each other and with previous analyses by Freilich et al. (2016) and Reyes-Velasco et al. (2018; Fig. 2, Suppl. material 2). The arboreal species of Ethiopian *Leptopelis* (*L. ragazzii*, *L. vannutellii* & *L. yaldeni*) form a monophyletic group, which is sister to the remaining species and populations, referred hereafter as the *L. gramineus* species complex. The complex consists of six distinct lineages: (1) a lineage consisting of frogs from the Harena forest, which correspond to *L. diffidens*; (2) a lineage corresponding to the arboreal species *L. susanae*; (3) a lineage consisting of frogs from the plateaus and mountains west of the GRV, *L. rugosus*; (4) a lineage corresponding to *L. gramineus* as defined by Tiutenko & Zinenko, 2021; (5) a lineage of frogs from the forests of the southeast corresponding to the “Kibre Mengist” clade of Freilich et al. (2016) and Reyes-Velasco et al. (2018) and (6) a lineage consisting of frogs from the plateaus and mountains east of the GRV. It should be noted that the *L. gramineus* lineage from the Chench Highlands was mistakenly assigned to *L. susanae* in Reyes-Velasco et al. (2018). However, upon closer examination and comparison with additional material, it was determined that these individuals, in fact, represent *L. gramineus*. The individuals of *L. susanae* in the present study were carefully

examined morphologically and fit the original description of Largen (1977). Despite the multiple clades being largely congruent with previous studies, the relationships amongst clades vary when compared to previous studies and many of the deeper nodes are not well supported (Suppl. material 2). These phylogenetic discordances have previously been reported by Reyes-Velasco et al. (2018). When only the 16s gene is analysed, the majority of the same groups were recovered; however, most of the nodes received poor support (bootstrap < 50; Suppl. material 3).

The uncorrected pairwise genetic distances between lineages in the mitogenome dataset ranged from 5.8% to 6.6% (Suppl. material 5: table S5), while those genetic distances, based on COX1, ranged from 5.3% to 10% (Suppl. material 5: table S6). These differences correspond to levels of inter-specific divergences previously reported in anurans (Smith et al. 2008).

Phylogenetic placement of the type specimens of *Pseudocassina ocellata* and *P. rugosa* in the *Leptopelis gramineus* species complex

The phylogenetic analysis of the whole mitogenomes placed the types of *Pseudocassina ocellata* and *P. rugosa* as sister to one another and together sister to an individual from Mehal Meda (Semien Shewa Zone, Amhara Region; Suppl. material 1: fig. S1A; see phylogenetic analyses above). These relationships received strong support (bootstrap support = 100). These samples formed the sister group to all other individuals, which consisted of a specimen from the Harena forest (*Leptopelis diffidens*) and multiple individuals from the Bale Mountains and Assela (Suppl. material 1: fig. S1A). The relationships amongst individuals did not change when we only included the COX1 gene (Suppl. material 1: fig. S1B).

In both COX1 and 16s phylogenies, the type specimens of *Pseudocassina ocellata* and *P. rugosa* grouped with individuals from northwest of the GRV (“Northern” clade of Reyes-Velasco et al. 2018), with strong support (bootstrap support > 95; Fig. 2, Suppl. materials 2, 3). These results show that the types of *Pseudocassina ocellata* and *P. rugosa* are conspecific. Both names are, thus, synonyms and correspond to the semi-fossorial *Leptopelis* found predominantly in the plateaus and mountains west of the GRV.

Linear morphometrics

Due to sexual dimorphism, we analysed male and female morphological measurements separately (Fig. 3; Table 1). The six species analysed morphologically can be split into three morphotype categories: a large, fully arboreal form, small, mostly arboreal forms and large, semi-fossorial forms. *Leptopelis susanae* is a truly arboreal form and can be distinguished from all other species of the group by enlarged finger and toe discs (FinDW and Toe4DW) and elongated hind-limbs (TL and THL; Suppl. material 5: table S9). Individuals from the Northern and Bale/Assela clades are semi-fossorial and distinguished from *L. gramineus*, *L. diffidens* and Kibre Mengist clade’s

individuals by a greater body size (SVL), a greater tympanum diameter (TD), longer snout (SL), inter-nares (IND) and snout-nostril distance (SN) and metatarsal tubercle length (MTL; Suppl. material 5: table S9). The Northern clade can be distinguished from the Bale/Assela clade by longer hind-limbs (TL and THL) and larger finger and toe discs (FinDW and Toe4WD; Suppl. material 5: table S9).

Within the arboreal group, head shape is most discriminant between species. The Kibre Mengist clade can be distinguished from the other small species of the complex (*L. gramineus* and *L. diffidens*) by a longer snout-nostril (SN) and a shorter inter-orbital distance (IOD). *Leptopelis gramineus* has a greater inter-nares (IND) and shorter snout-nostril (SN) distance than *L. diffidens* and the Kibre Mengist clade (Suppl. material 5: table S9).

Acoustic analysis

Advertisement calls of the *Leptopelis gramineus* species complex sound like a short rattle and species are difficult to distinguish by an untrained ear, except for *L. susanae*, which produces a call shorter in duration than the other species (Fig. 4; Table 2). The major differences between species lie in the number of pulses per note and pulse rate (Fig. 4; Table 2). The larger forms (*L. susanae*, the Northern and Bale/Assela clades) produce notes with fewer pulses than the smaller forms (*L. gramineus*, *L. diffidens* and the Kibre Mengist clade): 3–5 pulses vs. 5–9. These pulses are well spaced in the Northern clade (61 ± 14 pulses·s⁻¹) while they are emitted in very quick succession by males from the Bale Mountains and Assela clade (88 ± 3 pulses·s⁻¹) and *L. susanae* (209 ± 20 pulses·s⁻¹). Kibre Mengist males produces notes with lower pulse rate (39 ± 7 pulses·s⁻¹) than *L. gramineus* and *L. diffidens* (62 ± 9 and 53 ± 8 pulses·s⁻¹, respectively). Finally, the notes of *L. diffidens* are longer (130 ± 21 ms) than those of *L. gramineus* (93 ± 6 ms).

Table 2. Summary of call acoustic characters for the *Leptopelis gramineus* species complex.

Species	N individuals	N notes	Note duration (ms)	Inter-note interval (s)	Call rate	Pulses per note	Inter-pulse duration (ms)
<i>L. diffidens</i>	8	188	130 ± 21	12.08 ± 6.18	0.10 ± 0.04	7 ± 2	22 ± 4
<i>L. gramineus</i>	2	19	93 ± 6	16.46 ± 3.17	0.07 ± 0.01	6 ± 1	19 ± 2
<i>L. rugosus</i>	6	108	65 ± 21	13.12 ± 7.47	0.10 ± 0.04	4 ± 1	20 ± 5
<i>L. shebellensis</i> sp. nov.	4	89	57 ± 5	8.28 ± 1.34	0.13 ± 0.02	5 ± 0	11 ± 2
<i>L. susanae</i>	2	50	25.6 ± 2.1	11.21 ± 3.27	0.10 ± 0.02	5.2 ± 0	11 ± 2
<i>L. xeniae</i> sp. nov.	4	51	175 ± 25	14.16 ± 6.50	0.09 ± 0.03	7 ± 1	30 ± 5
	Pulse rate (s-1)	Peak frequency (Hz)	Min frequency (Hz)	Max frequency (Hz)	Frequency bandwidth (Hz)	Relative time of peak amplitude (ms)	
<i>L. diffidens</i>	53 ± 8	1928 ± 235	1489 ± 218	2880 ± 286	1386 ± 203	39 ± 10	
<i>L. gramineus</i>	62 ± 9	1863 ± 154	1445 ± 173	2832 ± 201	1385 ± 375	21 ± 9	
<i>L. rugosus</i>	61 ± 14	1769 ± 60	1448 ± 140	2192 ± 64	742 ± 82	9 ± 5	
<i>L. shebellensis</i> sp. nov.	88 ± 3	1616 ± 265	1211 ± 253	2192 ± 132	974 ± 163	21 ± 15	
<i>L. susanae</i>	209 ± 20	1986 ± 130	1611 ± 66	2445 ± 201	832 ± 133	7 ± 6	
<i>L. xeniae</i> sp. nov.	39 ± 7	2231 ± 585	1546 ± 73	3562 ± 505	2013 ± 573	44 ± 24	

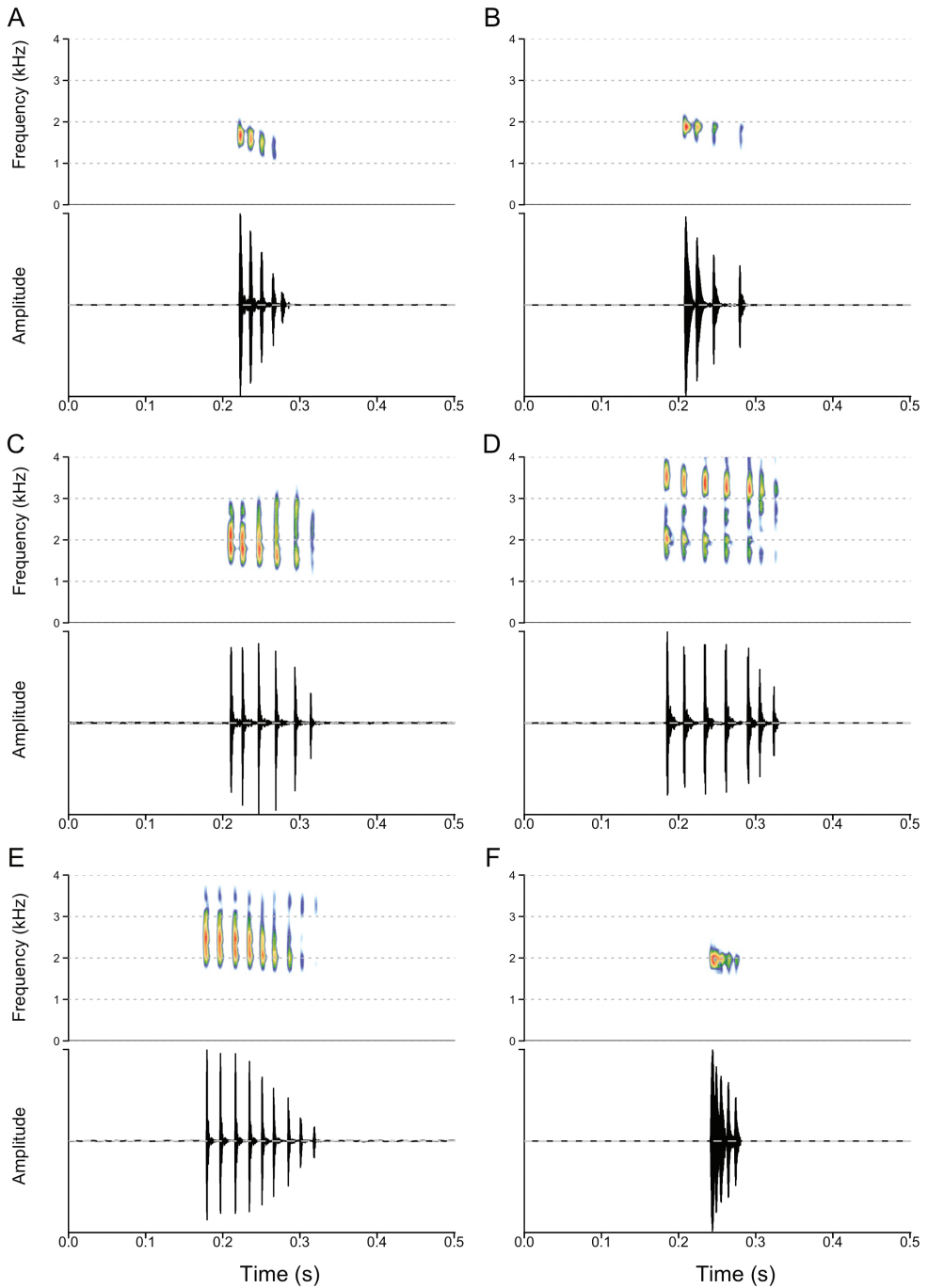


Figure 4. Advertisement calls of six *Leptopelis* species inhabiting the Ethiopian Highlands **A** *L. shebellensis* sp. nov. (SB61) **B** *L. rugosus* (SB609) **C** *L. gramineus* (SB212) **D** *L. xeniae* sp. nov. (SB169) **E** *L. diffidens* (SB134) **F** *L. susanae* (SB223).

Systematic accounts

Validity of the name *Leptopelis rugosus* (Ahl, 1924)

In 1924, Ahl described *Pseudocassina rugosa* and *Pseudocassina ocellata* as distinct species in the same article. Both names were subsequently synonymised with *Leptopelis gramineus* by Largen in 1977. In 2021, Tiutenko and Zinenko resurrected *L. ocellatus* from synonymy with *L. gramineus*, but because a senior homonym, *Leptopelis ocellatus* (Mocquard, 1902), existed, they assigned a new name to the species, *Leptopelis montanus* Tiutenko and Zinenko 2021. In the present study, we demonstrate that *Pseudocassina rugosa* Ahl, 1924 and *Pseudocassina ocellata* Ahl, 1924 (= *Leptopelis montanus* Tiutenko and Zinenko 2021) are synonyms. According to articles 60.1 and 60.2 of the International Code of Zoological Nomenclature, a junior homonym must be rejected and replaced by an available and valid synonym, if one exists. If multiple potentially valid synonyms exist, the oldest of these become the valid name. Therefore, being older than *Leptopelis montanus* Tiutenko and Zinenko 2021, *Leptopelis rugosus* (Ahl, 1924) becomes the valid name of the taxon.

Leptopelis rugosus (Ahl, 1924)

Pseudocassina rugosa Ahl, 1924.

Pseudocassina ocellata Ahl, 1924.

Leptopelis montanus Tiutenko & Zinenko, 2021.

Type material. Holotype. Adult female (ZMB–26915) collected during Oscar Neumann’s and Carlo von Erlanger’s expedition in 1900 in Meta, Kolla (approx. 9.17°N, 38.25°E, 2650 m a.s.l.).

Material examined. In addition to the holotype, we examined one female collected at the end of July 1900 during O. Neumann’s and C. von Erlanger’s expedition in “Hochebene Didda” (ZMB-26913), which is one of the two syntypes of *Leptopelis montanus* Tiutenko & Zinenko, 2021 (= *Pseudocassina ocellata*), synonymised here with *L. rugosus*. As this specimen was mentioned as “the holotype” by Largen (2001) and has a collection date and a more precise locality than the other syntype (ZMB-26914), which only states “Somaliand”, considered erroneous by (Largen 1977), we formally designate ZMB-26913 as the lectotype of *Pseudocassina ocellata* here (see remarks below regarding the locality and taxonomic status). We also examined one female (16–130), collected on 12 July 2016 by J. Reyes-Velasco and S. Boissinot east of Mehal Meda (10.3316°N, 39.7812°E, 3265 m a.s.l.), one male (16–103), collected on 12 July 2016 by J. Reyes-Velasco and S. Boissinot north of Debre Sina (9.9894°N, 39.7452°E, 3017 m a.s.l.), three males (16–109, 16–116, 16–129), collected on 12 July 2016 by J. Reyes-Velasco and S. Boissinot east of Mehal Meda (10.16–10.33°N, 39.76–39.80°E, 3167–3265 m a.s.l.), five males (16–150, 16–151, 16–152, 16–153,

16–154), collected on 13 July 2016 by J. Reyes-Velasco and S. Boissinot east of Debre Birhan (9.6979°N, 39.5628°E, 2833 m a.s.l.), three males (16–164, 16–168, 16–172), collected on 14 July 2016 by J. Reyes-Velasco and S. Boissinot south of Fiche (9.73–9.75°N, 38.74°E, 2657–2726 m a.s.l.), five males (SB530, SB531, SB532, SB533, SB540), collected on 1 and 2 July 2018 by S. Goutte and Y. Bourgeois east of Debre Birhan (9.6979°N, 39.5628°E, 2339 m a.s.l.), four males (SB541, SB542, SB544, SB545), collected on 2 July 2018 by S. Goutte and Y. Bourgeois between Debre Birhan and Ankober (9.6820°N, 39.7390°E, 3408 m a.s.l.), two females (SB555, SB558) and one male (SB556), collected on 4 July 2018 by S. Goutte and Y. Bourgeois east of Mehal Meda (10.31–10.33°N, 39.78–39.80°E, 3337–3429 m a.s.l.) and three males (SB608, SB609, SB610), collected on 11 July 2018 by S. Goutte and Y. Bourgeois south of Fiche (9.7307°N, 38.7439°E, 2365 m a.s.l.).

Diagnosis. A large (male (n = 22) SVL 38.7 ± 2.7 mm, female (n = 2) SVL 52.4 ± 0.2 mm) species of the *Leptopelis gramineus* species complex (Figs 5, 6). Robust, semi-fossorial form. It differs from other members of the *Leptopelis gramineus* species complex by the following combination of characters: (1) large tympanum (male TD/ED 0.57 ± 0.11, female TD/ED 0.54), (2) long snout (male SL/HL 0.25 ± 0.02, female SL/HL 0.27 ± 0.01), (3) well-developed metatarsal tubercle (male MTL/FL 0.17 ± 0.02, female MTL/FL 0.18 ± 0.02), (4) ventrum lacking any brown spots, (5) yellow colouration on the side of the ventrum and the inner thighs almost always present.

Comparison. Larger body size, longer head and snout and greater snout-nostril distance and larger tympanum and metatarsal tubercle than *L. gramineus*, *L. diffidens* and *L. sp.* Kibre Mengist (Table 1, Suppl. material 5: table S9). Longer hind-limbs than the Bale/Assela clade, but shorter than *L. susanae* (Table 1, Suppl. material 5: table S9). Finger and toe discs less developed and head narrower and shorter than *L. susanae* (Table 1, Suppl. material 5: table S9). *Leptopelis rugosus* is distinguished from the Bale/Assela clade by the lack of dark pigmentation on the ventrum, throat and ventral side of the limbs (Figs 6, 7).

Description of the holotype. Relatively large adult female (SVL 44.7 mm) in good condition of preservation (Fig. 5). Body robust and round. Head a third of body size in length, wider than long (HW/HL 1.21). Canthus rostralis obtuse and snout rounded and wide (IND/IOD 0.96). Nostril half-way between the tip of the snout and the eye (NS/SL 0.53). Tympanum partially hidden by flank skin rugosities and barely visible. Hind-limbs relatively long (TL/SVL 0.38 and THL/SVL 0.43). Finger and toe discs barely expanded, but distinct, ovoid. Finger formula: I < II < IV < III. Hand free of webbing. Foot longer than tibia (FL/TL 1.3). Inner metatarsal tubercle well-developed, oval in shape, 0.20× foot length. Outer metatarsal tubercle absent. Toe formula: I < II < V < III < IV. Toe webbing formula (toe internal/external sides, number of phalanges webbed): Ie(1), Ili/e(1–1), IIIi/e(1–2), IVi/e(2–2), Vi(2). Skin of the dorsum, flanks and ventrum highly rugose.

Colouration of the holotype in preservative. Dorsal ground colour and canthal region dark olive brown with no visible pattern, except for a large light brown blotch covering about a third of the dorsum (Fig. 5). This discolouration probably appeared during



Figure 5. Dorsal and ventral views of the female holotype (ZMB-26915) of *Leptopelis rugosus*.

the specimen preservation and after its original description, where Ahl described the dorsum as “solid dark olive-brown”. The thin light yellowish line noted by Ahl (1924) to extend to the upper arm is mostly faded away behind the tympanic region. Upper lip and flanks light yellowish-brown. Throat, ventrum, ventral side of the thighs and tibiae light yellowish-brown. Front and hind-limbs olive brown without any marking.

Variations. *Leptopelis rugosus* presents less colour polymorphism than the smaller members of the *L. gramineus* species complex. Dorsum is green to dark green and can be completely uniform or have a few to many irregular brown blotches (Fig. 6). In some individuals, these blotches form an irregular dorsal stripe extending from the top of the head to the lower back. A dark brown to black bar covers the canthal region and extends behind the eye, over the tympanum and sometimes behind the arm junction. This canthal stripe is overlined by a thin, more or less visible yellowish line. Flanks are the same colour as the dorsal ground colour and, in all individuals examined, except for the female SB558, have more or less well-defined brown ocelli. Limbs are the same colouration as the dorsum and rarely have irregular brown markings. Upper lip may be cream or a lighter shade of green than the dorsum without any markings. Iris sand colour to brown. Tympanum may be uniformly green or partially covered by a brown blotch joining the brown bar behind the eye. Throat and chest uniformly white to pale yellow. Ventrum generally white or cream with light to deep yellow zones on the sides extending to the ventral side of the thighs. In some individuals, the ventrum may be completely yellow. In gravid females, yellow eggs are visible through the thick ventral skin. In most individuals, the palms of the hands, ventral and inner sides of the limbs show very little to no dark pigmentation. Some individuals have a few irregular brown or black blotches on the inner tibia, forearm, hand and foot. Dorsal skin may be smooth, slightly or very rugose.

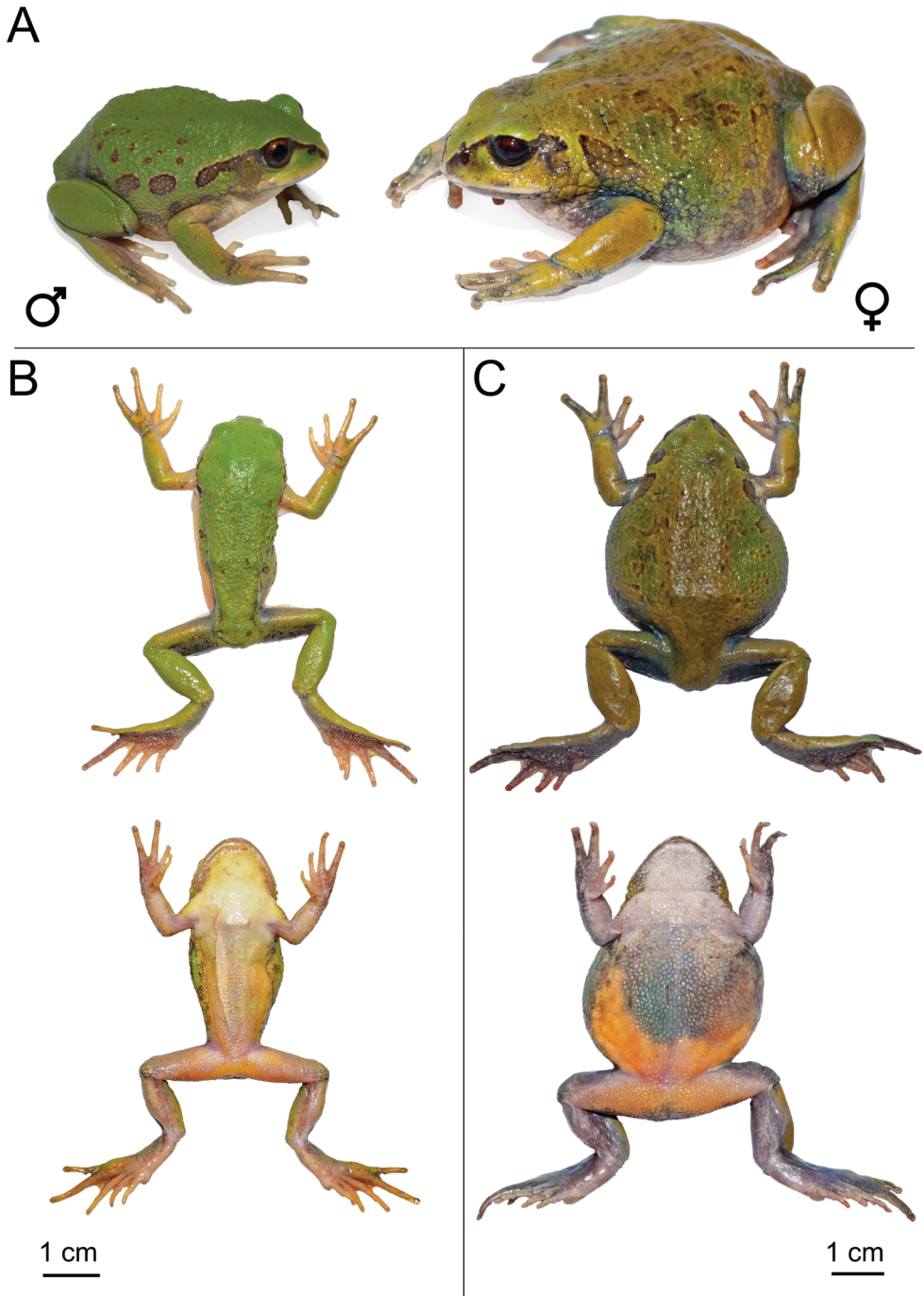


Figure 6. *Leptopelis rugosus* **A** live male (SB610; left) and female (SB558; right) **B** dorsal and ventral views of male (SB610) after euthanasia and before fixation **C** dorsal and ventral views of female (SB558) after euthanasia and before fixation.

Habitat, distribution and natural history. *Leptopelis rugosus* is found in grassy meadows of the Ethiopian Highlands north of the GRV at mid- to high elevations (2,339–3,337 m a.s.l.). This species occurs notably near Debre Birhan, Debre Sina, Fiche, Addis Ababa, Holeta and Ambo (Fig. 1, Suppl. material 5: table S1). The northernmost population was found near Mehal Meda (10.3171°N, 39.8024°E), while the southernmost individuals were found between Ambo and Wonchi (8.9007°N, 37.8928°E). One of the two types in Ahl's original description of *Pseudocassina ocellata* was collected on the Arussi Plateau, which, if the locality is correct, is the only known specimen east of the GRV (see remark on the type locality below).

Males are heard calling at night and sometimes during the day for extended periods of time. Advertisement calls are emitted from the ground, either on the grass or from a cavity in the ground or under a rock, generally near a stream or a flooded area. Several males were found calling from the banks of a completely dried-out stream, although it is unknown to us whether the reproduction period extends to the dry season or whether males keep calling only during shorter dry periods.

Advertisement call. The call of *Leptopelis rugosus* is a short rattle composed of a single note of 65 ± 21 ms in duration, containing 4 ± 1 pulses (Fig. 4B). In most individuals, the two first pulses are emitted at very short intervals, while the subsequent pulses are more spaced (average inter-pulse interval 20 ± 5 ms). Other individuals produce notes with regularly-spaced pulses. Amplitude is highest at the beginning of the note and decreases gradually. Within a call bout, calls are spaced by 13 ± 7 seconds, often with an acceleration of the call rate from a call every 10 seconds to one call per second. Call dominant frequency is $1,769 \pm 60$ Hz, with a bandwidth of 742 ± 82 Hz.

The call of *Leptopelis rugosus* is distinguishable from the calls of *L. gramineus*, *L. diffidens* and the Kibre Mengist and Bale/Assela clades by its lower number of pulses per note and narrower frequency band width. It is further distinguished from the call of *L. gramineus*, *L. diffidens* and *L. sp.* Kibre Mengist by its shorter note duration and from *L. sp.* Kibre Mengist by its lower peak frequency and higher pulse rate. Finally, it is distinguished from the call of *L. susanae* by its longer duration and lower pulse rate (Table 2).

Remarks. Diagnostic characters used in the original description.

Ahl described *Pseudocassina rugosa*, based on a single female and provided three main diagnostic characters when compared with *Pseudocassina ocellata*, which he described in the same article, based on one female and one male: (1) the texture of the skin (rugose for *P. rugosa* and smooth for *P. ocellata*), (2) the length of the tibia (*P. rugosa* TL/SVL 1/3.5 and *P. ocellata* TL/SVL 1/3), (3) the visibility of the tympanum (hidden for *P. rugosa* and visible for *P. ocellata*). Ahl also named *P. ocellata* after the presence of ocelli on the flanks of the individuals he examined, which reflects on its specificity, even though he did not use this trait as a diagnostic character.

We found individuals of *L. rugosus* and the Bale/Assela clade with either a completely smooth, slightly rugose or coarsely rugose dorsum. The rugosity of the skin thus seems to be variable amongst individuals and, perhaps, age or season. Additionally, we have noticed that the rugosity of the skin may disappear after euthanasia and/

or fixation of the specimen. Finally, even though almost all individuals of *L. diffidens*, *L. gramineus* and the *L. sp.* Kibre Mengist examined had smooth skin, we found two females *L. diffidens* and one female *L. sp.* Kibre Mengist with slightly rugose skin. The visibility of the tympanum seems to be variable across the individuals as well, perhaps linked to the size of the individual and the rugosity of the skin. While some female *L. rugosus* have a partially hidden tympanum, all males examined had a visible tympanum. The difference in tibia length between the specimens described by Ahl reflects individual variations as shown in our dataset. Finally, ocelli on the flanks and/or dorsum are present in certain individuals of *L. rugosus* and the Bale/Assela clade and is not a diagnostic character.

Type localities of *Pseudocassina ocellata* and *P. rugosa*

Ahl described *Pseudocassina ocellata*, based on one female and one male, collected at different localities during Oscar Neumann's and Carlo von Erlanger's 1900 expedition. The information given for the female is "Hochebene, Didda, end of July 1900", while for the male, only "Somaliland" is given. Although imprecise, both localities are clearly situated east of the Great Rift Valley (GRV). In contrast, the specimen used as holotype for the original description of *P. rugosa* and all recent *L. rugosus* specimens were collected west of the GRV. We propose two, non-exclusive explanations for this discrepancy.

First, based on Neumann's report and map of the expedition (Neumann 1902) and the collection date, "End of July 1900", the locality of collection of the first type of *P. ocellata* could be near Addis Ababa and not on the Arussi Plateau (i.e. Didda Plateau). Indeed, the expedition party crossed the Shebelle River the first time near Jabolo, east of Sheik Hussein on 10 June, continued west through Sheik Hussein, ascended a couple of mountains, crossed the Shebelle River a second time and ascended the Arussi Plateau. Neumann reports that it took them 12 days to cross the Arussi Plateau, after which they descended into the flooded Awash Valley and reached Addis Ababa from the southeast on 14 August 1900. Depending on their pace between Jabolo and the eastern edge of the Arussi Plateau and when ascending to Addis Ababa, at the end of July 1900, the expedition party could have been anywhere between the western Arussi Plateau and Addis Ababa. Notably, the specimen could have been collected on the Yerer Mountain, southeast of the capital and culminating above 2,800 m a.s.l.

Second, although the distribution range of *L. rugosus* is mostly west of the GRV, it is possible that a population occupies the west Arussi Plateau (or did in 1900). We found individuals of the grass frog *Ptychadena beka* Goutte, Reyes-Velasco, Freilich, Kassie and Boissinot 2021 at the north-western edge of the Arussi Plateau, even though the distribution range of this species is otherwise exclusively west of the GRV. We also found in the same area individuals of the river frog *Amietia nutti* (Boulenger 1896) carrying a mitochondrial haplotype restricted to the west of the GRV (Manthey et al. 2017). It is, thus, possible that conditions recently permitted the crossing of the GRV in that area for several anuran species and that *L. rugosus* is present or was recently present, east of the GRV.

***Leptopelis shebellensis* Goutte, Reyes-Velasco, Kassie & Boissinot, sp. nov.**

<https://zoobank.org/C3219B8F-7580-476A-BA0D-44F8D0822400>

Common name. English: Shebelle River burrowing African treefrog.

Type material. *Holotype.* Adult male (SB482), collected on 26 June 2018 by S. Goutte and Y. Bourgeois near the town of Ch'ange, Oromia, Ethiopia (8.1263°N, 39.4360°E, 2429 m a.s.l.). *Paratypes.* One male (15–46), collected on 5 August 2015 by X. Freilich, J. Reyes-Velasco and S. Boissinot, south of Assela (7.9068°N, 39.1238°E, 2520 m a.s.l.), one male (15–79) and one female (15–83), collected on 6 August 2015 by X. Freilich, J. Reyes-Velasco and S. Boissinot, southwest of Dinsho (7.1156°N, 39.7390°E, 3029 m a.s.l.), one male (15–84), collected on 6 August 2015 by X. Freilich, J. Reyes-Velasco and S. Boissinot southwest of Dinsho (7.1105°N, 39.7461°E, 3042 m a.s.l.), one male (15–143), collected on 8 August 2015 by X. Freilich, J. Reyes-Velasco and S. Boissinot between Robe and Ali (7.1720°N, 39.9722°E, 2431 m a.s.l.), one female (15–152), collected on 8 August 2015 by X. Freilich, J. Reyes-Velasco and S. Boissinot in Goba (7.0110°N, 39.9677°E, 2699 m a.s.l.), two females (16–8, 16–9), collected on 5 July 2016 by J. Reyes-Velasco and S. Boissinot south of Assela (7.8656°N, 39.1305°E, 2605 m a.s.l.), one females (16–25), collected on 6 July 2016 by J. Reyes-Velasco and S. Boissinot south of Assela (7.8836°N, 39.1245°E, 2531 m a.s.l.), two males (16–26, 16–28), collected on 6 July 2016 by J. Reyes-Velasco and S. Boissinot north of Bekoji (7.5585°N, 39.2520°E, 2721 m a.s.l.), one male (16–88), collected on 10 July 2016 by J. Reyes-Velasco and S. Boissinot east of Dinsho (7.1065°N, 39.8184°E, 3065 m a.s.l.), one male (16–93), collected on 10 July 2016 by J. Reyes-Velasco and S. Boissinot west of Dinsho (7.1204°N, 39.7358°E, 3048 m a.s.l.), three males (SB61, SB62, SB63), collected on 26 June 2018 by S. Goutte and J. Reyes-Velasco south of Dinsho (7.0915°N, 39.7834°E, 3079 m a.s.l.), two males (SB483, SB484), collected on 26 June 2018 by S. Goutte and Y. Bourgeois near Ch'ange (8.1263°N, 39.4360°E, 2429 m a.s.l.), three males (SB502, SB504, SB505), collected on 28 June 2018 by S. Goutte and Y. Bourgeois north of Arussi Robe (7.9190°N, 39.6091°E, 2433 m a.s.l.).

Diagnosis. Medium to large (male (n = 21) SVL 35.9 ± 3.5 mm, female (n = 5) SVL 53.4 ± 5.3 mm), robust semi-fossorial species of the *Leptopelis gramineus* species complex (Fig. 7). It differs from other members of the *Leptopelis gramineus* species complex by the following combination of characters: (1) short and robust hind-limbs (male TL/SVL 0.33 ± 0.03 , female TL/SVL 0.30 ± 0.02), (2) well-developed metatarsal tubercle (male MTL/FL 0.17 ± 0.03 , female MTL/FL 0.16 ± 0.02), (3) longer snout (male SL/HL 0.23 ± 0.03 , female SL/HL 0.24 ± 0.02), (4) toe and fingertips not enlarged and (5) ventrum often with dark brown spots and/or yellowish sides.

Comparison. Larger body size, longer head and snout and greater snout-nostril distance and larger tympanum and metatarsal tubercle than *L. gramineus*, *L. diffidens* and *L. sp. Kibre Mengist* (Table 1, Suppl. material 5: table S9). Shorter hind-limbs and smaller finger and toe discs than *L. rugosus* and *L. susanae* (Table 1, Suppl. material 5: table S9).

Description of the holotype. Medium size adult male (SVL 40.6 mm). Body robust (Fig. 7). Head a third of body size in length, wider than long (HW/HL 1.14). Snout wide (IND/IOD 0.87). Nostrils closer to the tip of the snout than the eyes (NS/SL 0.47). Canthus rostralis well-marked, but obtuse and loreal region slightly concave. Pupil vertical. Tympanum partially hidden on the posterior-dorsal edge, 0.40× eye diameter.

Fingers and toes robust with ovoid discs not expanded, but distinct. Finger formula: I < II < IV < III. Hand free of webbing. Hind-limbs short and robust (TL/SVL 0.31 and THL/SVL 0.38). Foot 1.32× tibia length. Inner metatarsal tubercle present, oval in shape, 0.16× foot length. Outer metatarsal tubercle absent. Toe formula: I < II < III < V < IV. Foot webbing minimal, except between toe III and toe IV where webbing extends to half-way between the first and the second phalanges. Skin of the dorsum, flanks and ventrum slightly rugose.

Colouration of the holotype in life. Dorsal ground colour sand, slightly iridescent, with green hues in the lower two-thirds (Fig. 7). One dorsal and two latero-dorsal irregular dark brown bands outlined with a thin cream line. Several small round or ovoid dark-brown spots, outlined with a thin cream line, are present in between the dorsal and latero-dorsal stripes and two larger and irregular in shape are present between the eyes. Dark brown canthal stripe, outline with a cream-coloured line, from the tip of the snout extending above and around the tympanum and behind the shoulder on the right side and to a fourth of the abdomen on the left side. Several large and irregular dark brown blotches, outlined by a cream line on the flank, in the continuation of the canthal stripe on each side. Tympanum golden light brown. Upper lip iridescent sand colour with a few irregular brown markings. Iris dark gold, lighter on the upper third, with heavy black reticulation. Flanks sand colour dorsally to forest green ventrally, with small black round spots. An irregular dark grey blotch marks the limit between the flank and the ventrum. Throat and ventrum mostly cream, yellowish towards the flanks, with small light brown blotches laterally. Hands, arms and forearms sand colour to green posteriorly, with a few irregular dark brown spots, except on the hands. Tibia light brown with irregular green blotches and a few small and irregular black spots. Thighs green dorsally to dark, bluish-green posteriorly, with a few irregular brown blotches. Feet green towards the heel to light olive green towards the toes.

Colouration of the holotype in preservative. Dorsal ground colour bluish-grey with large irregular black bands and spots outlined by a white line (Fig. 7B). Hands, feet and limbs bluish-grey with a few irregular black spots on the forearms and tibias, outlined with white. Throat and ventrum white to cream with a few faint brown spots. Ventral side of the hands, feet and tibiae heavily dusted with grey.

Variation. Dorsum can be green to dark green, sand or brown. All examined specimens had light or dark brown to black irregular markings, variable in size and number, on the dorsum. In many individuals, those markings are bi- or tricolour (yellowish-cream, light and dark brown) and form lateral and dorso-lateral ocelli in some animals. A thin yellowish line is present from the tip of the snout to behind the tympanum in all examined individuals. The canthal stripe can be light brown to black and can be underlined by a second yellowish line from the snout to the eye in some individuals. Flanks

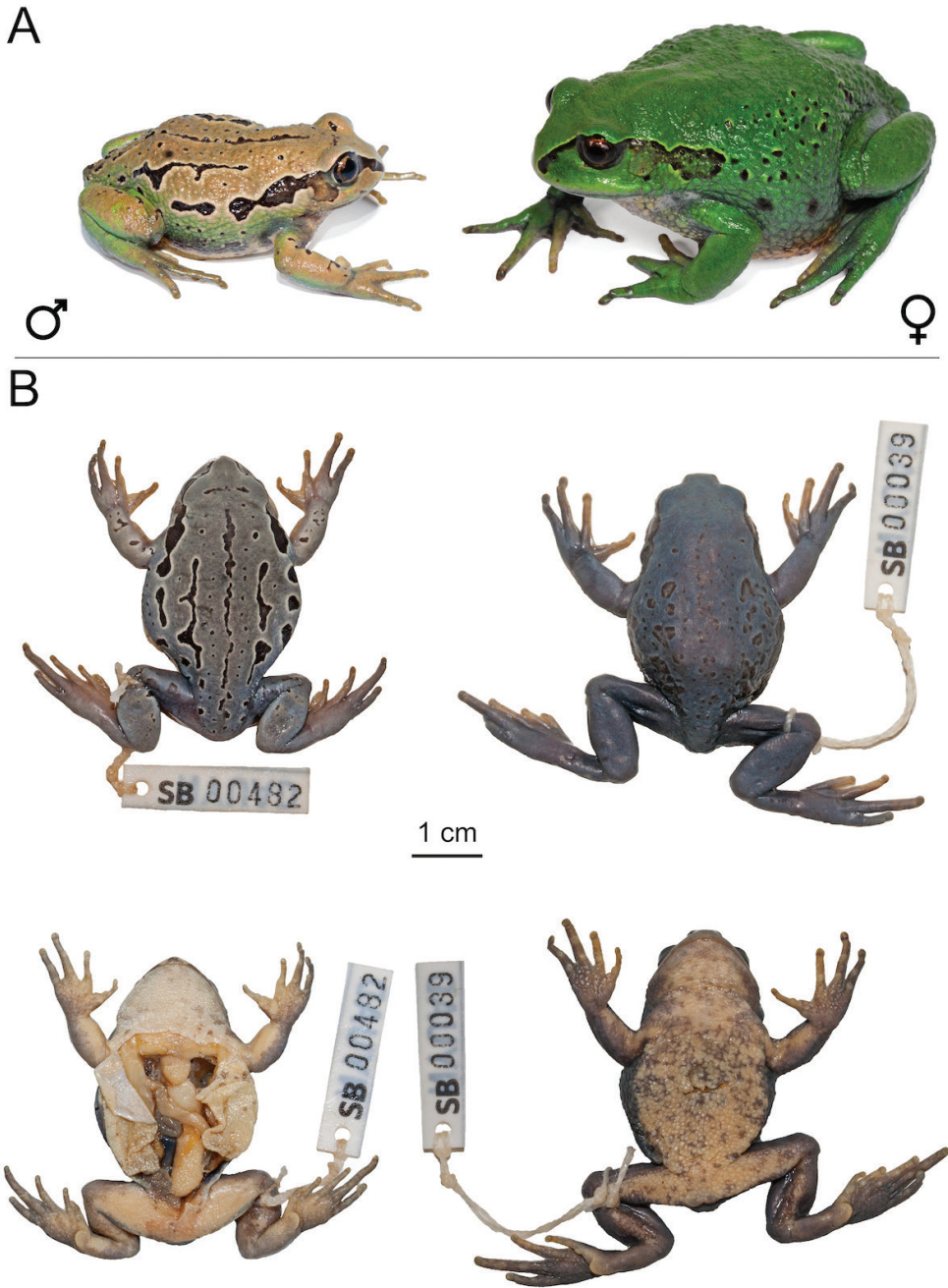


Figure 7. *Leptopelis shebellensis* sp. nov. **A** male holotype (SB482; left) and live female paratype (SB41; right) **B** male holotype (SB482; left) and dorsal and ventral views of female paratype (SB39; right) after fixation.

can be the same colour or a lighter version of the dorsal ground colour or green while the dorsum is brown or vice versa. Larger versions of the dorsal blotches are found on the flanks, sometime merging into an irregular band. Limbs are the same colouration

as the dorsum and sometimes have irregular brown markings. Upper lip may be light brown or the same colour as the dorsum without any markings. Iris golden to brown. Tympanum partially or completely covered with a brown blotch, either joining the brown bar behind the eye or as a separate blotch. Throat and chest uniformly white to pale yellow. Ventrums white to orange-yellow, sometimes with yellow to orange zones on the sides and extending to the ventral side of the thighs. In gravid females, yellow eggs are visible through the thick ventral skin. Palms of the hands, ventral sides of feet and tibia more or less heavily dusted with dark grey. Dorsal skin may be smooth, slightly or very rugose.

Etymology. The specific name refers to the Shebelle River, as the distribution range of the species appears restricted to the Shebelle River Basin, with populations found both north and south of the source of the river (Fig. 1).

Habitat, distribution and natural history. *Leptopelis shebellensis* sp. nov. inhabits the grassy meadows of the Didda Plateau and the northern Bale Mountains at mid- to high elevations (2,429–3,296 m a.s.l.). This species is notably found near Assela, Huruta, Dinsho, Adaba, Dodola, Goba and Chole (Fig. 1; Suppl. material 5: table S1). Males have been heard calling both during the dry (April, June) and rainy seasons (July, August) and call both at night and during the day, for extended periods of time. Males call on the bank of streams or side pools, generally from holes in the ground, sometimes from the ground under low vegetation.

Advertisement call. The call of *Leptopelis shebellensis* sp. nov. is a very short rattle. It is composed of one or two identical notes at 704 ± 85 ms interval (Fig. 4A). When they are produced, two-note calls make up about half of the calls within a call bout. Each note is 57 ± 5 ms in duration and contains five pulses, emitted regularly with very short inter-pulse intervals (11 ± 2 ms). The relative position of the note's amplitude peak is variable amongst individuals and may be on the first pulse, in the middle of the note or the amplitude may be equivalent for each pulse. Within a call bout, calls are spaced by 8 ± 1 seconds. Call dominant frequency is $1,616 \pm 265$ Hz, with a band width of 974 ± 163 Hz.

The call of *Leptopelis shebellensis* sp. nov. is distinguishable from the calls of *L. gramineus*, *L. diffidens*, *L. sp.* Kibre Mengist and *L. rugosus* by its higher pulse rate. It is further distinguished from the call of *L. gramineus*, *L. diffidens* and *L. sp.* Kibre Mengist by its shorter note duration and narrower frequency band width and from *L. susanae* by its longer note duration and lower pulse rate. Finally, it can be distinguished from the call of *L. rugosus* by its greater number of pulses per note.

***Leptopelis xeniae* Goutte, Reyes-Velasco, Kassie & Boissinot, sp. nov.**

<https://zoobank.org/1773A2C3-8562-4F29-96E3-7C809FD7FD74>

Common name. English: Xenia's African treefrog.

Type material. *Holotype.* Adult male (SB183), collected on 18 April 2018 by S. Goutte and J. Reyes-Velasco east of Kibre Mengist (5.8782°N, 39.1330°E, 1832 m a.s.l.). *Paratypes.* One female (SB151) and two males (SB152, SB153), collected

on 17 April 2018 by S. Goutte and J. Reyes-Velasco northwest of Kibre Mengist (5.9988°N, 38.8798°E, 2097 m a.s.l.), four males (SB167, SB168, SB169, SB170), collected on 17 April 2018 by S. Goutte and J. Reyes-Velasco northwest of Kibre Mengist (6.0093°N, 38.8576°E, 2105 m a.s.l.) and one male (SB184) collected on 18 April 2018 by S. Goutte and J. Reyes-Velasco east of Kibre Mengist (5.8782°N, 39.1330°E, 1832 m a.s.l.).

Other material examined. One female (SB197) and 12 males (SB186–SB196, SB206), collected on 19 April 2018 by S. Goutte and J. Reyes-Velasco southeast of Kofele (7.0226°N, 38.8701°E, 2,561 m a.s.l.).

Diagnosis. Small to medium-sized (male (n = 20) SVL 27.6 ± 2.0 mm, female (n = 2) SVL 43.5 ± 5.7 mm), robust arboreal species of the *Leptopelis gramineus* species complex (Fig. 8). It differs from other members of the *Leptopelis gramineus* species complex by the following combination of characters: (1) thin, elongated hind-limbs (male TL/SVL 0.36 ± 0.02 , female TL/SVL 0.37 ± 0.03), (2) small metatarsal tubercle (male MTL/SVL 0.07 ± 0.01 , female MTL/SVL 0.06 ± 0.00) (2) inter-orbital distance very short (male IOD/ED 0.88 ± 0.16 , female IOD/ED 0.69 ± 0.12), (3) dorsal skin always smooth, except in females where it may be slightly rugose, (4) absence of yellow colouration on the ventrum or inner thighs.

Comparison. Smaller body size, narrower head than *L. rugosus*, *L. shebellensis* sp. nov. and *L. susanae* (Table 1, Suppl. material 5: table S9). Tympanum and metatarsal tubercle smaller than *L. rugosus* and *L. shebellensis* sp. nov. Interorbital distance shorter than *L. gramineus* and *L. diffidens*. Snout narrower than *L. gramineus*, *L. rugosus* and *L. shebellensis* sp. nov. and more elongate (snout-nostril distance greater) than *L. gramineus* and *L. diffidens*. Hind-limbs and feet longer than in *L. gramineus*, *L. rugosus* and *L. shebellensis* sp. nov. (Table 1, Suppl. material 5: table S9).

Description of the holotype. Small-sized male (SVL 28.9 mm) adult (Fig. 8). Body robust. Head a third of body size in length, wider than long (HW/HL 1.16). Snout angular and narrow (IND/IOD 0.75). Nostril beyond half-way between the tip of the snout and the eye (NS/SL 0.56). Canthus rostralis well-marked and loreal region slightly concave. Pupil vertical. Tympanum clearly visible, and round, $0.71 \times$ eye diameter. Fingers and toes thin and elongated with discs barely expanded, but distinct, ovoid. Finger formula: I < II < IV < III. Hand free of webbing. Hind-limbs relatively long for the *L. gramineus* species complex (TL/SVL 0.38 and THL/SVL 0.42 vs. TL/SVL < 0.37 and THL/SVL < 0.40 in other species of the *L. gramineus* complex, except *L. susanae*). Foot $1.2 \times$ tibia length. Inner metatarsal tubercle present, oval in shape, $0.21 \times$ foot length. Outer metatarsal tubercle absent. Toe formula: I < II < V < III < IV. Foot webbing minimal. Skin of the dorsum and flanks smooth, ventrum rugose.

Colouration of the holotype in life. Dorsal ground colour grey-brown with three dark, but very faint, wide bands; the central band forming a triangle pointing towards the snout and each eye and extending along the spine to about three-fourths of the dorsum (Fig. 8A). Two similarly-coloured symmetrical bands on each side, starting behind the shoulder and fading away at the same level as the dorsal stripe. A few small

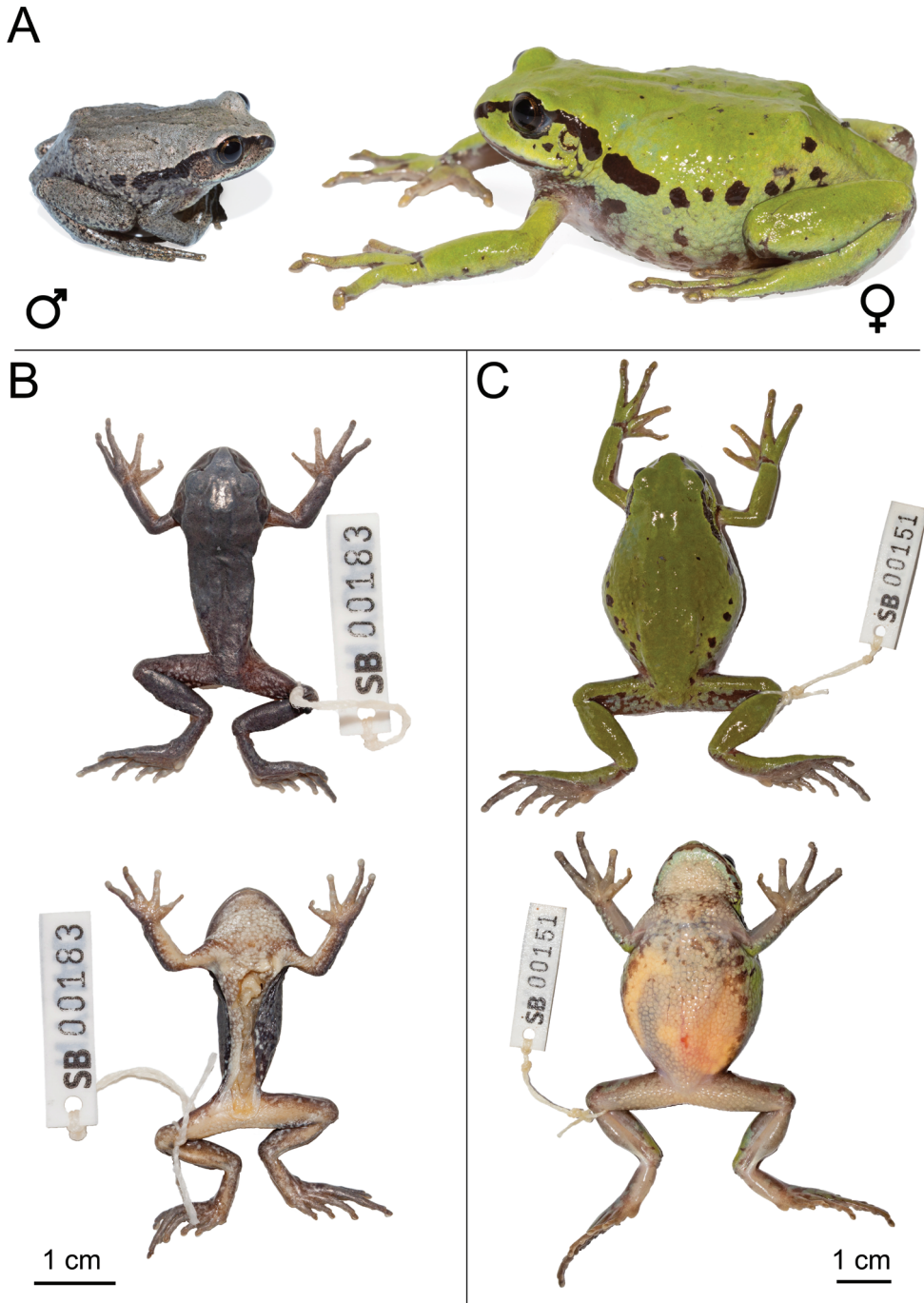


Figure 8. *Leptopelis xeniae* sp. nov. **A** live male holotype (SB183; left) and female paratype (SB151; right) **B** dorsal and ventral views of the male holotype (SB183) after fixation **C** dorsal and ventral views female paratype (SB151) after euthanasia and before fixation.

dark brown spots on the head and dorsum. Black canthal stripe from the tip of the snout extending above the tympanum and behind the shoulder on the left side and to a third of the abdomen on the right side. One large black blotch on the flank, in the continuation of the canthal stripe on each side. Tympanum light grey dusted with small black spots. Upper and lower lip light grey with small irregular black markings. Iris dark gold, lighter on the upper third, with heavy black reticulation. Flanks grey, yellow towards the thighs, with irregular black blotches. Ventrums and throats cream, reticulated with light grey on the chest. Limbs, hands and feet grey dusted with small black freckles. Back of the thighs dark brown with irregular bluish-grey and yellowish-grey markings.

Colouration of the holotype in preservative. Dorsal ground colour grey with a few small irregular dark grey spots (Fig. 8B). The faint three-bands pattern formed by these small dark grey spots is almost completely undistinguishable. Hands, feet and limbs grey with a few irregular dark grey spots. Back of the thighs dark brown with irregular light grey blotches. Throat and ventrum cream with some light brown or grey dusting. Ventral side of the thighs cream. Ventral side of the hands, feet and tibiae heavily dusted with brown and with a few irregular white spots.

Variations. As with other members of the *Leptopelis gramineus* species complex, *L. xeniae* sp. nov. shows significant colour polymorphism. Dorsal colouration varies from light grey (with or without some light green) or light brown to bright or dark green with important level of dark pigmentation. Most individuals examined display a similar dorsal pattern composed of three bands, which can be barely distinguishable to well-marked. The canthal stripe may extend as a wide dark brown to black stripe on the flank to four-fifths of the abdomen or be replaced by large blotches of the same colour. Limbs are the same colouration as the dorsum, with variable number of small to medium brown or black markings. Upper lip may be cream, light grey or green, with variable size and number of irregular brown or black markings. Iris golden to dark golden. Tympanum dark brown or black either entirely or on its upper half, with the lower half being the same colour as the dorsum. Rarely, the tympanum is entirely the same colour as the dorsum. Lower lip cream mottled with brown or grey or with a continuous brown blotch. In one female (SB151), the lower lip was light green with a few brown markings. Ventrums and throats white, with small brown blotches on either or both in most individuals. Inner thighs white or lacking any pigmentation, except dark brown and yellow spots towards the knee in some individuals. Cream-coloured eggs visible through the thick ventral skin of the gravid female SB151. Dorsal skin smooth in all specimens examined, except in the female SB197, which had a slightly rugose dorsal skin.

Etymology. *Leptopelis xeniae* sp. nov. is named after Xenia Freilich, who conducted her doctoral research on Ethiopian anurans, including the *Leptopelis gramineus* complex.

Habitat, distribution and natural history. *Leptopelis xeniae* sp. nov. is found in the forested areas around the towns of Kibre Mengist and Kofele, Oromia, Ethiopia (5.87–7.02°N, 38.80–39.13°E; Fig. 1, Suppl. material 5: table S1). The species occupies lower elevations than most other members of the *L. gramineus* species complex (1,832–2,561 m a.s.l.). Males are found calling at night from the ground or from vegetation up to 60 cm high, close to slow-flowing streams or in flooded forest clearings.

Reproductive biology is unknown beyond the calling behaviour and we have not encountered eggs or tadpoles.

Advertisement call. As for other members of the *Leptopelis gramineus* species complex, the call of *Leptopelis xeniae* sp. nov. is a short rattle (Fig. 4D). It is composed of a single note of 175 ± 25 ms in duration, containing 7 ± 2 pulses, which are clearly distinct. Within a note, pulses are spaced by intervals of 30 ± 5 ms. These inter-pulse intervals may be of equal length throughout the note or shorter between the last pulses. Amplitude is highest for the first quarter to half of the note and decreases in its last quarter. Within a call bout, calls are spaced by 14 ± 7 seconds, often with an acceleration of call rate starting with one call every 22 seconds to one note every four seconds. Call dominant frequency is $2,231 \pm 585$ Hz, with an important band width ($2,013 \pm 573$ Hz).

The call of *Leptopelis xeniae* sp. nov. is distinguishable from the calls of *L. gramineus*, *L. diffidens*, *L. shebellensis* sp. nov., *L. rugosus* and *L. susanae* by its longer note and longer inter-pulse intervals (Fig. 4, Table 2). It is further distinguished from the call of *L. shebellensis* sp. nov. and *L. rugosus* by a greater number of pulses per note, a higher peak frequency and a wider frequency band width (Table 2).

Remark on the Kofele population

Around the town of Kofele (7.0226°N, 38.8701°E, 2,561 m a.s.l.; Fig. 1), we found a population of *Leptopelis xeniae* sp. nov., which carried the mitochondrial genome of *L. shebellensis* sp. nov. suggesting gene flow between the two species in this area (Fig. 2; Reyes-Velasco et al. 2018). Individuals from this population are morphologically indistinguishable from other *L. xeniae* sp. nov. individuals and clearly different from *L. shebellensis* sp. nov. (Fig. 3). In addition, their nuclear genome is mostly of *L. xeniae* sp. nov. origin (Reyes-Velasco et al. 2018). Since the Kofele population shows evidence of past hybridisation, individuals from this locality have been excluded from the type series.

Remarks and notes on *Leptopelis diffidens*

Leptopelis diffidens shows substantial colour polymorphism, with dorsal colouration ranging from light yellow, brown, sand, orange to bright or bluish-green. Many individuals have a more or less marked three-banded pattern also shared with other species of the genus. Contrary to what is stated in the original description, we found *L. diffidens* in syntopy with *Leptopelis ragazzii* in multiple forest clearings, with males calling simultaneously. Male *L. diffidens* were found calling on flooded grass or reeds, while males *L. ragazzii* called from trees at 1.5–3 m above the ground. We also found multiple *L. diffidens* males calling on vegetation and under rocks around a rivulet running through the small town of Rira. Several female *L. diffidens* were found on shrubs as high as 1.5 m above the ground.

Beside the advertisement call produced by males, we recorded three calls, which we identified as aggressive calls, from two different males (Suppl. material 4: fig. S4A). These calls are longer than the species' advertisement call (1050 ± 148 ms) and composed of three pulse groups of 4 ± 1 , 4 ± 1 and 23 ± 1 pulses, respectively. The peak frequency of this call is lower than the advertisement call, at 1705 ± 34 Hz.

Identification key

- 1 Medium to large body size (male SVL 26–38 mm, female SVL 44–57 mm), finger and toe discs very enlarged, elongated hind-limbs (male TL/SVL 0.40–0.49, female TL/SVL 0.41–0.45; male THL/SVL 0.40–0.49, female THL/SVL 0.42–0.49 *L. susanae*
- Small to large body size (male SVL 21.5–45 mm, female SVL 35.9–61 mm), finger and toe discs barely expanded or not expanded at all, hind-limbs short to moderately elongated..... **2**
- 2 Medium to large body size (male SVL 30–45 mm, female SVL 45–61 mm), large tympanum (male TD/ED > 0.51, female TD/ED > 0.54), metatarsal tubercle spade-shaped and well developed..... **3**
- Small to medium body size (male SVL 21.5–38.8 mm, female SVL 35.9–50.2 mm), small tympanum (male TD/ED < 0.54, female TD/ED < 0.45), small ovoid metatarsal tubercle **4**
- 3 Ventral area and inner limbs with very little to no melanisation *L. rugosus*
- Palms of the hands, ventral sides of feet and tibia more or less heavily dusted with dark grey..... *L. shebellensis*
- 4 Inter-orbital distance very short (male IOD/ED 0.88 ± 0.16 , female IOD/ED 0.69 ± 0.12), snout narrow and elongate (male SN/SL 0.56 ± 0.05 , female SN/SL 0.57 ± 0.00 *L. xeniae*
- Inter-orbital distance not very short (male IOD/ED > 0.76, female IOD/ED > 0.77) snout less narrow (male and female SN/SL < 0.53 **5**
- 5 Finger tips barely enlarged *L. gramineus*
- Finger tips enlarged..... *L. diffidens*

Discussion

In the present work, we resolved issues related to the taxonomy of the *Leptopelis gramineus* species complex, which consists of at least six species. We described two new species found east of the GRV and clarified the status of montane populations west of the GRV. Using genetic and morphometric analyses of type specimens, we demonstrated that *Leptopelis rugosus* (= *Pseudocassina rugosa*) and *L. montanus* (= *Pseudocassina ocellata*) are, in fact, conspecific with the population northwest of the GRV and that the mountain populations east of the GRV belong to a new species, *L. shebellensis* sp. nov. In this species complex, including historical type specimens was necessary to assign the correct names to newly-discovered and previously-synonymised taxa. The present case is reminiscent of the situation reported in Ethiopian *Ptychadena*, where the analysis of type specimens allowed us to clarify the convoluted taxonomy of the group (Goutte et al. 2021; Reyes-Velasco et al. 2021).

The *Leptopelis gramineus* species complex comprises species living in most of the biotopes present in the Ethiopian Highlands, from mid-elevation forests

(~ 1,800 m a.s.l.) to high-elevation montane grasslands (> 3,200 m a.s.l.). Members of this clade show traits associated either with a semi-fossorial lifestyle (e.g. well-developed metatarsal tubercles, robust limbs and body shape) in species living in high elevation grasslands (*L. rugosus* and *L. shebellensis* sp. nov.) or with a more arboreal lifestyle (e.g. elongated limbs, slender body) in species inhabiting forests and forest edges (*L. diffidens*, *L. susanae* and *L. xeniae* sp. nov.). The *L. gramineus* species complex thus adds to a growing list of groups that have diversified in the Ethiopian Highlands (e.g. Goutte et al. 2019, 2021; Koppetsch 2020; Kostin et al. 2020; Soultan et al. 2020) and highlights the ecological importance of this unique region.

The restriction of *Leptopelis gramineus* to the south-eastern population near Chenchu and description of several species previously thought to be *L. gramineus* should impact the conservation status of Ethiopian *Leptopelis*. Currently, *Leptopelis susanae* is listed as “Endangered” by the IUCN because of its limited distribution range, while *L. gramineus*, considered widespread in Ethiopia, is listed as “Least concern” (IUCN 2022). Other species of the *L. gramineus* species complex are not currently listed. Based on our findings and on ongoing deforestation and land-transformation for pasture and agriculture in the region (Dessie and Christiansson 2008; Assefa and Bork 2014; Kindu et al. 2015), we expect that several species of the *L. gramineus* complex will be listed as “Near threatened”, “Endangered” or “Vulnerable” under IUCN Criteria B1ab (IUCN Standards and Petitions Committee 2022). Thus, we hope that our clarification of the *Leptopelis gramineus* species complex’s taxonomy will encourage conservation efforts in the Ethiopian Highlands, particularly in currently unprotected areas overlapping with *Leptopelis* spp. ranges.

Acknowledgements

We would like to thank the Ethiopian Wildlife Conservation Authority and the Ethiopian Biodiversity Institute for providing us with collecting and export permits for the samples. We are very grateful to Yann Bourgeois, Marcin Falis, Yejie Yun and Paula Mora Rojas who helped with the acoustic recordings in the field. Fieldwork in Ethiopia would not have been possible if not for the invaluable assistance of Megersa Kelbessa, Itbarek Kibret and Samuel Woldeyes of Rock Hewn Tours. This work could not have been possible without the assistance of many curators and collection managers from numerous institutions, including Bezawork Afework Bogale and M. Ketema (Zoological Natural History Museum, Addis Ababa University, Ethiopia), Jeff Streicher (The Natural History Museum, London, UK), Giuliano Doria and Enrico Borgo (Natural History Museum of Genova, Italy) and Mark-Oliver Rödel and Frank Tillack (Museum für Naturkunde Berlin, Germany). We thank Yann Bourgeois and Sebastian Kirchhof who helped with measuring specimens and Marcin Falis and Kole Utzinger who helped with lab work. We are indebted to Marc Arnoux and Nizar Drou from the Genome Core Facility and the Bioinformatics group at NYUAD. The NYUAD Sequencing Core is supported by NYUAD Research Institute grant G1205A to the NYUAD Center for Genomics and Systems Biology. This research was supported by New York University Abu Dhabi Research Funds AD180 (to SB).

References

- Ahl E (1924) Über eine Froschsammlung aus Nordost-Afrika und Arabien. Mitteilungen aus dem Zoologischen Museum in Berlin 11: 1–12. <https://doi.org/10.1002/mmnz.4830110102>
- Assefa E, Bork H-R (2014) Deforestation and Forest Management in Southern Ethiopia: Investigations in the Chenchä and Arbaminch Areas. *Environmental Management* 53(2): 284–299. <https://doi.org/10.1007/s00267-013-0182-x>
- Boulenger GA (1896) LXX.—Descriptions of two new frogs from Lake Tanganyika, presented to the British Museum by Mr. W. H. Nutt. *Annals & Magazine of Natural History* 18(108): 467–468. <https://doi.org/10.1080/00222939608680490>
- Boulenger GA (1898) Concluding report on the late Capt. Bottego's collection of reptiles and batrachians from Somaliland and British East Africa. *Annali del Museo Civico di Storia Naturale di Genova* 2: 715–722.
- Boulenger GA (1909) Descriptions of three new frogs discovered by Dr. P. Krefft in Usambara, German East Africa. *Annals & Magazine of Natural History* 4(24): 496–497. <https://doi.org/10.1080/00222930908692705>
- Dabney J, Meyer M, Pääbo S (2013) Ancient DNA damage. *Cold Spring Harbor Perspectives in Biology* 5(7): a012567. <https://doi.org/10.1101/cshperspect.a012567>
- Dessie G, Christiansson C (2008) Forest Decline and Its Causes in the South-Central Rift Valley of Ethiopia: Human Impact over a One Hundred Year Perspective. *Ambio* 37(4): 263–271. [https://doi.org/10.1579/0044-7447\(2008\)37\[263:FDAICI\]2.0.CO;2](https://doi.org/10.1579/0044-7447(2008)37[263:FDAICI]2.0.CO;2)
- Freilich X, Anadón JD, Bukala J, Calderon O, Chakraborty R, Boissinot S, Calderon D, Kanellopoulos A, Knap E, Marinos P, Mudasir M, Pirpinas S, Rengifo R, Slovak J, Stauber A, Tirado E, Uquilas I, Velasquez M, Vera E, Wilga A (2016) Comparative Phylogeography of Ethiopian anurans: Impact of the Great Rift Valley and Pleistocene climate change. *BMC Evolutionary Biology* 16(1): e206. <https://doi.org/10.1186/s12862-016-0774-1>
- Frost DR (2021) *Amphibian Species of the World: an Online Reference*. Version 6.1. <https://amphibiansoftheworld.amnh.org/index.php> [July 1, 2022]
- Gordon A, Hannon G (2010) FASTX-Toolkit: FASTQ/A short-reads preprocessing tools. http://hannonlab.cshl.edu/fastx_toolkit
- Goutte S, Reyes-Velasco J, Boissinot S (2019) A new species of puddle frog from an unexplored mountain in southwestern Ethiopia (Anura, Phrynobatrachidae, *Phrynobatrachus*). *ZooKeys* 824: 53–70. <https://doi.org/10.3897/zookeys.824.31570>
- Goutte S, Reyes-Velasco J, Freilich X, Kassie A, Boissinot S (2021) Taxonomic revision of grass frogs (Ptychadenidae, *Ptychadena*) endemic to the Ethiopian highlands. *ZooKeys* 1016: 77–141. <https://doi.org/10.3897/zookeys.1016.59699>
- Hahn C, Bachmann L, Chevreaux B (2013) Reconstructing mitochondrial genomes directly from genomic next-generation sequencing reads—A baiting and iterative mapping approach. *Nucleic Acids Research* 41(13): e129. <https://doi.org/10.1093/nar/gkt371>
- IUCN (2022) The IUCN red list of threatened species. <https://www.iucnredlist.org> [July 22, 2022]

- IUCN Standards and Petitions Committee (2022) Guidelines for Using the IUCN Red List Categories and Criteria. Version 15.1. <https://www.iucnredlist.org/documents/RedList-Guidelines.pdf>
- Katoh K, Standley DM (2013) MAFFT Multiple Sequence Alignment Software Version 7: Improvements in Performance and Usability. *Molecular Biology and Evolution* 30(4): 772–780. <https://doi.org/10.1093/molbev/mst010>
- Kindu M, Schneider T, Teketay D, Knoke T (2015) Drivers of land use/land cover changes in Munessa-Shashemene landscape of the south-central highlands of Ethiopia. *Environmental Monitoring and Assessment* 187(7): e452. <https://doi.org/10.1007/s10661-015-4671-7>
- Köhler J, Jansen M, Rodríguez A, Kok PJR, Toledo LF, Emmrich M, Glaw F, Haddad CFB, Rödel M-O, Vences M (2017) The use of bioacoustics in anuran taxonomy: Theory, terminology, methods and recommendations for best practice. *Zootaxa* 4251(1): 1–124. <https://doi.org/10.11646/zootaxa.4251.1.1>
- Koppetsch T (2020) A new species of *Trachylepis* (Squamata: Scincidae) from the Amhara Region, Ethiopia, and a key to the Ethiopian *Trachylepis*. *Zootaxa* 4859(1): 113–126. <https://doi.org/10.11646/zootaxa.4859.1.4>
- Kostin DS, Martynov AA, Komarova VA, Alexandrov DY, Yihune M, Kasso M, Bryja J, Lavrenchenko LA (2020) Rodents of Choke Mountain and surrounding areas (Ethiopia): The Blue Nile gorge as a strong biogeographic barrier. *Journal of Vertebrate Biology* 69(2): 1–12. <https://doi.org/10.25225/jvb.20016>
- Kumar S, Stecher G, Li M, Knyaz C, Tamura K (2018) MEGA X: Molecular Evolutionary Genetics Analysis across Computing Platforms. *Molecular Biology and Evolution* 35(6): 1547–1549. <https://doi.org/10.1093/molbev/msy096>
- Lanfear R, Calcott B, Ho SYW, Guindon S (2012) Partitionfinder: Combined selection of partitioning schemes and substitution models for phylogenetic analyses. *Molecular Biology and Evolution* 29(6): 1695–1701. <https://doi.org/10.1093/molbev/mss020>
- Largen MJ (1977) The Status of the Genus *Leptopelis* (amphibia Anura Hyperoliidae) in Ethiopia, Including Descriptions of Two New Species. *Monitore Zoologico Italiano. Supplemento* 9: 85–136. <https://doi.org/10.1080/03749444.1977.10736845>
- Largen MJ (2001) Catalogue of the amphibians of Ethiopia, including a key for their identification. *Tropical Zoology* 14(2): 307–402. <https://doi.org/10.1080/03946975.2001.10531159>
- Lê S, Josse J, Husson F (2008) FactoMineR: An R package for multivariate analysis. *Journal of Statistical Software* 25(1): 1–18. <https://doi.org/10.18637/jss.v025.i01>
- Lleonart J, Salat J, Torres GJ (2000) Removing Allometric Effects of Body Size in Morphological Analysis. *Journal of Theoretical Biology* 205(1): 85–93. <https://doi.org/10.1006/jtbi.2000.2043>
- Manthey JD, Reyes-Velasco J, Freilich X, Boissinot S (2017) Diversification in a biodiversity hotspot: Genomic variation in the river frog *Amietia nutti* across the Ethiopian Highlands. *Biological Journal of the Linnean Society. Linnean Society of London* 122(4): 801–813. <https://doi.org/10.1093/biolinnean/blx106>
- Mengistu AA (2012) Amphibian diversity, distribution and conservation in the Ethiopian highlands: morphological, molecular and biogeographic investigation on *Leptopelis* and *Ptychadena* (Anura), 219 pp.

- Miller MA, Pfeiffer W, Schwartz T (2010) Creating the CIPRES Science Gateway for inference of large phylogenetic trees. In: 2010 Gateway Computing Environments Workshop (GCE), 1–8. <https://doi.org/10.1109/GCE.2010.5676129>
- Neumann O (1902) From the Somali Coast through Southern Ethiopia to the Sudan. *The Geographical Journal* 20(4): 373–398. <https://doi.org/10.2307/1775561>
- Onn CK, Abraham RK, Grismer JL, Grismer LL (2018) Elevational size variation and two new species of torrent frogs from Peninsular Malaysia (Anura: Ranidae: *Amolops* Cope). *Zootaxa* 4434(2): 250. <https://doi.org/10.11646/zootaxa.4434.2.2>
- R Core Team (2020) R: A language and environment for statistical computing. R Foundation for Statistical Computing, Vienna. <http://www.R-project.org/>
- Reyes-Velasco J, Manthey JD, Freilich X, Boissinot S (2018) Diversification of African tree frogs (genus *Leptopelis*) in the highlands of Ethiopia. *Molecular Ecology* 27(9): 2256–2270. <https://doi.org/10.1111/mec.14573>
- Reyes-Velasco J, Goutte S, Freilich X, Boissinot S (2021) Mitogenomics of historical type specimens clarifies the taxonomy of Ethiopian *Ptychadena* Boulenger, 1917 (Anura, Ptychadenidae). *ZooKeys* 1070: 135–149.
- Ronquist F, Teslenko M, van der Mark P, Ayres DL, Darling A, Höhna S, Larget B, Liu L, Suchard MA, Huelsenbeck JP (2012) MrBayes 3.2: Efficient Bayesian Phylogenetic Inference and Model Choice across a Large Model Space. *Systematic Biology* 61(3): sys029. <https://doi.org/10.1093/sysbio/sys029>
- Rossing TD [Ed.] (2007) Springer Handbook of Acoustics. Springer New York, NY, XXIV, 1182 pp. <https://link.springer.com/book/10.1007/978-0-387-30425-0> [July 17, 2022]
- Shedlock AM, Haygood MG, Pietsch TW, Bentzen P (1997) Enhanced DNA extraction and PCR amplification of mitochondrial genes from formalin-fixed museum specimens. *BioTechniques* 22(3): 394–396, 398, 400. <https://doi.org/10.2144/97223bm03>
- Smith MA, Poyarkov Jr NA, Hebert PDN (2008) DNA BARCODING: CO1 DNA barcoding amphibians: take the chance, meet the challenge. *Molecular Ecology Resources* 8(2): 235–246. <https://doi.org/10.1111/j.1471-8286.2007.01964.x>
- Soultan A, Wikelski M, Safi K (2020) Classifying biogeographic realms of the endemic fauna in the Afro-Arabian region. *Ecology and Evolution* 10(16): 8669–8680. <https://doi.org/10.1002/ece3.6562>
- Sprecht R (2017) Avisoft-SASlab Pro. Avisoft Bioacoustics, Berlin. <http://avisoft.com/index.html>
- Sueur J, Aubin T, Simonis C (2008) Seewave, a free modular tool for sound analysis and synthesis. *Bioacoustics—the International Journal of Animal Sound and Its Recording* 18(2): 213–226. <https://doi.org/10.1080/09524622.2008.9753600>
- Tiutenko A, Zinenko O (2021) A new species of *Leptopelis* (Anura, Arthroleptidae) from the south-eastern slope of the Ethiopian Highlands, with notes on the *Leptopelis gramineus* species complex and the revalidation of a previously synonymised species. *ZooKeys* 1023: 119–150. <https://doi.org/10.3897/zookeys.1023.53404>
- Watters JL, Cummings ST, Flanagan RL, Siler CD (2016) Review of morphometric measurements used in anuran species descriptions and recommendations for a standardized approach. *Zootaxa* 4072(4): 477–495. <https://doi.org/10.11646/zootaxa.4072.4.6>

Supplementary material 1

Maximum Likelihood phylogenetic inference

Authors: Sandra Goutte, Jacobo Reyes-Velasco, Abeje Kassie, Stéphane Boissinot

Data type: jpg file

Explanation note: **Figure S1. A** Maximum Likelihood phylogenetic inference, based on 13 mitochondrial protein coding genes and the two ribosomal RNAs (12s and 16s) for members of the *Leptopelis gramineus* complex. Names in bold represent historical type specimens of *Pseudocassina rugosa* (ZMB-26915) and *Pseudocassina ocellata* (ZMB-26913). Bootstrap values are indicated at the nodes. Circles represent nodes with bootstrap values of 100. **B** Maximum Likelihood phylogenetic inference, based on the protein coding gene COX1 for members of the *Leptopelis gramineus* complex with complete mtDNA genomes. Names in bold represent historical type specimens of *Pseudocassina rugosa* (ZMB-26915) and *Pseudocassina ocellata* (ZMB-26913). Bootstrap values are indicated at the nodes. Circles represent nodes with bootstrap values of 100.

Copyright notice: This dataset is made available under the Open Database License (<http://opendatacommons.org/licenses/odbl/1.0/>). The Open Database License (ODbL) is a license agreement intended to allow users to freely share, modify, and use this Dataset while maintaining this same freedom for others, provided that the original source and author(s) are credited.

Link: <https://doi.org/10.3897/zookeys.1128.82176.suppl1>

Supplementary material 2

Bayesian phylogenetic inference of the *Leptopelis gramineus* species complex, based on COX1

Authors: Sandra Goutte, Jacobo Reyes-Velasco, Abeje Kassie, Stéphane Boissinot

Data type: jpg file

Explanation note: Posterior probabilities are given at the nodes. Names in bold represent historical type specimens of *Pseudocassina rugosa* (ZMB-26915) and *Pseudocassina ocellata* (ZMB-26913).

Copyright notice: This dataset is made available under the Open Database License (<http://opendatacommons.org/licenses/odbl/1.0/>). The Open Database License (ODbL) is a license agreement intended to allow users to freely share, modify, and use this Dataset while maintaining this same freedom for others, provided that the original source and author(s) are credited.

Link: <https://doi.org/10.3897/zookeys.1128.82176.suppl2>

Supplementary material 3

Maximum Likelihood phylogenetic inference, based on the ribosomal RNAs 16s for members of the *Leptopelis gramineus* complex

Authors: Sandra Goutte, Jacobo Reyes-Velasco, Abeje Kassie, Stéphane Boissinot

Data type: jpg file

Explanation note: Names in bold represent historical type specimens of *Pseudocassina rugosa* (ZMB-26915) and *Pseudocassina ocellata* (ZMB-26913). Bootstrap values are indicated at the nodes.

Copyright notice: This dataset is made available under the Open Database License (<http://opendatacommons.org/licenses/odbl/1.0/>). The Open Database License (ODbL) is a license agreement intended to allow users to freely share, modify, and use this Dataset while maintaining this same freedom for others, provided that the original source and author(s) are credited.

Link: <https://doi.org/10.3897/zookeys.1128.82176.suppl3>

Supplementary material 4

Aggressive call of *Leptopelis diffidens* and aggressive or warm-up call of *Leptopelis suanae*

Authors: Sandra Goutte, Jacobo Reyes-Velasco, Abeje Kassie, Stéphane Boissinot

Data type: jpg file

Explanation note: **A** Aggressive call of *Leptopelis diffidens* (SB128) and **B** aggressive or warm-up call of *Leptopelis suanae* (SB223).

Copyright notice: This dataset is made available under the Open Database License (<http://opendatacommons.org/licenses/odbl/1.0/>). The Open Database License (ODbL) is a license agreement intended to allow users to freely share, modify, and use this Dataset while maintaining this same freedom for others, provided that the original source and author(s) are credited.

Link: <https://doi.org/10.3897/zookeys.1128.82176.suppl4>

Supplementary material 5

Tables

Authors: Sandra Goutte, Jacobo Reyes-Velasco, Abeje Kassie, Stéphane Boissinot

Data type: localities, genetic, and morphometric data

Explanation note: **Tables: S1.** Localities of sampled specimens; **S2.** Number and average length of raw reads extracted from historical type specimens; **S3.** GenBank accession numbers; **S4.** PartitionFinder models; **S5.** Pairwise genetic distances (uncorrected P distances) of the whole mtDNA dataset; **S6.** Pairwise genetic distances (uncorrected P distances) of the COX1 dataset; **S7.** Linear morphometric measurements; **S8.** PCA loadings and scores for males and females of the *Leptopelis gramineus* complex; **S9.** Tukey HSD pairwise tests for linear morphometric measurements of males and females of the *Leptopelis gramineus* complex; **S10.** Acoustic characteristics of advertisement calls, averaged per individual.

Copyright notice: This dataset is made available under the Open Database License (<http://opendatacommons.org/licenses/odbl/1.0/>). The Open Database License (ODbL) is a license agreement intended to allow users to freely share, modify, and use this Dataset while maintaining this same freedom for others, provided that the original source and author(s) are credited.

Link: <https://doi.org/10.3897/zookeys.1128.82176.suppl5>

A new species of the genus *Podocerus* from the Seto Inland Sea, Japan (Crustacea, Amphipoda, Podoceridae)

Takanobu Arai¹, Yujiro Ohno¹, Ko Tomikawa²

1 Saijyo Agricultural High School, 3-16-1 Kagamiyama, Higashihiroshima 739-0046, Japan **2** Graduate School of Humanities and Social Sciences, Hiroshima University, 1-1-1 Kagamiyama, Higashihiroshima 739-8524, Japan

Corresponding author: Ko Tomikawa (tomikawa@hiroshima-u.ac.jp)

Academic editor: Rachael Peart | Received 2 August 2022 | Accepted 19 September 2022 | Published 8 November 2022

<https://zoobank.org/2377C791-A776-4794-A26E-CA354919A921>

Citation: Arai T, Ohno Y, Tomikawa K (2022) A new species of the genus *Podocerus* from the Seto Inland Sea, Japan (Crustacea, Amphipoda, Podoceridae). ZooKeys 1128: 99–109. <https://doi.org/10.3897/zookeys.1128.91155>

Abstract

A new podoceric amphipod, *Podocerus setouchiensis* **sp. nov.**, is described from the Etajima Island, the Seto Inland Sea, Japan. This new species differs from its congeners by the dorsal carination of pereonites and pleonites, and form of the antenna 1, gnathopods 1 and 2, uropods 1 and 2, and telson. Nucleotide sequence data of the mitochondrial cytochrome *c* subunit I (COI) from a paratype of *Podocerus setouchiensis* **sp. nov.** is provided for future molecular systematic studies.

Keywords

COI, intertidal, podoceric, *Podocerus setouchiensis*, systematics

Introduction

Podocerus Leach, 1814, is an amphipod crustacean genus belonging to the family Podoceridae Leach, 1814 and is cosmopolitan in world seas (Barnard and Karaman 1991). So far, 63 species of *Podocerus* have been described worldwide (Horton et al. 2022). In Japan, Nagata (1965b) recorded *P. inconspicuus* (Stebbing, 1888) from the sandy mud bottom of the Seto Inland Sea. Hughes (2012) noted morphological differences between Nagata's (1965b) description of *P. inconspicuus* recorded from Japan

and the original description of this species, and considered them to be distinct species. Yamato (1992) described *P. umigame* Yamato, 1992 from green algae growing on the shell of the loggerhead sea turtle *Caretta caretta*. However, this podoceric species is now considered a synonym of *P. chelonophilus* (Chevreux & Guerne, 1888) (Baldinger 2001; Kilgallen 2009; Hughes 2016). Recently, Tomikawa et al. (2019) described *P. jinbe* Tomikawa, Yanagisawa & Vader, 2019, a unique species that lives in the mouth of a whale shark (Tomikawa et al. 2019).

The Seto Inland Sea is the largest inland sea in Japan, surrounded by the three of four largest islands in Japan (excluding Okinawa), Honshu, Shikoku, and Kyushu, with more than 700 islands and a rich marine ecosystem. More than 90 species of amphipods have been reported from the Seto Inland Sea (Nagata 1965a; Hirayama 1987; Tomikawa et al. 2016). During our field survey of shallow-water amphipods in the Seto Inland Sea, an undescribed species of *Podocerus* was collected from coasts of Hiroshima and Okayama Prefectures. In this study, this undescribed species is described and illustrated. In addition, DNA sequence data will be provided for future taxonomic studies based on molecular data.

Materials and methods

Sampling and morphological observation

Specimens were collected using a hand net and fixed in 99% ethanol on-site (Fig. 1). Some specimens were frozen, then fixed and preserved with polyvinyl alcohol.

All appendages were dissected using insect pins in 80% ethanol and mounted in gum-chloral medium on glass slides using a stereomicroscope (Olympus SZX7). Slides were examined using a light microscope (Nikon Eclipse Ni), with appendages illustrated using a camera lucida. Bodies were dehydrated through a graded ethanol series, and dried using hexamethyldisilazane (HMDS) (Nation 1983). They were then sputter coated with gold and observed using scanning electron microscopy (SEM, JSM-6510LV). Body length was measured from the rostrum tip to the telson base, along the dorsal curvature to the nearest 0.1 mm. The specimens have been deposited in the National Museum of Nature and Science, Tsukuba (NSMT).

PCR and DNA sequencing

Genomic DNA extraction from body or appendage muscle followed Tomikawa et al. (2014). The cytochrome c oxidase subunit I (COI) gene [LCO1490 and HCO2198 (Folmer et al. 1994)] primer set was used for PCR and cycle sequencing reactions. PCR reactions and DNA sequencing were performed following Tomikawa et al. (2017). Sequences obtained from both strands of the gene segments were edited using MEGA11 (Tamura et al. 2021). DNA sequences have been deposited with the International Nucleotide Sequence Database Collaboration (INSDC) through the DNA Data Bank of Japan (DDBJ).

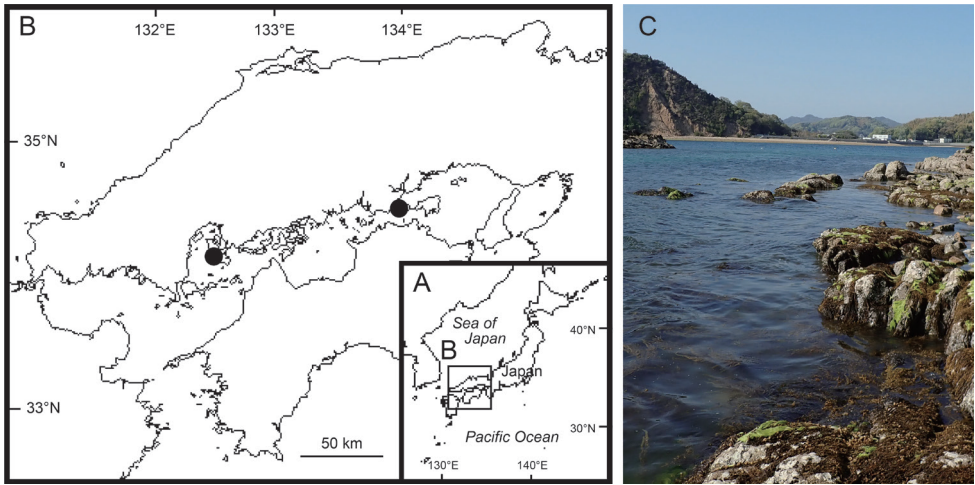


Figure 1. Map showing sampling locality and habitat of *Podocerus setouchiensis* sp. nov. **A** Japan **B** Seto Inland Sea **C** the type locality, Tsuruduki, Etajima, Hiroshima Prefecture, Japan. Circles indicate sampling localities.

Systematics

Suborder Senticaudata Lowry & Myers, 2013

Infraorder Corophiida Leach, 1814

Superfamily Caprelloidea Leach, 1814

Family Podoceridae Leach, 1814

Genus *Podocerus* Leach, 1814

Podocerus setouchiensis sp. nov.

<https://zoobank.org/0A9432E7-8420-431C-8FA8-243EC74DFDF3>

Figs 2–5

New Japanese name: Setouchi-doronomi

Material examined. Holotype: NSMT-Cr 30866, male (5.3 mm), intertidal zone of Tsuruduki, Etajima, Hiroshima Prefecture, Japan (34.1462°N, 132.4399°E), collected by K. Tomikawa on 18 April 2019. **Paratypes:** NSMT-Cr 30867 (female 4.6 mm), NSMT-Cr 30868 (male 6.0 mm, G1527), NSMT-Cr 30869 (male 4.7 mm), NSMT-Cr 30870 (male 4.2 mm), data same as for holotype; NSMT-Cr 30871, 2 males (5.9 mm, 5.1 mm), intertidal zone of Gokan, Tamano, Okayama Prefecture, Japan (34.5263°N, 133.9893°E), collected by H. Ogawa on 9 April 2019.

Diagnosis. Body weakly rugose; pereonites 6–7 and pleonites 1–2 with dorsal carina. Head dorsally smooth. Antenna 1 accessory flagellum 1-articulate. Antenna 2 flagellar article 1 elongate. Uropod 3 rami with setae. Telson shorter than wide, with 2 long robust setae apically, lower margin with short lateral setae.

Description (male, holotype, NSMT-Cr 30866). Body (Fig. 2A–C) weakly rugose; pereonites 6–7 and pleonites 1–2 with dorsal carina. Head (Fig. 2A, C) dorsally

smooth; rostrum absent; lateral cephalic lobe squarish. Gnathopod 2 palm of propodus slightly convex with long plumose setae. Uropods 1 and 2 with distoventral projection.

Antenna 1 (Fig. 3A, B) length $0.8\times$ body length; length ratio of peduncular articles 1–3 1.0: 2.1: 2.0; peduncular article 1 subquadrate, with long setae on posterior margin; peduncular articles 2 and 3 with 9 and 8 clusters of long setae on posterior margins, respectively; primary flagellum 6-articulate, $0.6\times$ peduncular articles 1–3 combined, article 1 long, $3.2\times$ article 2; accessory flagellum slender, 1-articulate. Antenna 2 (Fig. 3C, D) $1.5\times$ antenna 1; peduncular article 4 with long setae on posterior margin; peduncular article 5, $1.4\times$ article 4, with short setae on anterior and posterior margins; flagellum 4-articulate, $0.2\times$ peduncular articles 1–5 combined, article 1 slightly longer than articles 2–4 combined.

Upper lip (Fig. 3E) oval, ventral margin weakly concave, with minute setae. Lower lip (Fig. 3F) outer lobe broad, setulose; inner lobes distinct. Left and right mandibles (Fig. 3G, H) with 5-dentate incisor; molar process small, non-tritulative, with a short plumose seta apically; accessory setal row with 3 setae; palp 3-articulate, length ratio of articles 1–3 1.0: 2.7: 1.9, article 1 bare, article 2 with 20 setae on ventral margin and submargin, ventral margin of article 3 lined with plumose setae, inner surface of article 3 with cluster of setae. Maxilla 1 (Fig. 3I) inner plate indistinct; outer plate rectangular with 9 serrate robust setae; palp article 2 bearing 5 robust and 6 slender setae distally. Maxilla 2 (Fig. 3J) with broad outer plate longer than inner plate, inner and outer plates bearing long plumose setae on apical margin. Maxilliped (Fig. 3K–M) inner plate subrectangular, 3 small robust setae on apical margin and 1 on subapical margin; outer plate slightly exceeding half of palp article 2, medial margin with robust setae and long plumose setae; palp 4-articulate.

Gnathopod 1 (Fig. 3N) coxa slender, subtriangular, longer than broad; basis length $3.7\times$ width, lacking setae on anterior and posterior margins; carpus $2.0\times$ broad, ventral margin weakly lobate with long setae; propodus subtriangular, length $1.9\times$ wide, anterior margin with 4 clusters of slender setae, posterior margin convex with 3 robust setae at palmar corner; posterior margin of dactylus 6-dentate with short setae. Gnathopod 2 (Fig. 3O) coxa quadrate; basis $1.9\times$ broad, weakly concave anteriorly, anterodistal corner lobate; posterodistal corner of merus produced with simple and plumose setae; carpus indistinct, fused with propodus, with setae; propodus subovate, $2.1\times$ wide, anterior margin with 3 clusters of setae and single seta, medial surface with numerous plumose setae, palm slightly convex with long plumose setae, distal shelf well-developed, robust seta at palm defining corner; dactylus smooth, not reaching end of palm, with short setae.

Pereopods 3 and 4 (Fig. 4A–C) basis lacking anterodistal lobe; ischium subrectangular; merus slightly shorter than carpus, anterodistal corner weakly produced; propodus longer than carpus, lacking robust setae marginally. Pereopod 5 (Fig. 4D) basis without posterodistal lobe; posterodistal corner of merus weakly produced; length ratio of merus-dactylus 1.0: 1.2: 1.8: 1.0. Pereopod 6 (Fig. 4E) basis subrectangular, length $1.4\times$ wide, posterodistal corner weakly lobate; posterodistal corner of merus weakly produced; length ratio of merus-dactylus 1.0: 1.2: 2.0: 0.9. Pereopod 7 (Fig. 4F) basis length $1.2\times$ width, posterior margin expanded; merus produced posterodistally; length ratio of merus-dactylus 1.0: 1.2: 1.7: 1.2.

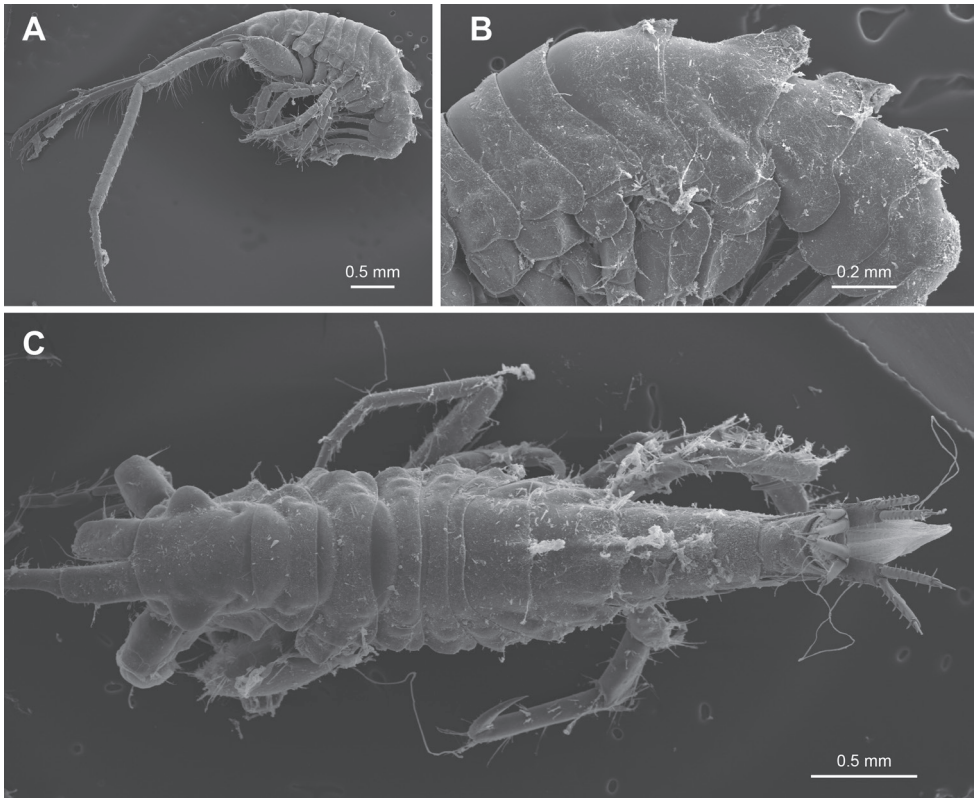


Figure 2. SEM photographs of *Podocerus setouchiensis* sp. nov. **A** habitus, lateral view (NSMT-Cr 30869, male 4.7 mm) **B** dorsal part of pereonites and pleonites, lateral view (NSMT-Cr 30869, male 4.7 mm) **C** habitus, dorsal view (NSMT-Cr 30870, male 4.2 mm).

Pleopods 1–3 (Fig. 4G) peduncle with short setae, inner distal corner with 4 retinacula (Fig. 4H).

Uropod 1 (Fig. 4I) biramous; peduncle 3.4× broad, medial and lateral margins each with 4 robust setae, distoventral projection length 0.3× peduncle; inner ramus 1.2× peduncle, with 7 medial and 2 lateral robust setae; outer ramus 0.8× length of inner ramus, with 3 robust setae on lateral margin. Uropod 2 (Fig. 4I) biramous; peduncle 1.3× broad, with short distoventral projection; inner ramus 1.9× peduncle, medial and lateral margins with 5 and 2 robust setae, respectively; outer ramus 0.7× length of inner ramus, bearing 2 lateral robust setae. Uropod 3 (Fig. 4K) uniramous, plate-like; with 4 apical, 1 medial and 1 lateral robust setae.

Telson (Fig. 4L) length 0.9× width, dorsal lobe with 2 long robust setae apically, lower margin with short lateral setae.

Female (paratype, NSMT-Cr 30867). Antenna 1 (Fig. 5A) length ratio of peduncular articles 1–3 1.0: 2.1: 1.9; primary flagellum 5-articulate, 0.4× peduncular articles 1–3 combined, article 1 long, 2.0× article 2. Antenna 2 (Fig. 5B) peduncular article 5, 1.4× article 4; flagellum 3-articulate, 0.3× peduncular articles 1–5 combined.

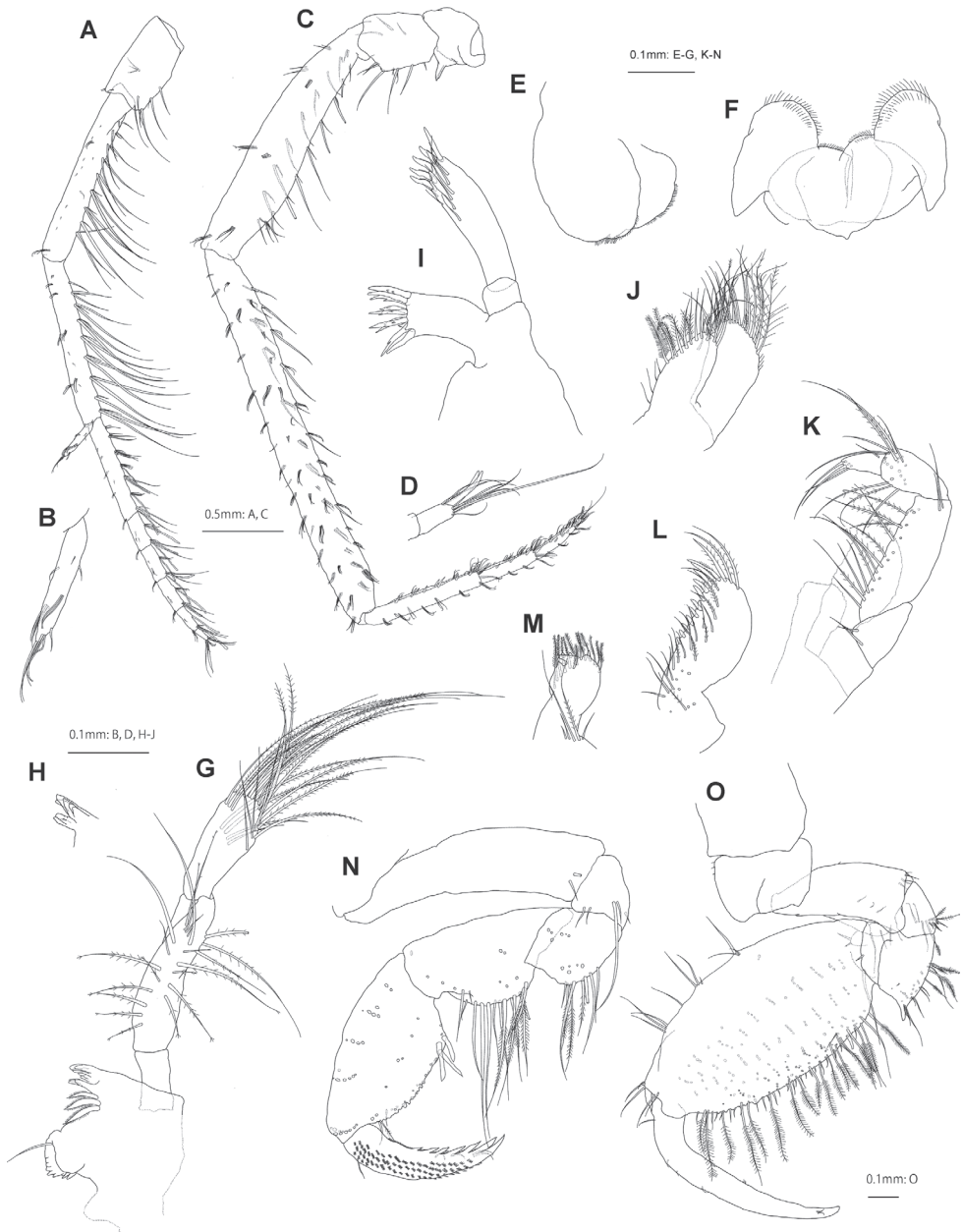


Figure 3. *Podocerus setouchiensis* sp. nov., holotype male, NSMT-Cr 30866 **A** antenna 1, medial view **B** accessory flagellum of antenna 1, medial view **C** antenna 2, medial view **D** distal part of antenna 2, medial view **E** upper lip, anterior view **F** lower lip, posterior view **G** right mandible, medial view **H** incisor and lacinia mobilis of left mandible, lateral view **I** maxilla 1, medial view **J** maxilla 2, medial view **K** palp of maxilliped, medial view **L** outer plate of maxilliped, medial view **M** inner plate of maxilliped, medial view **N** gnathopod 1, lateral view (coxa omitted) **O** gnathopod 2, lateral view.

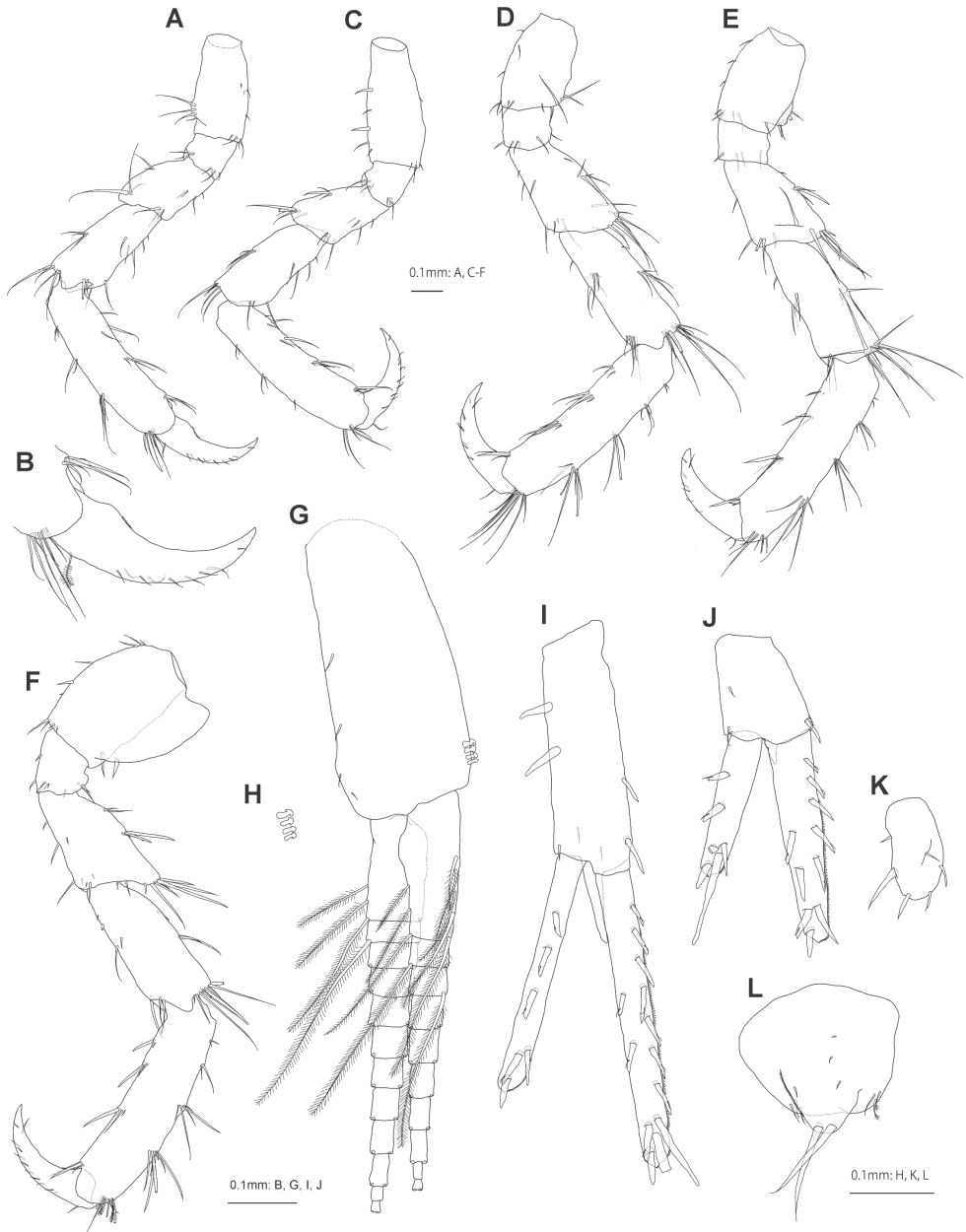


Figure 4. *Podocerus setouchiensis* sp. nov., holotype male, NSMT-Cr 30866 **A** pereopod 3, lateral view (coxa omitted) **B** dactylus of pereopod 3, lateral view **C-F** pereopods 4-7, lateral views (coxae omitted) **G** pleopod 1, posterior view **H** retinacula of pleopod 1, posterior view **I-K** uropods 1-3, dorsal views **L** telson, dorsal view.

Gnathopod 1 (Fig. 5A) basis almost straight; carpus 2.3× broad; palmar margin of propodus bearing robust setae; posterior margin of dactylus 4-dentate. Gnathopod 2 (Fig. 5B) basis with anterodistal robust setae; merus produced anterodistally with robust setae; carpus free, distinct from propodus; propodus ovate, length 1.4× width, palm convex with 3 robust setae near palmar corner.

Etymology. The specific name is derived from the Seto Inland Sea, where this new species is distributed.

DNA Sequence. A sequence of COI (GenBank accession number LC719250; 658 bp) was determined from the paratype female (NSMT-Cr 30868).

Distribution. Known from Hiroshima and Okayama Prefectures.

Remarks. *Podocerus setouchiensis* sp. nov. is similar to *P. andamanensis* (Giles, 1890), *P. casuarinensis* Kilgallen, 2009, *P. crenulatus* Myers, 1985, *P. fulanus* J.L. Barnard, 1962, *P. lazowasemi* Baldinger & Gable, 1994, *P. orontes* Hughes, 2013, and *P. walkeri* Rabindranath, 1972 in having dorsal carinae on pereonites 6 and 7, and pleonites 1 and 2. However, this new species differs from these species by the features shown in the following key. *Podocerus setouchiensis* sp. nov. is also similar to *P. ulreungensis* Kim & Kim, 1991

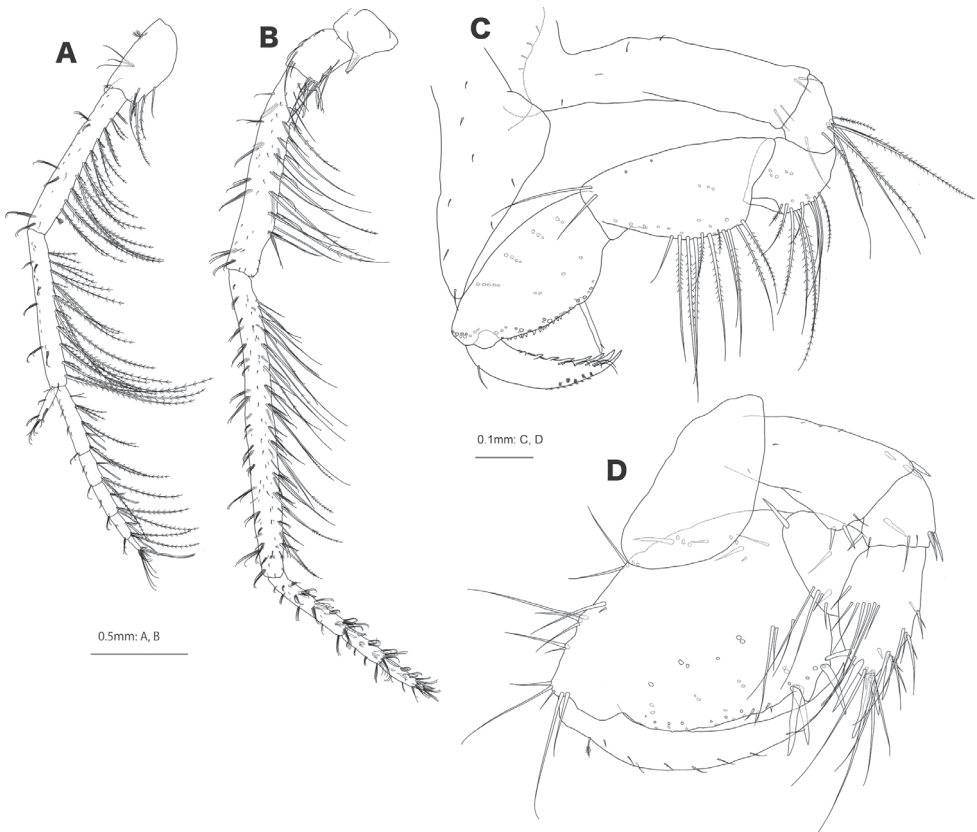


Figure 5. *Podocerus setouchiensis* sp. nov., paratype female, NSMT-Cr 30867 **A** antenna 1, medial view **B** antenna 2, medial view **C** gnathopod 1, lateral view **D** gnathopod 2, lateral view.

from Ulleung Island in the Sea of Japan in having antenna 2 with elongate flagellar article 1, gnathopod 1 with weakly lobate carpus, male gnathopod 2 merus pointed distally, male gnathopod 2 propodus with convex palmar margin bearing long marginal setae and robust seta at palm defining corner, uropod 1 peduncle with distoventral projection, and telson with 2 apical setae. However, this new species is distinguished from the latter by the following features (features of *P. ulreungensis* in parentheses): pereonite 6 with dorsal carina (absent); antenna 1 accessory flagellum 1-articulate (2-articulate); antenna 1 flagellar article 1 length 3.2 times as long as article 2 (2.3 times); uropod 2 peduncle with a short distoventral projection (lacking projection); and telson shorter than wide (longer).

Key to species of *Podocerus* with dorsal carina on pereonites 6 and 7 (lacking dorsal carina on pereonites 1–5).

- 1 Uropods 1 and 2 with peduncular distoventral projection.....2
- Uropods 1 and 2 without peduncular distoventral projection5
- 2 Telson with 2 apical setae..... *P. setouchiensis* sp. nov.
- Telson with 4 or 5 apical setae.....3
- 3 Male gnathopod 2 palmar margin of propodus concave, with long plumose setae, lacking robust setae; uropod 3 without setae on rami.....
.....*P. orontes* Hughes, 2013
- Male gnathopod 2 palmar margin of propodus convex, with short slender and robust setae; uropod 3 with setae on rami4
- 4 Coxa of gnathopod 1 triangular; gnathopod 2 palmar margin of propodus with robust setae on proximal corner*P. fulanus* J.L. Barnard, 1962
- Coxa of gnathopod 1 subquadrate; gnathopod 2 palmar margin of propodus lined with robust setae *P. lazowasemi* Baldinger & Gable, 1994
- 5 Antenna 1 accessory flagellum 2-articulate..... *P. crenulatus* Myers, 1985
- Antenna 1 accessory flagellum 1-articulate.....6
- 6 Uropod 1 inner ramus marginally bare *P. casuarinensis* Kilgallen, 2009
- Uropod 1 inner ramus with marginal robust setae.....7
- 7 Male gnathopod 1 palmar margin of propodus almost straight
.....*P. andamanensis* (Giles, 1890)
- Male gnathopod 1 palmar margin of propodus convex
.....*P. walkeri* Rabindranath, 1972

Acknowledgements

We thank Dr Naohisa Nishihara and staffs of Satoumi Science Museum for their support with the field survey. Thanks are also due to Hiroshi Ogawa for providing materials and Dr Alan Myers for the critical reading and valuable comments on our manuscript. This study was partly supported by the Japan Society for the Promotion of Science KAKENHI grants JP 21H00919, JP22H01011, and JP22K06373 to KT.

References

- Baldinger AJ (2001) An additional record of *Podocerus chelonophilus* (Chevreux and de Guerne, 1888) (Crustacea: Amphipoda: Podoceridae) from a sea turtle off the coast of Ecuador. *Poljskie Archiwum Hydrobiologii* 47: 441–455.
- Barnard JL, Karaman GS (1991) Families and genera of marine gammaridean Amphipoda (except marine gammaroids). Part 2. Records of the Australian Museum 13(2, Supplement 13): 419–866. <https://doi.org/10.3853/j.0812-7387.13.1991.367>
- Folmer O, Black M, Hoeh W, Lutz R, Vrijenhoek R (1994) DNA primers for amplification of mitochondrial cytochrome c oxidase subunit I from diverse metazoan invertebrates. *Molecular Marine Biology and Biotechnology* 3: 294–299.
- Giles GM (1890) Natural history notes from H. M. Indian marine survey steamer ‘Investigator’, commander Alfred Carpenter, R. N., D. S. O., commanding. No. 15. Descriptions of seven additional new Indian amphipods. *Journal of the Asiatic Society of Bengal* 59: 63–74.
- Hirayama A (1987) Two peculiar species of corophiid amphipods (Crustacea) from the Seto Inland Sea, Japan. *Zoological Science* 4: 175–181.
- Horton T, Lowry J, De Broyer C, Bellan-Santini D, Coleman CO, Corbari L, Costello MJ, Daneliya M, Dauvin J-C, Fišer C, Gasca R, Grabowski M, Guerra-García JM, Hendrycks E, Hughes L, Jaume D, Jazdzewski K, Kim Y-H, King R, Krapp-Schickel T, LeCroy S, Lörz A-N, Mamos T, Senna AR, Serejo C, Sket B, Souza-Filho JF, Tandberg AH, Thomas JD, Thurston M, Vader W, Väinölä R, Vonk R, White K, Zeidler W (2022) World Amphipoda Database. <https://doi.org/10.14284/368>
- Hughes LE (2012) New and little-known Podoceridae (Peracarida: Amphipoda) of Southern Australia. *Records of the Australian Museum* 64(1): 71–120. <https://doi.org/10.3853/j.0067-1975.64.2012.1588>
- Hughes LE (2016) Designation of neotypes for *Cyrtophium orientale* Dana, 1853, *Podocerus brasiliensis* (Dana, 1853) and *P. cristatus* (Thomson, 1879) and the description of a new species *Podocerus cyrenensis* (Crustacea: Amphipoda: Podoceridae). *The Raffles Bulletin of Zoology (Supplement 34)*: 312–330.
- Kilgallen NM (2009) Podoceridae. *Zootaxa* 2260(1): 841–860. <https://doi.org/10.11646/zootaxa.2260.1.47>
- Nagata K (1965a) Studies on marine gammaridean Amphipoda of the Seto Inland Sea. I. *Publications of the Seto Marine Biological Laboratory* 13(2): 131–170. <https://doi.org/10.5134/175398>
- Nagata K (1965b) Studies on marine gammaridean Amphipoda of the Seto Inland Sea. III. *Publications of the Seto Marine Biological Laboratory* 13(4): 291–326. <https://doi.org/10.5134/175410>
- Nation JL (1983) A new method using hexamethyldisilazane for preparation of soft insect tissues for scanning electron microscopy. *Stain Technology* 58(6): 347–351. <https://doi.org/10.3109/10520298309066811>
- Tamura K, Stecher G, Kumar S (2021) MEGA11: Molecular Evolutionary Genetics Analysis version 11. *Molecular Biology and Evolution* 38(7): 3022–3027. <https://doi.org/10.1093/molbev/msab120>

- Tomikawa K, Kobayashi N, Kyono M, Ishimaru S, Grygier MJ (2014) Description of a new species of *Sternomoera* (Crustacea: Amphipoda: Pontogeneiidae) from Japan, with an analysis of the phylogenetic relationships among the Japanese species based on the 28S rRNA gene. *Zoological Science* 31(7): 475–490. <https://doi.org/10.2108/zs140026>
- Tomikawa K, Tanaka H, Nakano T (2016) A new species of the rare genus *Priscomilitaris* from the Seto Inland Sea, Japan (Crustacea, Amphipoda, Priscomilitaridae). *ZooKeys* 607: 25–35. <https://doi.org/10.3897/zookeys.607.9379>
- Tomikawa K, Nakano T, Hanzawa N (2017) Two new species of *Jesogammarus* from Japan (Crustacea, Amphipoda, Anisogammaridae), with comments on the validity of the subgenera *Jesogammarus* and *Annanogammarus*. *Zoosystematics and Evolution* 93(2): 189–210. <https://doi.org/10.3897/zse.93.12125>
- Tomikawa K, Yanagisawa M, Higashiji T, Yano N, Vader W (2019) A new species of *Podocerus* (Crustacea: Amphipoda: Podoceridae) associated with the whale shark *Rhincodon typus*. *Species Diversity* 24(2): 209–216. <https://doi.org/10.12782/specdiv.24.209>
- Yamato S (1992) A new species of *Podocerus* (Amphipoda: Podoceridae) from the carapace of a loggerhead sea turtle in Japan. *Publications of the Seto Marine Biological Laboratory* 35(4–5): 281–288. <https://doi.org/10.5134/176201>

A new species of *Nitokra* Boeck, 1865 (Copepoda, Harpacticoida, Ameiridae) from the Caribbean coast of Colombia

Juan M. Fuentes-Reinés¹, Eduardo Suárez-Morales², Marcelo Silva-Briano³

1 Universidad del Magdalena, Grupo de Investigación en Biodiversidad y Ecología Aplicada, A.A 731 Santa Marta, Magdalena, Colombia **2** El Colegio de la Frontera Sur (ECOSUR), A.P. 424, 77014 Chetumal, Quintana Roo, Mexico **3** Departamento de Biología, Universidad Autónoma de Aguascalientes (UAA), 20131 Aguascalientes, Mexico

Corresponding author: Eduardo Suárez-Morales (esuarez@ecosur.mx)

Academic editor: Danielle Defaye | Received 27 May 2022 | Accepted 20 October 2022 | Published 8 November 2022

<https://zoobank.org/2BC60E0B-B619-4815-9AD9-5D4E8507B3A1>

Citation: Fuentes-Reinés JM, Suárez-Morales E, Silva-Briano M (2022) A new species of *Nitokra* Boeck, 1865 (Copepoda, Harpacticoida, Ameiridae) from the Caribbean coast of Colombia. ZooKeys 1128: 111–127. <https://doi.org/10.3897/zookeys.1128.86210>

Abstract

Biological samples obtained from a coastal system of northern Colombia yielded male and female specimens of an undescribed harpacticoid copepod of the diverse ameirid genus *Nitokra* Boeck, 1865. The new species is a member of the genus group III. We describe the new species based on adult male and female individuals. *Nitokra puebloviejensis* **sp. nov.**, appears to be most closely related to *N. vietnamensis* Tran & Chang, 2012, but they can be separated by the following characters: 1) number of setal elements on second segment of mandibular palp, 2) P1ENP/EXP ratio, 3) relative lengths of P2, P3ENP/EXP, 4) number of elements on male P5EXP and ENP, and 5) segmentation of male antennule. In addition, *N. puebloviejensis* **sp. nov.** can be confused with two other congeners: *N. taylori* Gómez, Carrasco & Morales-Serna, 2012 from South Africa and Colombia and *N. kastjanensis* Kornev & Chertoprud, 2008 from the White Sea, but the new species can be distinguished from them by: 1) number of setae on the maxillule coxa, 2) P1ENP/EXP ratio, 3) P2,P3ENP/EXP ratio, 4) female and male P5 setophore, 5) setation pattern of female P5EXP and ENP, 6) structure of female P6, 7) ornamentation of female anal operculum, 8) number of setae on male P5EXP, and 9) the male antennule segmentation. Most importantly, the presence of a group of five short setae on the medial surface of the maxilliped syncoxa allows the new species to be readily distinguished from its congeners. Only two subspecies and one species of this genus have been hitherto recorded from Colombia. A key to the 23 known American species of *Nitokra* is provided.

Keywords

Benthic copepods, brackish waters, harpacticoids, new species, northern Colombia, taxonomy

Introduction

The family Ameiridae Monard, 1927 is one of the most diverse of the copepod order Harpacticoida, and it has been divided into two subfamilies: Stenocopiinae Lang, 1944, and Ameirinae Boeck, 1865, the latter being the most diverse. Currently, the family comprises 49 genera and about 303 species (Walter and Boxshall 2022). Among ameirins, *Nitokra* Boeck, 1865 is the largest genus, with 80 described species and subspecies (Karanovic et al. 2015), 23 of them recorded in the Americas. Only *N. bisetosa* Mielke, 1993, *N. taylori* Gómez, Carrasco & Morales-Serna, 2012, *N. affinis affinis* Gurney, 1927, *N. lacustris richardi* Karanovic et al., 2015, *N. affinis colombiana* Reid, 1988, *N. minor minor* Willey, 1930, *N. lacustris lacustris* (Schmankevitch, 1875) and *N. lacustris sinoi* Marcus & Por, 1961 have been hitherto recorded from the Caribbean coasts (Chappuis 1933; Suárez-Morales et al. 1996, 2006; Suárez-Morales and Reid 1998; Fuentes-Reinés and Suárez-Morales 2014a, b; Karanovic et al. 2015). *Nitokra laingensis*, included in Suárez-Morales et al. (2006) list of Caribbean harpacticoids, was not considered in this paper because it could be an undescribed species. Members of the genus occur mainly in marine environments with a wide depth range (Hendrickx and Fiers 2010), but several species have been recorded from fresh- and brackish-water habitats (Suárez-Morales et al. 1996; Karanovic and Pesce 2002), a wide range of sediment types, and some are symbiotically associated with invertebrates including flatworms, isopods, and decapods (Boxshall and Halsey 2004).

The knowledge on the diversity of *Nitokra* in Colombia is still scarce. Hitherto, only one species and three subspecies have been recorded in the country: *N. lacustris colombianus* from Bahía Solano, Choco, *N. l. sinoi* from Ciénaga Grande de Santa Marta, Magdalena and Laguna Navío Quebrado, la Guajira, and *N. affinis colombiensis* and *N. taylori* from Laguna Navío Quebrado, La Guajira (Reid 1988; Fuentes-Reinés and Suárez-Morales 2014a, b).

The Ciénaga Grande de Santa Marta, a large costal system of northern Colombia, was biologically surveyed during 2017 as part of an ongoing effort aiming to increase our knowledge of the Colombian aquatic biodiversity. The samples obtained yielded male and female specimens of an undescribed species of *Nitokra*. The new species is described and compared it with its closest congeners. A key to the 23 species of *Nitokra* known to occur in the Americas is also provided.

Materials and methods

Biological samples were obtained monthly from littoral habitats of the Ciénaga Grande de Santa Marta, northern Colombia (10°52'11.25"N, 74°19'31.64"W) in July, 2022; samples were collected manually from areas with mangrove vegetation using a 25 L bucket. Water salinity, pH, and temperature were measured *in situ* with a WT-W350i Multimeter.

Samples were filtered with a plankton net (45 µm mesh size) and then fixed and preserved in 70% ethanol. Copepods were sorted from the original samples and then processed for taxonomical identification, including dissection and mounting of taxonomically relevant appendages. Dissected specimens were mounted in glycerin and sealed with Canada balsam. Drawings of the mounted appendages were prepared with a camera lucida; they were also photographed using a Kodak Easy Share C140 digital camera adapted to a compound microscope. Two adult male individuals were prepared for SEM examination with a JEOL LV 5900 microscope at the University of Aguascalientes (UAA), Mexico; one female individual was prepared for SEM examination with a JSM-6010LA microscope at El Colegio de la Frontera Sur, Chetumal, Mexico. The whole specimens were measured in lateral position, from the tip of rostrum to the posterior margin of the caudal rami. Morphological nomenclature follows Huys and Boxshall (1991). The following abbreviations were used in the morphologic description and tables: P1–P6, first to sixth swimming legs; EXP, exopod; ENP, endopod. Setae or spiniform setae are referred to as setal elements. The type specimens were deposited in the collection held at Museo De Historia Natural Marina De Colombia - MAKURIWA.

Results

Taxonomy

Order Harpacticoida G.O. Sars, 1903

Family Ameiridae Boeck, 1865

Subfamily Ameirinae Boeck, 1865

Genus *Nitokra* Boeck, 1865

Nitokra puebloviejensis sp. nov.

<https://zoobank.org/90D3530F-D17B-48E7-BC9A-90F41ED5C0E5>

Figs 1–6

Material examined. Adult female holotype (INV10139), ethanol-preserved, vial, Ciénaga Grande de Santa Marta, Colombia (10°52'11.25"N, 74°19'31.64"W), littoral plankton, coll. J.M. Fuentes-Reinés; adult male allotype (INV CRU10140), ethanol-preserved, vial, same sampling data as holotype. Paratypes: four females (INV CRU10141), and three males (INV CRU10142), same sampling data as holotype and allotype.

Additional material. Six adult females, four adult males in first authors' collection. One female and two male individuals prepared for SEM analysis.

Type locality. Puebloviejo, Ciénaga Grande de Santa Marta, northern Colombia (10°52'11.25"N, 74°19'31.64"W).

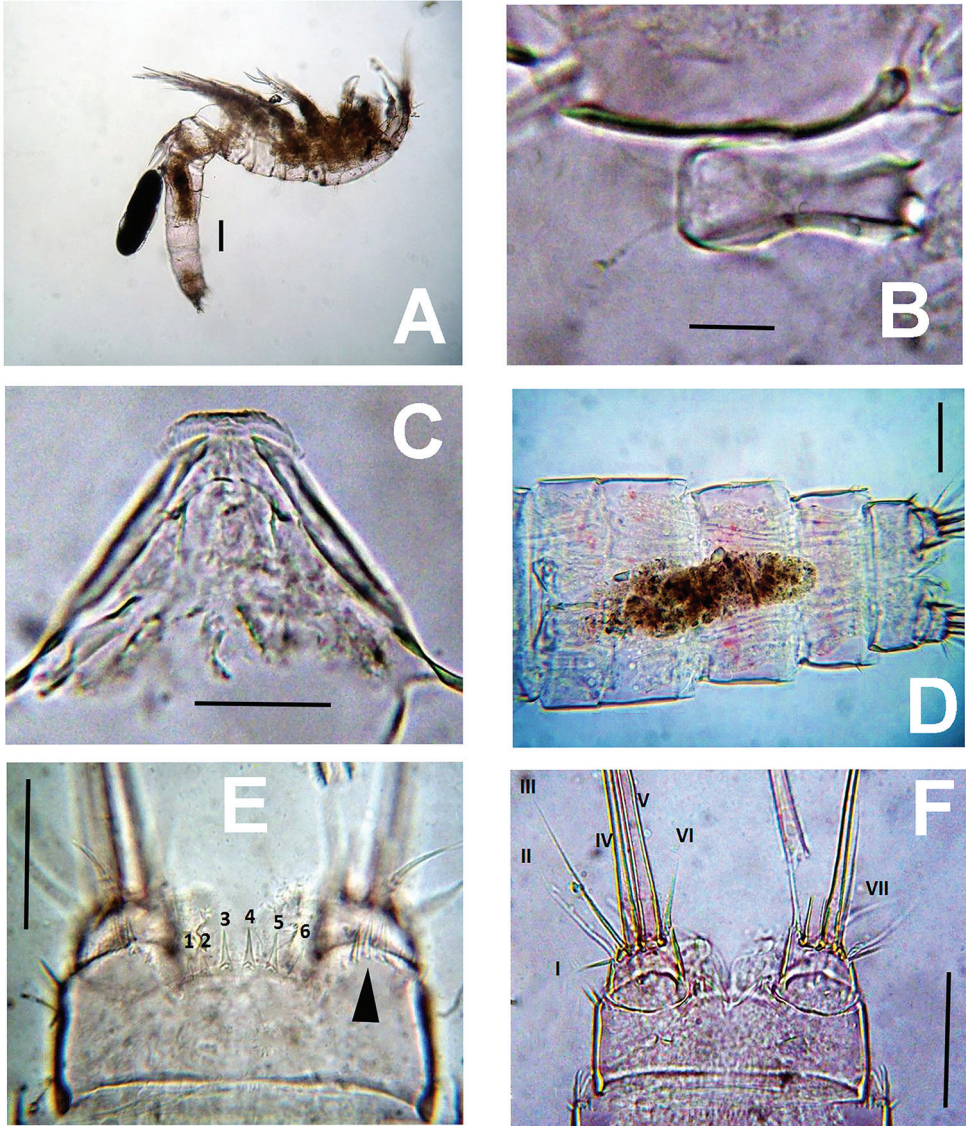


Figure 1. *Nitokra puebloviejensis* sp. nov. from Puebloviejo, Ciénaga Grande de Santa Marta, Colombia, digital photos. **A** holotype female, habitus, lateral view **B** rostrum, ventral view **C** labrum, ventral view **D** urosomites and caudal rami, ventral view **E** anal somite with anal operculum and spine ornamentation, dorsal view **F** anal somite and caudal rami showing caudal setae I–VII, ventral view. Scale bars: 50 μ m (**A**, **C**); 10 μ m (**B**); 20 μ m (**E**, **F**).

Etymology. The new species is named in reference to the type locality of the new species by adding the toponimic suffix in singular. The gender of the species suffix is feminine to match that of the genus.

Differential diagnosis. *Nitokra* with 1 inner seta and 5 setae on P1EXP2 and EXP3, respectively and 455 and 777 elements on P2–P4ENP3 and P2–P4EXP3, respectively, plus 111 inner setae on P2–P4ENP1, respectively. Female rostrum hourglass-shaped, distal segment of mandibular palp with 6 setal elements. P1ENP1 almost reaching distal margin of P1EXP3. Modified, club-shaped inner basipodal seta on leg1. Maxilliped with distinctive group of 5 setae inserted medially on the syncoxa.

Description of female. Body subcylindrical, tapering posteriorly (Fig. 1A), total body length 728–784 μm (average = 768 μm , $n = 6$; holotype length = 784 μm).

Rostrum small, slightly protruding, discernible in dorsal view; roughly hourglass-shaped, with flat tip; rostrum furnished apically with two pairs of short slender sensilla (Figs 1B, 2A). Labrum subtriangular, strong, heavily chitinized, with rugose edge apically (Figs 1C, 2B). Urosome short, thick (Figs 1D, 3D–F), comprising fifth pedigerous somite, genital double-somite and 3 free abdominal somites. Anal somite furnished with row of spinules on proximal ventral surface and along insertion of caudal rami (Figs 1F, 3D–F, 4A). Anal operculum semicircular, ornamented with 5 or 6 spines (Figs 1E, 4A). Caudal ramus short, subquadrate, armed with 7 caudal setae (Figs 1F, 4A), caudal seta I shorter than ramus; seta II about 2.6 \times as long as I, seta III on distal outer position, slightly longer than seta II. Setae IV and V thick, long, the former being longest; seta VI about 1.6 \times as long as seta I. Dorsal seta (VII) simple, about as long as caudal ramus, shorter than seta VI (Figs 1F, 4A).

Antennule 8-segmented, tapering distally (Fig. 4E), first segment robust, subquadrate, unornamented, with single seta. Aesthetasc on fourth segment long, reaching beyond distal end of terminal segment. Fourth segment as long as first. Segmental armature as follows (s = seta, ae = aesthetasc): 1(1s), 2(4s), 3(6s), 4(6+1ae), 5(3s), 6(2), 7(4), 8(7s+1ae).

Antenna (Figs 2E, 3A). Coxa short, subquadrate, smooth. Basis subrectangular, lacking abexopodal seta, armed with short distal spine and row of minute spinules at spine insertion. First endopodal segment subrectangular, smooth, second endopodal segment longer than first, furnished with subdistal row of spinules on inner margin (Fig. 3A), with 2 lateral inner spines and 6 apical setal elements, outermost 2 basally fused at insertion. EXP 1-segmented, cylindrical, armed with 3 subequal setal elements (Figs 2E, 3A, 6C, D).

Mandible (Fig. 2C, D). Gnathal blade armed with 13 teeth, 6 large, 7 small, 1 long spinule, and long dorsal seta ornamented with short spinules (Fig. 2D). Mandibular palp 2-segmented, basal segment short, subquadrate, with short robust seta (Fig. 2C). Endopodal segment subrectangular, armed with 1 short lateral and 5 apical setae (Fig. 2C).

Maxillule (Fig. 2F). With large praecoxa; precoxal arthrite (pca in Fig. 2F) rectangular, unornamented, armed with group of 4 apical and 2 subapical spiniform elements. Coxal endite shorter than precoxal arthrite, armed with 1 curved serrate spiniform element and 2 smooth setae (cxe in Fig. 2F). Basis (bas in Fig. 2F) shorter than coxal endite, seemingly with five subequal apical and subapical setae; exopod reduced, represented by 1 seta; endopod (enp in Fig. 2F) 1-segmented, armed with 2 subequal plumose setae inserted apically (Fig. 2F).

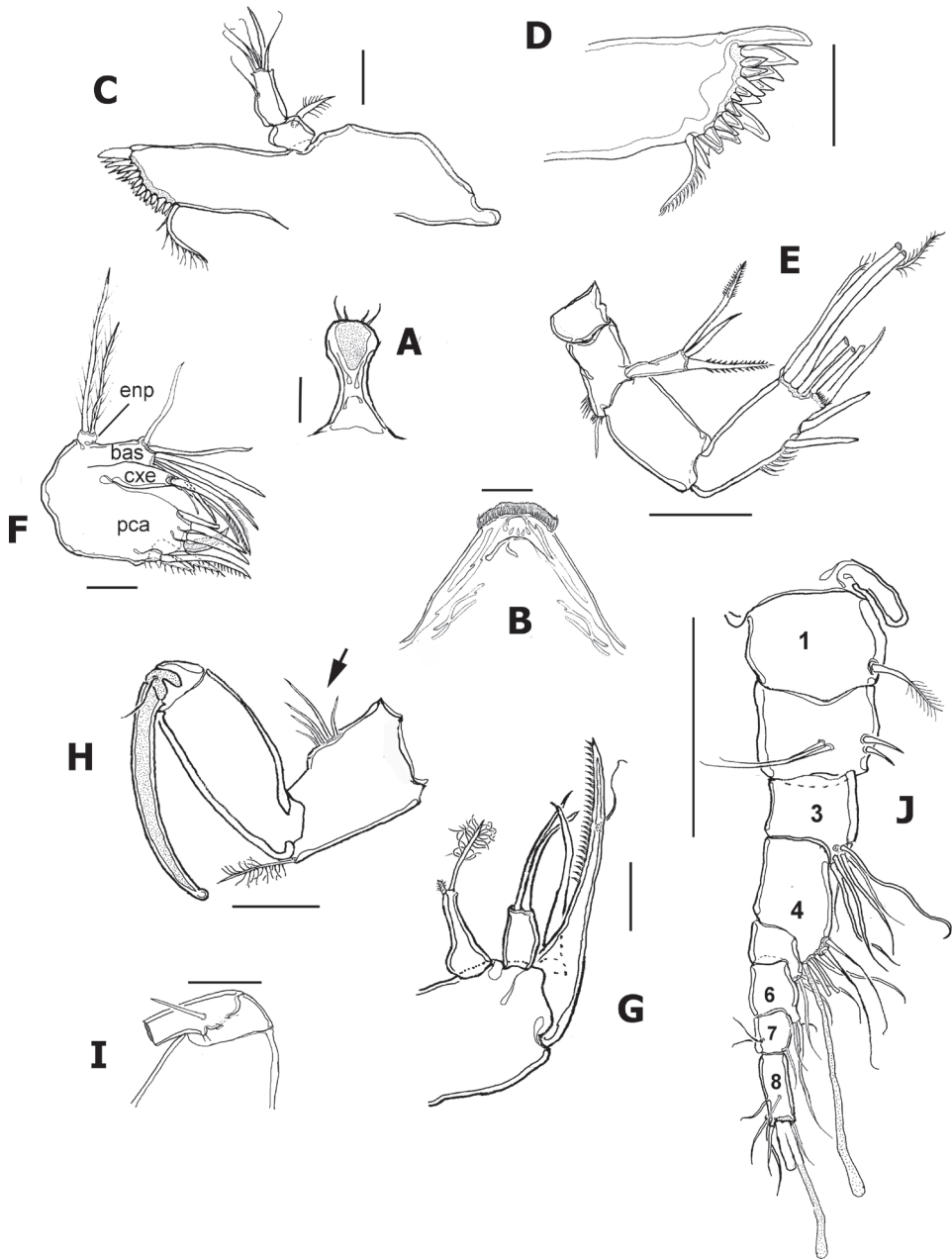


Figure 2. *Nitokra puebloviejensis* sp. nov. from Puebloviejo, Ciénaga Grande de Santa Marta, Colombia. Adult female holotype. **A** rostrum **B** labrum **C** mandible with palp **D** gnathal blade with teeth and dorsal seta **E** antenna (some setae cut short) **F** maxillule showing armature of lobes **G** maxilla **H** maxilliped showing row of setal elements on syncoxa **I** detail of accessory seta of maxilliped ENP **J** antennule showing segmentation. Scale bars: 15 μ m (**A–D, I**); 20 μ m (**D–F**); 25 μ m (**G, H, J**).

Maxilla (Fig. 2G). Syncoxa unornamented, with 2 endites, proximalmost armed with short spiniform element and slender modified seta furnished with distal tuft of setules; second endite with 2 slender apical setae. Allobasis produced into strong serrate claw with short, curved adjacent spiniform element and slender seta. ENP 1-segmented, armed with 2 setae.

Maxilliped (Fig. 2H, I). Subchelate. Syncoxa with single setulated seta on inner distal corner and distinctive group of 4 or 5 short slender elements inserted medially on the outer margin of the syncoxa, as in male (Fig. 2H, arrowhead in Fig. 6E). ENP represented by long, slender claw with short accessory seta (Fig. 2I).

P1 (Fig. 5A). Intercoxal sclerite smooth. Coxa with transverse row of spinules proximally and spinules row distally. Basis with spinules bordering insertion of exopodal and endopodal rami, inner basipodal spine short, reaching proximal 1/3 of length of first ENP segment. Outer basipodal spine short. EXP and ENP 3-segmented. Exopodal ramus shorter than endopod, reaching about the margin end of second exopodal segment. EXP1 lacking inner setae, EXP2 with inner seta; EXP3 with 3 outer spines and 2 geniculate apical setae. ENP 3-segmented; ENP 2 with inner seta, ENP1 subrectangular. ENP3 with 1 apical spiniform seta, 1 geniculate apical seta, and short plumose inner seta.

P2 (Fig. 5B–D). Intercoxal sclerite with transverse rows of long spinules (Fig. 6C). Coxa with transverse row of long spinules plus 2 rows of minute spinules (Fig. 6D). Outer basipodal spine short (“obs” in Fig. 6B). EXP and ENP 3-segmented. EXP1 lacking inner seta, EXP2 with long, slender inner seta, EXP3 with 3 outer spines, 1 apical and 3 inner setae. ENP shorter than EXP, reaching slightly beyond halfway of EXP3. ENP-3 with 2 inner setae (Fig. 5B).

P3 (Fig. 5E). Intercoxal sclerite smooth. Coxa and basis as in P2. EXP and ENP 3-segmented. ENP slightly shorter than EXP. ENP as in P2 except for additional inner plumose seta on ENP3.

P4 (Fig. 5F). Intercoxal sclerite, coxa and basis as in P2 and P3. EXP and ENP 3-segmented. ENP shorter than EXP, barely reaching 1/3 of EXP3. EXP as in P3 except for thinner outer spines on EXP3. ENP as in P3.

P5 (Fig. 3C at arrow, 4C). EXP and baseoendopod not fused, baseoendopod subtriangular, reaching EXP midlength, segment bearing 5 setae, apical being longest. EXP subquadrate, with spinules row along inner margin; EXP armed with 5 unequally long setae (Fig. 4C).

P6 (Fig. 4D). Represented by narrow transverse plate with subdistal lobe-like processes marked by a rounded notch. Plate bearing a small seta on each side (Fig. 4D at arrows).

Armature formula of female P1–P5 as follows:

	Exopod	Endopod
P1	I-0; I-1; III,2,0	0-1;0-1;I,I,2,0
P2	I-0; I-1;III,2,2	0-1;0-1; I,2,1
P3	I-0; I-1;III,2,2	0-1;0-1; I,2,2
P4	I-0;I-1;III,2,2	0-1;0-1;I,2,2
P5	5	5

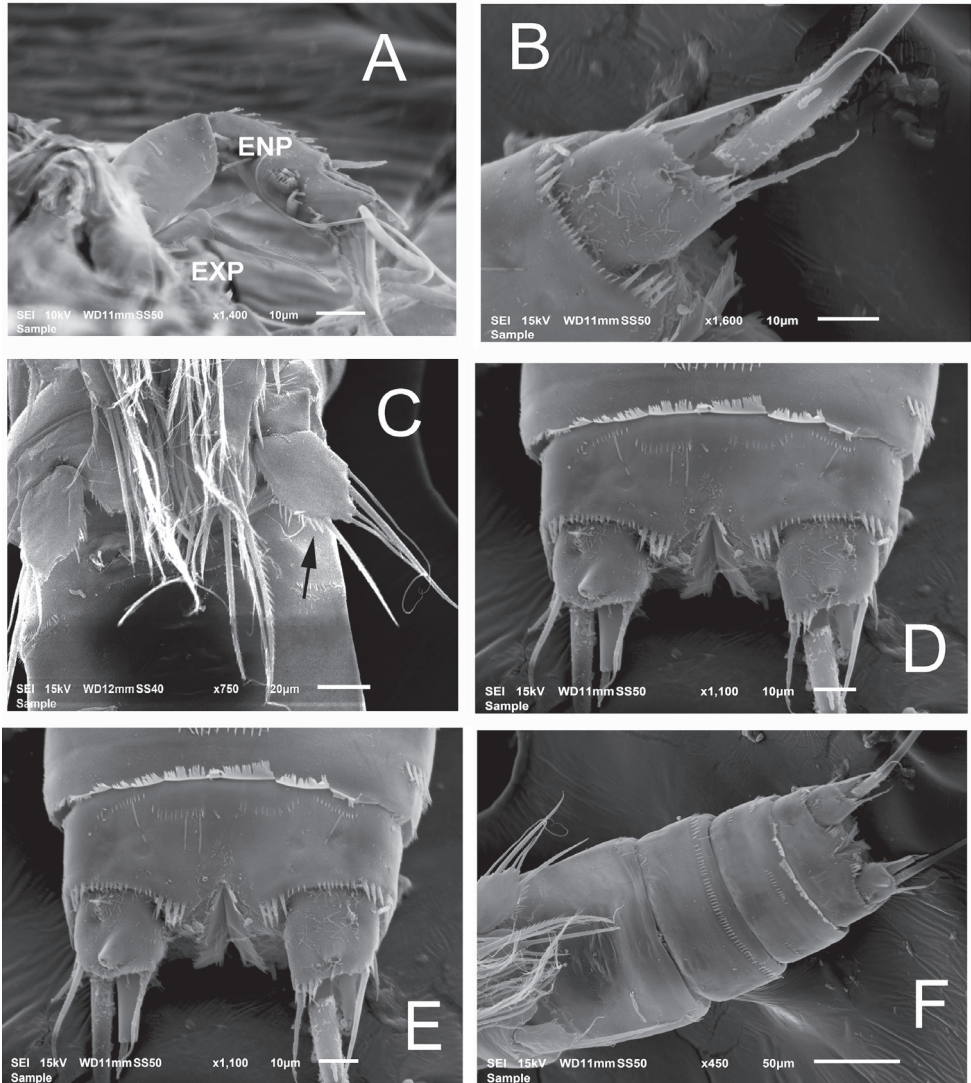


Figure 3. *Nitokra puebloviejensis* sp. nov. from Puebloviejo, Ciénaga Grande de Santa Marta, Colombia. SEM-prepared adult female. **A** antenna showing EXP and ENP **B** posterior end of anal somite and insertion of caudal rami showing ornamentation, semi-lateral view **C** fifth leg exopods (at arrow), ventral view **D** anal somite and caudal rami, ventral view **E** anal somite, ventral view **F** urosome, ventral view.

Male. Smaller than female, total body length 578–588 μm (average length = 578 μm , $n = 3$; allotype specimen length = 588 μm).

Anal operculum, rostrum, antennae (Fig. 6C, D), and mouthparts as in female. Sexual dimorphism expressed in the antennule, urosome, P1basis, distal inner seta of P3ENP3, P5, and P6.

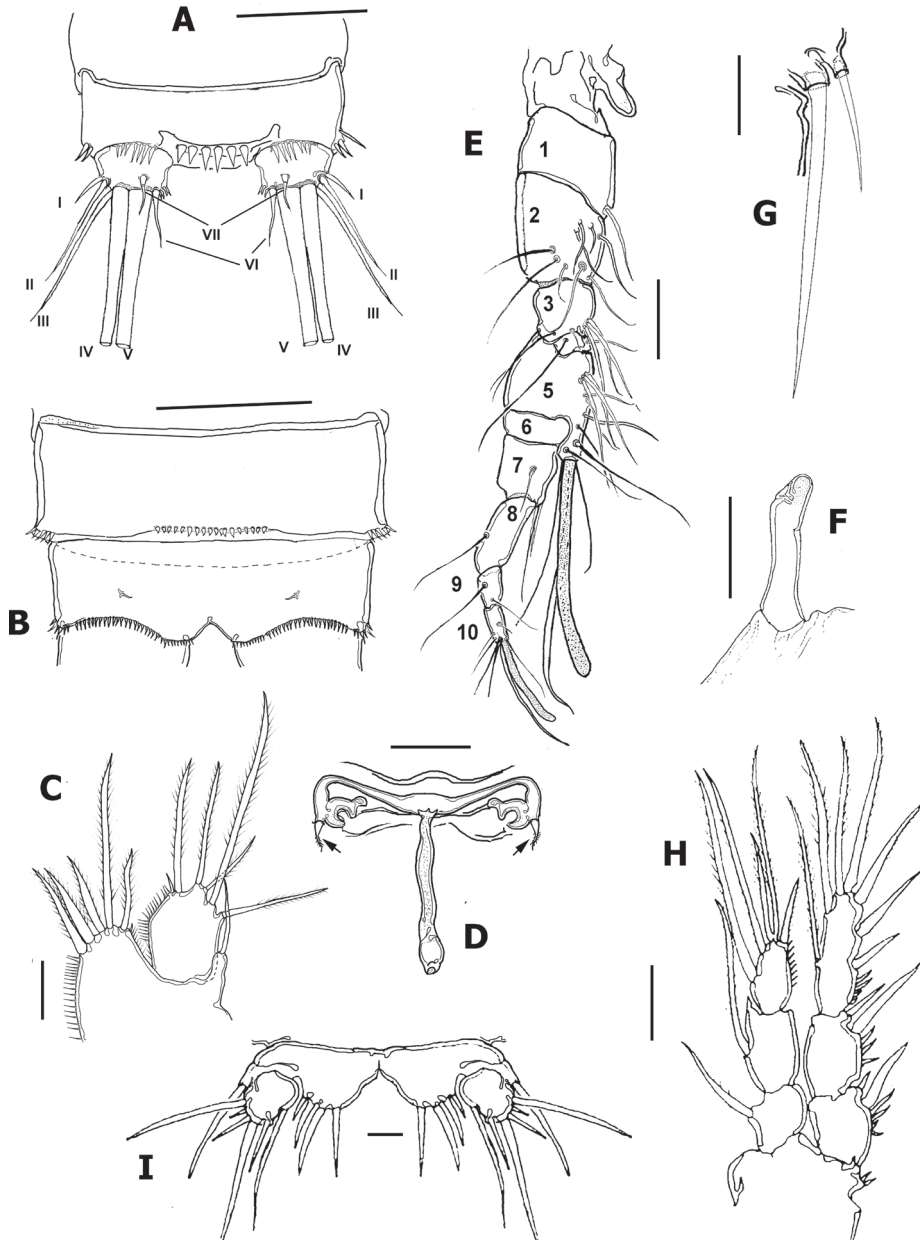


Figure 4. *Nitokra puebloviejensis* sp. nov. from Puebloviejo, Ciénaga Grande de Santa Marta, Colombia. **A** adult female anal and preanal urosomites, dorsal view showing anal operculum and caudal setae I–VII **B** female anal and preanal urosomites, ventral view **C** female P5 **D** female genital field and P6 with setae (arrowed) **E** male geniculated antennule **F** modified, club-shaped basipodal spine of male P1 **G** male leg 6 **H** male P3, anterior view **I** male P5, ventral view. Scale bars: 25 μm (**A–D, I**); 10 μm (**E–G**); 20 μm (**H**).

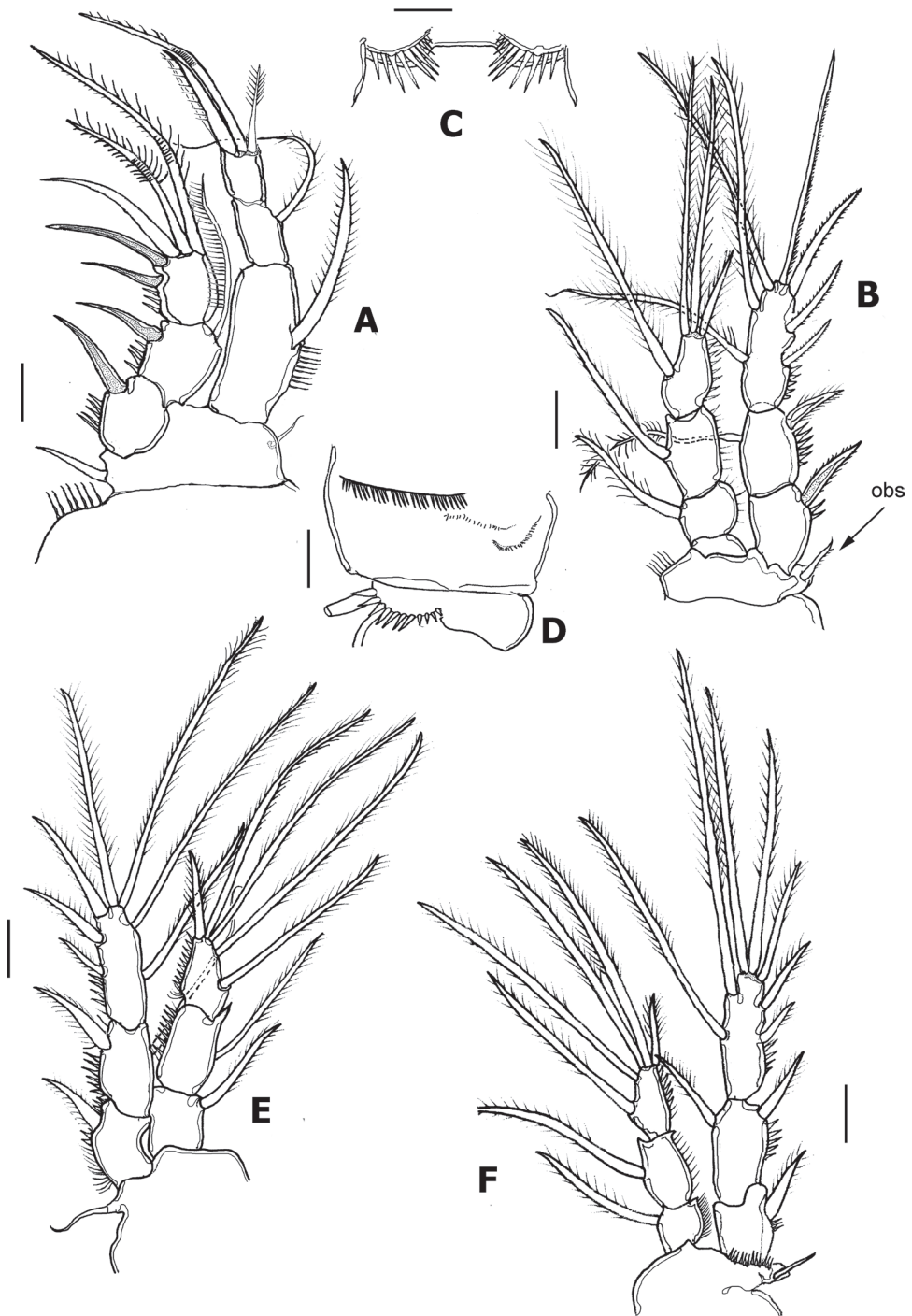


Figure 5. *Nitokra puebloviejensis* sp. nov. from Puebloviejo, Ciénaga Grande de Santa Marta, Colombia. Adult female holotype **A** leg 1 **B** leg 2 **C** leg 2 intercoxal sclerite **D** leg 2 coxa and basipod ornamentation, anterior view **E** leg 3 **F** leg 4. Scale bars: 20 μm (**A, B, D–F**); 10 μm (**C**).

Antennule (Fig. 6A, B) haplocer, 10-segmented; armature formula difficult to discern, purportedly as follows: 1(1s), 2(9s), 3(6s), 4(2s), 5(9+ae), 6(1s), 7(3s), 8(1s), 9(2s), 10(7+ae).

Antenna (Fig. 6C, D), maxilliped (Fig. 6E), mouthparts, and P1–P4 as in female. Ventral ornamentation of urosomites as in female except urosomite 2. Posterior margins of urosomites with row of small spinules.

P1 basis and P3ENP3. P1 basis with modified, club-shaped inner spine (Fig. 4F, arrowheads in Fig. 6F). P3ENP3 with distal inner spine thinner than in female.

P5 (Fig. 4I). EXP and baseoendopod separated. The former subquadrate, with 5 or 6 setae, Baseoendopod reaching about proximal 1/3 of EXP, armed with 4 elements.

P6. With 2 unequal setae, inner one about 3× as long as outer seta. Caudal rami as in female.

Variability. One male with 3 setal elements (instead of 4) on P5ENP. Another male was observed to possess 6 setae instead of 5 on P5EXP.

Habitat. The new species is known only from the type locality, Puebloviejo, Ciénaga Grande de Santa Marta (northern Colombia). The site where it was collected is a shallow mangrove area, 0.7 m deep, with water temperature 26–31 °C; local salinity was 15–20 PSU, and pH values was 7.5–8.1.

Discussion

There are 23 species of the genus reported from the Americas, as follows: *N. typica typica* Boeck, 1865, *N. spinipes spinipes* Boeck, 1865, *N. lacustris lacustris* (Schmankevitch, 1875), *N. hibernica hibernica* (Brady, 1880), *N. lacustris sinoi* Marcus & Por, 1961, *N. pusilla* Sars, 1911, *N. bdelluræ* (Liddell, 1912), *N. affinis affinis* Gurney, 1927, *N. affinis affinis colombiensis* Fuentes-Reinés & Suárez-Morales, 2014, *N. dubia* G. O. Sars, 1927, *N. minor minor* Willey, 1930, *N. chelifera* Wilson, 1932, *N. hyperidis* Jakobi, 1956, *N. fragilis paulistana* Jakobi, 1956, *N. spinipes armata* Lang, 1965, *N. affinis californica* Lang, 1965, *N. lacustris colombiana* Reid, 1988, *N. sphaeromata* Bowman, 1988, *N. galapagoensis* Mielke, 1993, *N. bisetosa* Mielke, 1993, *N. evergladensis* Bruno et al., 2002, *N. taylori* Gómez, Carrasco & Morales-Serna, 2012, and *N. lacustris richardi* Karanovic et al., 2015 (Willey 1930; Lang 1948; Humes 1953; Jakobi 1956; Reid 1987, 1988; Mielke 1993; Suárez-Morales et al. 1996, 2006, 2009; Suárez-Morales and Gasca 1998; Bruno et al. 2002; Reid and Williamson 2010; Fuentes-Reinés and Zoppi de Roa 2013; Fuentes-Reinés and Suárez-Morales 2014a).

In a partial revision of *Nitokra*, Gómez et al. (2012) divided the genus into three morphological groups based on the combination of the armature formula of the P1EXP2 and 3. Species in the first group carry one inner seta and four elements on P1EXP2 and EXP3, respectively. The second group is distinguished by the absence of an inner seta on P1EXP2 but bears five setae on P1EXP3. The third, most diverse group contains species bearing one inner seta and five setae on P1EXP2 and EXP3, respectively (as in Fig. 5A). Up to 13 species and subspecies have been assigned to this group, whose members also

share a pattern of 4,5,5 and 7,7,7 setal elements on P2–P4ENP3 and P2–P4EXP3, respectively, plus 1,1,1 inner setae on P2–P4ENP1, respectively. The group includes: *N. spinipes* Boeck, 1864, *N. fragilis fragilis* Sars, 1905, *N. fragilis paulistana* Jakobi, 1956, *N. spinipes orientalis* Sewell, 1924, *N. pietschmanni* Chappuis, 1933, *N. australis* Soyer, 1974, *N. intermedia* Pesce, 1983, *N. laingensis* Fiers, 1986, *N. husmanni* Kunz, 1976, *N. koreanus* Chang, 2007, *N. taylori* Gómez, Carrasco & Morales-Serna, 2012, *N. vietnamensis* Tran & Chang, 2012, and now *N. puebloviejensis* sp. nov. Within this group, the new species most closely resembles *N. vietnamensis* because they share of several characters including the number of elements on the maxillule coxa, the setation pattern on female P5EXP and P1–P4, relative length of female P5 setophore, number of spines on anal operculum, and relative length of P5ENP inner seta. These two species can be distinguished by the following characters: 1) the distal segment of the mandibular palp has 6 elements in *N. puebloviejensis* (Fig. 2C) vs. only 4 in *N. vietnamensis* (Tran and Chang 2012: fig. 4E), 2) in the new species, *N. puebloviejensis*, the P1ENP1 almost reaches the distal margin of P1EXP3, whereas in *N. vietnamensis* the P1ENP1 is relatively shorter, barely reaching half length of P1EXP2 (Tran and Chang 2012), 3) in *N. puebloviejensis* sp. nov. both the P2ENP and P3ENP reach about half of P2EXP3 and P3EXP3, respectively (Fig. 5B, E), whereas in *N. vietnamensis* these rami are relatively shorter, barely reaching the proximal 1/3 of P2EXP3 and P3EXP3, respectively (Tran and Chang 2012), 4) the female P5EXP is subquadrate, robust in *N. puebloviejensis* (Fig. 4C) vs clearly narrower and elongate in *N. vietnamensis* (Tran and Chang 2012), 5) the male P5EXP and P5ENP are armed with 5 or 6 and 4 elements, respectively, vs 3 and 6 elements, respectively, in *N. vietnamensis* (Tran and Chang 2012), 6) the male antennule is 10-segmented in *N. puebloviejensis* (Fig. 6A, B) vs 8-segmented in *N. vietnamensis* (Tran and Chang 2012).

Furthermore, *N. puebloviejensis* can be confused with *N. taylori*, another congener known from the Colombian Caribbean, but these two species can be distinguished by the following characters: 1) maxillule coxa with 3 setal elements in *N. puebloviejensis* (Fig. 2F) vs 2 in *N. taylori* (Gómez et al. 2012: fig. 4C), 2) P1ENP1 almost reaches the distal margin of P1EXP3 (Fig. 5A) vs relatively shorter, reaching only half length of P1EXP3 in *N. taylori* (Gómez et al. 2012: fig. 4D; Fuentes-Reinés and Suárez-Morales 2014a: fig 6D), 3) P2ENP and P3ENP reach half the length of P2 EXP3 and P3EXP3, respectively (Fig. 5B, E) vs barely reach the proximal 1/3 of P2EXP3 and P3EXP3, respectively in *N. taylori* (Gómez et al. 2012: figs 5B, 6C; Fuentes-Reinés and Suárez-Morales 2014a: fig. 6E, F), 4) intercoxal sclerite of P3 is smooth vs with 2 conspicuous spinule rows in *N. taylori* (Gómez et al. 2012, fig 6C), 5) the female P5 EXP is armed with 5 setae in the new species (Figs 3C, 4C) vs 6 such setae in *N. taylori* (Gómez et al. 2012, fig. 7B, 9C, 10C, Fuentes-Reinés & Suárez-Morales, 2014a, fig 7B, 8G), 6) the female P6 bears a short seta in *N. puebloviejensis* (Fig. 4D) vs 2 slender setae in *N. taylori* (Gómez et al. 2012, fig. 3D, Fuentes-Reinés & Suárez-Morales, 2014a, fig 8H), 7) female anal operculum with 5 or 6 spines in *N. puebloviejensis* (Fig. 4A) vs 3–5 in *N. taylori* (Gómez et al. 2012: fig. 3A; Fuentes-Reinés and Suárez-Morales 2014a: fig. 7C–E), 8) male P5ENP with 4 setae (Fig. 4I) vs 3 in *N. taylori* (Gómez et al. 2012: figs 9C, 10C; Fuentes-Reinés and Suárez-Morales 2014a: fig 8G), 9) male antennule 10-segmented (Fig. 6A, B) vs 9-segmented in *N. taylori* (Gómez et al. 2012; Fuentes-Reinés and Suárez-Morales 2014a), and 10) dorsal caudal seta VII simple (Fig. 4A) vs articulated in

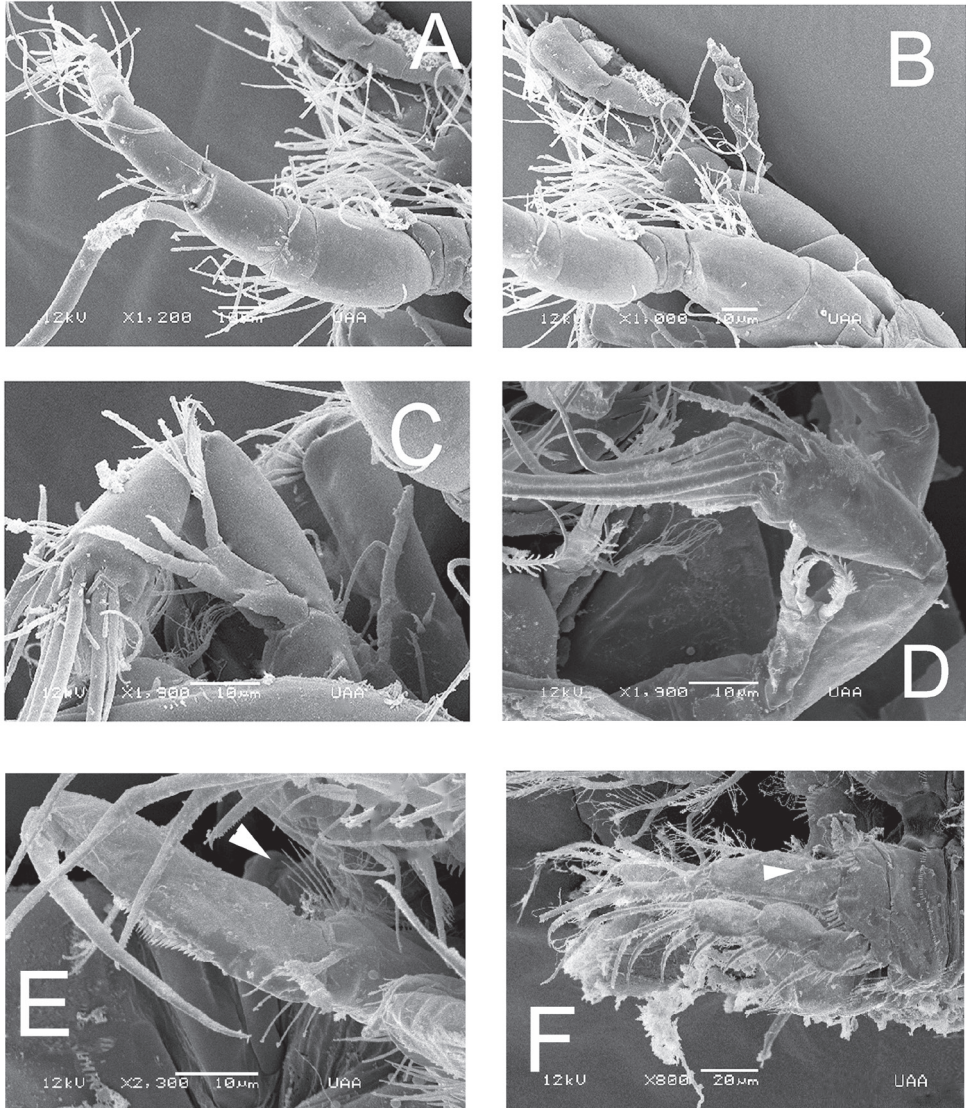


Figure 6. *Nitokra puebloviejensis* sp. nov. from Puebloviejo, Ciénaga Grande de Santa Marta, Colombia. SEM-prepared adult male individual **A** antennules, semi-lateral view **B** same, showing detail of proximal segments **C** antenna, posterior view **D** same showing exopodal ramus and endopodal segments **E** maxilliped, ventral view showing row of setal elements on syncoxal medial surface (arrowhead) **F** leg 1 showing modified, club-shaped basipodal spine (at arrow).

N. taylori (Gómez et al. 2012). Overall, the new species can be readily distinguished from its known congeners by the maxilliped armature, with a group of five elements on the medial surface of the syncoxa (Fig. 2H, arrowhead in Fig. 6E).

The diversity of the ameirid harpacticoid fauna could be underestimated and deserves further study in the Caribbean region.

Key to species of *Nitokra* reported in the Americas

1	P4EXP3 with 6 elements	2
1a	P4EXP3 with 7 elements	3
1b	P4EXP3 with 8 elements	21
2	P2 and P3EXP3 with 7 and 7 elements, respectively.....	<i>N. bisetosa</i> Mielke, 1993
–	P2 and P3EXP3 with 6 and 5 elements, respectively	<i>N. lacustris richardi</i> (Karanovic, 2015)
3	P5 female endopodite and exopodite with 6 and 5 elements. respectively.....	4
–	P5 female endopodite and exopodite with 5 and 5 elements, respectively	13
4	P4ENP1 with inner seta	5
–	P4ENP1 without inner seta	8
5	P2EXP3 with seven elements	6
–	P2EXP3 with six elements	7
6	P1EXP3 almost reaching P1ENP3, anal operculum with 3 or 4 spines.....	<i>N. taylori</i> Gómez, Carrasco & Morales-Serna, 2012
–	P1EXP3 reaching the end margin of P1ENP2, anal operculum without spines... ..	<i>N. bdelluræ</i> (Liddell, 1912)
7	P1ENP1 reaching the half of P1EXP3, anal operculum about 15 spines, P5EXP male with 5 elements	<i>N. chelifer</i> Wilson, 1932
–	P1ENP1 overpassing P1EXP3, anal operculum with 9 spines, P5EXP male with 4 elements.....	<i>N. typica typica</i> Boeck, 1865
8	P1ENP1 overpassing P1EXP3	9
–	P1ENP1 not reaching beyond P1EXP3	10
9	P2 and P3ENP3 with 4 and 5 elements, respectively; P3EXP3 with 6 elements; anal operculum lacking spines.....	<i>N. pusilla</i> Sars, 1911
–	P2 and P3ENP3 with 2 and 3 elements, respectively; P3EXP3 with 5 elements; anal operculum with about 10 spines.....	<i>N. hibernica hibernica</i> (Brady, 1880)
10	P1ENP1 as long as EXP1 and EXP2 combined	11
10a	P1ENP1 reaching 1/3 or 1/2 of P1EXP3	<i>N. lacustris sinoi</i> Marcus & Por, 1961
10b	P1ENP1 reaching 1/2 of P1EXP2.....	12
11	Anal operculum with 7 spines, baseoendopodite of P5 female almost reaching distal end of EXP	<i>N. evergladensis</i> Bruno & Reid, 2002
–	Anal operculum with about 10 spines, P5 baseoendopodite reaching middle of EXP	<i>N. dubia</i> Sars, 1927
12	With a spinulate medial surface of the caudal rami and caudal seta II about 2.2 as long as seta I	<i>N. lacustris colombiana</i> Reid, 1988
–	Spinulate medial surface absent in the caudal rami and caudal seta II less 2 times as long as seta I	<i>N. lacustris lacustris</i> (Schmankevitch, 1875)
13	P4ENP3 with 4 elements.....	<i>N. hyperidis</i> Jakobi, 1956
–	P4ENP3 with 5 elements.....	14
14	P2ENP3 with 4 elements, P4ENP2 with 1 element.....	15
–	P2ENP3 with 3 elements, P4ENP2 unarmed.....	<i>N. galapagoensis</i> Mielke, 1997

15	P2ENP1 and P4ENP1 without inner seta	<i>N. minor minor</i> Willey, 1930
–	P2ENP1 and P4ENP1 with inner seta.....	16
16	P1ENP1 reaching the margin end of P1EXP2	<i>N. fragilis paulistana</i> Jakobi, 1956
–	P1ENP1 longer than P1EXP2	17
17	P1EXP3 reaching the insertion point of inner seta of ENP1	<i>N. sphaeromata</i> Bowman, 1988
–	P1EXP3 going beyond the insertion point of inner seta ENP1	18
18	Anal operculum with 6 spines; female and male P6 with 1 and 2 setal elements, respectively; male P5EXP with 5 elements; maxilliped with 4 or 5 setal elements on the syncoxa medial surface	<i>N. puebloviejensis</i> sp. nov.
–	Characters not as above.....	19
19	Anal operculum with 10–15 spines, female and male P6 with 2 and 3 setal elements, respectively; male P5EXP with 6 elements; maxilliped lacking medial setae on the syncoxa	20
20	Anal operculum with 10–12 spines, posterior margin of genital double somite with row of long lateral spinules	<i>N. spinipes armata</i> Lang, 1965
–	Anal operculum with 12–15 spines, posterior part of double genital somite with short row of lateral spinules	<i>N. spinipes spinipes</i> Boeck, 1865
21	Rostrum with long projection	<i>N. affinis colombiensis</i> Fuentes-Reinés & Suárez-Morales, 2014
–	Rostrum without long projection.....	23
23	P1ENP1 longer than exopodite, posterior edge of antepenultimate somite spinulose dorsal to ventrolateral.....	<i>N. affinis affinis</i> Gurney, 1927
–	P1ENP1 as long as exopodite, posterior edge of antepenultimate somite encircled by spinules.....	<i>N. affinis californica</i> Lang, 1965

Acknowledgements

Dr Samuel Gómez (UNAM, Unidad Académica Mazatlan) provided useful taxonomic literature during our work on Colombian *Nitokra*. Araceli Adabache (University of Aguascalientes, Mexico) kindly helped us in processing specimens of the new species for SEM examination and guided our observations. MS-B was supported by University of Aguascalientes project PIB19-2 UAA. We appreciate the editorial processing of our work by the Associate Editor Danielle Defaye.

References

- Boxshall GA, Halsey SH (2004) An Introduction to Copepod Diversity. The Ray Society Series 166. The Ray Society, London, 966 pp.
- Bruno MC, Reid JW, Perry SA (2002) New records of harpacticoid copepods from Everglades National Park (Florida, U.S.A.): Description of *Nitokra evergladensis*, new species (Ameiridae),

- supplementary description of *Attheyella americana*, and redescription of *Bryocamptus newyorkensis* (Canthocamptidae). *Journal of Crustacean Biology* 22(4): 834–854. <https://doi.org/10.1163/20021975-99990296>
- Chappuis PA (1933) Süß- und Brackwasser-Copepoden von Bonaire, Curaçao und Aruba. In: *Zoologische Ergebnisse einer Reise nach Bonaire, Curaçao und Aruba im Jahre 1930*. *Zoologische Jahrbücher, Abteilung für Systematik Ökologie und Geographie der Tiere* 64: 391–404.
- Fiers F (1986) New and interesting copepods (Crustacea, Copepoda) from brackish waters of Laing Island (Northern Papua New Guinea); Léopold III biological station, Laing Island, contribution no. 96. *Bulletin de l'Institut Royal des Sciences Naturelles de Belgique Biologie* 56: 99–120.
- Fuentes-Reinés JM, Suárez-Morales E (2014a) A new subspecies of *Nitokra affinis* Gurney, 1927 (Copepoda, Harpacticoida) from the Caribbean coast of Colombia. *ZooKeys* 378: 1–15. <https://doi.org/10.3897/zookeys.378.6695>
- Fuentes-Reinés JM, Suárez-Morales E (2014b) Annotated checklist and new records of Harpacticoida (Copepoda) from a coastal system of northern Colombia, South America. *Crustaceana* 87(2): 212–255. <https://doi.org/10.1163/15685403-00003283>
- Fuentes-Reinés JM, Zoppi de Roa E (2013) Harpacticoid copepods from Ciénaga Grande de Santa Marta, Colombia. *Métodos en Ecología y Sistemática* 8: 5–28. <https://doi.org/10.15560/9.6.1580>
- Gómez S, Carrasco NK, Morales-Serna N (2012) A new species of *Nitocra* Boeck, 1865 (Harpacticoida, Ameiridae, Ameirinae) from South Africa, with notes on its ecology and remarks on the status of *Nitocra sewelli busmanni* Kunz, 1976. *ZooKeys* 244: 33–58. <https://doi.org/10.3897/zookeys.244.2633>
- Hendrickx ME, Fiers F (2010) Copépodos Harpacticoida asociados con crustáceos decápodos. *Ciencias Marinas* 14(41): 3–30.
- Humes AG (1953) Two new semiparasitic harpacticoid copepods from the coast of New Hampshire. *Journal of the Washington Academy of Sciences* 43: 360–373.
- Huys R, Boxshall GA (1991) *Copepod evolution*. The Ray Society Series 159. The Ray Society, London, 468 pp.
- Jakobi H (1956) Novas espécies de Harpacticoida (Copepoda-Crustacea) provenientes de regiões de água salobra da costa São Paulo-Paraná. (Neue Harpacticoiden-Arten (Copepoda-Crustacea) aus den Brackwassergebieten der Küste Sao Paulo-Paraná). *Dusenía Curitiba* 7: 159–171.
- Karanovic T, Pesce GL (2002) Copepods from ground waters of Western Australia, VII. *Nitokra humphreysi* sp. nov. (Crustacea: Copepoda: Harpacticoida). *Hydrobiologia* 470(1/3): 5–12. <https://doi.org/10.1023/A:1015694015451>
- Karanovic T, Eberhard S, Cooper SJB, Guzik MT (2015) Morphological and molecular study of the genus *Nitokra* (Crustacea, Copepoda, Harpacticoida) in a small palaeochannel in Western Australia. *Organisms, Diversity & Evolution* 15(1): 65–99. <https://doi.org/10.1007/s13127-014-0193-3>
- Lang K (1948) *Monographie der Harpacticiden*, 1–2: Håkan Ohlsson's Böktryckeri, Lund & Nordiska Bökhandeln, Stockholm, 1–1682.

- Mielke W (1993) Species of the taxa *Orthopsyllus* and *Nitokra* (Copepoda) from Costa Rica. *Microfauna Marina* 8: 247–266.
- Reid JW (1987) Some cyclopoid and harpacticoid copepods from Colombia, including descriptions of three new species. *Proceedings of the Biological Society of Washington* 100: 262–271.
- Reid JW (1988) Cyclopoid and harpacticoid copepods (Crustacea) from Mexico, Guatemala and Colombia. *Transactions of the American Microscopical Society* 107(2): 190–202. <https://doi.org/10.2307/3226461>
- Reid JW, Williamson CE (2010) Copepoda. In: Thorpe JH, Covich AP (Eds) *Ecology and Classification of North American Freshwater Invertebrates* (3rd edn.). Academic Press, New York, 829–899. <https://doi.org/10.1016/B978-0-12-374855-3.00021-2>
- Suárez-Morales E, Gasca R (1998) Updated checklist of the marine Copepoda (Crustacea) of Mexico. *Anales del Instituto de Biología. Universidad Nacional Autónoma de México. Serie Zoológica* 69(1): 105–119.
- Suárez-Morales E, Reid JW (1998) An updated list of free-living freshwater copepods (Crustacea) of Mexico. *The Southwestern Naturalist* 43: 256–265. <http://www.jstor.org/stable/30055363>
- Suárez-Morales E, Reid JW, Iliffe TM, Fiers F (1996) Catálogo de los copépodos (Crustacea) continentales de la Península de Yucatán, México. CONABIO/ ECOSUR, 298 pp.
- Suárez-Morales E, De Troch M, Fiers F (2006) A checklist of the marine Harpacticoida (Copepoda) of the Caribbean Sea. *Zootaxa* 1285: 1–19. <https://doi.org/10.11646/zootaxa.1285.1.1>
- Suárez-Morales E, Fleegeer JW, Montagna PA (2009) Free-living Copepoda (Crustacea) of the Gulf of Mexico. In: Felder DL, Camp DK (Eds) *Gulf of Mexico-Origins, Waters, and Biota Biodiversity*. Texas A&M Press, College Station, 841–869.
- Tran DL, Chang CY (2012) Two new species of harpacticoid copepods from anchialine caves in karst area of North Vietnam. *Animal Cells and Systems* 16(1): 57–68. <https://doi.org/10.1080/19768354.2011.621979>
- Walter TC, Boxshall G (2022) World of Copepods Database. *Nitokra* Boeck, 1865. World Register of Marine Species. <https://www.marinespecies.org/aphia.php?p=taxdetails&id=115198>
- Willey A (1930) Harpacticoid Copepoda from Bermuda. – Part I. *Annals and Magazine of Natural History (Series 10)* 6: 81–114. <https://doi.org/10.1080/00222933008673192>

Revision of *Vanuatubasis* Ober & Staniczek, 2009 (Odonata, Coenagrionidae), with description of seven new species

Natalie A. Saxton^{1,2,3}, Milen G. Marinov⁴, Seth M. Bybee³

1 Research and Collections Division, The Cleveland Museum of Natural History, Cleveland, OH, 44106, USA **2** Department of Biology, Case Western Reserve University, Cleveland, OH, 44106, USA **3** Department of Biology and Monte L. Bean Museum, Brigham Young University, Provo, UT 84604, USA **4** Biosecurity Surveillance and IncurSION Investigation Plant Health Team, Ministry for Primary Industries, 14 Sir William Pickering Drive, Christchurch 8053, New Zealand

Corresponding author: Natalie A. Saxton (nsaxton@cmnh.org)

Academic editor: Jan van Tol | Received 13 July 2022 | Accepted 27 September 2022 | Published 9 November 2022

<https://zoobank.org/7AC1EB83-EE91-4109-892A-E5714A65EFB9>

Citation: Saxton NA, Marinov MG, Bybee SM (2022) Revision of *Vanuatubasis* Ober & Staniczek, 2009 (Odonata, Coenagrionidae), with description of seven new species. ZooKeys 1128: 129–169. <https://doi.org/10.3897/zookeys.1128.89751>

Abstract

Vanuatubasis Ober & Staniczek, 2009 is an endemic genus of damselfly found on the island archipelago of Vanuatu. Previously only three species were assigned to the genus. Here, all known species of *Vanuatubasis* are formally described and treated, including the association of females for known species. The following new congeners are also described: *V. discontinua* sp. nov., *V. evelynae* sp. nov., *V. insularivorum* sp. nov., *V. kapularum* sp. nov., *V. nunggoli* sp. nov., *V. rhomboides* sp. nov., and *V. xanthochroa* sp. nov. from material collected across six different islands. An illustrated key to both males and females of all species within *Vanuatubasis* is provided as well as distributions for all known species.

Keywords

Damselflies, *Nesobasis*, South Pacific, taxonomy, Vanuatu

Introduction

Vanuatu is a small island nation in the South Pacific whose Odonata diversity is largely unknown (Marinov et al. 2019). Prior to this study, the most notable work in the region was performed by the early twentieth century entomologist, L. Evelyn Cheesman,

and the 2006 expedition to the northwest coast of the island of Espiritu Santo (SANTO Expedition) (Ober and Staniczek 2009). Cheesman is recognized for her work collecting insects across the South Pacific and specifically in Vanuatu (Touzel and Garner 2018). Among the many species described as a result of her work, are two species, *Vanuatubasis malekulana* (Kimmins, 1936) and *V. bidens* (Kimmins, 1958), formerly classified under the genus *Nesobasis* Selys, 1891. Donnelly (1990) noted that these specimens collected from Vanuatu differed from *Nesobasis* in having characters which may justify the establishment of a new genus: e.g., short cerci and a raised pronotal hind lobe. However, it was not until after the SANTO Expedition when additional specimens were collected, that *Vanuatubasis* Ober & Staniczek, 2009 was formally introduced (Ober and Staniczek 2009).

Several authors have suggested that due to their similarity *Nesobasis* and *Vanuatubasis* are closely related, however, no published phylogeny has yet investigated this relationship (Donnelly 1990; Ober and Staniczek 2009; Dijkstra et al. 2014). Furthermore, the subfamilial placement of *Vanuatubasis* and its hypothesized sister genera have been disputed (see Dijkstra et al. 2014). Donnelly (1990) considered *Melanesobasis* Donnelly, 1984, *Nesobasis*, and what is now *Vanuatubasis* as part of “*Nesobasis* group.” Phylogenetic work, however, has shown that *Melanesobasis* is not closely related to *Nesobasis* as previous authors had suggested (Beatty et al. 2017). De Marmels (2007) excluded *Nesobasis* from the Teinobasinae due to the lack of a cercal spur, noting that this character was different from the basal spine present in many other Coenagrionidae. Following Donnelly (1990) Ober and Staniczek (2009) grouped *Vanuatubasis* with *Nesobasis* and excluded them from the subfamily. In Dijkstra et al. (2014), *Vanuatubasis* was tentatively placed back within Teinobasinae, however, many of the genera in question were not included in Dijkstra et al.’s (2014) phylogeny. A more thorough morphological assessment also needs to be done to support their placement here. Thus, the composition of Teinobasinae and the placement of *Vanuatubasis* remains uncertain.

Vanuatubasis is just beginning to be understood in terms of diversity and natural history (Marinov et al. 2019; Saxton et al. 2020, 2021). Previous work suggests that *Vanuatubasis* requires alkaline streams and there have been several records of spider-feeding (Marinov et al. 2019; Saxton et al. 2021). Much work remains to be done in the region, as Vanuatu is undersampled compared to other South Pacific countries (Marinov 2015). Here, we formally revise the genus with the treatment of all known species and the formal description of seven new species.

Materials and methods

A series of expeditions in the country took place from 2017–2019 visiting ten different islands in total (i.e., Aneityum, Tanna, Efate, Erromongo, Malekula, Ambrym, Pentecost, Maewo, Espiritu Santo, and Gaua) (Fig. 1). Specimens were collected using aerial nets and subsequently placed in 95% EtOH. Specimens were examined using an

Olympus SZ51 stereo microscope. Images were taken using a Vision Digital passport imaging system and stitched using Zerene v. 1.04 (Zerene Systems LLC, Richland, WA, USA). Scale bars in images represent ~ 0.5 mm.

Terminology employed here mostly follows Garrison et al. (2010) for the general body morphology and Riek and Kukulová-Peck (1984) for wing venation. Three main measurements are given here including full-body length, abdominal length, and hindwing length. Full body length is measured from the labrum to the posterior end of the terminal appendages, while the abdominal length is measured from the anterior edge of the first abdominal segment to the end of the terminal appendages. Abdominal segments are abbreviated in the text to S1–S10, as are hindwing (**HW**) and forewing (**FW**). Nodal indices are given as the number of postnodals in the first row counted from the distal part of the wing/number of antenodals in the first row counted from the distal part of the wing followed by the number of corresponding antenodals in the second row/ the number of corresponding postnodals in the sec-

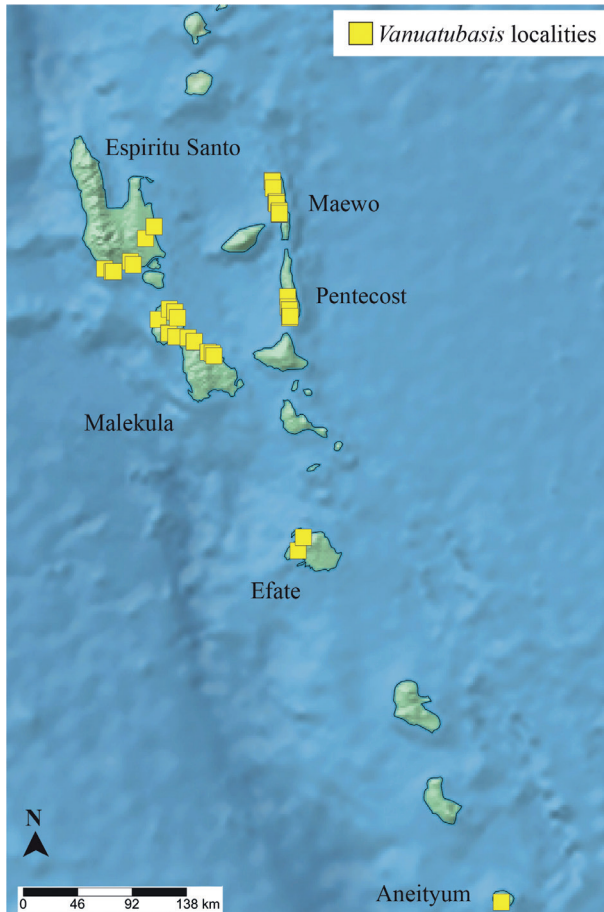


Figure 1. Collecting localities for *Vanuatubasis*. See Saxton et al. (2021) for more details.

ond row. Female specimens were associated and described only for those collected in tandem with males.

Label data for types is given verbatim within quotations with “ | ” to indicate line breaks. Specimens housed in the BYU frozen tissue collection and not in the general collection are indicated as such by the abbreviation “cryo”. All distributions given are in the country of Vanuatu. The following abbreviations for institutions are used throughout the text:

BPBM	Bernice P. Bishop Museum, Honolulu, Hawaii, USA;
BYU	Monte L. Bean Museum, Brigham Young University, Provo, Utah, USA;
MNHN	Muséum National d’Histoire Naturelle, Paris, FR;
NHM	Natural History Museum, London, UK;
NZAC	New Zealand Arthropod Collection, Auckland, NZ;
SMNS	Staatliches Museum für Naturkunde, Stuttgart, DE.

Results

Order Odonata Fabricius, 1793

Suborder Zygoptera Selys, 1854

Family Coenagrionidae Kirby, 1890

Genus *Vanuatubasis* Ober & Staniczek, 2009

Type species. *Nesobasis malekulana* Kimmins, 1936 (by original designation).

Diagnosis (adapted from Ober & Staniczek, 2009). *Vanuatubasis* resembles *Nesobasis* but can be distinguished by the following characters: cerci of males broad and short, always shorter than the paraprocts, paraprocts forceps-like, apically curved inwards (continuously curved medially), each ending with a dark tip; protonal hind lobe raised and medially protruding to obtuse or acute apex, ventral lobe expanding dorsally, and leveling up approximately with the dorsal carina.

Etymology (feminine). The name of the genus is derived from its distribution within Vanuatu, and the Latin suffix *-basis* which means base or foundation (see Ober and Staniczek 2009).

Vanuatubasis bidens (Kimmins, 1958)

Figs 2, 20A, 21A

Nesobasis bidens Kimmins, 1958: 239–241 (species description); Ober and Staniczek 2009: 490–492; Marinov et al. 2019: 14.

Material examined. Holotype. (1♂ NHM) “Type” “NEW HEBRIDES;| Aneityum. | Red Crest: 1,200ft. [sic] | 3m.N.E.of Anelcauhat. | vi .1955.” “L.E.Cheesman. | B.M.1955–217.” “Nesobasis | ♂ bidens Kim | D.E.Kimmins det. 1957 | TYPE.”

Additional material. (3♂♂, 3♀♀ BYU) “Vanuatu: Aneityum: | Anijemhag River, 12.v.2017 | 20.2180°S 169.8012°E, coll. | S.M.Bybee, M.Marinov” *Vanuatubasis bidens* was known by males only. Here we describe the female.

Description of female. Head: Labium overall pale beige; labrum pale green, darkening posteriorly, with dark brown postero-lateral edges and medially, a black spot at posterior edge; anteclypeus, genae, and mandibles (except for reddish tips) greenish yellow; postclypeus greenish yellow medially, with a black bar that begins medially and extends to the anterior edge, not extending to anterior corners; frons yellow, abruptly changing to black posteriorly; scapes and pedicels black, flagella dark brown and lightening apically; vertex and rear of head black, with bronze shimmer and white pruinescence; three pale ocelli with beige patch apical of the median ocellus; eyes cream-colored, although likely different color in life.

Thorax: Prothorax dorsally black with bronze shimmer; laterally yellowish green; pronotum black medially with greenish yellow edges, postero-lateral corners rounded to obtuse angles and weakly explanate, hind lobe raised and slightly curved outward medially, extending to point that protrudes posteriorly; mesostigmal plate black with green lateral edges, roughly triangular and staying approximately level across the outer surface. Pterothorax with black carina; laterally, mesepisternum with black stripe reaching the dorsal carina and reaching the mesopleural suture posteriorly across ~ 0.5 mm, but only reaching ~ 2/3 of the mesepisternum on the anterior and medial portion; yellow stripe located on anterior 1/3 of mesepisternum, not quite reaching mesinfraepisternum, and extending just past the mesopleural suture; mesepimeron overall pale green with yellow extending down from mesepisternum, short, dark brown line on posterior end of interpleural suture; metepisternum overall pale green with short, black line located on metapleural suture near the base of the wings, extending ~ 1/6 the suture's length; mesinfraepisternum yellow-green with small, dark-brown spot located medially; metepimeron pale green and turning beige dorsally; coxae, trochanters, and femora dorsally pale brown and ventrally pale beige with black spines; tibiae pale brown with slightly darker, and smaller, spines than that of the femora; tarsi beige with dark brown edges and smaller spines; pale brown tarsal claws that darken apically to reddish tips, claws with a small tooth located on the basal 1/4 of their length.

Wings: Hyaline; venation dark brown; pterostigma elongated rhomboidal dark brown and lightening towards the edges; CuP approximately halfway between antenodals in all wings; arculus originates slightly distal of second antenodal crossvein in all wings; discoidal cells unequal with FW dorsal edge being 1/2 as long as HW. Nodal index: 14/2–2/13 in FW and 13/2–2/12 in HW.

Abdomen: Overall, yellow with black dorsal stripe, that lightens laterally, extending from S1–9, dark brown lines encircling the posterior end of S1–S5, and pale brown setae; S1 with anterior 1/2 beige and latter 1/2 pale green; S2 pale green; S3–S8 laterally yellow; S9 yellow, with dorsal stripe extending $\frac{3}{4}$ of lateral view posteriorly; S10 laterally blue with brown edges, dorsally with blue patch extending $\frac{3}{4}$ of its length. Ovipositor overall pale yellow and reddish brown ventrally; stylus rounded, dark brown and lightening apically; gonapophysis reddish brown. Cerci roughly triangular, brown, and narrowing to a slightly rounded apex.

Measurements (mm): total length 35–36 mm, abdomen 29–30 mm, HW 21–22 mm ($n = 3$).

Diagnosis. Male. *Vanuatubasis bidens* can be distinguished from other known species of *Vanuatubasis* by a black pterostigma, bright blue abdominal S9 and S10, relatively straight black cerci that only curve medially on their apical 1/3, the presence of cercal teeth (although difficult to see in some specimens), and by having the lateral lobes of the genital ligula covering the sclerotized portion of the first genital segment. **Female.** *Vanuatubasis bidens* can be distinguished from other females in this genus by green thoracic coloring, and pale colored cerci surpassing the length of the stylus.

Variation. Male. The sinusoidal shape of the cerci is not as pronounced in some individuals nor are the cerci “teeth” as prominent. Color varies from yellow to green, likely due to the maturity of the specimen. **Female.** Variation in color due to maturity of specimens, yellow immatures and green mature. Terminal ends of cerci are sometimes more pointed than that of the description above.

Distribution. Aneityum, Vanuatu.

Notes. This species was previously only known from one male. Here, we expand the number of known males collected as well as confidently associate the female. Kimmins (1958) noted that the holotype of this species, described as having yellow thorac-

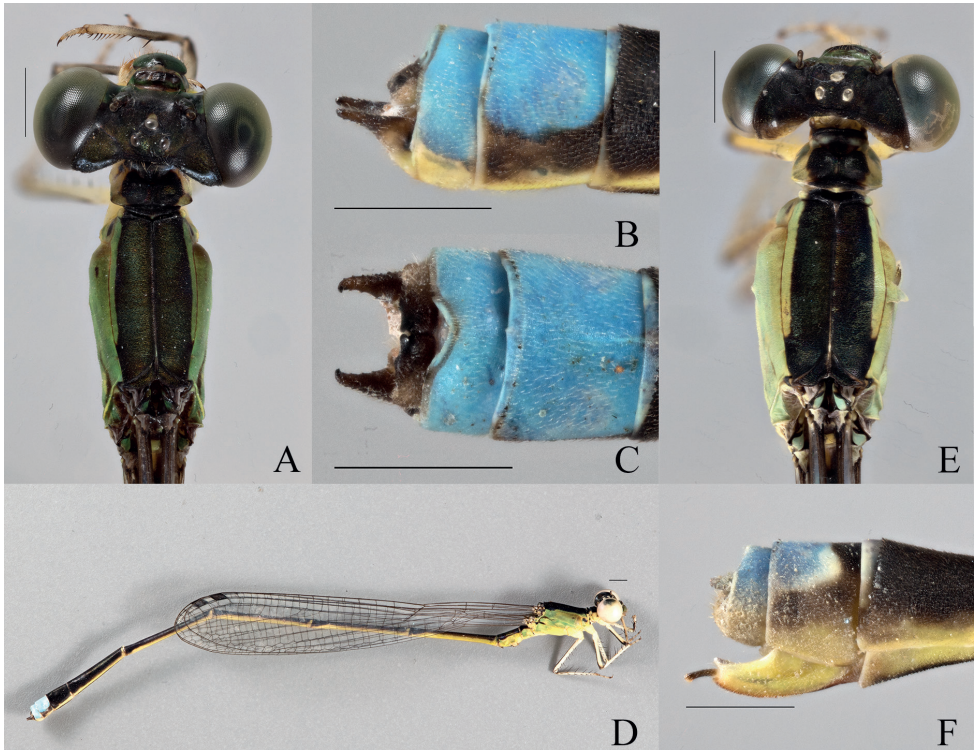


Figure 2. *Vanuatubasis bidens* (♂ BYU) **A** dorsal thorax **B** lateral terminalia **C** dorsal terminalia **D** lateral habitus *V. bidens* (♀ BYU) **E** dorsal thorax **F** lateral terminalia. Scale bars: 0.5 mm.

ic coloring, was likely an immature specimen but only had a single specimen and could not confirm this hypothesis. Additional collection efforts have confirmed Kimmins' hypothesis and found that the mature individuals are green and immature individuals are yellow (see Marinov et al. 2019: fig. 9).

***Vanuatubasis discontinua* sp. nov.**

<https://zoobank.org/CF66CBD3-F145-46C1-8A7D-549189814285>

Figs 3, 21B

Type material. Holotype (1♀ NZAC). (NZAC04230977, New Zealand Arthropod Collection, Auckland, New Zealand), locality data: Malekula Island, Litslits (-16.1460, 167.4653; 45 m a.s.l.): 24 May 2018; S. Bybee & G. Powell leg.

Paratypes (5♀♀ NZAC). Malekula Island: 1♀ (NZAC04231068), Losinwei (-16.1079, 167.3273, 29 m a.s.l.), 06 May 2019; 3♀♀ (NZAC04231069-71), Brenwe (-16.083, 167.275; 180 m a.s.l.), 22 May 2019; 1♀ (NZAC04231072), Wiaru River (-16.0787, 167.2726; 188 m a.s.l.), 13 May 2019); all S. Bybee & G. Powell leg.

Additional material (1♀ NZAC). Malekula Island, Stretch of Lakatchkach River flowing through Postanle Area (-16.1437, 167.4671 to -16.1474, 167.4649; 15–51 m a.s.l.): 17 May 2017; M. Marinov & S. Bybee leg.

Description of holotype. Head: Labium pale yellow; labrum, mandibles (except the reddish tips), clypeus and frons up to the midline between antennal bases and genae along the eyes up to dorsal level of scapes yellow with darker spots as follows: dull fulvous spot (to pale brown) along the posterior edge of the labrum; on postclypeus three areas with darker centers and diffused edges which connect to each other and with a transverse bar at the middle dorsal surface forming a T-shaped structure and dark fuscous to dark reddish at the dorsal corners of the mandibles at the ends of the lateral proximal corners of the postclypeus plus lateral sides of labrum running down for almost the whole length to the anterior edge; scapes yellow, pedicels pale brownish, flagella missing, scape: pedicel 0.3; vertex black with slight dark red sheen with a dull yellow spot in front of the median ocellus; rear part of the head yellow continuing up to occipital area and visible from the dorsum, yellow almost fully interrupted dorsally on the occipital bar between the postocular lobes except a small elongated spot in the middle area.

Thorax: Dark wide parallel sided bar with slight reddish sheen passing on the dorsal part of pro- and pterothorax encompassing $\frac{3}{4}$ of the dorsal part of the mesostigmal plate and $\frac{2}{3}$ of mesepisternum with a faint light line on the posterior edge of the middle prothoracic lobe and dorsal carina, at the posterior ends the dark area curves ventrally towards the mesopleural suture with its edges making two consecutive semicircles joining the suture at its very posterior ends; dark elongated spots with same color developed also as follows: one oblique occupying the upper part of the mesinfraepisternum, two sitting on the dorsal edges of the meso- and metapleural sutures at their posterior ends and faintly connecting to two dark shiny



Figure 3. *Vanuatubasis discontinua* Holotype (♀ NZAC) **A** dorsal thorax **B** lateral terminalia. Scale bars: 0.5 mm.

spots at the alar areas by a tiny bridge with the same color; legs almost entirely yellow saved for the faint barred dorsal area on all femora (very weakly developed to almost invisible on the front legs and darken like a dashed line towards the hind legs), dark spots at the joints between femora and tibiae and all the leg spines, claws orange with darker reddish tips; mesostigmal plate roughly triangular shape with tip wide rounded to almost straight; posterior edge of posterior edge of the prothorax dorsal edge interrupted at the middle.

Wings: Hyaline; venation generally dark especially at the distal ends becoming lighter towards the bases with pale spots at the nodus at the outer sides; pterostigma elongated rhomboidal light fulvous to almost transparent; CuP approximately halfway between antenodals in all wings situated very closely to the wing petiolation almost at the point where CuP ad AA is leaving the wing edge; arculus originates at the second

antenodals in front wings and slightly distal to it in hind wings; discoidal cells dissimilar in shape – in front wings anterior side is $\sim 1/3$ of the posterior and in hind wings anterior side is slightly longer than $1/2$ of posterior; nodal index: 12/2–2/12 in front wings and 10/2–2/11 in hind wings.

Abdomen: Almost uniformly dark fulvous on the dorsum from S1 to S9 with yellow developed as follows: isosceles triangular spot on at the base of S1, all segment from S3 to S7 with lines at the base coming from the ventral and continuing up to almost meeting at the dorsum with yellow fainting in intensity towards the posterior segments; dark on S9 occupies a little more than $1/3$ on the dorsal part, descends laterally and ends at the posterior end of the segment as a very faint dark area, rest of S9 beige on the dorsum; S10 dark base as deep reddish line overarching the dorsum and descending towards the venter, rest of dorsum beige; ventral side of the abdomen yellow except for: narrow dark lines running on almost entire length of the ridges of the sternites 2 to 8 (slightly to widely expanded on second and eight segments respectively); cerci pale brownish; posterior end of sternite 8 ending in a very low blunt tooth; ovipositor orange yellow aligned with the posterior end of S10 and styli surpassing the posterior ends of the cerci by $1/5$ of their length.

Measurements: total length 38.5, abdomen 32.0, hind wings 23.5.

Diagnosis. Female. *Vanuatubasis discontinua* is characterized with pale yellow ground color with dark markings on the thorax and dorsal part of the abdomen. It can be distinguished from other congeners where females exhibit similar type of coloration at various stages of their life (e.g., *V. bidens*, *V. rhomboides* sp. nov.) by the following combination of characters: long pedicel (scape: pedicel < 0.5), maculation on postclypeus present and brown cerci.

Variation. Female. Greatest variations observed on the shape of the markings on the postclypeus where the T-shaped structure could be reduced to two isolated spots. Dorsal carina along the posterior edge of prothorax not interrupted in two specimens. Dark elongated spots on the mesinfraepisternum diffused in most specimens and missing in one paratype. Two paratypes with pale markings on the dorsum of S9 close to the posterior end of the segment. Ovipositor surpassing S10 in one specimen.

Measurements (mm): total length 35.0–38.0, abdomen 29.5–31.5, HW length 21–23 ($n = 5$).

Distribution. Malekula, Vanuatu.

Etymology. The specific epithet for this species is derived from the modern Latin word *discontinuus*, *-a*, *-um* = discontinuous, referring to the interrupted dorsal carina on the prothorax (declinable adjective).

Notes. This species is only known from female specimens as no males were able to be associated. One female was excluded from the type material as it generally resembles the paratypes, but has the following differences: (1) posterior edge of the middle lobe of prothorax with incision having bilobed shape, (2) elongated spot on mesinfraepisternum darker than other paratypes, (3) dorsum of S10 with a diffused longitudinal bar joining the posterior end of the segment enclosing two pale spots, (4) smaller size than paratypes: total length 30.5, abdomen 25.2, HW length 19.5.

***Vanuatubasis evelynae* sp. nov.**

<https://zoobank.org/5974BE63-DD97-411B-998E-6BD01F582838>

Figs 4, 20B, 21C

Type material. *Holotype* (1♂ **BYU**). “VANUATU: Santo Is: | Coulons, -15.2957 | 167.1616092, 28 v. 2018, | coll. S. Bybee and G. Powell”.

Paratypes (1♂ 1♀ **BPBM**, 7♂♂ **BYU**, 3♂♂ **NHM**, 3♂♂ **NZAC**). (1♂ 1♀ **BPBM**, 3♂♂ **BYU**, 3♂♂ **NHM**, 3♂♂ **NZAC**) Same label data as holotype. (1♂ **BYU**) “VANUATU: Santo Is., | Coulons, May 20, 2019 | -15. 2955, 167.1614 | coll. SM. Bybee, GS. Powell | #BYU-VU-2019” “OD1710” (1♂ **BYU cryo**) “VANUATU: Santo Is: | Pelmol, -15.6078, 166.7849, | 4.vi.2018, | coll. S. Bybee and | G. Powell” “OD1709” (1♂ **BYU cryo**) same data as holotype; “OD1710” (1♂ **BYU cryo**) “VANUATU: Santo Is: | Coulons, -15.2957 | 167.1616092, 28 v. 2018, | coll. S. Bybee and G. Powell” “OD1711”.

Allotype (1♀ **BYU**). same label data as holotype.

Description of holotype. *Head:* Labium overall pale beige; labrum blue-green, darkening posteriorly, with dark brown postero-lateral edges and medially, a black spot at posterior edge; anteclypeus dark green; genae, and mandibles (except for reddish brown tips) green with paler anterolateral edges; postclypeus overall covered by a black bar that begins medially and extends to the anterior edge, not extending to the dark green, lateral corners; frons dark green, with medial black and extending posteriorly; scapes, and pedicels black, flagella dark brown and lightening apically; vertex and rear of head black with line of setae, a bronze shimmer, and white pruinescence; a pair of white post-ocular spots present; three pale ocelli with a yellow patch apical of the median ocellus; line of setae behind vertex; eyes yellowish green.

Thorax: Prothorax dorsally dark green to black with a bronze shimmer; laterally blue and green; pronotum black, latero-posterior corners rounded to obtuse angles and explanate, mid-line obviously indented across the pronotum, hind lobe with raised ridge that is shorter than the width of the pronotum, is curved outward medially, and extends to a sharp point that protrudes posteriorly; mesostigmal plate dark brown with yellow-green edges, interior edges raised to form protruding lobes. Pterothorax with black carina; laterally, mesepisternum with black stripe reaching the dorsal carina and extending to the mesopleural suture posteriorly across ~0.5 mm, but only reaching ~ 2/3 of the mesepisternum on the anterior and medial portion; green stripe located on latter 1/3 of mesepisternum and extending past the dark brown mesopleural suture; mesepimeron overall blue with green extending down from mesepisternum, metepisternum overall blue with short, brown line located on metapleural suture near the base of the wings, extending ~ 1/6 the suture’s length; mesinfraepisternum bluish green with dark brown spot located medially; metepimeron pale blue with white pruinescence; coxae, trochanters, and femora dorsally brown to black and ventrally pale beige with black spines; tibiae pale brown with smaller spines than that of the femora; tarsi beige with dark brown edges and small, dense spines; pale brown tarsal claws that darken apically to reddish tips, claws with a small tooth located on the basal 1/4 of their length.

Wings: Hyaline; venation dark brown and thickening towards the dorsal edge; pterostigma dark brown and rhombus-shaped, with edges being the darkest; CuP slightly distal than halfway between antenodals in HW; arculus originates just distal of the second antenodal crossvein in HW and slightly proximal to it in HW; discoidal cells unequal with FW dorsal edge being $1/2$ as long as HW. Nodal index: $12/2-2/12$ in FW and $11/2-2/10$ in HW.

Abdomen: Overall yellowish green with black dorsal stripe extending from S1–S9 and lightening to brown laterally, brown reaching ventrally at posterior edge of S1–S4, pale brown setae; segment 1 blue; S2 blue with patch of beige at anterior end; S3 anteriorly dark blue, turning yellow posteriorly, S4–S8 yellow with patches of blue on terminal end of each segment; S9 overall brown with blue dorsal stripe extending medially lengthwise, and light patch medially in lateral view; S10 with blue patch laterally that extends to ventral surface, terminal edge raised medially to form protrusion; cerci dark brown with gold setae and appearing as a curved crescent shape dorsally, excavated medially on each lobe and sloping posteriorly; paraprocts in dorsal view dark brown and darkening apically, with bumpy texture; in the lateral perspective the lobes are roughly triangular and tapering apically to form small, acutely rounded lobes, with dorsal edge slightly uneven and ventral edge expanded to form small “hump”, terminating in small, acutely rounded lobe.

Measurements (mm): total length 38 mm, abdomen 33 mm, HW 20 mm.

Description of allotype. Head: Labium overall pale beige; labrum blue-green, with black latero-posterior edges and a medially black spot at posterior edge; anteclypeus, genae, and mandibles (except for reddish tips) blue-green; postclypeus darker blue with a small bar located on the medial, anterior edge; frons blue-green, abruptly changing to black posteriorly; scapes, and pedicels black, flagella dark brown and lightening apically; vertex and rear of head black with line of setae, a bronze shimmer, and white pruinescence; a pair of white post-ocular spots present; three pale ocelli with a yellow patch apical of the median ocellus; eyes green.

Thorax: Prothorax dorsally dark green to black with bronze shimmer; laterally blue; pronotum black medially with blue edges, latero-posterior corners rounded to obtuse angles and weakly explanate, mid-line obviously indented across the pronotum, hind lobe with raised ridge that is shorter than the width of the pronotum, is curved outward medially, and extends to a sharp point that protrudes posteriorly; mesostigmal plate black with green lateral edges, roughly triangular and not significantly raised. Pterothorax with black carina; laterally, mesepisternum with black stripe reaching the dorsal carina and reaching the mesopleural suture, but only reaching $\sim 2/3$ of the mesepisternum; dark green stripe located on latter $1/3$ of mesepisternum, not quite reaching mesinfraepisternum, turning yellow as it passes the mesopleural suture; mesepimeron overall blue with yellow extending down from mesepisternum; dark brown line on posterior end of mesopleural suture extending $\sim 1/6$ the sutures length; metepisternum overall blue with short, black line located on metapleural suture near the base of the wings, extending \sim the suture's length; mesinfraepisternum blue; metepimeron blue; coxae, trochanters, and femora dorsally pale brown with blue patches, and ventrally

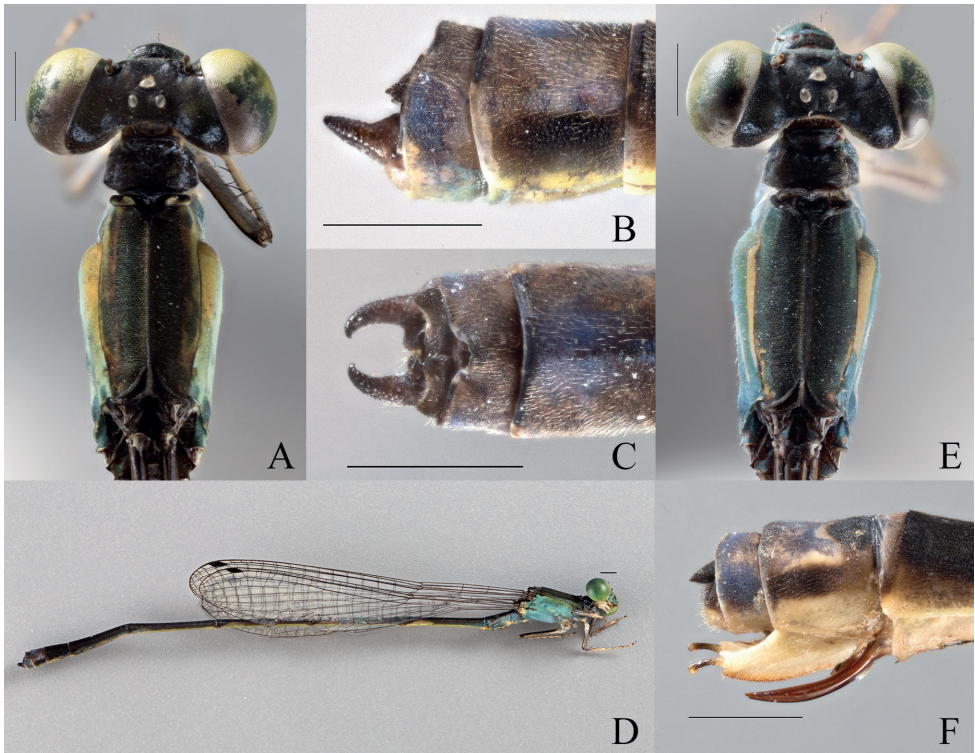


Figure 4. *Vanuatuabasis evelynae* Holotype (♂ BYU) **A** dorsal thorax **B** lateral terminalia **C** dorsal terminalia **D** lateral habitus *V. evelynae* Allotype (♀ BYU) **E** dorsal thorax **F** lateral terminalia. Scale bars: 0.5 mm.

pale beige with black spines; tibiae pale brown with slightly darker, and smaller, spines than that of the femora; tarsi beige with dark brown edges and small, dense spines; pale brown tarsal claws that darken apically to reddish tips, claws with a small tooth located on the basal 1/4 of their length.

Wings: Hyaline with dark brown venation, thickening towards the dorsal edge. Pterostigma dark brown and rhombus-shaped, with edges being the darkest; CuP slightly distal than halfway between antenodals in HW, and approximately halfway in FW; arculus originates at the second antenodal crossvein in front wings and slightly distal to it in HW; discoidal cells unequal with FW dorsal edge being 1/2 as long as HW. Nodal index: 13/2–2/11 in FW and 13/2–2/11 in HW.

Abdomen: Overall yellow with black dorsal stripe extending from S1–S9 and lightening laterally, with pale brown setae; S1 and S2 blue laterally; S3 blue anteriorly but turns to pale yellow posteriorly; S4–S8 pale yellow laterally; S9 with dorsal blue patch extending 3/4 of its length; S10 blue dorsally and laterally. Ovipositor overall pale yellow and reddish brown ventrally, with serrated ventral edge; stylus with rounded edges, dark brown and lightening apically; gonapophysis dark reddish-brown with

slightly serrated dorsal edge. Cerci roughly triangular, dark brown, and narrowing to a rounded apex, dorsal edge slightly rounded.

Measurements (mm): total length 35 mm, abdomen 28 mm, HW 20 mm.

Diagnosis. Male. *Vanuatubasis evelynae* can be distinguished from other *Vanuatubasis* species by a black pterostigma, forked (longer than wide) lateral lobes of the genital ligula, cerci curving medially their entire length, and black postclypeus with green lateral margins. **Female.** *Vanuatubasis evelynae* can be distinguished from other females in this genus, by their dark colored cerci, postclypeus with dark maculation, and uneven dorsal black area on S9 appearing almost sinusoidal.

Variation. Male. Immature specimens are pale blue with less thoracic coloring.

Measurements (mm): length 37–38 mm, abdomen 29–33 mm, HW 19–20 mm ($n = 5$). **Female.** The color of the pterostigma is lighter. **Measurements (mm):** total length 35–36, abdomen 28–29 mm, HW 20–21 ($n = 2$).

Distribution. Espiritu Santo, Vanuatu.

Etymology. The specific epithet of this species is a Latinized noun in the genitive case of the name ‘Evelyn’ in honor of L. Evelyn Cheesman, a prominent female entomologist whose early expeditions in Vanuatu significantly paved the way for future work in this region.

Notes. This species is likely the one referred to as “*Vanuatubasis* sp.” in Staniczek (2011). With the exception of one individual, all specimens were collected at the same site (Coulons, Espiritu Santo). One individuals’ label data reflects a locality on the other side of the island (Pelmol, Espiritu Santo). While this disjunct range is possible, it does seem suspect and is likely an error.

Vanuatubasis insularivorum sp. nov.

<https://zoobank.org/B70ED116-B861-42C4-AEC4-6DFC0D091B61>

Figs 5, 20C, 21D

Type material. Holotype (1♂ BYU). Male. “VANUATU: Maewo Is., | Betarara, May 23, 2019; | -15.1130, 168.0926 | Coll: SM Bybee, GS Powell | #BYU-VU-2019”.

Paratypes (2♂♂ 1♀ BPBM, 12♂♂ BYU, 3♂♂ 1♀♀ NHM, 4♂♂ 1♀♀ NZAC). (1♀ BPBM, 1♀ BYU, 1♂ NHM) same label data as holotype. (2♂♂ BPBM, 2♂♂ BYU, 1♂ NHM) “VANUATU: Maewo Is., | Betarara, May 21, 2019 | -15.1263, 168.0937 | Coll:SM Bybee,GS Powell | #BYU-VU-2019” (3♂♂ BYU) “VANUATU: Maewo Is., | Betarara, May 21, 2019 | -15.1191, 168.0891 | Coll:SM Bybee,GS Powell | #BYU-VU-2019” (1♂ BYU, 1♂ NHM) “VANUATU: Maewo Is., | Naone, May 24, 2019; | -15.01197, 168.0667 | Coll:SM Bybee,GS Powell | #BYU-VU-2019” (3♂♂ BYU, 1♂ NHM) “VANUATU: Maewo Is., | Marino, May 23, 2019; | -14.9616, 168.0605 | Coll:SM Bybee,GS Powell | #BYU-VU-2019” (1♂ BYU) “VANUATU: Maewo Is., | Baitora, May 22, 2019 | -15.1980, 168.1138 | Coll:SM Bybee,GS Powell | #BYU-VU-2019” (1♂ BYU, 1♂ NZAC) “VANUATU: Maewo Is., | Marino, May 23, 2019; | -14.9654, 168.0604 | Coll:SM Bybee,GS Powell | #BYU-VU-2019” (1♂

NZAC “VANUATU: Maewo Is., | Marino, May 23, 2019; | -14.9600, 168.0614 | Coll:SM Bybee,GS Powell | #BYU-VU-2019” (1♀ **NZAC**) “VANUATU: Maewo Is., | Betarara, May 23, 2019 | -15.1130, 168.0926 | Coll:SM Bybee,GS Powell | #BYU-VU-2019” (1♂ **NZAC**) “VANUATU: Maewo Is., | Betarara, May 21, 2019 | -15.1263, 168.0937 | Coll:SM Bybee,GS Powell | #BYU-VU-2019” (1♂ **NZAC**) “VANUATU: Maewo Is., | Baitora, May 22, 2019 | -15.1901, 168.1107 | Coll:SM Bybee,GS Powell | #BYU-VU-2019”.

Allotype (1♀ **BYU**). same label data as holotype.

Description of holotype. Head: Labium overall pale beige; labrum blue, with dark brown latero-posterior edges and a medial brown spot at posterior edge; anteclypeus, genae, and mandibles (except for reddish tips) blue; postclypeus blue, with a dark brown bar extending laterally, reaching the posterior edge medially, and not quite extending to anterior corners; frons greenish blue abruptly changing to black posteriorly; scapes, and pedicels greenish blue, flagella dark brown and lightening apically; vertex and rear of head dark brown; three pale ocelli with a beige patch apical of the median ocellus; eyes green.

Thorax: Prothorax dorsally dark brown; laterally blue; pronotum dark brown medially lightening towards the edges, latero-posterior corners rounded to obtuse angles and explanate, mid-line obviously indented across the pronotum hind lobe with raised ridge that is shorter than the width of the pronotum, appears sinusoidal with a median that extends to a sharp point that protrudes posteriorly; mesostigmal plate dark brown with blue lateral edges, roughly quadrilateral, and not raised. Pterothorax with dark brown carina; laterally, with dark brown stripe that extends laterally over the mesepisternum, reaching the mesopleural suture posteriorly across ~ 0.5 mm, but only reaching ~ 2/3 of the mesepisternum on the anterior and medial portion; pale brown stripe beginning at the mesopleural suture and extending to mesepimeron; mesepimeron overall blue with brown extending down from mesepisternum on first 1/3; metepisternum overall blue with short, dark brown line located on metapleural suture near the base of the wings, extending ~ 1/6 the suture’s length; mesinfraepisternum with dark brown spot that encompasses all but the blue posterior ventral corner; metepimeron blue and turning beige dorsally; coxae, trochanters, and femora dorsally pale brown and ventrally pale beige with dark brown spines; tibiae pale brown with slightly darker, and smaller, spines than that of the femora; tarsi beige with dark brown edges and small, dense spines; pale brown tarsal claws that darken apically to reddish tips, claws with a small tooth located on the basal 1/4 of their length.

Wings: Hyaline with brown venation. Pterostigma pale brown and rhombus-shaped; CuP halfway between antenodals in HW, and slightly proximal to halfway in FW; arculus originates just distal of the second antenodal crossvein in both wings; discoidal cells unequal with FW dorsal edge being 1/2 as long as HW. Nodal index: 13/2–2/12 in FW and 11/2–2/11 in HW.

Abdomen: Overall beige with brown dorsal stripe extending from S1–S10 and lightening laterally, brown reaching ventrally at posterior edge of S4–S6, pale brown setae; S1 and S2 blue with beige patches; S3 blue at anterior 1/3, and beige for latter

2/3; S4–S7 beige with dark brown dorsal strip reaching ventrally at posterior edge of segments; S8 brown; S9 brown with dorsal medial blue patch; S10 pale brown with darker edges. Cerci pale brown with gold setae and appearing as a curved sinusoidal shape dorsally, with abrupt ridge medially; in the lateral perspective the lobes are roughly triangular, with dorsal edge slightly sloped ventrally and appearing hooked apically. Paraprocts with dense pale brown setae that thins apically across the appendages.

Measurements (mm): total length 38 mm, abdomen 32 mm, HW 19 mm.

Description of allotype. Head: Labium overall pale beige; labrum pale green with brown latero-posterior edges and slightly indented medially brown spot at posterior edge; anteclypeus, genae, and mandibles (except for reddish tips) pale green; postclypeus translucent brown darker bar stretching across on the medial, anterior edge; frons pale green, abruptly changing to dark brown posteriorly, with a reddish brown spot on apex of head; scapes, and pedicels pale brown, flagella pale brown and lightening apically; vertex and rear of head dark brown with line of setae and a bronze shimmer; three pale ocelli with beige patch apical of the median ocellus; eyes pale green.

Thorax: Prothorax dorsally dark brown; laterally pale brown with hints of green; pronotum dark brown medially with beige edges, latero-posterior corners rounded to acute angles and weakly explanate, mid-line obviously indented across the pronotum, hind lobe with raised ridge that is shorter than the width of the pronotum, is curved outward medially, and extends to a sharp, rounded point that protrudes posteriorly; mesostigmal plate brown with green lateral edges, roughly triangular and not significantly raised. Pterothorax with dark brown carina; laterally, mesepisternum with dark brown stripe reaching the dorsal carina and reaching approximately 1/2 the mesepisternum; pale green on latter 1/3 of mesepisternum; mesepimeron overall pale green with hints of blue; dark brown line on posterior end of mesopleural suture extending $\sim 1/6$ the sutures length; metepisternum overall blue with short, brown line located on metapleural suture near the base of the wings, extending $\sim 1/6$ the suture's length; mesinfraepisternum pale brown; metepimeron beige; coxae, trochanters, and femora dorsally pale brown and ventrally pale beige with black spines; tibiae pale brown with slightly darker, and smaller, spines than that of the femora; tarsi beige with dark brown edges and small, dense spines; pale brown tarsal claws that darken apically to reddish tips, claws with a small tooth located on the basal 1/4 of their length.

Wings: Hyaline with brown venation; pterostigma pale brown and rhombus-shaped; CuP halfway between antenodals in both wings; arculus at second antenodal crossvein in both wings; discoidal cells unequal with FW dorsal edge being 1/2 as long as HW. Nodal index: 15/2–2/14 in FW and 12/2–2/11 in HW.

Abdomen: Overall beige with brown dorsal stripe extending from S1–S8 and lightening laterally, with pale brown setae; S1 and S2 with hints of blue laterally; S3–S8 pale beige laterally, with dorsal stripe reaching ventral at terminal ends of S3–S7; S9 with pale dorsal patch extending $\frac{3}{4}$ of its length; S10 pale brown; ovipositor overall beige, with serrated ventral edge; stylus with rounded edges, pale brown and lightening

apically; gonapophysis reddish brown with slightly serrated dorsal edge. Cerci roughly triangular, dark brown, and narrowing to a rounded apex, dorsal edge straight.

Measurements (mm): total length 38 mm, abdomen 31 mm, HW 23 mm.

Diagnosis. Male. *Vanuatubasis insularivororum* can be distinguished from all other species of *Vanuatubasis* by its distinctly pointed posterior edge of the pronotum, mesostigmal plates with dorso-posterior corner not raised in an auricle, and a postclypeus with a transverse bar on the anterior edge. **Female.** *Vanuatubasis insularivororum* can be distinguished from other *Vanuatubasis* females by a postclypeus with pale maculation, a frons with dark triangle extending from base of the median ocelli, and a distinctly pointed posterior edge of the pronotum.

Variation. Male. This species is highly variable in overall color. Some specimens are dark brown to black dorsally. Wings with dark brown venation and pterostigma. Wings with brown pigmentation. Shape of maculation on S9 somewhat variable.

Measurements (mm): total length 37–41 mm, abdomen 31–35 mm, HW 19–23 mm ($n = 12$). **Female.** Overall color varies the same as in males. **Measurements (mm):** total length 38–41 mm, abdomen 31–35 mm, HW 23–24 mm ($n = 5$).

Distribution. Maewo, Vanuatu.

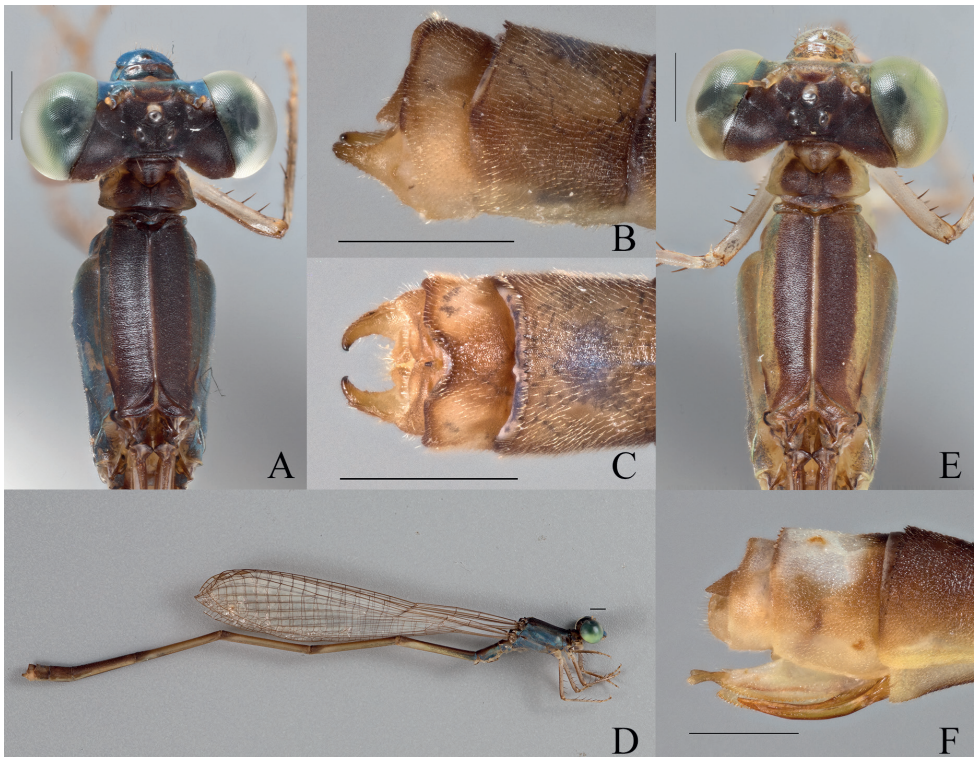


Figure 5. *Vanuatubasis insularivororum* Holotype (♂ BYU) **A** dorsal thorax **B** lateral terminalia **C** dorsal terminalia **D** lateral habitus *V. insularivororum* Allotype (♀ BYU) **E** dorsal thorax **F** lateral terminalia. Scale bars: 0.5 mm.

Etymology. The specific epithet of this species a combination of the Latin words *insula*, meaning island, and *rivorum* (genitive plural noun) meaning of small streams, which accurately describes the island of Maewo.

***Vanuatubasis kapularum* sp. nov.**

<https://zoobank.org/B7579D85-263D-4251-82AC-67AD6AD1DD4E>

Fig. 6, 20D, 21E

Type material. Holotype (1♂ **BYU**). “VANUATU: Efate Is., | Ulei, June 11 2019; | -17.5768, 168.2960 | Coll: SM Bybee, GS Powell | #BYU-VU-2019”.

Paratypes (2♂♂ **BPBM**, 7♂♂ **BYU**, 3♂♂ **NHM**, 4♂♂ 1♀ **NZAC**). (6♂♂ **BYU**, 3♂♂ **NHM**, 2♂♂ **NZAC**). “VANUATU: Efate Is., | Ulei, June 11 2019; | -17.5768, 168.2960 | Coll: SM Bybee, GS Powell | #BYU-VU-2019” (1♂ **BYU**, 2♂♂ **NZAC**) “VANUATU: Efate Is., | Mele Maat, June 11, 2019; -17.6754, 168.2559 | Coll: SM Bybee, GS Powell | #BYU-VU-2019” (1♀ **NZAC**) “VANUATU: Efate Is., | Devil’s Point Rd., -17.684167 | 168.253638, 12.vi.2018, | coll. S. Bybee & G. Powell”.

Allotype (1♀ **BYU**). “VANUATU: Efate Is., | Mele Maat, June 11, 2019; -17.6754, 168.2559 | Coll: SM Bybee, GS Powell | #BYU-VU-2019”.

Description of holotype. Head: Labium overall pale beige; labrum blue, with black latero-posterior edges and medially, a depressed black spot at posterior edge; anteclypeus blue; genae, and mandibles (except for reddish brown tips) blue with dark brown anterolateral edges; postclypeus overall covered by a black bar that begins medially and extends to the anterior edge, not extending to the blue, anterior corners; frons black medially, with blue lateral edges, abruptly changing to black posteriorly; scapes, and pedicels black, flagella dark brown and lightening apically; vertex and rear of head black with line of setae, a bronze shimmer, and white pruinescence; a pair of white post-ocular spots present; three pale ocelli with beige patch apical of the median ocellus; eyes green.

Thorax: Prothorax dorsally black with a bronze shimmer; laterally mottled appearance with dark brown, blue and hints of green; pronotum black with white pruinescence, latero-posterior corners rounded to obtuse angles and slightly explanate, mid-line obviously indented across the pronotum, hind lobe with raised ridge that is shorter than the width of the pronotum, overall sinusoidal, is curved outward medially, and extends to a sharp point that protrudes posteriorly; mesostigmal plate black with blue edges, interior edges protruding posteriorly, and raised to form very short lobes. Pterothorax with black carina; laterally, mesepisternum with black stripe reaching the dorsal carina and reaching over 1/2 the mesepimeron; blue stripe across the interpleural suture; metepisternum overall dark brown with black line located on metapleural suture near the base of the wings, extending ~ 1/6 the suture’s length; mesinfraepisternum black; metepimeron dark black and lightening anteriorly with white pruinescence; coxae, trochanters, and femora dorsally dark brown and ventrally beige with black spines; tibiae beige with smaller spines than that of the femora;

tarsi beige with brown edges and small, dense spines; pale brown tarsal claws that darken apically to reddish tips, claws with a small tooth located on the basal 1/4 of their length.

Wings: Hyaline with dark brown to black venation that thickens dorsally; pterostigma pale brown and rhombus-shaped, darkest on the edges; CuP halfway between antenodals in both wings; arculus just distal of second antenodal crossvein in both wings; discoidal cells unequal with FW dorsal edge being 1/2 as long as HW. Nodal index: 15/2–2/13 in FW and 12/2–2/12 in HW.

Abdomen: Overall with dark brown to black dorsal stripe extending from S1–S10 and lightening to brown laterally, brown reaching ventrally at posterior edge of S3–S6, pale brown setae; S1 blue with white pruinescence; S2–S9 yellow; S9 with dorsal blue spot on posterior end; S10 with a pair of blue patches laterally; cerci dark brown with pale brown setae and appearing as a curved crescent shape dorsally, internal margins touching continuously with black, bulbous tips; paraprocts in dorsal view dark brown and darkening apically, with bumpy texture; in the lateral perspective the lobes are roughly triangular and tapering apically to form small, acutely rounded lobe, dorsal edge sloping ventrally and ventral edge expanding ventrally to form a small lump before abruptly tapering to rounded apex.

Measurements (mm): total length 41 mm, abdomen 35 mm, HW 21 mm.

Variation. Male. Blue dorsal patch on S9 variable in shape and size; S10 lateral blue spots appear cream colored in some specimens. Size of the brown stripe on the metepisternum is somewhat variable. Immature males are yellow to dark beige. **Measurements (mm):** total length 39–42 mm, abdomen 33–36 mm, HW 21–22 mm ($n = 10$).

Description of allotype. Head: Labium overall pale beige; labrum brown medially lightening towards the edges, except for dark brown postero-lateral edges and slightly indented medially dark brown spot at posterior edge; anteclypeus, genae, and mandibles (except for reddish tips) pale brown; postclypeus translucent pale brown, with darker bar stretching across on the medial, anterior edge; frons pale brown abruptly changing to dark black posteriorly; scapes, and pedicels light brown, flagella pale brown and lightening apically; vertex and rear of head black with line of setae, a bronze shimmer, and faint white pruinescence; three pale ocelli with a beige patch apical of the median ocellus; eyes green.

Thorax: Prothorax dorsally black; laterally yellow with pale brown stripes; pronotum black medially with yellow lateral edges, latero-posterior corners rounded to obtuse angles and weakly explanate, mid-line obviously indented across the pronotum, hind lobe with raised ridge that is shorter than the width of the pronotum, is curved outward medially, and extends to a sharp point that protrudes posteriorly; mesostigmal black with yellow lateral edges, roughly triangular and not slightly raised medially. Pterothorax with black carina, laterally mesepisternum with black stripe reaching the dorsal carina and extending $\sim 1/3$ of the mesepisternum; latter 1/3 of mesepisternum yellow; mesepimeron yellow with short, black medial stripe; pale brown mesepister-

num; metepisternum overall yellow, with short, black line located on metapleural suture near the base of the wings, extending $\sim 1/6$ the suture's length; mesinfraepisternum yellow with dark brown medial spot; metepimeron pale yellow and lightening ventrally; coxae, trochanters, and femora dorsally brown and ventrally pale beige with black spines; tibiae pale brown with slightly darker, and smaller, spines than that of the femora; tarsi beige with dark brown edges and small, dense spines; pale brown tarsal claws that darken apically to reddish tips, claws with a small tooth located on the basal $1/4$ of their length.

Wings: Hyaline with dark brown venation; pterostigma pale brown and rhombus-shaped; CuP halfway between antenodals in FW, and slightly proximal to halfway in HW; arculus at second antenodal crossvein in both wings; discoidal cells unequal with FW dorsal edge being $1/2$ as long as HW. Nodal index: $13/2-2/12$ in FW and $12/2-2/11$ in HW.

Abdomen: Overall yellow with black dorsal stripe extending from S1–S9 and lightening towards the edges, with pale brown setae; black carina stripe extending ventrally on terminal edges of S2–S6; S9 with pale dorsal patch extending $3/4$ of its length; S10 pale dorsally. Ovipositor overall beige, with brownish red serrated ventral edge, and pale brown setae; stylus with rounded edges, pale brown and lightening apically; gonapophysis reddish brown with slightly serrated dorsal edge. Cerci roughly triangular, dark brown, and narrowing to a rounded, acute point, dorsal edge straight.

Measurements (mm): total length 37 mm, abdomen 32 mm, HW 21 mm.

Diagnosis. Male. *Vanuatubasis kapularum* can be distinguished from all other *Vanuatubasis*, besides *V. nunggoli* by the presence of dark brown thoracic coloring on the metepisternum. It can be distinguished from *V. nunggoli* due to by having pale yellow paraprocts with dark tips, dorsally with inner angles forming $\sim 90^\circ$ angle and by the bright blue labrum. **Female.** *Vanuatubasis kapularum* can be distinguished from other *Vanuatubasis* females by having a black area dorsally on S9 with relatively straight edges, dark colored cerci, and having the dorso-posterior corners of the mesostigmal plates raised in a small auricle.

Variation. Male. Blue dorsal patch on S9 variable in shape and size; S10 lateral blue spots appear cream colored in some specimens. Size of the brown stripe on the metepisternum is somewhat variable. Immature males are yellow to dark beige.

Measurements (mm): total length 39–42 mm, abdomen 33–36 mm, HW 21–22 mm ($n = 10$). **Female.** S9 and S10 dorsal patch blue in some specimens; thoracic coloring more blue than yellow in mature specimens. **Measurements (mm):** total length 37–40 mm, abdomen 32–34 mm, HW 21–22 mm ($n = 2$).

Distribution. Efate, Vanuatu.

Etymology. The specific epithet *kapularum* is here treated as a noun in the genitive case, in honor of the Kapula family who were among the first to show us the wonders of Vanuatu.

Notes. This species was observed feeding on spiders at the Ewor River locality. One male specimen was collected with a spider in its mandibles.

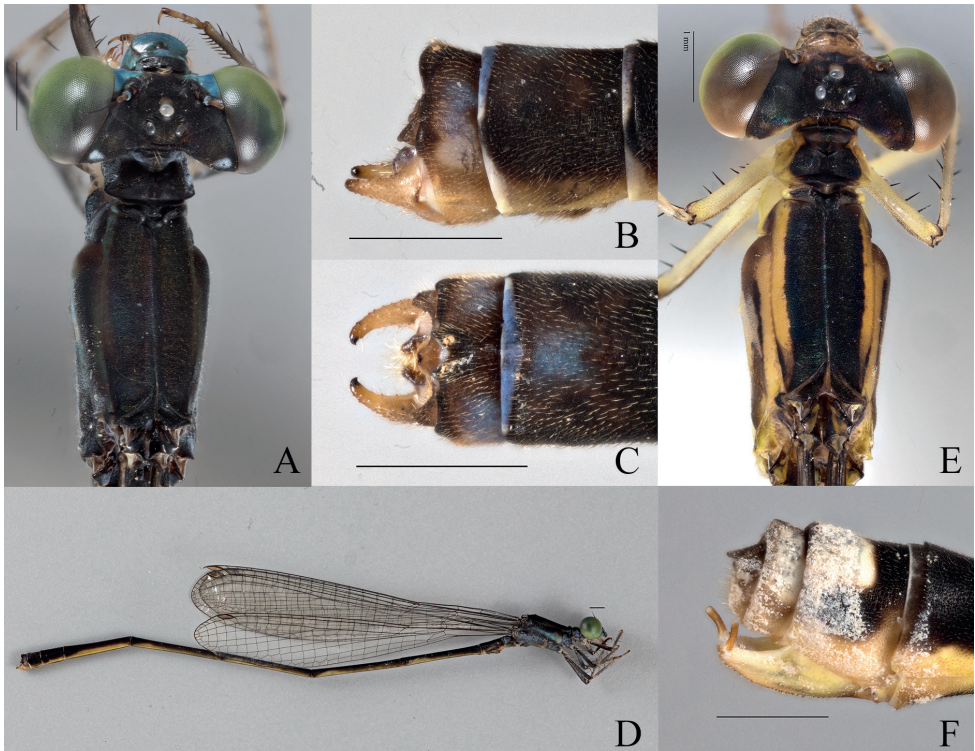


Figure 6. *Vanuatubasis kapularum* Holotype (♂ BYU) **A** dorsal thorax **B** lateral terminalia **C** dorsal terminalia **D** lateral habitus *V. kapularum* Allotype (♀ BYU) **E** dorsal thorax **F** lateral terminalia. Scale bars: 0.5 mm.

***Vanuatubasis malekulana* (Kimmins, 1936)**

Figs 7, 20E, 21F

Neosbasis malekulana Kimmins, 1936: 72–73; Ober and Staniczek 2009: 492–495.

Remark. *Vanuatubasis malekulana* was known by males only. Here we tentatively assign and describe the female.

Material examined. Holotype (1♂ NHM). “Holo- | type” “New Hebrides: | Malekula, | Ounua. | Mar .and Apl. 1929 | Miss L.E. Cheesman. | B.M.1929–343.” “331.” “NESOBASIS | malekulana | ♂ Holotype sp.n. | det.D.E.Kimmins.” **Additional material** (2♂♂ BYU). “VANUATU: Malekula Is: | Litslits, -16.1459 | 167.465, 18, 24.v.2018, | coll. S. Bybee and G. Powell”.

Paratypes (2♂♂ NHM). “Para- | type” “New Hebrides: | Malekula, | ounua. | Feb.1929. | Miss L.E.Cheesman. | B.M.1929-234.” “231.” “NESOBASIS | malekulana | ♂ sp.n. | det.D.E.Kimmins.”.

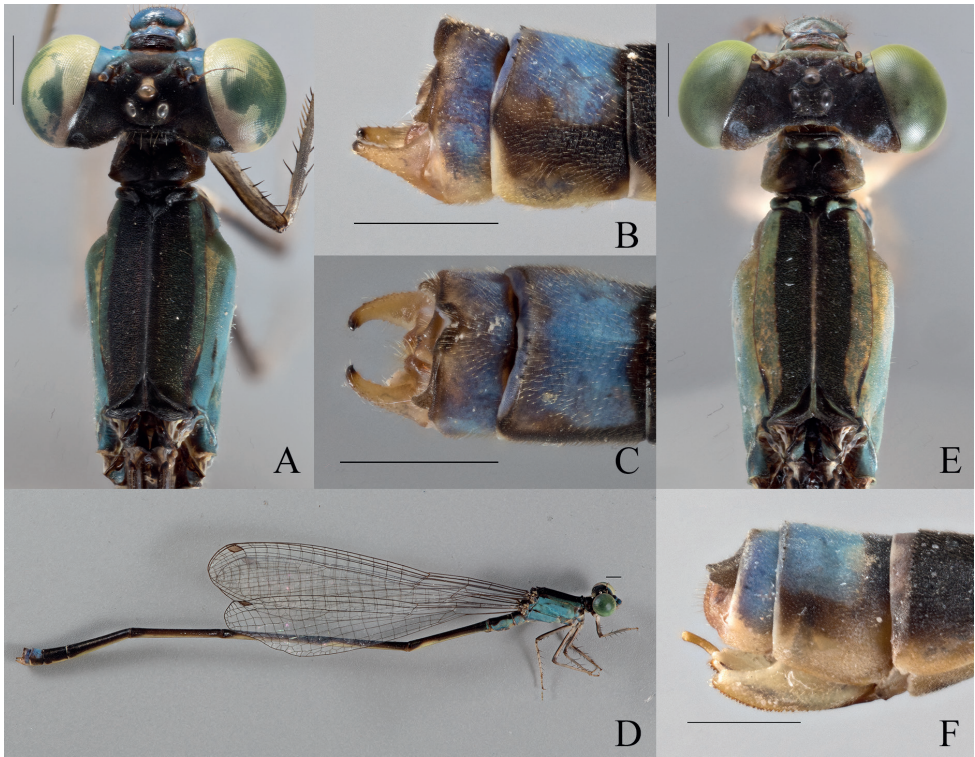


Figure 7. *Vanuatubasis malekulana* (♂ BYU) **A** dorsal thorax **B** lateral terminalia **C** dorsal terminalia **D** lateral habitus *V. malekulana* (♀ BYU) **E** dorsal thorax **F** lateral terminalia. Scale bars: 0.5 mm.

Description of female. Head: Labrium overall pale beige; labrum pale green with brown latero-posterior edges and a small, slightly indented medial pale spot at posterior edge; anteclypeus, genae, and mandibles (except for reddish tips) pale green; postclypeus green with faint brown maculation medially; frons pale green, turning black posteriorly; scapes, pedicels, and flagella dark brown; vertex of head black, back of head pale green; three pale ocelli with small green patch apical of the median ocellus; eyes green.

Thorax: Prothorax dorsally black; laterally green; pronotum black medially with green edges, latero-posterior corners rounded to acute angles and weakly explanate, mid-line obviously indented across the pronotum, hind lobe with raised ridge that is curved outward medially, and extends to a sharp, acute point that protrudes posteriorly; mesostigmal plate black with green lateral edges, internal margins raised and protruding posteriorly. Pterothorax with black carina; laterally mesepisternum with black stripe reaching the dorsal carina and extending more than 3/4 of the mesepisternum, dark green on latter 1/4 of mesepisternum except for short brown strip at posterior edge of mesopleural suture; mesepimeron overall pale green with hints of yellow; me-

tepi sternum overall green with short, brown line located on metapleural suture near the base of the wings; mesinfraepisternum pale green to yellow; metepimeron pale green, with beige anterior portion; coxae and trochanters beige, femora dorsally dark brown and ventrally beige with black spines; tibiae pale brown with slightly darker, and smaller, spines than that of the femora; tarsi beige with dark brown edges and small, dense spines; pale brown tarsal claws that darken apically to reddish tips, claws with a small tooth located on the basal 1/4 of their length.

Wings: Hyaline with dark brown; pterostigma dark brown and rhombus-shaped, darkest on the edges; CuP halfway between antenodals in both wings; arculus just distal of second antenodal crossvein in both wings; discoidal cells unequal with FW dorsal edge being 1/2 as long as HW. Nodal index: 12/2–2/11 in FW and 10/2–2/9 in HW.

Abdomen: Overall pale green to yellow with black dorsal stripe from S1–S8 and lightening towards the edges, with pale brown setae; S1 and S2 green laterally; S3–S8 yellow laterally; S9 with pale blue dorsal stripe; S10 pale blue; Ovipositor overall beige, with darker serrated ventral edge; stylus with rounded edges, pale brown and lightening apically; gonapophysis reddish brown with slightly serrated dorsal edge. Cerci roughly triangular, brown, and narrowing to a rounded apex, dorsal and ventral edge straight.

Measurements (mm): total length 34–35 mm, abdomen 24–28 mm, HW 21–22 mm ($n = 3$).

Diagnosis. Male. *Vanuatubasis malekulana* can be distinguished from all other *Vanuatubasis*, by the dorso-posterior corner of the mesostigmal plate raised in an auricle, lack of dark color on the metepimeron. **Female.** Females of *V. malekulana* can be distinguished by the dorsal, black area on S9 having an almost straight posterior edge, and having distinctly raised dorso-posterior corners of the mesostigmal plate in an auricle.

Variation. Male. Postclypeal maculation sometimes extending to posterior edge of postclypeus; internal projects of cerci vary from rounded to more pointed; variable extent to which internal margins of mesostigmal plates are raised; dorsal patch on S9 variable in shape and ranging in color from cream to blue. **Female.** Postclypeal maculation variable in extent; sometimes having small, brown maculation on the mesinfraepisternum.

Distribution. Malekula, Vanuatu.

Notes. The male of this species was recently treated in Ober and Staniczek (2009). This species is the most variable within the genus with regional differences in size and coloration that do not represent any consistent structural differences. The female is tentatively associated here as variation among the males makes it difficult to determine species limits. Future work may lead to additional new species.

Vanuatubasis nunggoli sp. nov.

<https://zoobank.org/89FC33DA-7362-4654-9ACD-D223677DFE50>

Figs 8, 20F, 21G

Type material. Holotype. (1♂ BYU) “VANUATU: Pentecost Is., | Wali, May 26–27, 2019; | -15.9310, 166.1897 | Coll: SM Bybee, GS Powell | #BYU-VU-2019”.

Paratypes (2♂♂ 1♀ **BPBM**, 12♂♂ 1♀ **BYU**, 3♂♂ 1♀ **NHM**, 8♂♂ 2♀♀ **NZAC**). (4♂♂ **BYU**, 2♂♂ **NZAC**) “VANUATU: Pentecost Is., | Ranmawat, May 30, 2019; | -15.8126, 168.1770 | Coll:SM Bybee,GS Powell | #BYU-VU-2019” (1♂ **BYU**, 1♂ **NHM**) “VANUATU: Pentecost Is., | Salap, May 28, 2019; | -15.9589, 168.1948 | Coll:SM Bybee,GS Powell | #BYU-VU-2019” (2♂♂ 1♀ **BPBM**, 6♂♂ 1♀ **BYU**, 2♂♂ 1♀ **NHM**, 2♂♂ 2♀♀ **NZAC**) same label data as holotype. (1♂ **BYU**, 3♂♂ **NZAC**) “VANUATU: Pentecost Is., | Panas, May 31, 2019; | -15.9088, 168.1904 | Coll:SM Bybee,GS Powell | #BYU-VU-2019” (1♂ **NZAC**) “VANUATU: Pentecost Is., | St Joseph, May 31, 2019; | -15.8886, 168.1803 | Coll:SM Bybee,GS Powell | #BYU-VU-2019”.

Allotype (1♀ **BYU**). same label data as holotype.

Description of holotype. Head: Labium overall pale beige; labrum blue-green, with black latero-posterior edges and medially, a depressed black spot at posterior edge; anteclypeus blue-green; genae, and mandibles (except for reddish brown tips) blue-green with darker anterolateral edges; postclypeus overall covered by a black bar that begins medially and extends to the anterior edge, not extending to the dark blue-green, anterior corners; frons black medially with blue-green lateral edges, abruptly changing to black posteriorly; scapes, and pedicels black, flagella dark brown and lightening apically; vertex and rear of head black with line of setae, a bronze shimmer, and a white pruinescence; a pair of white post-ocular spots present; three pale ocelli with small pale patch apical of the median ocellus; eyes green.

Thorax: Dorsally black with a bronze shimmer and white pruinescence; laterally blue and green; pronotum black, latero-posterior corners rounded to obtuse angles and explanate, mid-line obviously indented across the pronotum, hind lobe with raised ridge that is shorter than the width of the pronotum, is curved outward medially, and extends to a sharp point that protrudes posteriorly; mesostigmal plate black with blue-green lateral edges, interior edges raised dorsally to form protruding lobes. Pterothorax with black carina laterally, mesepisternum with black stripe reaching the dorsal carina and reaching the mesopleural suture posteriorly across ~0.5 mm, but only reaching ~ 2/3 of the mesepisternum on the anterior and medial portion; green stripe located on latter 1/3 of mesepisternum and extending past the dark brown mesopleural suture; mesepimeron overall blue with green extending down from mesepisternum; dark brown stripe extending from mesinfraepisternum to ~ 0.25 mm from the base of the wings; metepisternum overall blue with short, brown line located on metapleural suture near the base of the wings, extending ~ 1/6 the suture's length; mesinfraepisternum dark brown; metepimeron dark brown on dorsal 1/2, and blue ventrally, with white pruinescence; coxae, trochanters, and femora dorsally dark brown and ventrally pale beige with brown spines; tibiae pale brown with smaller spines than that of the femora; tarsi beige with dark brown edges and small, dense spines; pale brown tarsal claws that darken apically to reddish tips, claws with a small tooth located on the basal 1/4 of their length.

Wings: Hyaline with dark brown venation; pterostigma pale brown and rhombus-shaped, darkest on the edges; CuP slightly proximal to halfway between antenodals in

both wings; arculus just distal of second antenodal crossvein in both wings; discoidal cells unequal with FW dorsal edge being $1/2$ as long as HW. Nodal index: $14/2-2/13$ in FW and $12/2-2/11$ in HW.

Abdomen: Overall yellowish with black dorsal stripe extending from S1–S9 and lightening to brown laterally, brown reaching ventrally at posterior edge of segments 2–5, with pale brown setae; S1 and S2 mottled blue and brown; S3 anteriorly dark blue, turning yellow posteriorly, S4–S8 yellow; S9 overall brown with blue dorsal stripe medially; S10 with blue lateral spots, terminal edge raised medially to form protrusion. cerci dark brown with pale brown setae and appearing as a curved crescent shape dorsally, medial edges touching at base and apex, terminating in darkened round lobes; paraprocts in dorsal view dark brown and darkening apically, with bumpy texture, slightly converging medially continuously that form sharp terminal hooks; in the lateral perspective the cerci are roughly triangular and tapering apically, with dorsal edge slightly uneven and ventral edge slightly expanded, terminating in small, acutely rounded lobe.

Measurements (mm): total length 42 mm, abdomen 35 mm, HW 21 mm.

Description of allotype. Head: Labium overall pale beige; labrum pale blue with brown latero-posterior edges and a slightly indented medially brown spot at posterior edge; anteclypeus, genae, and mandibles (except for reddish tips) pale blue; postclypeus translucent brown; frons yellow, abruptly changing to black posteriorly; scapes, and pedicels pale blue, flagella pale brown and lightening apically; vertex and rear of head black with line of setae and a bronze shimmer; three pale ocelli with small beige patch apical of the median ocellus; eyes pale green.

Thorax: Dorsally black; laterally yellow with hints of blue; pronotum black medially with yellow lateral edges, latero-posterior corners rounded to obtuse angles and weakly explanate, mid-line obviously indented across the pronotum, hind lobe with raised ridge that is shorter than the width of the pronotum, is curved outward medially, and extends to a sharp, rounded point that protrudes posteriorly; mesostigmal plate brown with yellow lateral edges, not significantly raised dorsally. Pterothorax with black carina; laterally, mesepisternum with black stripe reaching the dorsal carina and extending $\sim 1/2$ of the mesepisternum, reaching the mesopleural suture posteriorly across ~ 0.5 mm, but only reaching $\sim 1/2$ of the mesepisternum on the anterior and medial portion; pale green on ventral $1/2$ of mesepisternum with hint of a brown stripe; metepisternum overall yellow with short, brown line located on metapleural suture near the base of the wings, extending $\sim 1/6$ the suture's length; mesepimeron overall pale blue; dark brown line on posterior end of mesopleural suture extending $\sim 1/6$ the sutures length; mesinfraepisternum pale yellow with apical brown spot; metepimeron light yellow; coxae and trochanters beige, femora dorsally pale brown and ventrally pale beige with black spines; tibiae pale brown with slightly darker, and smaller, spines than that of the femora; tarsi beige with dark brown edges and small, dense spines; pale brown tarsal claws that darken apically to reddish tips, claws with a small tooth located on the basal $1/4$ of their length.

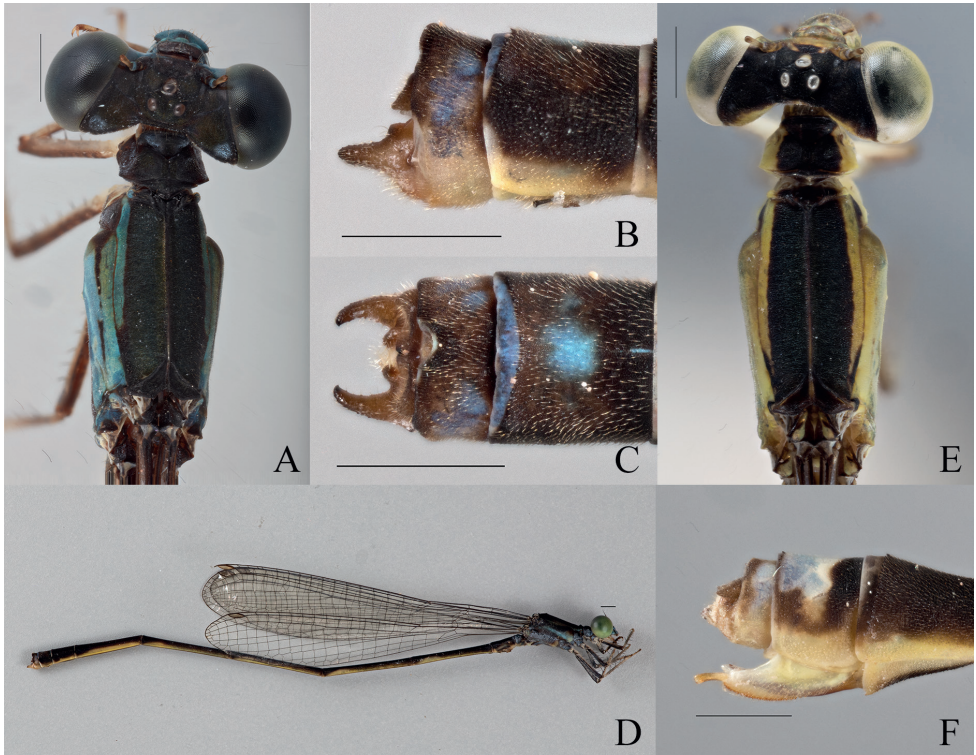


Figure 8. *Vanuatubasis nunggoli* Holotype (♂ BYU) **A** dorsal thorax **B** lateral terminalia **C** dorsal terminalia **D** lateral habitus *V. nunggoli* Allotype (♀ BYU) **E** dorsal thorax **F** lateral terminalia. Scale bars: 0.5 mm.

Wings: Hyaline with dark brown to black venation that thickens dorsally; pterostigma pale brown and rhombus-shaped, darkest on the edges; CuP halfway between antenodals in both wings; arculus just distal of second antenodal crossvein in both wings; discoidal cells unequal with FW dorsal edge being 1/2 as long as HW. Nodal index: 15/2–2/13 in FW and 12/2–2/12 in HW.

Abdomen: Overall yellow with black dorsal stripe extending from S1–S8 and lightening towards the edges, with pale brown setae; S1 and S2 with hints of blue and green laterally; S3 apically blue and turning yellow posteriorly; S3–S7 pale yellow laterally, with dorsal stripe reaching ventral at terminal ends; S8 yellow; S9 with pale dorsal patch extending $\frac{3}{4}$ of its length; S10 pale brown with pale dorsal patch; ovipositor overall beige, with darker serrated ventral edge; stylus with rounded edges, pale brown and lightening apically; gonapophysis reddish brown with slightly serrated dorsal edge. Cerci roughly triangular, dark brown, and narrowing to a rounded apex, dorsal and ventral edge straight.

Measurements (mm): total length 38 mm, abdomen 32 mm, HW 21 mm.

Diagnosis. Male. *Vanuatubasis nunggoli* can be distinguished from all other *Vanuatubasis*, besides *V. kapularum* by the presence of dark brown thoracic coloring on

the metepisternum. It can be distinguished from *V. kapularum* by the inner posterior angle of the paraprocts forming an obtuse angle and the green-blue labrum. **Female.** *Vanuatubasis nunggoli* can be distinguished from other females in this genus, by the dorsal black area on S9 with an uneven posterior edge (this coloring on S9 is sharper than that in *V. evelynae* and not extending as far), a short pedicel, a brown pterostigma, and a blueish hue on the pterothorax.

Variation. Male. The males of this species exhibit variable thoracic coloring, with some males almost black and others blue-green with only traces of black striping. This variation may be connected to populations as males from certain localities seemed to have more dark thoracic coloring than others. **Measurements (mm):** total length 39–42 mm, abdomen 34–37 mm, HW 21–23 mm ($n = 14$). **Female. Measurements (mm):** total length 37–40 mm, abdomen 31–33 mm, HW 21–24 mm ($n = 6$).

Distribution. Pentecost, Vanuatu.

Etymology. The specific epithet of this species is a noun in apposition, derived from the local word for “land diving,” a cultural practice that originated on the island of Pentecost.

Vanuatubasis rhomboides sp. nov.

<https://zoobank.org/3B882901-4835-4CC1-ADFA-B9EE493D41AD>

Figs 9, 21H

Type material. Holotype (1♀ NZAC). (NZAC04230978, New Zealand Arthropod Collection, Auckland, New Zealand), locality data: Republic of Vanuatu, Malekula Island, Stretch of Lakatchkach River flowing through Postanle Area (-16.1437, 167.4671 to -16.1474, 167.4649; 15–51 m a.s.l.): 17 May 2017; M. Marinov & S. Bybee leg.

Paratype (1♀ NZAC). NZAC04231074, Malekula Island, Litslits (-16.1435, 167.4671; 15 m a.s.l.): 07 May 2019, S. Bybee & G. Powell leg.

Description of holotype. Head: Labium pale yellow, labrum, mandibles (except for the reddish tips), whole clypeus, frons and genae along the eyes up to the dorsal ends of the scapes, scapes citron yellow except for dark fuscous to dark reddish spots at the dorsal corners of the mandibles at the ends of the lateral proximal corners of the postclypeus plus lateral sides of labrum running down for almost the whole length to the anterior edge; pedicels brownish; flagella dark red; scape: pedicel 0.5; vertex black with slight dark red sheen with three yellow spots – two are horn-like expansions of the yellow on the postfrons into the dark vertex and the third is just in front of the median ocellus; rear part of the head yellow which is continuing up toward the occipital area and visible from the dorsum in a shape of two pear-like yellow areas on the postocular lobes and a small spot on the occipital bar; two roughly circular occipital spots formed by pale pruinescence; eyes orange yellow with pale fulvous areas on the dorsal part.

Thorax: Dark wide bar (slightly tapering towards posterior end) with slight reddish sheen passing on the dorsal part of pro- and pterothorax encompassing ~ 3/4 of

the dorsal part of the mesostigmal plate and 1/2 of mesepisternum (faint pale line along the dorsal carina starting approximately midway and gradually becoming lighter towards the pre-alar area), at the posterior end the dark bar abruptly curves ventrally at a near 90° angle and joins the posterior end of mesopleural suture with a semicircular curvature; dark elongated spots with same color developed also as follows: two sitting on the dorsal edges of the meso- and metapleural sutures at their posterior ends and connecting to two dark shiny spots at the alar areas by a tiny bridge with the same color and a solid bar on the posterior edge of poststernum; legs almost entirely yellow save for darken areas on the inner surfaces of the front tibia in the proximal 2/3 and dorsal part of all femora occupying as follows: distal 1/2 of front femora, 9/10 of the distal part in the middle and hind legs, all dark areas with characteristic pale spots giving a barred-like appearance, pale spots on front femora weakly developed forming serrated outer edges; dark spots at the joints between femora and tibiae and distal tips of the last tarsal segments; claws orange with darker reddish tips; all the leg spines black; mesostigmal plate triangular in shape with dorsoposterior end enlarged and extruded into an auricle-like lobe, ventral side wide rounded and slightly elevated and separated from the thorax; hind lobe of the prothorax is triangular with two parallel carinae ventrally arising out from the lateral sides of the hind lobe and running posteriorly to the dorsal edge.

Wings: Hyaline; venation generally dark especially at the distal ends becoming paler towards the bases with pale spots at the nodus at both outer and inner sides; pterostigma with protruding posterior proximal end into a sharp angle which is dissimilar in both front and hind wings differing in the following: front wing smaller with central fuscous area outlined with pale yellow, hind wing larger with anterior end 2/3 of the length of posterior, bicolored with dark area continuing towards the sharp proximal end of the pterostigma and pale yellow anterior part; CuP slightly proximal to halfway between antenodals in front wings and halfway in hind wings sitting on the top CuP and AA distal at the point where the latter is leaving the wing edge; arculus at second antenodal in front wings and slightly distal to it in hind wings; discoidal cells dissimilar in shape – in front wings anterior side is ~ 1/3 of the posterior and in hind wings anterior side is more than 1/2 of posterior; two postdiscoidal cells before nodus; nodal index: 12/2–2/12 in front wings and 10/2–2/10; MA and MP very long reaching to surpassing the midway between nodus and pterostigmas, CuA surpassing the nodus and ends proximal to the midway between nodus and pterostigma.

Abdomen: Black dorsal area running from S1 to S8 continuing on the dorsal 1/2 of S9 where it descends on the lateral side of the segment outlining a wide circular beige spot on each side of the segment and joining the posterior end of the segment, dark area on the dorsum of S9 ends up at two round lobes, posterior dorsal 1/2 of S9 with a pale brownish bar, S10 with a dark area on the dorsum which is constricted at both lateral sides by the beige expansions from the lateral sides of the segment giving the dark area a roughly X-shape when viewed from the dorsum; dark area with dorsal invaginations forming lateral bulbous expansions at proximal ends on S2 and S3 and yellow bars continuing up almost meeting on the dorsum of S3–S5; ventral side of

the abdomen yellow with slim dark lines on the ridges of the sternites 2–8, those lines faint on second segment occupying approximately mid-area and continuing more towards the anterior part of the segment, slightly skewed towards the anterior end on segments 3–5 and equidistant from both ends of the segments on 6–8; posterior end of the eighth sternite lacking tooth; cerci fuscous with pale tips; ovipositor yellow surpassing the posterior end of S10 with the tip reaching just before the distal tips of the cerci, styli yellow at the extreme base and gradually darkening becoming deep dark red distally with very weak yellow lightening at the tips, styli surpassing the cerci.

Measurements (in mm): total length 35.5, abdomen 30.0, hind wing 22.5.

Diagnosis. *Vanuatubasis rhomboides* has a mesostigmal plate with the dorso-posterior end raised as an auricle. This shape is found only in three other congeners:



Figure 9. *Vanuatubasis rhomboides* Holotype (♀ NZAC) **A** dorsal thorax **B** lateral terminalia. Scale bars: 0.5 mm.

V. kapularum, *V. nunggoli*, and *V. malekulana*. The height of the auricle is less pronounced in the first two species, but *V. malekulana* has a similarly high auricle to *V. rhomboides*. The latter is distinguished by all other congeners by the rhomboidal shape of the pterostigmata which are characteristically bicolored in HW.

Variation. Body overall green and predominantly yellow on the ventral side; dark area on the dorsum of S9–10 reduced. **Measurements** (in mm): total length, abdomen 30.0, hind wing 22.5.

Distribution. Malekula, Vanuatu.

Etymology. The name *rhomboides* is Latinized form of Greek *ῥομβοειδής*, *-ής*, *-ές* = like a rhombus, rhomboid, in reference to the shape of the pterostigmata {adjective}.

Notes. This species is only known from female specimens as no males were able to be associated.

Vanuatubasis santoensis Ober & Staniczek, 2009

Figs 10, 20G, 21I

Vanuatubasis santoensis Ober & Staniczek (2009): 487–490.

Remark. *Vanuatubasis santoensis* was known by males only. Here we describe the female.

Material examined. Holotype (1♂ SMNS). “*Vanuatubasis santoensis* ♂ HOLOTYPE | Ober and Staniczek 2009 | Vanuatu, Sanma Province | Espiritu Santo, surroundings of | Penaoru, Penaoru River | leg. A.H. Staniczek and M. Pallmann, 13.XI.2006 | det. S.V. Ober, 21.VII.2008 | coll.- | Ober and Staniczek 2009 | 14.96105°S. 166.63316°E 90 m | ODO 000242 K.” (4♂♂ BYU) “VANUATU: Santo Is: | Wailapa, -15.5781 | 167.0024, 6.vi.2018, coll, | S. Bybee and G. Powell” (1♂ BYU) “VANUATU: Santo Is: | Narango, -15.6274 | 166.8535, 4.vi.2018, | coll, S. Bybee and G. Powell” (2♂♂ BYU) “VANUATU: Santo Is: | Narango, -15.5538 | 166.9814, 4.vi.2018, | coll, S. Bybee and G. Powell” (12♂♂ 4♀♀ BYU) “VANUATU: Santo Is: | Ipayato, -15.6296 | 166.8426, 4 vi.2018. | coll. S. Bybee and G. Powell” (5♀♀ BYU) “VANUATU: Santo Is: Felea | -15.3839 166.8426, 4.vi.2018, | coll, S. Bybee and G. Powell”

Paratypes (2♂♂ SMNS). same label data as Holotype with the following barcode numbers: ODO 000246 K, ODO 000247 K. (1♂ SMNS). “Vanuatu, Sanma Province | Espiritu Santo, surroundings of Tasmate, Paé River, 15.2175°S, 166.68706°E, 139 m, 11.XI.2006, leg. A.H. Staniczek and M. Pallmann”, with the following barcode number: ODO 000245 K. (2♂♂ SNMS, 2♂♂ MNHN). “Vanuatu, Sanma Province, Espiritu Santo, surroundings of Tasmate, Mamasa River, 15.20976°S, 166.67705°E, 20 m, 9.XI.2006, leg. A. H. Staniczek and M. Pallmann”, SNMS specimens with the following barcodes: ODO 000243 K, ODO 000244 K.

Description of the female. Head: Labium overall pale beige; labrum pale green with brown latero-posterior edges and small, slightly indented medially brown spot at posterior edge; anteclypeus, genae, and mandibles (except for reddish tips) pale green; postclypeus translucent brown with green lateral edges; frons pale green, turning black

posteriorly; scapes, pedicels, and flagella pale brown; vertex and rear of head black with line of setae and a bronze shimmer; three pale ocelli with small beige patch apical of the median ocellus; two white post-ocular spots; eyes pale green.

Thorax: Prothorax dorsally black; laterally green; pronotum black medially with brown edges, latero-posterior corners rounded to acute angles and weakly explanate, mid-line obviously indented across the pronotum, hind lobe with raised ridge that is shorter than the width of the pronotum, is curved outward medially, and extends to a sharp, rounded point that protrudes posteriorly; mesostigmal plate black with green lateral edges and not significantly raised. Pterothorax with black carina; laterally mesepisternum with black stripe reaching the dorsal carina and extending more than $3/4$ of the mesepisternum, pale green on latter $1/4$ of mesepisternum; mesepimeron overall pale green with hints of yellow; metepisternum overall green with short, brown line located on metapleural suture near the base of the wings, extending $\sim 1/6$ the suture's length; mesinfraepisternum pale green with apical brown spot; metepimeron green, with beige anterior portion; coxae and trochanters beige, femora dorsally dark brown and ventrally beige with black spines; tibiae pale brown with slightly darker, and smaller, spines than that of the femora; tarsi beige with dark brown edges and small, dense spines; pale brown tarsal claws that darken apically to reddish tips, claws with a small tooth located on the basal $1/4$ of their length.

Wings: Hyaline with dark brown; pterostigma dark brown and rhombus-shaped, darkest on the edges; CuP halfway between antenodals in both wings; arculus just distal of second antenodal crossvein in both wings; discoidal cells unequal with FW dorsal edge being $1/2$ as long as HW. Nodal index: $13/2-2/12$ in FW and $12/2-2/11$ in HW.

Abdomen: Overall beige yellow with black dorsal stripe from S1–8 and lightening towards the edges, with pale brown setae; S1 and S2 green laterally; S3–S8 yellow laterally; S9 with pale dorsal stripe; S10 pale brown; ovipositor overall beige, with darker serrated ventral edge; stylus with rounded edges, pale brown and lightening apically; gonapophysis reddish brown with slightly serrated dorsal edge. Cerci roughly triangular, dark brown, and narrowing to a rounded apex, dorsal edge straight a ventral edge slightly rounded ventrally.

Measurements (mm): total length 36–39 mm, abdomen 29–33 mm, HW 22–24 mm ($n = 9$).

Diagnosis. Male. *Vanuatubasis santoensis* can be distinguished from other *Vanuatubasis* by its black pterostigma, pale blue postclypeus without any bars or maculations, dorso-posterior corner of mesostigmal plate not raised in an auricle (or if elevated, only slightly so). **Female.** *Vanuatubasis santoensis* can be distinguished from other females in this genus, by its dark brown to black pterostigma, uniformly colored postclypeus (sometimes with pale spots), frons with a dark triangle extending from the base of the median ocelli, and the dark area on the mesepisternum reaching the black spot at the posterior end of the mesopleural suture.

Variation. Male. Postclypeal maculation more prominent than in some individuals. Pterothorax sometimes with variable short black stripes. **Female.** Thoracic coloring varies from yellow to green, presumably due to the age of the individual.

Distribution. Espiritu Santo, Vanuatu.

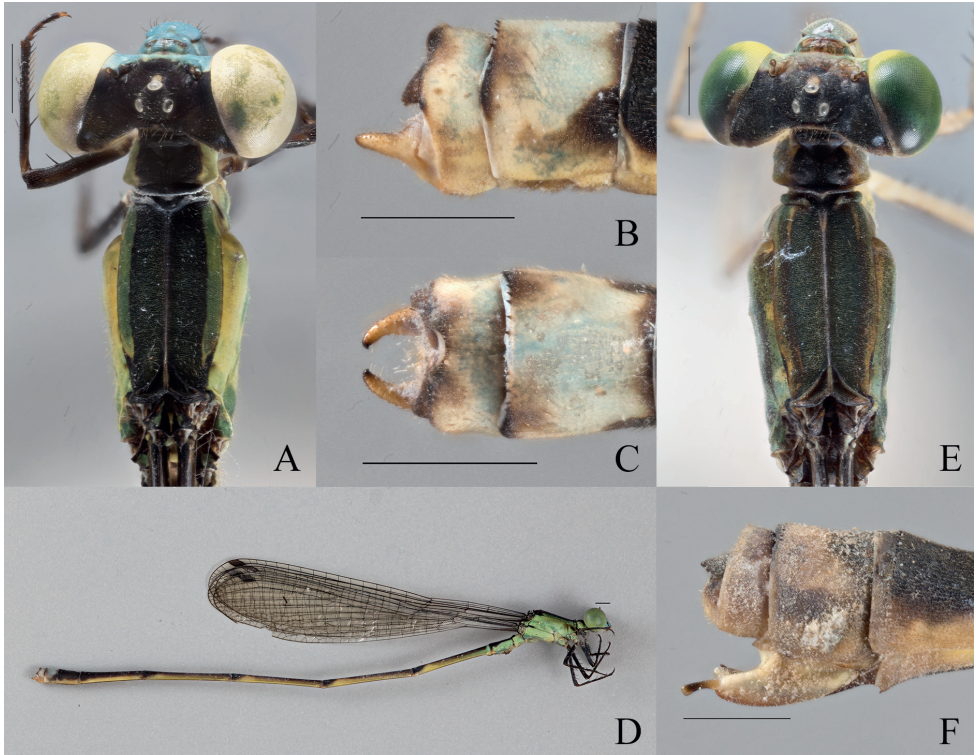


Figure 10. *Vanuatubasis santoensis* (♂ BYU) **A** dorsal thorax **B** lateral terminalia **C** dorsal terminalia **D** lateral habitus *V. santoensis* (♀ BYU) **E** dorsal thorax **F** lateral terminalia. Scale bars: 0.5 mm.

***Vanuatubasis xanthochroa* sp. nov.**

<https://zoobank.org/3F3CD171-A876-49FE-93EA-D69D512A288B>

Figs 11, 21J

Type material. Holotype (1♀ NZAC). “REPUBLIC OF VANUATU, Malekula Island, | Stretch of Lakatchkach River flowing through Postanie Area | 16.1437S, 167.4671E; 15 m a.s.l. | 17 May 2017 | M. Marinov & S. Bybee leg.” “*Vanuatubasis* sp.2., female | M. Marinov det., August 2017” “NZ Arthropod Collection | Private Bag 92170 | Auckland | New Zealand | NZAC04230976”.

Paratypes (2♀♀ BPBM, 5♀♀ BYU, 3♀♀ NHM, 4♀♀ NZAC). (2♀♀ BPBM, 4♀♀ BYU, 3♀♀ NHM, 3♀♀ NZAC) “VANUATU: Malekula Is. | Litslits, -16.14594705 | 167.4653247, 18, 24.v.2018 | coll. S. Bybee and G. Powell.” (1♀ BYU, 1♀ NZAC) “VANUATU: Malekula Is., | Litslits, May 7th 2019 | -116.1435, 167.4671 | Coll:SM Bybee, GS Powell | VU-BYU-2019”.

Description of holotype. Head: Labium pale yellow; labrum, mandibles (except for the reddish tips), whole clypeus, frons and genae along the eyes up to the dorsal ends of the scapes, scapes and pedicels citron yellow except for a dull fulvous (to pale

brownish) spot at the middle of the labrum along its posterior edge with triangular shape and two fuscous spots at the postero-lateral corners of the labrum; flagella dark red; scape: pedicel 0.5; vertex black with slight dark red sheen with three yellow spots – two are expansions of the yellow face into the dark vertex and the third is just in front of the median ocellus; rear part of the head yellow which is continuing up toward the occipital area and visible from the dorsum on the posterior ends of postocular lobes and occipital bar; two roughly circular occipital spots formed by pale pruinescence; eyes orange yellow with pale fulvous areas on the dorsal part; eyes with three transverse lines in right eye and one in left which are unclear if are post mortem or present in life.

Thorax: Entire thorax including the legs yellow with pale fulvous area starting from the dorsal part of the thorax and diffusing around the level of mesepimeron; five dark spots as follows: two faint sitting on the dorsal end of mesopleural and metapleural sutures (metapleural very obscure) almost touching the posterior corners of both sutures; two dark red at the dorsal posterior corners of both mesepimeron and metepimeron and one at the posterior end of the poststernum; leg spines deep dark red to almost black, claws fulvous becoming darker at the tips; mesostigmal plate, roughly quadrilateral-shaped with expanded dorsoanterior side thus wider than ventral side; hind lobe of the prothorax raised, roughly triangular shape with two parallel carinae, dorsal angulated and ventral rounded arising out from the lateral sides of the hind lobe, running posteriorly to the dorsal edge.

Wings: Hyaline; venation generally dark especially at the distal ends becoming paler towards the bases with pale spots at the nodus at the outer sides; pterostigma rhomboidal fulvous with pale yellow lines along the edges that are wider on the dorsal edge and faint to almost not existing at the anterior edge; CuP halfway between antenodals in front wings and closer to second antenodal in hind wings situated proximally to the wing petiolation and distant from the point where CuP and AA is leaving the wing edge for nearly a whole of its length; arculus distal from the second antenodal in all wings; discoidal cells dissimilar in shape – in front wings anterior side is $\sim 1/4$ of the posterior and in hind wings anterior side is $\sim 1/2$ of posterior; three postdiscoidal cells before nodus; nodal index: 12/2–2/11 in front wings and 10/2–2/11; MA, MP and CuA very long reaching to surpassing the midway between nodus and pterostigmas.

Abdomen: Generally dark fulvous on the dorsum and pale yellowish on the ventral side with the following peculiarities: fulvous dorsal area is very faint to almost missing on S1 and gradually becoming darker towards the posterior end finishing abruptly at $\sim 1/4$ of S9, remainder of S9 and S10 pale cream with a touch of a faint blue on the dorsum, dorsum of S10 at the intersegmental membrane to S9 with a very narrow dark red bar not continuing on the lateral sides of the segment; dorsum of S2–S7 with anterior part paler, becoming darker at the posterior $\sim 1/6$ – $1/7$ end of the segments, all with yellow bars at the anterior end continuing from the venter and almost touching on the dorsum, S8 uniformly dark; small tooth at the posterior end of the eighth sternite; cerci pale yellow; ovipositor orange yellow surpassing the posterior end of S10 with the tip aligned with the tips of cerci and styles surpassing the cerci.

Measurements (in mm): total length 33.5, abdomen 28.0, hind wing 20.5.

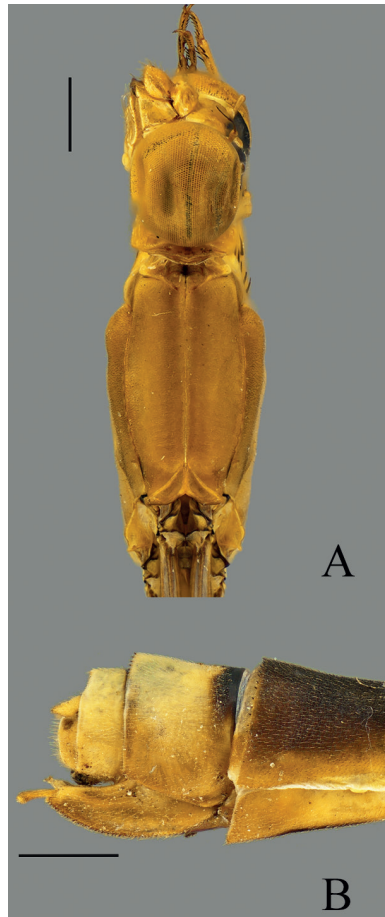


Figure 11. *Vanuatubasis xanthochroa* Holotype (♀ NZAC) **A** dorsal thorax **B** lateral terminalia. Scale bars: 0.5 mm.

Diagnosis. Female. *Vanuatubasis xanthochroa* can be distinguished from all other *Vanuatubasis* females by the lack of a black dorsal stripe across the carina and no post-clypeal maculation.

Variation. Female. Dark spot on the labrum larger; both eyes with transverse lines; posterior end of the posterior edge of the prothorax triangular shape and not as wide as in the holotype; CuP situated at the petiolation at the base of CuP and AA where the later leaves the wing edge, pterostigma with yellow lines all around the edges, nodal index: 11/2–2/11 in front wings and 9/2–2/9 in hind wings, spine on the ventral side of eight sternite large and sharp.

Distribution. Malekula, Vanuatu

Etymology. The name *xanthochroa* is Latinized feminine form of Greek *ξανθόχρους*, *-οῦς*, *-οῦν* = yellow colored, in reference to the color of the thorax {declinable adjective}.

Notes. This species is only known from female specimens as no males were able to be associated.

Key to species of *Vanuatusbasis* using mature males

- 1 Terminal segment of genital ligula with lobes laterally covering the sclerotized portion of the first segment (Fig. 12A), or lobes extended in parallel sided, longer than wide, projections (Fig. 12C)..... **2**
- Terminal segment of genital ligula with lobes laterally not covering the sclerotized portion of the first segment (Fig. 12B); lobes not extended in parallel sided projections (Fig. 12D) **3**
- 2 Paraprocts subparallel, only curving medially at apical 1/3. Cerci with two acute teeth. Aneityum Is. ***V. bidens***
- Paraprocts strongly curving medially their entire length. Cerci lacking two teeth. Espiritu Santo Is. ***V. evelynae***
- 3 Mesostigmal plate with dorso-posterior corner not raised in an auricle; if elevated then height of the projection is less than 1/2 the distance between the tip of the auricle and the dorsal carina (Fig. 13A)..... **4**
- Mesostigmal plate with dorso-posterior corner raised in an auricle; the height of the projection is greater than or equal to 1/2 the distance between the tip of the auricle and the dorsal carina (Fig. 13B)..... **5**
- 4 Postclypeus pale blue (sometimes with yellow dots) but lacking dark markings (Fig. 14A). Espiritu Santo Is. ***V. santoensis***
- Postclypeus pale blue with black transverse bar at the anterior edge (Fig. 14B); Maewo Is. ***V. insularivororum***
- 5 Mes- and metinfraepisterna almost entirely black (Fig. 15A)..... **6**
- Mes- and metinfraepisterna almost entirely pale saved for a black dot on the anterior corner of mesinfraepisternum (Fig. 15B); Malekula Is. ... ***V. malekulana***
- 6 Cerci dorsally having the inner posterior angle form a slightly acute to quadrate (~90°) angle (Fig. 16A); Efate Is. ***V. kapularum***
- Cerci dorsally having the inner posterior angle form a broadly rounded, obtuse angle (Fig. 16B); Pentecost Is. ***V. nunggoli***

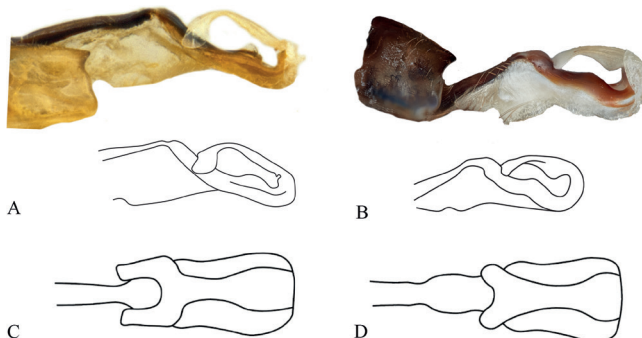


Figure 12. Characters of the genital ligula **A** *V. bidens* image and line drawing of lateral lobes covering the sclerotized portion of the first segment **B** *V. kapularum* image and line drawing of lateral lobes not covering the sclerotized portion of the first segment **C** *V. evelynae* dorsal view of lateral lobes being longer than wide **D** *V. malekulana* dorsal view of lateral lobes not being longer than wide.

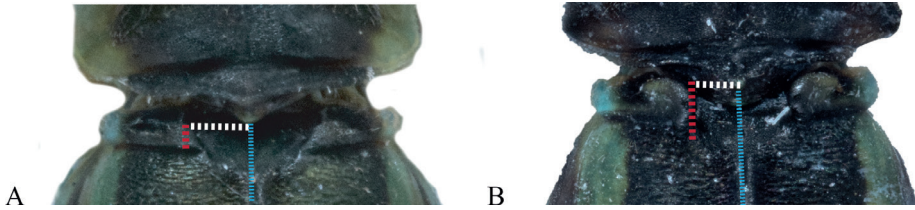


Figure 13. Dorsal view of mesostigmal plates showing the relative heights of the auricles **A** *V. santoensis*, height < distance between tip and the dorsal carina **B** *V. nunggoli*, height > distance between tip and the dorsal carina. The red dotted line represents the height of the mesostigmal plate, the white dotted line shows the distance from the the tip of the plate to the dorsal carina, and the blue dotted line runs along the dorsal carina.

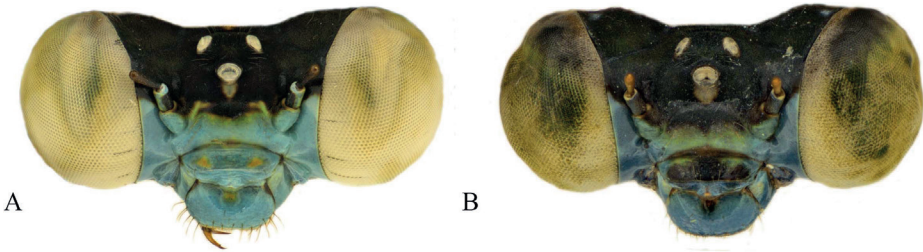


Figure 14. Face of male **A** *V. santoensis* **B** *V. insularivorum*.

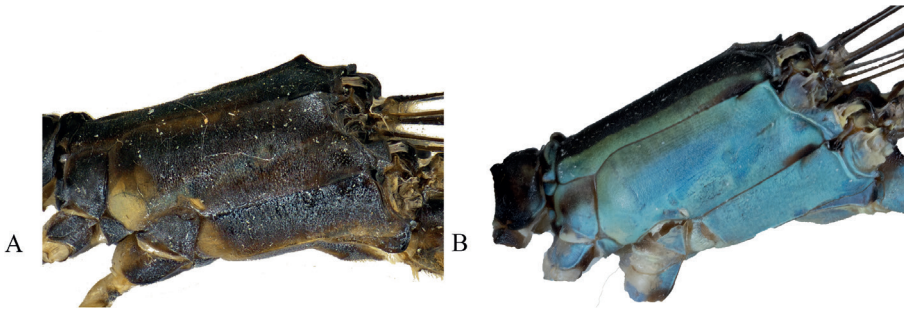


Figure 15. Mes- and metinfraepisterna **A** *V. kapularum* **B** *V. malekulana*.

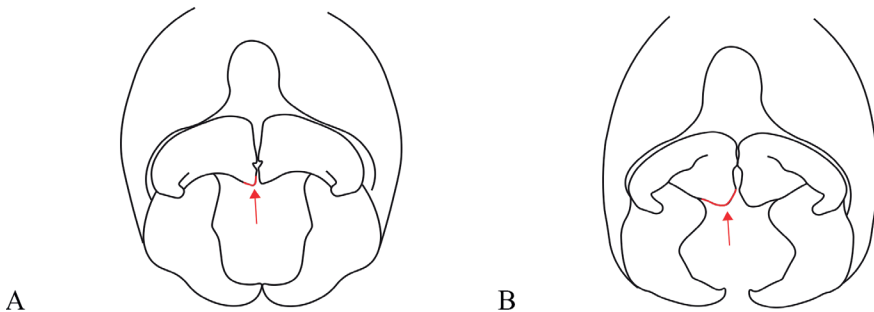


Figure 16. Paraprocts with inner posterior angle highlighted **A** *V. kapularum* angle slightly acute to 90° **B** *V. nunggoli* angle obtuse.

Key to species of *Vanuatubasis* using mature females

- 1 Postclypeus uniformly colored (Fig. 21H, J) OR with pale spots (Fig. 21A, D, I) **2**
 – Postclypeus not uniformly colored; spots or darker area brown or black (Fig. 21B, C, E, F, G) **6**
- 2 Cerci brown; frons various colors but always with dark semicircle on apical 1/3 (Fig. 17A) **3**
 – Cerci pale yellow; frons yellow and lacking dark semicircle on apical 1/3 (Fig. 17B) **5**
- 3 Pterostigmata of HW unicolored (Fig. 18A) **4**
 – Pterostigmata of HW bicolored (Fig. 18B); Malekula Is. *V. rhomboides*
- 4 Wing venation pale brown; pterostigmata pale yellow; black on the mesepisterna does not cover the dorsal carina; sternum of S8 without spine above the ovipositor (Fig. 5E, F); Maewo Is. *V. insularivorum*
 – Wing venation black; pterostigmata dark; black on the mesepisterna partly cover the dorsal carina; sternum of S8 with spine above the ovipositor (Fig. 10E, F); Espiritu Santo Is. *V. santoensis*
- 5 Pterothorax unicolored; Malekula Is. *V. xanthochroa*
 – Pterothorax not unicolored; Aneityum Is. *bidens*
- 6 Black area on the disk of S9 with uneven posterior edge (Fig. 21B, C, G, H) **7**
 – Black area on the disk S9 with almost straight posterior (Fig. 21E, F) **9**
- 7 Cerci brown **8**
 – Cerci black. Espiritu Santo Is. *V. evelynae*
- 8 Pedicel long (scape: pedicel < 0.4); dark area (if present) on mesinfraepisternum with a maximum width of ~1/6 of the disk; pterothorax with no blueish hue; Malekula Is. *V. discontinua*
 – Pedicel short (scape: pedicel ≥ 0.4); dark area on mesinfraepisternum with width ≥ 1/4 of the disk; pterothorax with blueish hue; Pentecost Is. *V. nunggoli*
- 9 Height of the dorso-posterior corners of mesostigmal plates equal or longer than the distance between the tip of the plate and dorsal carina (Fig. 19A); Malekula Is. *V. malekulana*
 – Height of the dorso-posterior corners of mesostigmal plates shorter than the distance between the tip of the plate and dorsal carina (Fig. 19B); Efate Is. *V. kapularum*

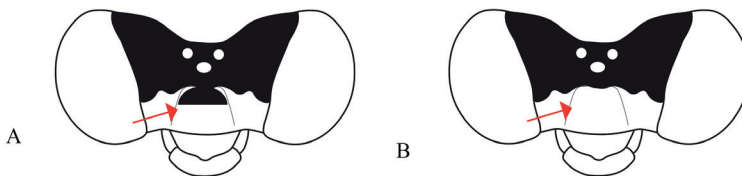


Figure 17. Head of females **A** with a dark semicircle on frons **B** without a dark semicircle on frons.

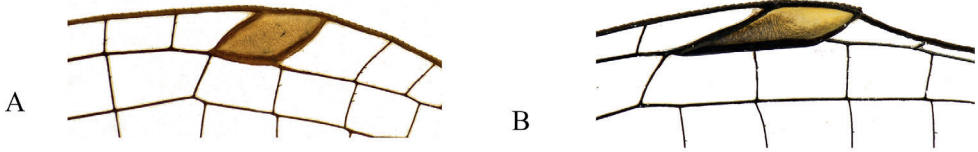


Figure 18. Female pterostigma **A** *V. insularivorum* unicolored **B** *V. rhomboides* bicolored.

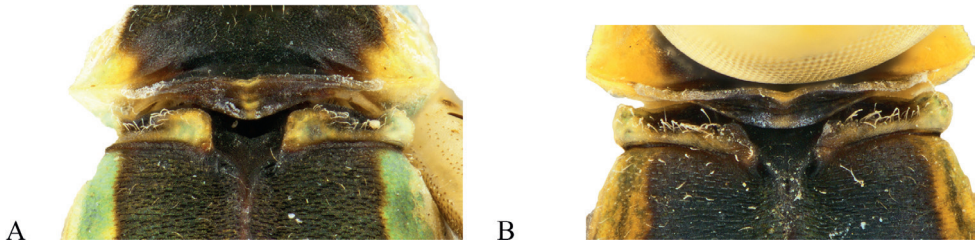


Figure 19. Female mesostigmal plates **A** *V. malekulana* **B** *V. kapularum*.

Discussion

Vanuatubasis exhibits great levels of island endemism, a pattern also seen in other endemic damselfly genera on Pacific island systems such as *Nesobasis* in Fiji (Donnelly 1990) and *Megalagrion* in Hawaii (Polhemus 1997). *Vanuatubasis* in overall appearance and structure most closely resembles *Nesobasis*, with the most obvious difference being the length of the cerci compared to the paraprocts. *Vanuatubasis* species, in contrast to those of *Nesobasis*, do not display a wide diversity of color to the human eye. Almost all specimens collected (excluding teneral individuals) are generally dark blue and green hues, with few exceptions (e.g., a few females of *Vanuatubasis* are yellow). In *Nesobasis* the color variation includes bright red or yellow males, as well as both pale and dark blue species.

It appears likely that small stretches of ocean between islands provide some sort of barrier between populations allowing for speciation events to occur. This is illustrated by each species only being found on a single island in the archipelago. The high level of endemism that these species have puts them at risk due to the rapid environmental change currently taking place in Vanuatu. Over the course of several years of fieldwork, the authors noted alteration of stream habitats, such as increased agriculture and removal of native vegetation. In one instance, we noted a difference in the actual presence of some of these species on particular streams. For example, in 2018 specimens of *V. kapularum* were collected on Ewor River in Efate. The following year at the same time of year no specimens were found on the same river, and there was an overall difference in the amount of the native vegetation, with many ferns being replaced by agricultural crops. This revision looked over material collected on six islands. Continued sampling is particularly pressing, especially on additional islands, as much of the preferred habitat for the genus is quickly being altered (Wairiu 2017; Saxton et al. 2021).

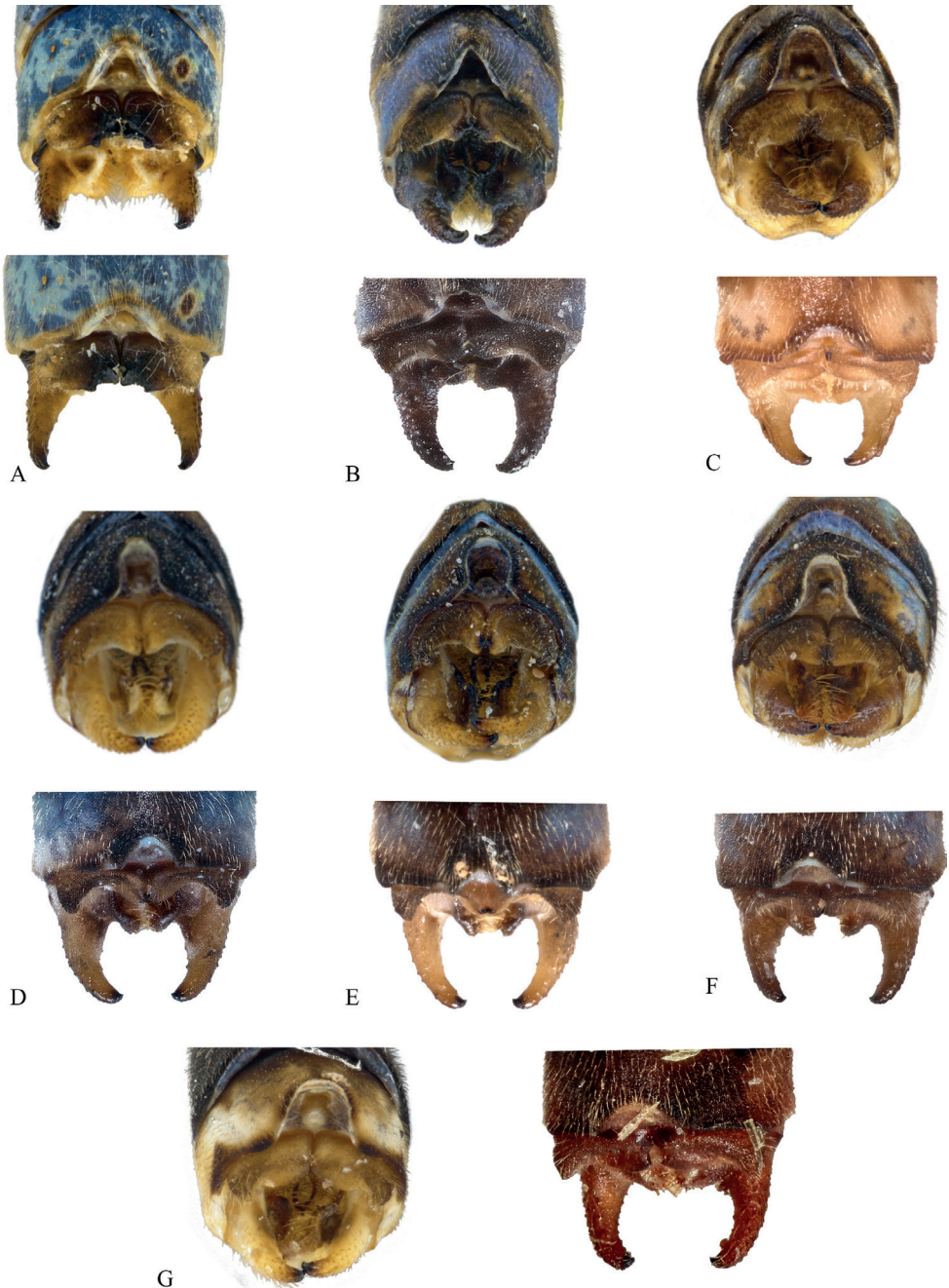


Figure 20. Male dorso-posterior and dorsal terminalia of **A** *V. bidens* **B** *V. evelynae* **C** *V. insularivorum* **D** *V. kapularum* **E** *V. malekulana* **F** *V. nunggoli* **G** *V. santoensis*.

Vanuatubasis diversity further demonstrates the need for more odonate research in the South Pacific region. This research lays the groundwork for future research on their ecology, biogeography, and evolutionary history. Work in this region should further

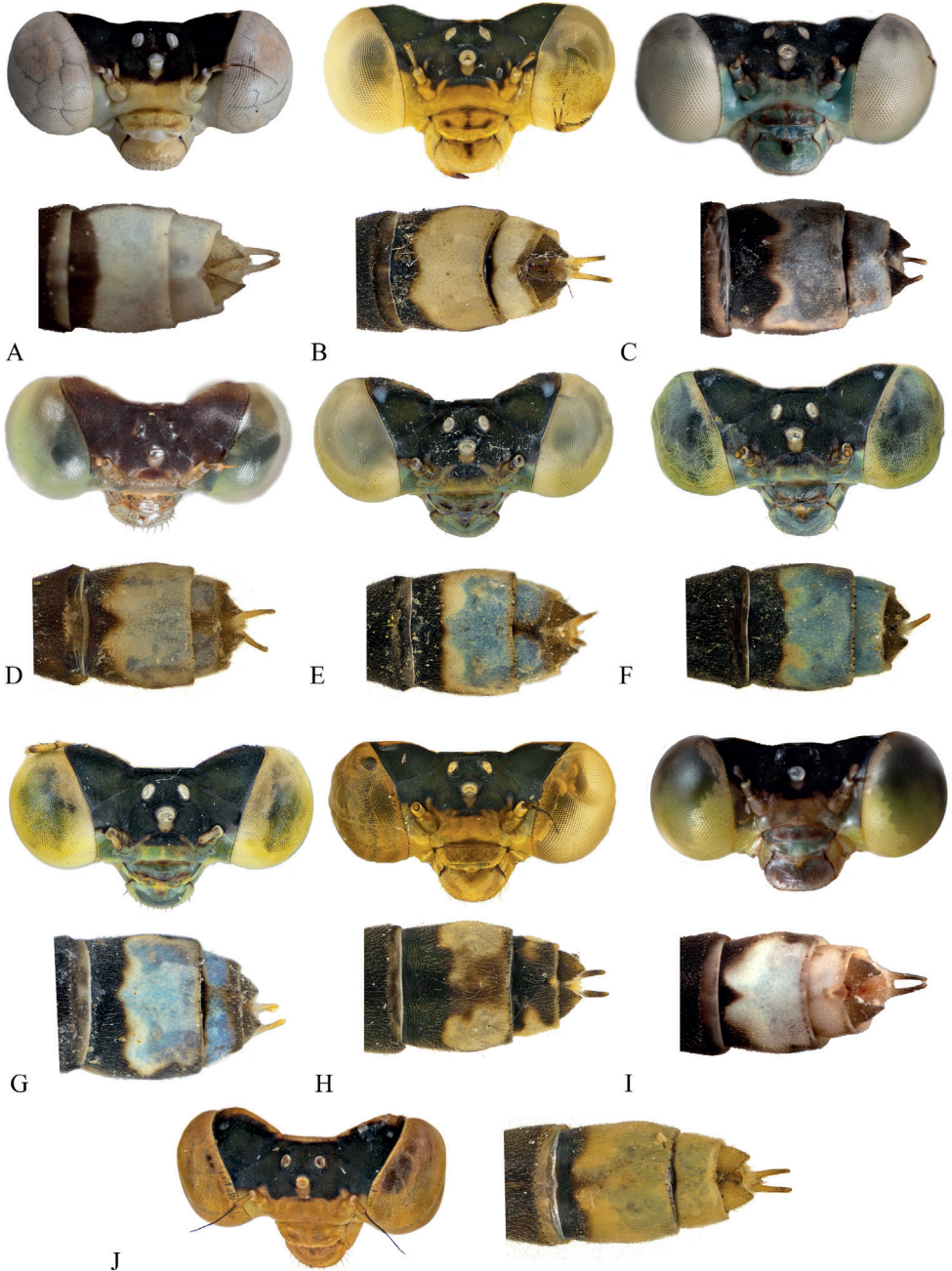


Figure 21. Female face and dorsal terminalia of **A** *V. bidens* **B** *V. discontinua* **C** *V. evelynae* **D** *V. insularivororum* **E** *V. kapularum* **F** *V. malekulana* **G** *V. nunggoli* **H** *V. rhomboides* **I** *V. santoensis* **J** *V. xanthochroa*.

focus on the relationships among endemic genera in Fiji and Vanuatu (e.g., *Nesobasis*, *Melanesobasis*, *Vanuatubasis*) and their placement within the larger subfamilies of Coenagrionidae. A broader understanding of their phylogenetic position will help to answer questions relating to their biogeography.

Acknowledgements

We would like to thank our Vanuatu government contacts Donna Kalfatakvoli and Mimosa Bethel for their assistance in obtaining the required permits and visas in order to complete our research. Additional thanks to all the local ni-Vanuatu landowners and guides who helped us. Thanks to Ben Price (NHM) for allowing us access to museum specimens, Heinrich Fliedner for nomenclatural advice, and Gareth Powell for assistance with imaging. Additional thanks to Martin Schorr and the International Dragonfly Fund. Finally, we thank Dan Polhemus and Jan van Tol for their comments that greatly improved this manuscript. This research was funded through the National Science Foundation Division of Environmental Biology grants (#1265714 to SMB), the BYU Sant Grant, BYU Research Experience for Undergrads, and the BYU Kennedy Center for International Studies.

References

- Beatty CD, Sánchez Herrera M, Skevington JH, Rashed A, Van Gossum H, Kelso S, Sherratt TN (2017) Biogeography and systematics of endemic island damselflies: The *Nesobasis* and *Melanesobasis* (Odonata: Zygoptera) of Fiji. *Ecology and Evolution* 7(17): 7117–7129. <https://doi.org/10.1002/ece3.3175>
- De Marmels J (2007) *Tepuibasis* gen. nov. from the Pantepui region of Venezuela, with descriptions of four new species, and with biogeographic, phylogenetic and taxonomic considerations on the Teinobasinae (Zygoptera: Coenagrionidae). *Odonatologica* 36(1): 117–146.
- Dijkstra KDB, Kalkman VJ, Dow RA, Stokvis FR, van Tol J (2014) Redefining the damselfly families: A comprehensive molecular phylogeny of Zygoptera (Odonata). *Systematic Entomology* 39(1): 68–96. <https://doi.org/10.1111/syen.12035>
- Donnelly TW (1990) The Fijian genus *Nesobasis* Part 1: Species of Viti Levu, Ovalau, and Kadavu (Odonata: Coenagrionidae). *New Zealand Journal of Zoology* 17(1): 87–117. <https://doi.org/10.1080/03014223.1990.10422587>
- Garrison RW, von Ellenrieder N, Louton JA (2010) Damselfly genera of the New World. An illustrated and annotated key to the Zygoptera. The Johns Hopkins University Press, Baltimore, MD, [xiv +] 490 pp.
- Kimmins DE (1958) Miss LE Cheesman's expedition to New Hebrides, 1955: Orders Odonata, Neuroptera and Trichoptera. *Bulletin of the British Museum* 6(9): 237–250. [Natural History] <https://doi.org/10.5962/bhl.part.17108>
- Marinov M (2015) The seven “oddities” of Pacific Odonata biogeography. *Journal of the International Dragonfly Fund* 11: 1–58.
- Marinov M, Bybee S, Doscher C, Kalfatakvolis D (2019) Faunistic studies in South-east Asian and Pacific Island Odonata. *Journal of the International Dragonfly Fund* 26: 1–46.
- Ober S, Staniczek A (2009) A new genus and species of coenagrionid damselflies (Insecta, Odonata, Zygoptera, Coenagrionidae) from Vanuatu. *Zoosystema* 31(3): 485–497. <https://doi.org/10.5252/z2009n3a6>

- Polhemus DA (1997) Phylogenetic analysis of the Hawaiian damselfly genus *Megalagrion* (Odonata: Coenagrionidae): implications for biogeography, ecology, and conservation biology. *Pacific Science* 51(4): 395–412.
- Riek EF, Kukalová-Peck J (1984) A new interpretation of dragonfly wing venation based upon Early Upper Carboniferous fossils from Argentina (Insecta: Odonatoidea) and basic character states in pterygote wings. *Canadian Journal of Zoology* 62(6): 1150–1166. <https://doi.org/10.1139/z84-166>
- Saxton NA, Powell GS, Bybee SM (2020) Prevalence of leg regeneration in damselflies reevaluated: A case study in Coenagrionidae. *Arthropod Structure & Development* 59: 100995. <https://doi.org/10.1016/j.asd.2020.100995>
- Saxton NA, Paxman EM, Dean AM, Jensen CR, Powell GS, Bybee SM (2021) Factors influencing the distribution of endemic damselflies in Vanuatu. *Insects* 12(8): 670. <https://doi.org/10.3390/insects12080670>
- Staniczek A (2011) Focus on aquatic insects. In: Bouchet PH, Guyader HL, Pascal O (Eds) *The natural history of Santo*. Muséum national d'Histoire naturelle, Paris, 251–257.
- Touzel G, Garner B (2018) “The Person Herself Is Not Interesting” Lucy Evelyn Cheesman’s life dedicated to the faunistic exploration of the Southwest Pacific. *Collections - A Journal for Museum and Archives Professionals* 14(4): 497–532. <https://doi.org/10.1177/155019061801400407>
- Wairiu M (2017) Land degradation and sustainable land management practices in Pacific Island Countries. *Regional Environmental Change* 17(4): 1053–1064. <https://doi.org/10.1007/s10113-016-1041-0>

Two new millipede species of the genus *Coxobolellus* Pimvichai, Enghoff, Panha & Backeljau, 2020 (Diplopoda, Spirobolida, Pseudospirobolellidae)

Piyatida Pimvichai¹, Henrik Enghoff², Thierry Backeljau^{3,4}

1 Department of Biology, Faculty of Science, Mahasarakham University, Maha Sarakham 44150, Thailand

2 Natural History Museum of Denmark, University of Copenhagen, Universitetsparken 15, DK-2100 Copenhagen Ø, Denmark

3 Royal Belgian Institute of Natural Sciences, Vautierstraat 29, B-1000 Brussels, Belgium

4 Evolutionary Ecology Group, University of Antwerp, Universiteitsplein 1, B-2610 Antwerp, Belgium

Corresponding author: Piyatida Pimvichai (piyatida.p@msu.ac.th)

Academic editor: Didier VandenSpiegel | Received 30 August 2022 | Accepted 4 October 2022 | Published 9 November 2022

<https://zoobank.org/63453838-8BCC-44BF-8C4C-46EF32B29283>

Citation: Pimvichai P, Enghoff H, Backeljau T (2022) Two new millipede species of the genus *Coxobolellus* Pimvichai, Enghoff, Panha & Backeljau, 2020 (Diplopoda, Spirobolida, Pseudospirobolellidae). ZooKeys 1128: 171–190. <https://doi.org/10.3897/zookeys.1128.94242>

Abstract

Two new millipede species of the genus *Coxobolellus* Pimvichai, Enghoff, Panha & Backeljau, 2020 from Thailand are described: *Coxobolellus saratani* sp. nov. from Loei Province and *Coxobolellus serratoligulatus* sp. nov. from Uttaradit Province. The descriptions are based on gonopod morphology and two mitochondrial gene fragments (COI and 16S rRNA). The phylogenetic mtDNA analysis assigned the two new species unequivocally to the consistently well-supported *Coxobolellus* clade, in which they form a fifth subclade that was well supported by maximum likelihood analysis of 16S rRNA, though neither by Bayesian inference nor by COI. The two new *Coxobolellus* species share four conspicuous gonopodal synapomorphies of the genus: (1) the protruding process on the coxae of the 3rd (and sometimes 4th) pair of male legs, (2) a large, triangular coxae on the 4th–5th pair of legs, (3) a short process of the preanal ring protruding as far as, or slightly beyond, the anal valves, and (4) the posterior gonopod telopodite divided into two parts, with a conspicuous pore opening at the mesal margin at the end of the coxal part of the posterior gonopod. Thus, the two new species provide further evidence of the well-defined monophyly of the genus *Coxobolellus*. Finally, the paper provides an updated morphological identification key to all currently described *Coxobolellus* species.

Keywords

DNA barcode, gonopod morphology, identification key, taxonomy, Thailand

Introduction

Until recently, the poorly known millipede family Pseudospirobolellidae Brölemann, 1913 included only four species in two genera, viz. *Pseudospirobolellus* Carl, 1912 and *Benoitolus* Mauriès, 1980 (Enghoff et al. 2015). Yet, the past few years fieldwork in Thailand has led to the discovery of 13 new pseudospirobolellid species and their assignment to two new genera, viz. *Coxobolellus* Pimvichai, Enghoff, Panha & Backeljau, 2020 (10 species) and *Siliquobolellus* Pimvichai, Enghoff, Panha & Backeljau, 2022 (3 species) (Pimvichai et al. 2020, 2022b). As such, the genus *Coxobolellus*, with its unique synapomorphic protruding process on the coxae of the 3rd (and sometimes 4th) pair of male legs, appears to be a particularly well supported and species-rich clade (Pimvichai et al. 2020). It was therefore expected that additional *Coxobolellus* species were bound to be discovered. The present study complies with this expectation as it combines morphological and mtDNA sequence data to describe two new species of the genus *Coxobolellus* from Thailand.

Material and methods

Live specimens were hand-collected. They were partly preserved in 70% ethanol for morphological study and partly placed in a freezer at -20°C for DNA analysis.

This research was conducted under the approval of the Animal Care and Use regulations (numbers U1-07304-2560 and IACUC-MSU-037/2019) of the Thai government.

Morphology

Gonopods were photographed with a digital microscope camera (Zeiss Stemi 305). Samples for scanning electron microscopy (SEM: Hitachi TM4000Plus) were air-dried directly from alcohol and sputter-coated for 60 s with gold (Hitachi: MC1000). Scanning electron micrographs were taken at the Central Lab of Mahasarakham University. Drawings were made using a stereomicroscope and photographs. Voucher specimens were deposited in the collections of the Museum of Zoology, Chulalongkorn University, Bangkok, Thailand (CUMZ).

DNA extraction, amplification and sequencing

Total genomic DNA was extracted from legs of specimens of *Coxobolellus saratani* sp. nov. (CUMZ-D00153 and CUMZ-D00153) from Loei Province and *Coxobolellus serratoligulatus* sp. nov. (CUMZ-D00154-1 and CUMZ-D00154) from Uttaradit Province, Thailand using the PureDireX column based genomic DNA extraction kit (tissue) (Bio-Helix) following the manufacturer's instructions. PCR amplifications and sequencing of the standard mitochondrial COI and 16S rRNA gene fragments were done as described by Pimvichai et al. (2020). The COI and 16S rRNA gene fragments

were amplified with the primers LCO-1490 and HCO-2198 (Folmer et al. 1994) for COI and 16Sar and 16Sbr (Kessing et al. 2004) for 16S rRNA. All new nucleotide sequences have been deposited in GenBank under accession numbers OP580097–OP580100 and OP580512–OP580515 for the partial COI and 16S rRNA fragment sequences respectively. Sample data and voucher codes are provided in Table 1.

Table 1. Specimens from which the COI and/or 16S rRNA gene fragments were sequenced. CUMZ, Museum of Zoology, Chulalongkorn University, Bangkok, Thailand; NHMD, Natural History Museum of Denmark; NHMW, Naturhistorisches Museum, Vienna, Austria; NHM, The Natural History Museum, London, United Kingdom. Names of countries are in capitals. Abbreviations after species names refer to the isolate of each sequence. GenBank accession numbers are indicated for each species. — means no sequences were obtained.

	Voucher code	Locality	COI	16S rRNA
Genus <i>Apeutbes</i>				
<i>A. maculatus</i> Amc	NHMW-Inv. No.2395	South Annam, VIETNAM	MF187404	MF187360
<i>A. maculatus</i> Am26	NHMD-621697	Nha Trang, Bao Dai Villas Hotel, in garden, VIETNAM	MZ567159	MZ568653
<i>A. fimbriatus</i> BMP	CUMZ-D00144	Bach Ma Peak, Da Nang, VIETNAM	MZ567160	MZ568654
<i>A. longeligulatus</i> TPP	CUMZ-D00140	Tham Phet Po Thong, Klong Hard, Sa Kaco, THAILAND	MZ567161	MZ568655
<i>A. pollex</i> SMR	CUMZ-D00141	Sra Morakot, Klongthom, Krabi, THAILAND	MZ567162	MZ568656
<i>A. pollex</i> SML	CUMZ-D00142	Koh 8, Similan islands, Phang-Nga, THAILAND	MZ567163	MZ568657
<i>A. pollex</i> WTS	CUMZ-D00143	Tham Sue Temple, Muang, Krabi, THAILAND	MZ567164	MZ568658
? <i>A. spininavis</i> ABB	CUMZ-D00145	Air Banun, Perak, MALAYSIA	MZ567165	MZ568659
Genus <i>Atopochetus</i>				
<i>A. anaticeps</i> SVL	CUMZ-D00091	Srivilai temple, Chalermprakiet, Saraburi, THAILAND	MF187405	—
<i>A. dollfusii</i> DOL	NHM	Cochinchina, VIETNAM	MF187412	MF187367
<i>A. helix</i> SPT	CUMZ-D00094	Suan Pa Thong Pha Phum, Kanchanaburi, THAILAND	MF187416	MF187371
<i>A. moulmeinensis</i> TAK	CUMZ-D00095	Km 87, Tha Song Yang, Tak, THAILAND	MF187417	MF187372
<i>A. setiferus</i> HPT	CUMZ-D00097	Hub Pa Tard, Lan-Sak, Uthaithani, THAILAND	MF187419	MF187374
<i>A. spinimargo</i> Ton27	NHMD-00047013	Koh Yo, Songkhla, THAILAND	MF187423	MF187377
<i>A. truncatus</i> SML	CUMZ-D00101	Koh 8, Similan islands, Phang-Nga, THAILAND	MF187424	MF187378
<i>A. uncinatus</i> KMR	CUMZ-D00102	Khao Mar Rong, Bangsapan, Prachuapkhirikhan, THAILAND	MF187425	MF187379
<i>A. weseneri</i> Tos29	NHMD-00047003	Supar Royal Beach Hotel, Khanom, Nakhonsrithammarat, THAILAND	MF187431	MF187384
Genus <i>Aulacobolus</i>				
<i>A. uncopogus</i> Auc	NHMW-Inv. No.2375	Nilgiris, South India, INDIA	MF187433	MF187386
Genus <i>Benoitulus</i>				
<i>B. birgatae</i> BBG	NHMD 621687	Chiang Dao, Chiang-Mai, THAILAND	MT328992	—
Genus <i>Coxobolellus</i>				
<i>C. albiceps</i> Stpw	CUMZ-D00121	Tham Pha Tub, Muang District, Nan Province, THAILAND (green individual)	MT328994	MT328211
<i>C. albiceps</i> Stpl	CUMZ-D00122	Tham Pha Tub, Muang District, Nan Province, THAILAND (small, brown individual)	MT328993	—
<i>C. albiceps</i> TPB	CUMZ-D00123	Wat Tham Bampen Bun, Pan District, Chiang-Rai Province, THAILAND	MT328996	MT328213
<i>C. albiceps</i> Stvd	CUMZ-D00124	Tham Wang Daeng, Noen Maprang District, Phitsanulok Province, THAILAND	MT328995	MT328212
<i>C. compactogonus</i> SKR	CUMZ-D00134	Sakaerat Environmental Research Station, Wang Nam Khiao District, Nakhon Ratchasima Province, THAILAND	MT328998	MT328215
<i>C. compactogonus</i> KLC	CUMZ-D00135	Khao Look Chang, Pak Chong District, Nakhon Ratchasima Province, THAILAND	MT328997	MT328214

	Voucher code	Locality	COI	16S rRNA
<i>C. fuscus</i> HKK	CUMZ-D00133	Kroeng Krawia waterfall, Sangkhla Buri District, Kanchanaburi Province, THAILAND	MT328999	MT328216
<i>C. nodosus</i> SPW	CUMZ-D00126	Chao Por Phawo Shrine, Mae Sot District, Tak Province, THAILAND	MT329000	MT328217
<i>C. serratus</i> KKL	CUMZ-D00132	Khao Kalok, Pran Buri District, Prachuap Khiri Khan Province, THAILAND	MT329001	MT328218
<i>C. simplex</i> TNP	CUMZ-D00136	Tham Pha Pha Ngam, Mae Prik District, Lampang Province, THAILAND	MT329002	—
<i>C. tenebris</i> KWP	CUMZ-D00119	Wat Khao Wong Phroh-m-majan, Ban Rai District, Uthai Thani Province, THAILAND	MT329003	MT328219
<i>C. tenebris</i> TPL	CUMZ-D00120	Wat Tham Phrom Lok Khao Yai, Sai Yok District, Kanchanaburi Province, THAILAND	MT329004	MT328220
<i>C. tigris</i> TKP	CUMZ-D00130	Wat Tham Khao Plu, Pathio District, Chumphon Province, THAILAND	MT329005	MT328221
<i>C. tigris</i> TYE	CUMZ-D00131	Tham Yai I, Pathio District, Chumphon Province, THAILAND	MT329006	MT328222
<i>C. transversalis</i> Stpg	CUMZ-D00125	Tham Pha Tub, Muang District, Nan Province, THAILAND	MT329007	MT328223
<i>C. valvatus</i> TCD	CUMZ-D00127	Wat Tham Chiang Dao, Chiang Dao District, Chiang-Mai Province, THAILAND	MT329009	—
<i>C. valvatus</i> BRC	CUMZ-D00128	Tham Borichinda, Chom Thong District, Chiang-Mai Province, THAILAND	MT329008	MT328224
<i>C. valvatus</i> TST	CUMZ-D00129	Tham Sam Ta, Muang District, Mae Hong Son Province, THAILAND	MT329010	MT328225
<i>C. saratani</i> sp. nov. PPLL2	CUMZ-D00153	Phu Pha Lom, Muang District, Loei Province, THAILAND	OP580097	OP580512
<i>C. saratani</i> sp. nov. PPLL	CUMZ-D00153-1	Phu Pha Lom, Muang District, Loei Province, THAILAND	OP580098	OP580513
<i>C. serratoligulatus</i> sp. nov. TCU	CUMZ-D00154	Tham Chan, Thong Saen Khan District, Uttaradit Province, THAILAND	OP580099	OP580514
<i>C. serratoligulatus</i> sp. nov. TCU2	CUMZ-D00154-1	Tham Chan, Thong Saen Khan District, Uttaradit Province, THAILAND	OP580100	OP580515
Genus <i>Leptogoniulus</i>				
<i>L. sorornus</i> BTN	CUMZ- D00109	Botanical Garden, Penang, MALAYSIA	MF187434	MF187387
Genus <i>Litostrophus</i>				
<i>L. chamaeleon</i> PPT	CUMZ- D00111	Phu Pha terb, Mukdahan, THAILAND	MF187436	MF187389
<i>L. sarabuwensis</i> PKS	CUMZ- D00113	Phukhae Botanical Garden, Saraburi, THAILAND	MF187438	MF187391
<i>L. segregatus</i> Ls19	NHMD 621686	Koh Kut, Trad, THAILAND	MF187440	MF187394
Genus <i>Macrurobolus</i>				
<i>M. macrurus</i> INT	CUMZ- D00147	Wat Tham Inthanin, Mae Sot District, Tak Province, THAILAND	MZ905519	—
Genus <i>Madabolus</i>				
<i>M. maximus</i> Mm4	NHMD-00047007	de Toliara Province, Parc National de Bernaraha, South Bank of Manambolo River, Near Tombeau Vazimba, MADAGASCAR	MF187441	MF187395
Genus <i>Narceus</i>				
<i>N. annularis</i>			NC_003343.1	—
Genus <i>Parabolus</i>				
<i>P. dimorphus</i> Pd34	NHMD-00047004	Dar es Salaam, TANZANIA	MF187442	MF187396
Genus <i>Paraspirobolus</i>				
<i>P. lucifugus</i>			AB608779.1	—
Genus <i>Pelmatojulus</i>				
<i>P. tigrinus</i> Pt2	NHMD-00047008	Southern part of the Comoé N.P., 30 km north of Kakpin, CÔTE D'IVOIRE	MF187443	MF187397
<i>P. togoensis</i> Pto6	NHMD-00047006	Biakpa, GHANA	MF187444	MF187398
Genus <i>Pseudospirobolellus</i>				
<i>Pseudospirobolellus avernis</i> GPG	CUMZ-D00117	Gua Pulai, Gua Musang, Kelantan, MALAYSIA	MT329011	MT328226
<i>Pseudospirobolellus</i> sp. KCS	CUMZ-D00118	Koh Chuang, Sattahip, Chonburi, THAILAND	MT329012	MT328227

	Voucher code	Locality	COI	16S rRNA
Genus <i>Rhinocricus</i>				
<i>R. parvus</i> Rp49	NHMD-00047009	Puerto Rico, USA	MF187449	MF187403
Genus <i>Siliquobolellus</i>				
<i>S. amicusdraconis</i>	CUMZ- D00149	Hub Pa Tard, Lan-Sak, Uthaithani, THAILAND	OP174621	—
<i>S. constrictus</i>	CUMZ- D00150	Ban Yang Chum, Kui Buri, Prachuap Khiri Khan, THAILAND	OP174622	—
<i>S. prasankokae</i>	CUMZ- D00148	Pha Thai, Ngao, Lampang, THAILAND	OP174623	—
Genus <i>Trachelomegalus</i>				
<i>T. sp.</i> Tr54	NHMD-00047012	Borneo Sabah, MALAYSIA	MF187445	—
Genus <i>Trigoniulus</i>				
<i>T. corallinus</i> Tco15	NHMD-00047010	Vientiane, LAOS	MF187446	MF187400
Outgroup				
Genus <i>Anurostreptus</i>				
<i>A. barthelemyae</i> Tlb	CUMZ-D00003	Thale-Ban N.P., Khuan-Don, Satun, THAILAND	KC519469	KC519543
Genus <i>Chonecambala</i>				
<i>C. crassicauda</i> Ttp	CUMZ-D00001	Ton-Tong waterfall, Pua, Nan, THAILAND	KC519467	KC519541
Genus <i>Thyropygus</i>				
<i>T. allevatus</i> Bb	CUMZ-D00013	BangBan, Ayutthaya, THAILAND	KC519479	KC519552

Alignment and phylogenetic analysis

The 16S rRNA data included 51 specimens, representing 12 genera and 37 nominal species of ingroup taxa (Table 1). Three species of the order Spirostreptida, viz. *Anurostreptus barthelemyae* Demange, 1961 (Harpagophoridae), *Chonecambala crassicauda* Mauriès & Enghoff, 1990 (Pericambalidae) and *Thyropygus allevatus* (Karsch, 1881) (Harpagophoridae) were used as the outgroup. The same ingroup and outgroup taxa were used for COI, with the addition of: (1) *Coxobolellus simplex* Pimvichai, Enghoff, Panha & Backeljau, 2020, (2) *C. albiceps* (Stpl) Pimvichai, Enghoff, Panha & Backeljau, 2020, (3) *C. valvatus* (TCD) Pimvichai, Enghoff, Panha & Backeljau, 2020, (4) *Siliquobolellus amicusdraconis* Pimvichai, Enghoff, Panha & Backeljau, 2022, (5) *S. constrictus* Pimvichai, Enghoff, Panha & Backeljau, 2022, (6) *S. prasankokae* Pimvichai, Enghoff, Panha & Backeljau, 2022, (7) *Paraspirobolus lucifugus* (Gervais, 1836), (8) *Narceus annularis* Rafinesque, 1820, (9) *Trachelomegalus* sp., (10) *Macrurobolus macrurus* (Pocock, 1893), (11) *Atopochetus anaticeps* Pimvichai, Enghoff, Panha & Backeljau, 2018, and (12) *Benoitolus birgitae* (Hoffman, 1981). Hence, the COI data set included 63 specimens, representing 18 genera and 47 nominal species of ingroup taxa (Table 1).

CodonCode Aligner (ver. 4.0.4, CodonCode Corporation) was used to assemble the forward and reverse sequences and to check for errors and ambiguities. All sequences were checked with the Basic Local Alignment Search Tool (BLAST) provided by NCBI and compared with reference sequences in GenBank. They were aligned using MUSCLE (ver. 3.6, see <http://www.drive5.com/muscle>; Edgar 2004). The COI alignment consisted of 660 bp and that of 16S rRNA consisted of 458 bp (gaps were excluded by complete-deletion). The sequences were checked for ambiguous nucleotide sites, saturation and phylogenetic signal using DAMBE (ver. 5.2.65; see <http://www.dambe.bio.uottawa.ca/DAMBE/dambe.aspx>; Xia 2018). MEGA (ver. X, see <http://www.megasoftware.net>; Kumar et al. 2018) was used to (1) check for stop codons, (2)

translate COI protein-coding sequences into amino acids, and (3) calculate uncorrected pairwise p-distances among sequences.

Phylogenetic trees were constructed using maximum likelihood (ML) and Bayesian inference (BI) applied to either the COI and 16S rRNA data separately or combined. The shape parameter of the gamma distribution, based on 16 rate categories, was estimated using maximum likelihood analysis. ML trees were inferred with RAxML (ver. 8.2.12, see http://www.phylo.org/index.php/tools/raxmlhpc2_tgb.html; Stamatakis 2014) through the CIPRES Science Gateway (Miller et al. 2010) using a GTR+G substitution model and 1000 bootstrap replicates to assess branch support. BI trees were constructed with MrBayes (ver. 3.2.7a, see http://www.phylo.org/index.php/tools/mrbayes_xsede.html; Huelsenbeck and Ronquist 2001). Substitution models were inferred using jModeltest (ver. 2.1.10, see <https://www.github.com/ddarriba/jmodeltest2/releases>; Darriba et al. 2012) applying Akaike Information Criterion weights as selection criterion. This yielded as best models GTR+I+G ($-\ln L = 17117.3442$, gamma shape = 0.6820) for the combined dataset, TrN+ I+G ($-\ln L = 12352.6533$, gamma shape = 0.4820) for COI, and TIM3+ I+G ($-\ln L = 6495.3310$, gamma shape = 0.8870) for 16S rRNA.

BI trees were run for 2 million generations for the combined dataset, 3 million generations for the separate 16S rRNA, and 4 million generations for the separate COI datasets (heating parameter: 0.01 for the combined dataset and 16S rRNA, and 0.02 for COI), sampling every 1000 generations. Convergences were confirmed by verifying that the standard deviations of split frequencies were below 0.01. Then the first 1000 trees were discarded as burn-in, so that the final consensus tree was built from the last 3002 trees for the combined dataset, 4502 trees for the 16S rRNA, and 6002 trees for the COI datasets. Branch support was assessed by posterior probabilities.

For ML trees we consider branches with bootstrap values (BV) of $\geq 70\%$ to be well supported (Hillis and Bull 1993) and $< 70\%$ as poorly supported. For BI trees, we consider branches with posterior probabilities (PP) of ≥ 0.95 to be well supported (San Mauro and Agorreta 2010) and below as poorly supported.

Results

Phylogeny

The uncorrected p-distance between the COI sequences (660 bp) ranged from 0.00 to 0.26 (Suppl. material 1). The mean interspecific sequence divergence within *Coxobolellus* was 0.12 (range: 0.06–0.15). The mean intergeneric sequence divergence between *Coxobolellus* and *Pseudospirobolellus* was 0.21 (range: 0.20–0.23), between *Coxobolellus* and *Siliquobolellus* it was 0.17 (range: 0.14–0.20), and between *Coxobolellus* and *Benoitulus birgita* it was 0.21 (range: 0.20–0.23).

The uncorrected p-distance between the 16S rRNA (458 bp) sequences ranged from 0.00 to 0.30 (Suppl. material 2). The mean interspecific sequence divergence within *Coxobolellus* was 0.11 (range: 0.05–0.15). The mean intergeneric sequence di-

vergence between *Coxobolellus* and *Pseudospirobolellus* was 0.21 (range: 0.18–0.24). Currently, there are no 16S rRNA sequences for *Siliquobolellus* and *Benoitolus*.

The uncorrected p-distance between the combined COI + 16S rRNA (1118 bp) sequences ranged from 0.00 to 0.27 (Suppl. material 3). The mean interspecific sequence divergence within *Coxobolellus* was 0.11 (range: 0.05–0.14). The mean intergeneric sequence divergence between *Coxobolellus* and *Pseudospirobolellus* was 0.21 (range: 0.19–0.23).

The ML and BI trees based on the separate and combined datasets (COI, 16S rRNA and COI + 16S rRNA) were largely congruent with respect to the well-supported branches (by visual inspection of the branching pattern). The combined COI + 16S rRNA tree is used for further discussion (Fig. 1). The separate COI and 16S rRNA trees are presented in Suppl. materials 4, 5, respectively.

The genus *Coxobolellus* (Clade 1) is consistently well supported in the three trees and can be subdivided into five generally well supported subclades (1A–E; cf. Pimvichai et al. 2020), one of which is formed by the two new species (subclade 1E). Yet, this latter subclade is only well supported by ML of the 16S rRNA (and combined) data, but not by BI and the COI data. Moreover, the position of two other species, viz. *C. fuscus* (COI and 16S rRNA) and *C. simplex* (COI only), remains ambiguous, even if both species seem to be somehow associated with subclades 1C and 1D.

Subclade 1A comprises *C. nodosus* and *C. valvatus*, two species that are distributed in western and northern Thailand, respectively. They differ in their posterior gonopod telopodite: in *C. nodosus* the telopodital part (pt) is as long as the coxal part (pcx), while in *C. valvatus* the telopodital part (pt) is much shorter than the coxal part (pcx). Their COI sequence divergence is 0.06–0.07.

Subclade 1B comprises the sympatric species *C. albiceps* and *C. transversalis*. They mainly differ in the following two aspects: (1) in *C. albiceps* the tip of the anterior gonopod coxa is apically obliquely truncated, while in *C. transversalis* it is transversely truncated; (2) the telopodital part (pt) of the posterior gonopod telopodite is fairly long in *C. transversalis*, while in *C. albiceps* it is short. Their COI sequence divergence is 0.08.

Subclade 1C comprises *C. compactogonus* and *C. tenebris*, two species that are distributed in northeastern and central to western Thailand, respectively. They mainly differ in the following two aspects: (1) the anterior gonopod telopodite (at) ends in a rounded lobe in *C. compactogonus*, while in *C. tenebris* there is a tiny triangular laterad denticle near the tip of the anterior gonopod telopodite (at); (2) the telopodital part (pt) of the posterior gonopod telopodite is with three processes in *C. compactogonus*, while in *C. tenebris* this part ends in a rounded, smooth lobe. Their COI sequence divergence is 0.10 (range: 0.09–0.10).

Subclade 1D comprises *C. serratus* and *C. tigris*, two species that are distributed in southern Thailand. They mainly differ in the following two aspects: (1) in *C. serratus* the posterior gonopod telopodite with a long coxal part (pcx), while this part is short in *C. tigris*; and (2) the telopodital part (pt) laterally is with a serrate margin in *C. serratus*, while in *C. tigris* only the apical part with a serrate margin. Their COI sequence divergence is 0.12.

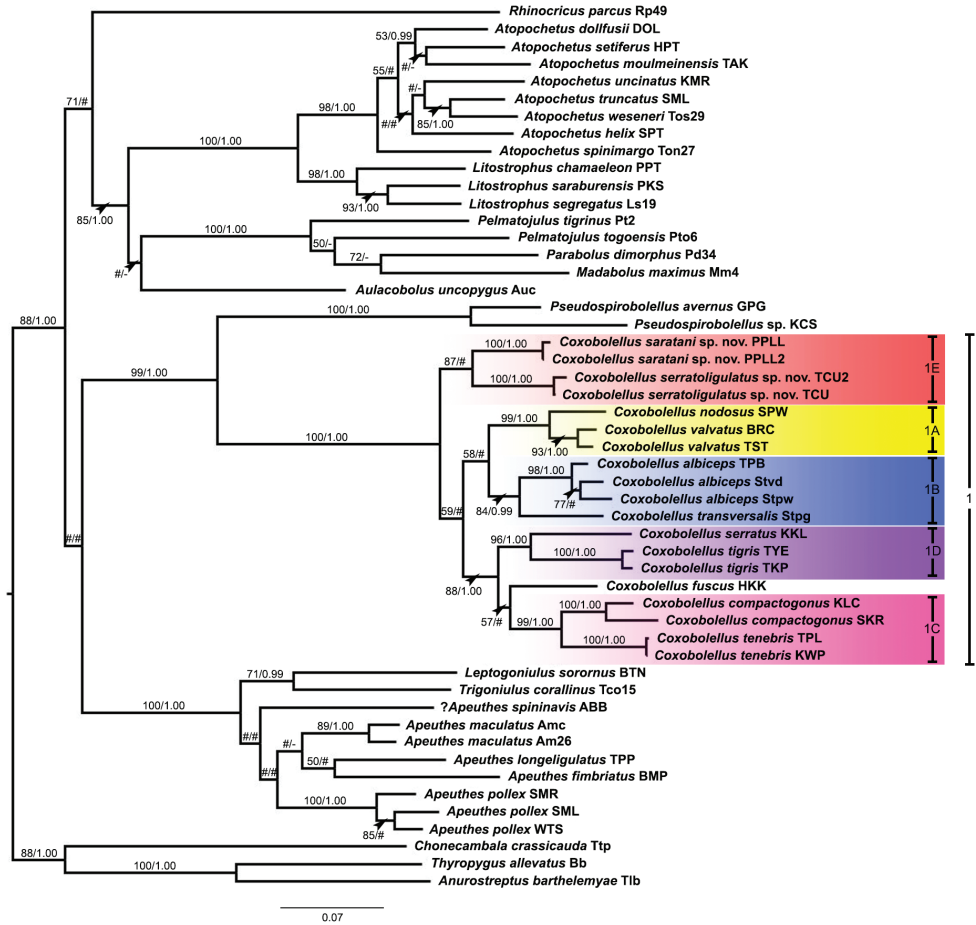


Figure 1. Phylogenetic relationships of *Coxobolellus* species based on maximum likelihood analysis (ML) and Bayesian inference (BI) of 1118 bp in the combined COI + 16S rRNA alignment. Numbers at nodes indicate branch support based on bootstrapping (ML) / posterior probabilities (BI). Scale bar = 0.07 substitutions/site. # indicates branches with <50% ML bootstrap support and <0.95 Bayesian posterior probability. - indicates non-supported branches. The colored areas mark the subclades of *Coxobolellus* and are labelled as in Pimvichai et al. (2020).

Subclade 1E (only supported by ML of 16S rRNA) comprises the two new species: *C. saratani* sp. nov. and *C. serratoligulatus* sp. nov., which are distributed in northeastern and northern Thailand, respectively. They differ in both the anterior gonopod and the posterior gonopod telopodite, and will be treated in detail further below. Their COI sequence divergence is 0.08 (range: 0.07–0.08).

The combined COI + 16S rRNA (Fig. 1) and the separate 16S rRNA (Suppl. material 5) trees showed *Pseudospirobolellus* as a well-supported sister group of *Coxobolellus*. However, this sister group relation was no longer supported when the genus *Siliquobolellus* was included, i.e. in the separate COI tree (Suppl. material 4).

Taxonomy

Class Diplopoda de Blainville in Gervais, 1844

Order Spirobolida Bollman, 1893

Suborder Spirobolidea Bollman, 1893

Family Pseudospirobolellidae Brölemann, 1913

Genus *Coxobolellus* Pimvichai, Enghoff, Panha & Backeljau, 2020

Diagnosis. Differing from the other genera of Pseudospirobolellidae by having (1) the coxae of the 3rd pair of male legs with extremely large, protruding processes (in *C. albiceps* and *C. transversalis*, this condition also applies to the 4th pair of male legs), (2) the 4th and 5th leg-pairs with large, triangular coxae, (3) short process of preanal ring protruding as far as, or slightly beyond, anal valves, and (4) the posterior gonopod telopodite divided into a coxal part (pcx) and a telopodital part (pt); with opening of efferent groove (oeg) at mesal margin at the end of coxal part (pcx).

Species description. The two new species share all of the diagnostic characters of the genus *Coxobolellus*, as described in the general description section in Pimvichai et al. (2020: 599–601).

***Coxobolellus saratani* sp. nov.**

<https://zoobank.org/C8EB9916-1AFE-465E-A630-12970577E4E5>

Figs 2, 4, 5

Material studied. *Holotype* ♂ (CUMZ-D00153-1), THAILAND, Loei Province, Muang District, Phu Pha Lom; 17°32'30"N, 101°51'38"E; 370 m a.s.l.; 25 September 2021; P. Pimvichai, P. Prasankok and S. Saratan leg. *Paratypes*. 7 ♂♂, 9 ♀♀; same data as holotype (CUMZ-D00153-2).

Etymology. The species is named after Mr Sathit Saratan, who always supports the authors during fieldwork and who is a devoted millipede collector.

Diagnosis. Differing from all other species in the genus by having the tip of the telopodital part (pt) forming a flattened, pointed lobe, directed distad (Fig. 2C, F–H), whereas in the other 11 *Coxobolellus* species the tip of the telopodital part of the posterior gonopod curves mesad or forms a rounded lobe.

Description. Adult males with 51–55 podous rings. Length ca 6–7 cm, diameter ca 4.9–5.2 mm. Adult females with 52 or 53 podous rings. Length ca 6–8 cm, diameter ca 5.6–6.1 mm.

Colour. Living animal greenish grey except for dark brown antennae and legs (Fig. 4A).

Anterior gonopods (Fig. 2A, B, D, E) with high coxae, apically obliquely truncated, mesal margins straight, diverging, delimiting a V-shaped space between both coxae, posterior surface with relatively high ridge laterally for accommodation of telopodite. Telopodite (at) projecting slightly over anterior gonopod coxa (cx), subapically

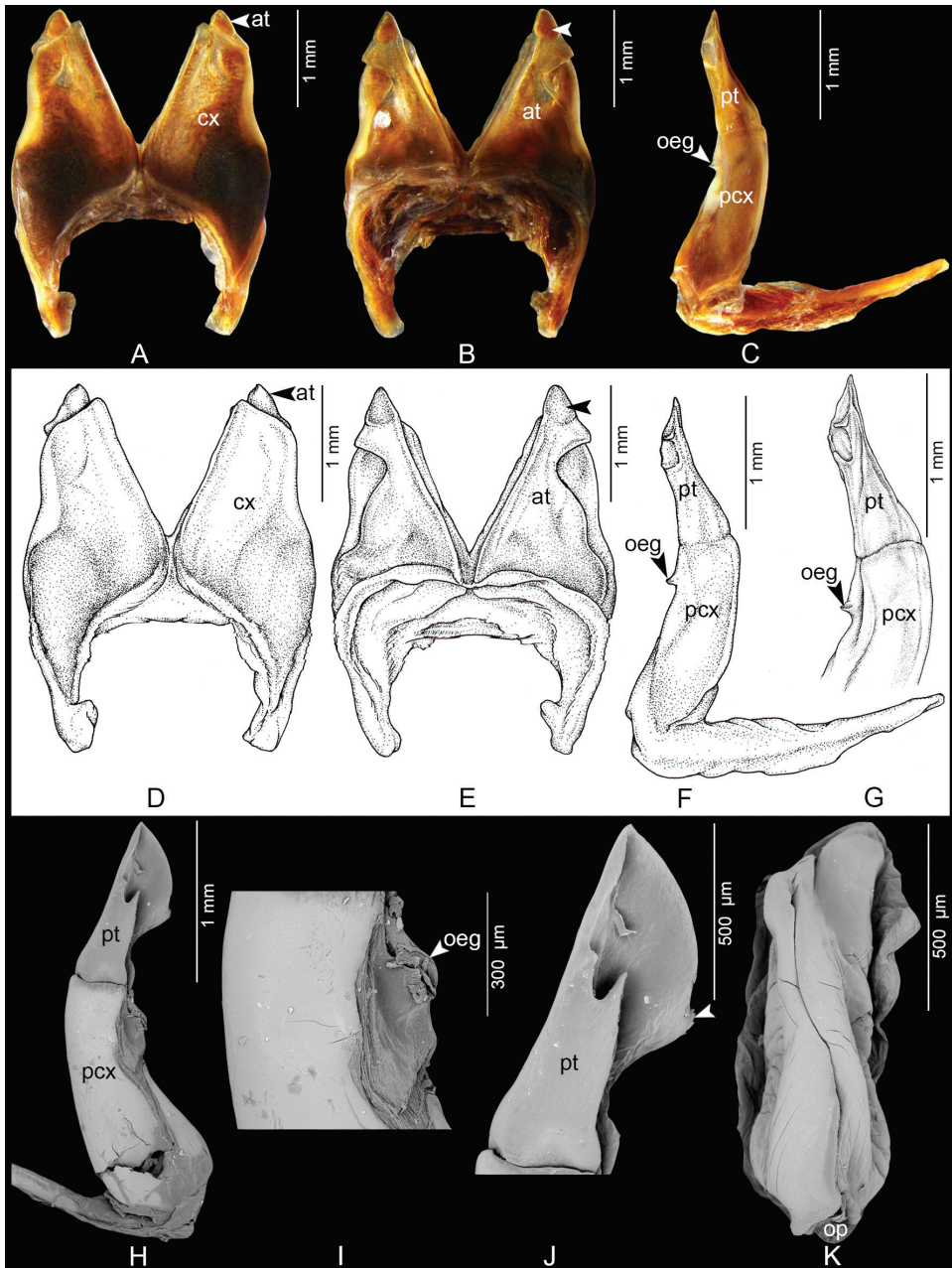


Figure 2. *Coxobolellus saratani* sp. nov., holotype, gonopods (CUMZ-D00153-1) **A, D** anterior gonopod, anterior view **B, E** anterior gonopod, posterior view, unlabeled arrows indicate a pigmented brown node **C, F, G** left posterior gonopod **H** SEM, right posterior gonopod, posterior-mesal view **I** SEM, mesal part of posterior gonopod, posterior-mesal view **J** SEM, tip of posterior gonopod, posterior-lateral view **K** SEM, left female vulva, posterior-mesal view. at = anterior gonopod telopodite; cx = coxa; oeg = opening of efferent groove; op = operculum of vulva; pcx = coxal part of the posterior gonopod telopodite; pt = telopodital part of the posterior gonopod telopodite.

strongly constricted, apically forming a triangular process with pointed tip and a pigmented brown node (Fig. 2B, E, unlabeled arrow).

Posterior gonopods (Fig. 2C, F–J) simple, rounded, with long, smooth coxal part (pcx); telopodital part (pt) fairly long, apically pointed, directed distad, with a sharp, pointed, folded process in the middle (Fig. 2C, F–H), with a small transverse ridge near tip protruding from mesal surface, with serrate mesal margin (Fig. 2J, unlabeled arrow).

Female vulvae (Fig. 2K): valves prominent, of equal size.

DNA barcodes. The GenBank accession numbers are:

Holotype CUMZ-D00153-1: COI = OP580098; 16S rRNA = OP580513.

Paratype CUMZ-D00153: COI = OP580097; 16S rRNA = OP580512.

Habitat. Found under leaf litter and crawling around (on the rock and stairs).

Distribution. Known only from the type locality in Loei Province, Thailand (Fig. 5).

Coxobolellus serratoligulatus sp. nov.

<https://zoobank.org/BDE726D9-4EC8-44F8-93D2-AE742C88A793>

Figs 3–5

Material studied. **Holotype** ♂ (CUMZ-D00154-1), THAILAND, Uttaradit Province, Thong Saen Khan District, Tham Chan; 17°35'4"N, 100°25'10"E; 230 m a.s.l.; 31 July 2020; P. Pimvichai, P. Prasankok and S. Saratan leg. **Paratypes.** 2 ♀♀; same data as holotype (CUMZ-D00154-2).

Etymology. The species epithet is a Latin adjective meaning “with a serrated tongue” and refers to the characteristic process of the posterior gonopod.

Diagnosis. Anterior gonopods with high coxae, apically obliquely truncated (Fig. 3A, D). Similar in this respect to *C. albiceps*. Differing from all other species in the genus by having the posterior gonopod with a massive, broad, flattened, serrate process protruding from the mesal surface, forming a tongue-like process (Fig. 3C, F–H), whereas in the other 11 *Coxobolellus* species the telopodital part of the posterior gonopod has no distinct tongue-like process.

Description. Adult male with 54 podous rings. Length ca 5 cm, diameter ca 4.0 mm. Adult females with 51–53 podous rings. Length ca 5 cm, diameter ca 3.9–4.1 mm.

Colour. Living animal dark green except for dark brown antennae and legs (Fig. 4B).

Anterior gonopods (Fig. 3A, B, D, E) with high coxae, apically obliquely truncated, mesal margins straight, posterior surface with relatively high ridge laterally for accommodation of telopodite. Telopodite (at) projecting over anterior gonopod coxa (cx), subapically strongly constricted, apically forming a big triangular process with pointed tip and a pigmented brown node (Fig. 3B, E, unlabeled arrow).

Posterior gonopods (Fig. 3C, F–H) very simple, rounded, with long, smooth coxal part (pcx); telopodital part (pt) fairly long, curving mesad, ending in a rounded lobe, forming a canopy, with a large, broad, flattened, serrate process protruding from mesal surface, forming a tongue-like process (Fig. 3H, unlabeled arrow).

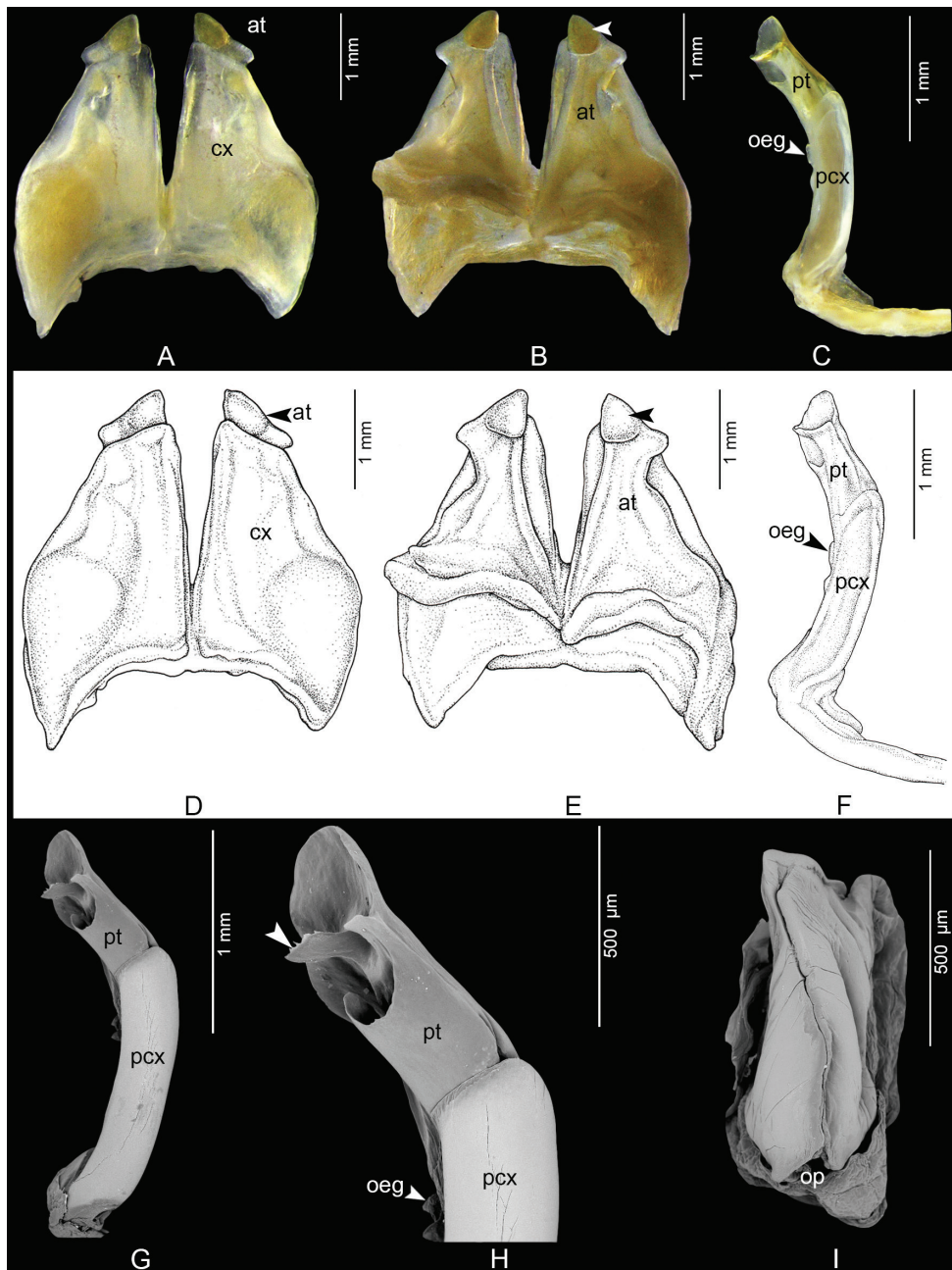


Figure 3. *Coxobolellus serratoligulatus* sp. nov., holotype, gonopods (CUMZ-D00154-1) **A, D** anterior gonopod, anterior view **B, E** anterior gonopod, posterior view, unlabeled arrows indicate a pigmented brown node **C, F** left posterior gonopod **G** SEM, left posterior gonopod, posterior-mesal view **H** SEM, tip of posterior gonopod, posterior-lateral view, unlabeled arrow indicates the tongue-like process **I** SEM, left female vulva, posterior-mesal view. at = anterior gonopod telopodite; cx = coxa; oeg = opening of efferent groove; op = operculum of vulva; pcx = coxal part of the posterior gonopod telopodite; pt = telopodital part of the posterior gonopod telopodite.



Figure 4. Live *Coxobolellus* species from Thailand **A** *C. saratani* sp. nov., male (paratype, CUMZ-D00153-2) **B** *C. serratoligulatus* sp. nov., male (holotype, CUMZ-D00154-1).

Female vulvae (Fig. 3I): valves prominent, of equal size.

DNA barcodes. The GenBank accession numbers are:

Holotype CUMZ-D00154-1: COI = OP580100; 16S rRNA = OP580515.

Paratype CUMZ-D00154: COI = OP580099, 16S rRNA = OP580514.

Habitat. Found under leaf litter.

Distribution. Known only from the type locality in Uttaradit Province, Thailand (Fig. 5).

Key to species of the genus *Coxobolellus* (based on adult males, update of the key of Pimvichai et al. 2020)

- 1 Tip of anterior gonopod coxa truncated.....2
- Tip of anterior gonopod coxa concave/bilobed or forming a triangular process....5
- 2 Tip of anterior gonopod coxa transversely truncated; telopodital part (pt) of posterior gonopod long compared to coxal part (pcx).....
..... *C. transversalis* Pimvichai, Enghoff, Panha & Backeljau, 2020
- Tip of anterior gonopod coxa obliquely truncated.....3
- 3 Telopodital part (pt) of posterior gonopod short compared to coxal part (pcx)....
..... *C. albiceps* Pimvichai, Enghoff, Panha & Backeljau, 2020
- Telopodital part (pt) of posterior gonopod fairly long compared to coxal part (pcx)4
- 4 Telopodital part (pt) directed distad, pointed (Fig. 2C), with a sharp, pointed, folded process in the middle, with a small transverse ridge near tip, with serrate mesal margin (Fig. 2J, unlabeled arrow) *C. saratani* sp. nov.
- Telopodital part (pt) curving mesad, ending in a rounded lobe, forming a canopy, with a broad, flattened, serrate, tongue-like process protruding from mesal surface, (Fig. 3H, unlabeled arrow) *C. serratoligulatus* sp. nov.
- 5 Tip of anterior gonopod coxa concave/bilobed.....6
- Tip of anterior gonopod coxa forming triangular process7

- 6 Tip of anterior gonopod coxa bilobed, outer process broadly rounded, inner process triangular, protruding higher than outer process; telopodital part (pt) of posterior gonopod ending in a rounded margin with a sharp spine protruding from mesal surface near tip..... ***C. valvatus* Pimvichai, Enghoff, Panha & Backeljau, 2020**
- Tip of anterior gonopod coxa concave, forming equal outer and inner lobes; telopodital part of posterior gonopod (pt) ending in a long, sharp spine, with a flattened lamella protruding from mesal surface near tip ***C. nodosus* Pimvichai, Enghoff, Panha & Backeljau, 2020**
- 7 Tip of anterior gonopod coxa ending in an abruptly narrowed, pointed, triangular process **8**
- Tip of anterior gonopod coxa ending in a simple triangular process **10**
- 8 Tip of anterior gonopod telopodite (at) long, narrow, curving mesad; tip of telopodital part (pt) of posterior gonopod ending in coarsely serrate lamella with a sharp point..... ***C. fuscus* Pimvichai, Enghoff, Panha & Backeljau, 2020**
- Tip of anterior gonopod telopodite (at) forming a triangular process **9**
- 9 Telopodital part (pt) of posterior gonopod with a sharp, curling lamella at base....
..... ***C. tenebris* Pimvichai, Enghoff, Panha & Backeljau, 2020**
- Telopodital part (pt) of posterior gonopod without a sharp, curling lamella at base..... ***C. simplex* Pimvichai, Enghoff, Panha & Backeljau, 2020**
- 10 Anterior gonopod telopodite (at) projecting slightly over anterior gonopod coxa (cx), with rounded tip
..... ***C. compactogonus* Pimvichai, Enghoff, Panha & Backeljau, 2020**
- Anterior gonopod telopodite (at) far overreaching anterior gonopod coxa (cx), with narrowed tip **11**
- 11 Anterior gonopod telopodite (at) directed distad; telopodital part (pt) of posterior gonopod ending in a rounded, serrate margin
..... ***C. tigris* Pimvichai, Enghoff, Panha & Backeljau, 2020**
- Anterior gonopod telopodite (at) curving laterad; telopodital part (pt) of posterior gonopod laterally with serrate margin.....
..... ***C. serratus* Pimvichai, Enghoff, Panha & Backeljau, 2020**

Discussion

The two new species described here obviously belong to the genus *Coxobolellus* because they share the unique synapomorphic characters of this genus viz., (1) the coxae of the 3rd male leg-pair with extremely large, protruding processes, (2) the 4th and 5th leg-pairs with large, triangular coxae, (3) preanal ring with a short process protruding as far as, or slightly beyond, anal valves, and (4) posterior gonopod telopodite divided into a coxal part (pcx) and a telopodital part (pt); with opening of efferent groove (oeg) at mesal margin at the end of coxal part (pcx) (Pimvichai et al. 2020). In line with this, the mtDNA trees provided maximum support for the placement of the two new species in the monophyletic genus *Coxobolellus*.



Figure 5. Distribution of the species of *Coxobolellus* in Thailand. Droplets vary in size to improve readability.

The mtDNA data further confirmed the trends observed in earlier studies dealing with levels of COI sequence divergence among millipede species and genera, i.e. high interspecific COI sequence divergences among congeneric species (overall range: 0.05–0.18) (Pimvichai et al. 2014, 2018, 2022a, b; Reip and Wesener 2018), but still clearly higher COI sequence divergences between genera (overall range: 0.16–0.23) (e.g. Pimvichai et al. 2022a, b). Yet, it would be premature to

draw taxonomic conclusions from these trends in terms of potential DNA barcode threshold levels.

Similarly, the subdivision of *Coxobolellus* into five subclades should not be interpreted as a prelude to some sort of taxonomic subdivision. Instead, it is an attempt to look for phylogenetic patterns that can help to decide about new species. In the present case, for example, the fact that the two new species tend to form a separate subclade is indeed an additional argument that supports their recognition as new species, even if this subclade is only supported by ML of 16S rRNA.

The inclusion of the two new *Coxobolellus* species in the phylogenetic analysis did not resolve the ambiguous sister group relationships of *Coxobolellus*, *Pseudospirobolellus* and *Siliquobolellus* (Pimvichai et al. 2022b) and neither provided new evidence about the enigmatic position of *Benoitolus*. Obviously, the phylogenetic relationships of the Pseudospirobolellidae need further research.

The present results further reinforce the expectation that new pseudospirobolellid, and in particular *Coxobolellus*, species remain to be discovered in Southeast Asia (cf. Pimvichai et al. 2022b). Although the systematic study of Pseudospirobolellidae started only recently, it has already convincingly shown that this group is far more diverse than hitherto was assumed. The present paper is another testimony of this.

Acknowledgements

This research was funded by the Thailand Science Research and Innovation (TSRI) together with Mahasarakham University as a TRF Research Career Development Grant (2019–2022; RSA6280051) (to P. Pimvichai). Additional funding was provided by the Royal Belgian Institute of Natural Sciences (RBINS). We thank, Sathit Saratan (Sirindhorn Museum) and Pongpun Prasankok (Suranaree University of Technology) for assistance in collecting material. We are indebted to Thita Krutchuen (College of Fine Arts, Bunditpatanasilpa Institute) for the excellent drawings. We are grateful to Sergei Golovatch (Russian Academy of Sciences, Moscow) and Nesrine Akkari (Naturhistorisches Museum Wien) for their critical comments which helped to improve the manuscript.

References

- Darriba D, Taboada GL, Doallo R, Posada D (2012) jModelTest 2: More models, new heuristics and parallel computing. *Nature Methods* 9(8): 772–772. <https://doi.org/10.1038/nmeth.2109>
- Edgar RC (2004) MUSCLE: Multiple sequence alignment with high accuracy and high throughput. *Nucleic Acids Research* 32(5): 1792–1797. <https://doi.org/10.1093/nar/gkh340>
- Enghoff H, Golovatch S, Short M, Stoev P, Wesener T (2015) Diplopoda – Taxonomic overview. In: A. Minelli (Ed.) *The Myriapoda 2. Treatise on Zoology – Anatomy, Taxonomy, Biology*, 363–453. [Brill: Leiden.] https://doi.org/10.1163/9789004188273_017

- Folmer O, Black M, Hoeh W, Lutz R, Vrijenhoek R (1994) DNA primers for amplification of mitochondrial cytochrome c oxidase subunit I from diverse metazoan invertebrates. *Molecular Marine Biology and Biotechnology* 3: 294–299.
- Hillis D, Bull J (1993) An empirical test of bootstrapping as a method for assessing confidence in phylogenetic analysis. *Systematic Biology* 42(2): 182–192. <https://doi.org/10.1093/sysbio/42.2.182>
- Huelsenbeck JP, Ronquist F (2001) MRBAYES: Bayesian inference of phylogeny. *Bioinformatics* 17(8): 754–755. <https://doi.org/10.1093/bioinformatics/17.8.754>
- Kessing B, Croom H, Martin A, McIntosh C, McMillan WO, Palumbi S (2004) PCR primers. In: *The Simple Fool's Guide to PCR*. University of Hawaii, Department of Zoology: Honolulu, HI, USA. Version 1.0, 17–18.
- Kumar S, Stecher G, Li M, Knyaz C, Tamura K (2018) MEGA X: Molecular evolutionary genetics analysis across computing platforms. *Molecular Biology and Evolution* 35(6): 1547–1549. <https://doi.org/10.1093/molbev/msy096>
- Mauriès J-P (1980) Contributions à l'étude de la faune terrestre des îles granitiques de l'archipel des Séchelles (Mission P.L.G. Benoit – J.J. Van Mol 1972). *Myriapoda – Diplopoda. Revue de Zoologie Africaine* 94: 138–168.
- Miller MA, Pfeiffer W, Schwartz T (2010) Creating the CIPRES Science Gateway for inference of large phylogenetic trees. In: *Proceedings of the Gateway Computing Environments Workshop (GCE)*, 14 November 2010, New Orleans, LA, USA. INSPEC Accession Number: 11705685, 1–8. [IEEE] <https://doi.org/10.1109/GCE.2010.5676129>
- Pimvichai P, Enghoff H, Panha S (2014) Molecular phylogeny of the *Thyropygus allevatus* group of giant millipedes and some closely related groups. *Molecular Phylogenetics and Evolution* 71: 170–183. <https://doi.org/10.1016/j.ympev.2013.11.006>
- Pimvichai P, Enghoff H, Panha S, Bäckeljau T (2018) Morphological and mitochondrial DNA data reshuffle the taxonomy of the genera *Atopochetus* Attems, *Litostrophus* Chamberlin and *Tonkinbolus* Verhoeff (Diplopoda: Spirobolida: Pachybolidae), with descriptions of nine new species. *Invertebrate Systematics* 32(1): 159–195. <https://doi.org/10.1071/IS17052>
- Pimvichai P, Enghoff H, Panha S, Bäckeljau T (2020) Integrative taxonomy of the new millipede genus *Coxobolellus*, gen. nov. (Diplopoda : Spirobolida : Pseudospirobolellidae), with descriptions of ten new species. *Invertebrate Systematics* 34: 591–617. <https://doi.org/10.1071/IS20031>
- Pimvichai P, Panha S, Bäckeljau T (2022a) Combining mitochondrial DNA and morphological data to delineate four new millipede species and provisional assignment to the genus *Apeuthes* Hoffman & Keeton (Diplopoda: Spirobolida: Pachybolidae: Trioniulinae). *Invertebrate Systematics* 36(2): 91–112. <https://doi.org/10.1071/IS21038>
- Pimvichai P, Enghoff H, Panha S, Bäckeljau T (2022b) A new genus of Pseudospirobolellidae (Diplopoda, Spirobolida) from limestone karst areas in Thailand, with descriptions of three new species. *Zoosystematics and Evolution* 98(2): 313–326. <https://doi.org/10.3897/zse.98.90032>
- Reip HS, Wesener T (2018) Intraspecific variation and phylogeography of the millipede model organism, the black pill millipede *Glomeris marginata* (Villers, 1789) (Diplopoda, Glomerida, Glomeridae). *ZooKeys* 741: 93–131. <https://doi.org/10.3897/zookeys.741.21917>

- San Mauro D, Agorreta A (2010) Molecular systematics: A synthesis of the common methods and the state of knowledge. *Cellular & Molecular Biology Letters* 15(2): 311–341. <https://doi.org/10.2478/s11658-010-0010-8>
- Stamatakis A (2014) RAxML version 8: A tool for phylogenetic analysis and post-analysis of large phylogenies. *Bioinformatics* 30(9): 1312–1313. <https://doi.org/10.1093/bioinformatics/btu033>
- Xia X (2018) DAMBE7: New and improved tools for data analysis in molecular biology and evolution. *Molecular Biology and Evolution* 35(6): 1550–1552. <https://doi.org/10.1093/molbev/msy073>

Supplementary material 1

Estimates of COI sequence divergences within and among *Coxobolellus* species and related taxa expressed as uncorrected p-distances (rounded to two decimals)

Authors: Piyatida Pimvichai, Henrik Enghoff, Thierry Backeljau

Data type: COI sequence divergences

Copyright notice: This dataset is made available under the Open Database License (<http://opendatacommons.org/licenses/odbl/1.0/>). The Open Database License (ODbL) is a license agreement intended to allow users to freely share, modify, and use this Dataset while maintaining this same freedom for others, provided that the original source and author(s) are credited.

Link: <https://doi.org/10.3897/zookeys.1128.94242.suppl1>

Supplementary material 2

Estimates of 16S rRNA sequence divergences within and among *Coxobolellus* species and related taxa expressed as uncorrected p-distances (rounded to two decimals)

Authors: Piyatida Pimvichai, Henrik Enghoff, Thierry Backeljau

Data type: 16S rRNA sequence divergences

Copyright notice: This dataset is made available under the Open Database License (<http://opendatacommons.org/licenses/odbl/1.0/>). The Open Database License (ODbL) is a license agreement intended to allow users to freely share, modify, and use this Dataset while maintaining this same freedom for others, provided that the original source and author(s) are credited.

Link: <https://doi.org/10.3897/zookeys.1128.94242.suppl2>

Supplementary material 3

Estimates of combine datasets (COI + 16S rRNA) sequence divergences within and among *Coxobolellus* species and related taxa expressed as uncorrected p-distances (rounded to two decimals)

Authors: Piyatida Pimvichai, Henrik Enghoff, Thierry Backeljau

Data type: COI + 16S rRNA sequence divergences

Copyright notice: This dataset is made available under the Open Database License (<http://opendatacommons.org/licenses/odbl/1.0/>). The Open Database License (ODbL) is a license agreement intended to allow users to freely share, modify, and use this Dataset while maintaining this same freedom for others, provided that the original source and author(s) are credited.

Link: <https://doi.org/10.3897/zookeys.1128.94242.suppl3>

Supplementary material 4

Phylogenetic relationships of *Coxobolellus* species based on maximum likelihood analysis (ML) and Bayesian inference (BI) of 660 bp of the COI alignment

Authors: Piyatida Pimvichai, Henrik Enghoff, Thierry Backeljau

Data type: Figure (PDF file)

Explanation note: Numbers at nodes indicate branch support based on bootstrapping (ML) / posterior probabilities (BI). Scale bar = 0.3 substitutions/site. # indicates branches with <50% ML bootstrap support and <0.95 Bayesian posterior probability. - indicates non-supported branches.

Copyright notice: This dataset is made available under the Open Database License (<http://opendatacommons.org/licenses/odbl/1.0/>). The Open Database License (ODbL) is a license agreement intended to allow users to freely share, modify, and use this Dataset while maintaining this same freedom for others, provided that the original source and author(s) are credited.

Link: <https://doi.org/10.3897/zookeys.1128.94242.suppl4>

Supplementary material 5

Phylogenetic relationships of *Coxobolellus* species based on maximum likelihood analysis (ML) and Bayesian inference (BI) of 458 bp of the 16S rRNA alignment

Authors: Piyatida Pimvichai, Henrik Enghoff, Thierry Backeljau

Data type: Figure (PDF file)

Explanation note: Numbers at nodes indicate branch support based on bootstrapping (ML) / posterior probabilities (BI). Scale bar = 0.06 substitutions/site. # indicates branches with <50% ML bootstrap support and <0.95 Bayesian posterior probability. - indicates non-supported branches.

Copyright notice: This dataset is made available under the Open Database License (<http://opendatacommons.org/licenses/odbl/1.0/>). The Open Database License (ODbL) is a license agreement intended to allow users to freely share, modify, and use this Dataset while maintaining this same freedom for others, provided that the original source and author(s) are credited.

Link: <https://doi.org/10.3897/zookeys.1128.94242.supl5>